Proteome analysis of the differential adaptation of *Pseudomonas aeruginosa* morphotypes isolated from Cystic Fibrosis patients, to iron limiting conditions, oxidative stress and anaerobic conditions

Von dem Fachbereich Biologie der Universität Hannover

zur Erlangung des Grades

DOKTOR DER NATURWISSENSCHAFTEN
Dr. rer.nat.

genehmigte Dissertation
von

Master of Science, Senthil Selvan Saravanamuthu

geboren am 28. April 1977 in Chennai, India

Hannover
2004

Referent: Prof. Dr. D. Bitter-Suermann
Koreferrent: PD Dr. I. Steinmetz

Tag Der Promotion: 04 May 2004

Prüfungskollegium:

Vorsitz: Prof. Dr. G. Auling

Prüfende: Prof. Dr. D. Bitter-Suermann
                   Prof. Dr. K. Kloppstech
                   PD Dr. I. Steinmetz

Abstract

The occurrence of diverse colony morphotypes of *Pseudomonas aeruginosa* is a common finding in the chronically infected cystic fibrosis (CF) lung. A previous study from our laboratory showed that the isolation of *P. aeruginosa* Small Colony Variants (SCVs) could be correlated with parameters revealing poor lung function and the use of inhalative antibiotics. Among the heterogenous group of clinical SCVs, recently a subgroup of hyperpiliated SCVs that exhibited autoaggregative growth behaviour and enhanced ability to form biofilms was identified. Role of these variants in the pathogenesis is poorly understood.

In this study we compared the ability of these SCVs to survive harsh conditions like iron limitation and hydrogen peroxide induced oxidative stress compared to their corresponding wild types. The autoaggregative SCV 20265 showed better growth and survival under iron limiting and oxidative stress conditions compared to the clonal wild type. In agreement with these functional characteristics extensive comparative proteome analysis of SCV 20265 was indicative of a better adaptation to oxidative stress and iron limitation as compared to the corresponding wildtype, WT 20265. Proteome profile of SCV 20265 showed differential expression of some oxidative stress combat proteins like peroxidases, superoxide dismutases and iron acquisition related proteins like FeoB, HasAp, FpvA.

Since occurrence of anaerobic biofilms in the CF lung is known, differential adaptation of SCV and WT 20265 to anaerobic mode of growth using nitrate was tested. Results indicate that SCV 20265 grows better than the WT 20265 under this condition. Proteome analysis of anaerobically grown cells revealed the differential regulation of some key genes involved in the anaerobic mode of growth using nitrate.

Membrane and supernatant sub proteomes of morphotypes of strain 20265 were subjected to a gel-less proteome analysis using nanoflow LC/MS to obtain an overview of the expression differences and pick up candidates for more detailed analysis. Accordingly, expression of a putative ferrous iron transporter (PA 4358) was further monitored using real time PCR analysis and its differential expression confirmed at a transcription level too. As an interesting offshoot from the main study, polyadenylation of mRNAs of *Pseudomonas aeruginosa* has been reported in this study for the first time. DNA microarray analysis of log phase RNA preparation of strain PAO1 has revealed that up to 42% of the expressed mRNA was polyadenylated.

Taken together our data suggest that some SCVs like the SCV 20265, represent clonal variants which are especially adapted to oxidative stress and iron limitation, conditions which are likely to be encountered in the CF lung. It is speculated that polyadenylation of a significant number of expressed mRNAs might have some significance in the post-transcriptional modification and mRNA stability.

Key words: Small colony variant (SCV), Cystic fibrosis, *Pseudomonas aeruginosa*, iron, proteome analysis, H_2O_2, Polyadenylation

Kurzfassung

Das Auftreten verschiedener Kolonie-Morphotypen von *Pseudomonas aeruginosa* ist ein häufiger Befund bei der chronisch infizierten Lunge von Patienten mit Cystischer Fibrose(CF). Frühere Untersuchungen unseres Labors haben gezeigt, dass das Vorkommen so genannter „*P. aeruginosa* Small Colony Variants" (SCVs) mit schlechter Lungenfunktion und inhalativer Antibiotikatherapie korreliert. Aus dieser heterogenen Gruppe klinischer SCVs wurde unlängst eine Untergruppe hyperpilierter SCVs identifiziert, die ein autoaggregatives Wachstumsverhalten und eine erhöhte Fähigkeit zur Biofilm-Bildung aufwiesen. Über die Rolle dieser Varianten in der Pathogenese ist nur wenig bekannt.

In dieser Arbeit wurden die Auswirkungen verschiedener Faktoren, wie Eisen-Mangel und durch Wasserstoffperoxid ausgelöster oxidativer Stress, auf das Überleben der SCVs mit denen der entsprechenden Wildtypen verglichen. Die autoaggregative SCV 20265 zeigte ein besseres Wachstum und Überleben unter diesen Bedingungen im Vergleich zum klonalen Wildtyp. Diese funktionellen Charakteristikan wurden durch umfangreiche Proteom-Analysen der SCV 20265 unterstützt, die ebenfalls auf eine bessere Anpassung der SCV an oxidativen Stress und Eisen-Mangel im Vergleich zum entsprechenden Wildtyp deuten. Das Proteom-Profil der SCV 20265 zeigte eine unterschiedliche Expression einiger Schutzproteine gegen oxidativen Stress, wie Peroxidasen und Superoxid-Dismutase und einiger Proteine, die bei der Eisen-Aufnahme eine Rolle spielen, wie FeoB und HasAp.

Da bekannt ist, dass anaerobe Biofilme in der CF-Lunge auftreten, wurde die unterschiedliche Anpassung von SCV und WT 20265 an anaerobe Wachstumsbedingungen in gegenwart von Nitrat untersucht. Die Ergebnisse weisen darauf hin, dass die SCV 20265 besser als der WT 20265 unter diesen Bedingungen wächst. Proteom-Analysen von unter anaeroben Bedingungen gewachsenen Zellen zeigten eine unterschiedliche Regulation einiger Schlüsselgene, die bei der Nitrat-Nutzung unter anaeroben Wachstumsbedingungen involviert sind.

Membranen und sezernierte proteinen von Morphotypen des Stammes 20265 wurden mittels eines Gel-unabhängigen Proteom-Analyse Verfahrens namens Nanoflow LC/MS untersucht, um eine Übersicht über Expressionsunterschiede zu erhalten und um mögliche Kandidaten für eine ausführlichere Analyse zu finden. Folglich wurde die Expression eines vermeintlichen Fe^{2+}-Eisen-Transporters (PA 4358) mittels RT-PCR genauer untersucht, wodurch seine unterschiedliche Expression auch auf Transkriptionsebene bestätigt werden konnte. Als interessantes „Nebenprodukt" dieser Studie wurde eine Polyadenylierung der mRNA in *Pseudomonas aeruginosa* gezeigt. DNA-Mikroarray Analysen von isolierter RNA aus der exponentiellen Wachstumsphase des sequenzierten Stammes PAO1 haben gezeigt, dass bis zu 42% der exprimierten mRNA polyadenyliert war.

Letztlich deuten unsere Ergebnisse darauf hin, dass einige SCVs, wie die SCV 20265, klonale Varianten bilden, die besonders gut an oxidativen Stress und Eisen-Mangel angepasst sind; eben solchen Bedingungen, wie sie in der CF-Lunge vorherrschen. Polyadenylierung des grössten Teils der mRNA könnte eine entscheidende Rolle bei posttranskriptionalen Modifikationen und bei der Stabilität der mRNA haben.

Schlagworte: Small Colony Variants (SCV), Cystische Fibrose, *Pseudomonas aeruginosa*, Eisen, Proteom-Analyse, H_2O_2, Polyadenylierung

Acknowledgements

Abbreviations

16-BAC	Benzyldimethyl-n-hexadecylammonium chloride
2D-Gel	Two dimensional Gel
AA	Acrylamide
ADP	Adenosine Phosphate
APS	Ammonium persulphate
Aqua dest.	Distilled Demineralised Water
ASB14	N-Tetradecyl-N, N-dimethyl-3-ammonio-1-propanesulphate
ATP	Adenosine tri phosphate
bp	Basepair
BSA	Bovine Serum Albumin
C	Celcius
CF	Cystic Fibrosis
CFU	Colony Forming Units
CHAPS	3-((3-Chloramidopropyl)-di-Methylammonio)-1-Propane-Sulphonate
Da	Dalton
DNA	Deoxyribonucleic Acid
dNTPs	Deoxynucleoside triphosphates
DTT	Dithiothreitol (1,4-Dimercapto-2,3-butanediol)
EDTA	Ethylene dinitrilo tetra acetic acid
EtOH	Ethanol
hr	Hour
IEF	Isoelectric Focussing
IPG	Immobilised pH gradient
Kb /Kbp	Kilobase/Kilobasepair
LB-Medium	Luria-Bertani-Medium
LC/MS	Liquid Chromatography/ Mass Spectrometry
Leupeptin	N-Acetyl-Leu-Leu-Arginal X ½ H_2SO_4 X H_2O
m	meter
m/z	Mass by Charge ratio
MALDI	Matrix Assisted Laser Desorption/Ionization
min	Minute
mRNA	Messenger RNA
MS	Mass Spectrometry
MS/MS	Tandem Mas Spectrometry
MW	Molecular Weight
OD	Optical Density
ORF	Open Reading Frame
PAGE	Polyacrylamide Gel Electrophoresis
PBS	Phosphate Buffered Saline
Pefablock SC	4-(2-Aminoethyl)-benzolsulphonylfluoride-hydrochloride
PI	Isoelectric point
REV	Revertant
RNA	Ribonucleic acid
rpm	Rotations per minute

SB	Sulphobetaine
SCV	Small Colony Variant
SDS	Sodium Dodecyl Sulphate
s	Seconds
sp.	Species
TBP	Tributyl Phosphine
TCA	Trichloro acetic acid
TEMED	N,N,N'N'-Tetramethylethylenediamine
TOF	Time of Flight
Tris	Tris-(hydroxymethyl)-aminomethane
v/v	Volume/ Volume
V/w	Volume/ Weight
VB Medium	Vogel Bonner Medium
Vol	Volume
WT	Wildtype

Contents

1.   Introduction

1.1 *Pseudomonas aeruginosa*

Pseudomonas aeruginosa is a gram-negative rod shaped bacterium having polar flagella belonging to the group of α-proteobacteria (Olsen *et al.*, 1994). The genus *Pseudomonas* belongs to the γ-subclass of the Proteobacteria and contains more than 140 species including fluorescent Pseudomonads such as *Pseudomonas putida*, *Pseudomonas fluorescens*, *Pseudomonas chlororaphis*, *Pseudomonas aeruginosa*, phytopathogenic species like *Pseudomonas syringae*, *Pseudomonas cichorii*, *Pseudomonas marginalis* and *Pseudomonas tolaasii* as well as non-fluorescent Pseudomonads like *Pseudomonas stutzeri*, *Pseudomonas mendocina* or *Pseudomonas alcaligenes*.

Most pseudomonads are saprophytic organisms and are well known for their broad metabolic and physiological versatility. They are free-living ubiquitous bacteria that are frequently found in soil, aquatic habitats or associated with host organisms like plants and animals and play an important role in decomposition, biodegradation, carbon and nitrogen cycles and disease production. Unlike other Pseudomonads, *P. aeruginosa* has the capacity to cause disease in humans, because of its large repertoire of virulence factor (Stover *et al.,* 1983). It can cause serious infections in immuno-suppressed patients such as burn victims, cancer and intensive care unit patients. *P. aeruginosa* infections of the respiratory tract are the major cause of death in cystic fibrosis patients. *P. aeruginosa* causes bacteraemia in burn victims, urinary-tract infections in catheterized patients, and hospital-acquired pneumonia in patients on respirators (Bodey *et al.*, 1983).

A   **B**
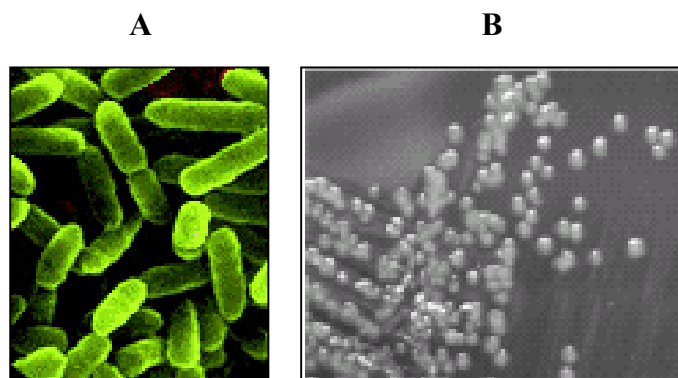
Fig 1.1.1 *Pseudomonas aeruginosa* morphology in a Scanning Electron Micrograph (A) and streaks on agar plates (B). (Illustration adopted from http://www.pseudomonas.com (A) and von Götz (2003) (B))

Today, in the era of genome sequencing and whole genome analysis, the genome of one *Pseudomonas* strain, *P. aeruginosa* PAO1 has been completely sequenced (Stover *et al.,* 2000). The sequencing project of *P. putida* KT2440 was started in 1998, five more

Pseudomonas sequencing projects are currently underway, including three *P. fluorescen*s and two *P. syringae* strains (Bernal, 2001). During the last 15 years, physical and genetic chromosome maps were constructed for a number of *Pseudomonas* species shedding additional light on the genome structure and variability of Pseudomonads (Romling and Tummler, 2000; Wechter *et al.,* 2002; Rainey and Bailey, 1996)

1.2 *Pseudomonas aeruginosa* in Cystic Fibrosis

CF is the most common genetic disease among the Caucasians. The affected gene encodes for a 1480 amino acid chloride channel called the Cystic Fibrosis Transmembrane Conductance Regulator (CFTR). 70% of the patients are affected with EF 508 (Phenly alanine deletion) in a critical portion of the protein that leads to its being misfolded and retained in the endoplasmic reticulum (ER), where it seems to be pulled out of the ER membrane and degraded on proteosomes.

Thus these patients suffer from lack of any chloride channels in the membrane because they have been degraded before they ever became functional in the membrane. A large number of mutations have been described. In general, there is a direct correlation between severity of disease symptoms and the severity of the effect on chloride channel function.The opportunistic pathogen *P. aeruginosa* being a key etiological agent of hospital acquired infections in the immunocompromised host, is also responsible for chronic lung infection in cystic fibrosis (CF) patients (Gilligan, 1991; Lyczak *et al.,* 2002; Govan & Deretic, 1996; Breitenstein *et al.,*1997).

Once CF patients become colonized by *P. aeruginosa*, there is a subsequent gradual deterioration in lung function, which determines the course and prognosis in most CF patients. In normal individuals, the function of airway epithelia is to promote proper transport of Cl^-, Na^+ and water from the basolateral to the apical surface (**Fig. 1.2.1**). A major role of CFTR is to transport Cl^- across the apical surface of secretory cells. Thus, a major defect in CF is either little or no Cl^- transport across the apical surface. This can occur as a result of either (i) no CFTR produced, (ii) mutated CFTR, (iii) or mutated and truncated CFTR. Without CFTR, Na^+, Cl^- and water are reabsorbed in an unopposed and accelerated fashion. The fact that goblet cells in CF airway disease secrete mucus to the apical surface despite the failure to clear mucus from the airway surface further exacerbates the disease process (**Fig. 1.2.1**).
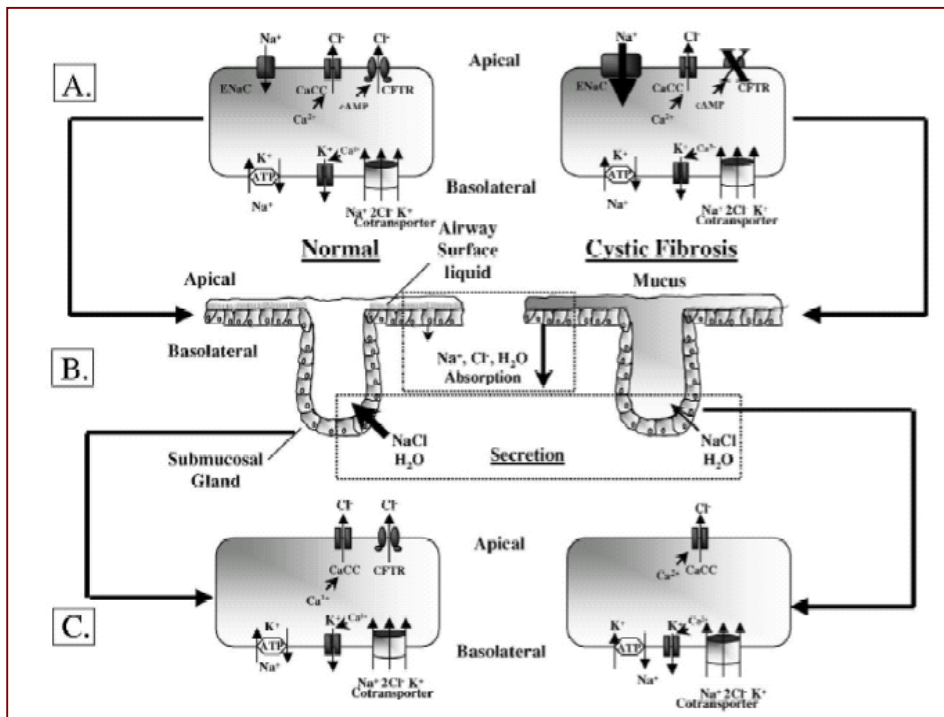
Figure 1.2.1. **Model of ion transport** in normal (left) and CF (right) absorptive (A) and secretory (C) epithelia. Transepithelial Cl^- transport occurs through movement of Cl^- through the basolateral membrane $Na^+ K^+ 2Cl^-$ co-transporter, and across the lumenal (apical) membrane by Cl^- channels. This model shows that CFTR is activated by increased intracellular cAMP through protein kinase A, and alternative Cl^- channels, as well as the amiloride-sensitive sodium channel, ENaC. The basolateral membrane contains the Na^+/K^+ ATPase and basolateral membrane calcium and cAMP activated K^+ channels. K^+ channels help drive Cl^- across the cell. Tight junctions provide a transepithelial resistance to the movement of other ions and molecules. In CF, CFTR mutants have altered unit conductance, or altered trafficking, maturation or stability. ENaC activity is increased in CF, leading to hyper-absorption of sodium. This leads to a decrease in the airway surface liquid volume, and thickened mucus. This thickened mucus layer, plus oxygen-consuming metabolism of airway epithelia and bacteria, provides a hypoxic environment ideal for anaerobic growth of *P. aeruginosa*. (Illustration adopted from Hassett *et al.,* 2002)

The cilia that beat freely and efficiently on normal epithelia are matted down by the thick mucus and either do not beat or beat inefficiently. Thus, the thickened, poorly cleared mucus becomes a veritable breeding ground for opportunistic pathogens in CF that include *P.aeruginosa*, *Staphylococcus aureus*, *Hemophilus influenzae*, *Burkholderia cepacia*, and other opportunists, as well as some true pathogens (e.g. *Mycobacterium tuberculosis*). However, with progression of CF airway disease, *P. aeruginosa* predominates and its mode of growth *in vitro* is dramatically different from that *in vivo*. The *in vivo* mode of growth in CF airway disease has been termed a 'biofilm'(Singh *et al.,* 2000).

The lung infection with *P. aeruginosa* is regarded as one of the major causes of health decline in patients with cystic fibrosis (CF). The CF host response to the persistent bacterial antigen load in the endobronchiolar lumen is characterized by a pronounced humoral response, local production of cytokines, influx of neutrophils into the lung and a

protease-protein inhibitor imbalance predominantly sustained by released neutrophil elastase. The epidemiology of the infection with *P. aeruginosa*, investigated by quantitative macro restriction fragment pattern analysis, revealed that the distribution and frequency of clones found in CF patients match that found in other clinical and environmental aquatic habitats, but the over-representation of specific clones at a CF clinic indicates a significant impact of nosocomial transmission. Most patients remain colonized with the initially acquired *P. aeruginosa* clone. According to direct sputum analysis the majority of patients carry a single clonal variant at a concentration of 10^7-10^9 CFU. Co-colonization with other species or other clones is infrequent (Tummler *et al.,* 1997). Independent of the underlying genotype, the CF lung habitat triggers a uniform, genetically fixed conversion of bacterial phenotype. Most CF *P. aeruginosa* strains become non-motile, mucoid, LPS-, pyocin- and phage-deficient, secrete less virulence determinants and shift the production of cytokines evoked in neutrophils. On the other hand, other properties such as antimicrobial susceptibility or adherence to bronchial mucins remain highly variable reflecting the capacity of *P. aeruginosa* to adapt to ongoing changes in the CF lung habitat.

1.3 Virulence Factors of *Pseudomonas aeruginosa*

Pseudomonas aeruginosa has several virulence factors. They fall into two broad categories: either cell associated or secreted virulence factors. Cellular appendages including motility structures like flagella and adhesive structures like Type IV pili and other nonpilus adhesins are important for attachment and establishment of infection in the epithelial cells (de Bentzmann *et al.,* 1996; Feldman *et al.,* 1998), which are the frontlines in the host-pathogen interaction. The inherent ability of *P. aeruginosa* to adapt a biofilm mode of growth is also considered as a virulence trait (Watnik and Kolter, 2000).

Secreted virulence factors include exotoxins, type III toxins, elastases, alkaline metallo proteases, siderophores and hemolysins. These virulence factors are secreted out of the bacteria by one of the four types of secretion pathways (Type I–IV) known in gram-negative bacteria. Some of them like the exotoxin A are secreted by Type II secretion system. Exotoxin A (ExoA), ADP ribosylates elongation factor 2 (EF–2), which stops the protein synthesis and elicits apoptosis of the affected cells. Secretion of ExoA by the Type II secretion mechanism is common to most if not all gram-negative. The secretion can be described as the Sec dependent export of ExoA into the periplasmic space followed by

folding of the polypeptide chain. Uptake of ExoA by epithelial cells is by the alpha 2-macroglobulin / LDL receptor. Mechanism of entry to the cytosol in other cells is very similar to that of the cholera toxin. Once toxin is internalised, it is transported backwards through the secretory pathway: endosomes, golgi apparatus and endoplasmic reticulum (from where the catalytic portion of the toxin is transported to the cytosol). Regulation of gene (toxA) is under the control of environmental iron levels (low iron means increased toxA). Inspite of being a potential cytotoxin, it seems to have relatively minor role in virulence in the airways. Folded ExoA is then recognized by a specifically assembled secretion machinery consisting in part of the Xcp genes and the pil genes (pil B,C,D). Thus, Type II secretion and Type IV pili are interconnected. Some components of the Type II secretion machinery, XcpT,U,V,W are exported by prepilin type signal peptides to be assembled into a supramolecular structure in the periplasmic space. Assembly of pilA into Type IV pili requires all the xcp genes. One component of the secretion machinery XcpP has a homolog in Type II secretion mechanisms of *Salmonella, Shigella, Helicobacter, Yersinia, E.coli* and others. This protein seems to form a 12 mer in the outer membrane that functions as a gated channel. It is presumed that all Type II and Type II secreted proteins as well as the type IV pili must pass the outer membrane through a similar type of channel.

Elastases (LasA and LasB) break down elastin, an important connective tissue protein in the lungs (maintains lung elasticity so that recoil occurs properly during exhalation). LasB is not strictly an elastase, but a Zinc metalloprotease (i.e., needs some Zn in the solution) that is somewhat non-specific but also works on elastin. LasA is a serine protease that nicks elastin but does not degrade it. Over all, Las A and LasB operate together to behave as an elastase, even though they have different individual functions. The concerted activity of two enzymes, LasB elastase and LasA elastase, is responsible for elastolytic activity (Galloway, 1991). Early damage to lungs may occur from LasA and LasB, which also degrade complement components and a protease inhibitor (which prevents damage due to neutrophil-produced proteases). Thus, LasA and LasB will inhibit immune cell response and could also enhance activity of neutrophil elastase.

Metalloproteases in bacterial-conditioned medium, as well as purified alkaline protease and elastase, degrade human RANTES, monocyte chemotactic protein-1 (MCP-1), and epithelial neutrophil-activating protein-78 (ENA-78) (Leidal, 2003). Neuraminidase is an

enzyme that works on sialic acid (neuraminic acid), leading to increased amounts of asialo-GM1 and endash GM2 on surfaces of airway cells, which will then likely bind increased numbers of bacteria. Neuraminidase production is regulated by osmolarity of medium (increases with higher osmolarity), and it has been proposed that the luminal airway surface liquid (ASL) has a higher than normal NaCl and osmolarity in CF than in normal individuals. Phospholipase C (plcS) and alkaline protease (apr) are also virulence genes.

In general, all type III toxins are ineffective when they are applied to the outsides of cells, indicating that they must gain access into the cells to bring about cytotoxicity. Exoenzyme S (ExoS) is an ADP ribosylase. It targets include Ras and perhaps related G proteins Rap, Ral and Rab, but not Rho and ARF and it also works on vimentin, an intermediate filament protein. The toxin is produced as an aggregate of two immunologically related proteins ExoS (53 KDa) and ExoT (49 KDa). Although these proteins share about 75% amino acid homology, ExoT has a catalytic defect and operates at < 1% of the ADP-ribosyl transferase activity of ExoS. ExoS is involved in virulence.

Siderophores are the most important virulence factors. Iron chelated to the *P. aeruginosa* siderophore pyochelin enhances oxidant-mediated injury to pulmonary artery endothelial cells by catalyzing hydroxyl radical (HO*) formation (DeWitte, 2001). Pyoverdine, the yellow-green, water-soluble, fluorescent pigment of the fluorescent Pseudomonas species, is a powerful iron (III) scavenger and an efficient iron (III) transporter. As a fluorescent pigment, it represents a ready marker for bacterial differentiation and, as a siderophore, it plays an important physiological function in satisfying the absolute iron requirement (Meyer, 2000). Pyoverdin competes directly with transferrin for iron and that it is an essential element for in vivo iron gathering and virulence expression in *P. aeruginosa* (Meyer, 1996). Pyocyanin, produced by *P. aeruginosa*, has many deleterious effects on human cells that relate to its ability to generate reactive oxygen species (ROS), such as superoxide and hydrogen peroxide (O'Malley, 2003). Other virulence factors include LPS, pilin assembled into type IV pili and possibly other not so well described iron uptake systems.

1.4 Iron and *Pseudomonas aeruginosa*

Iron is a first row transition metal that under physiological conditions, mainly exists in one of the two readily inter-convertible redox states: the reduced Fe^{2+} (Ferrous) and the oxidised Fe^{3+} (Ferric). It can also adopt different spin states (high or low) in both the ferric and ferrous form, depending on its ligand environment. These properties make iron an extremely versatile prosthetic component for incorporation into proteins as a biocatalyst or electron carrier. Iron is considered to be absolutely required for life of all forms (except for a few exceptions like the *Lactobacilli, Borrelia burgdorferi*). It participates in many major biological processes, such as photosynthesis, N_2 fixation, methanogenesis, H_2 production and consumption, respiration, the trichloroacetic acid (TCA) cycle, oxygen transport, gene regulation and DNA biosynthesis. With the evolution of oxygenic photosynthesis (about 2.2 to 2.7 billion years ago), the predominant form of iron switched from the relatively soluble (0.1M at pH 7.0) ferrous state to the extremely insoluble (10^{-18}M at pH 7.0) ferric form. Thus, this valuable minor nutrient upon which life is now so dependent became scarce and growth limiting within many ecological niches. Iron limitation has profound consequences for all but a few microbial organisms so far identified on our planet. There is always a paucity of soluble, biologically useful iron in aerobic environments. Bacterial cells each contain 10^5 to 10^6 iron ions, which are essential for many metabolic pathways. Typical bacterial organisms require approx. $0.3 - 1.8$ µM of iron for optimal growth, whereas the concentration in the soil is < 0.1 µM and only 10^{-9} in mammalian host (Vasil and Ochsner, 1999). *P. aeruginosa* is found in a remarkable variety of environments, which furnish a variety of exigencies, both in terms of how to obtain iron from its surroundings and how to deal with potentially toxic levels once it starts to increase its uptake. Consequently, in comparison with many other frank pathogens that need to acquire iron only from the limited ecological niches to which they are restricted, i.e. a human host, *P. aeruginosa* has to use an assortment of strategies for accessing iron and for regulating its intake (refer **Table 1.4.1**).

Siderophores are the chief iron scavengers. They are highly efficient in chelating Ferric iron from a variety of sources. Pyoverdin and pyochelin are the two siderophores of *P aeruginosa*. *P. aeruginosa* is also capable of utilizing heterologous siderophores (siderophores produced by other microbes) and henceforth expresses cognate receptors for these too apart from the ferripyoverdine and ferripyochelin receptors.

Table.1.4.1. Iron uptake systems of *Pseudomonas aeruginosa*

Iron source	Protein	Function	References
Haemoglobin / Haemin	PhuR	Heme/Hb OM receptor	(Ochsner *et al.,* 2000))
	PhuSTUVW	Heme ABC transport system	(Ochsner *et al.,* 2000)
	HasRADEF	Heme receptor, hemophore, ABC transporter for HasA export	(Ochsner *et al.,* 2000)
Reduced iron - Fe(II)	FeoAB	Fe^{2+}	(Vasil and Ochsner, 1999)
Siderophores – Fe(III)	FptA	Ferric Pyochelin OM receptor	(Ankenbauer, 1992)
	FpvA	Ferric pyoverdine OM receptor	(Poole *et al,* 1993)
	FiuA	Ferrioxamine OM receptor	(Ochsner and Vasil, 1996)
	PfeA PirA	Ferric enterobactin OM receptor	(Dean *et al,* 1993; Ochsner and Vasil, 1996)
	PiuA, PfuA, UfrA	Unknown OM receptor	(Ochsner and Vasil, 1996)

Haemophores are found to enhance the efficiency of haem uptake by100 folds (Letoffe *et al.,* 1999). *P. aeruginosa* has two distinct haemophore mediated iron uptake systems namely, Haem Acquisition System (Has) and Pseudomonas Haem Uptake (Phu) system (Ochsner *et al.,* 2000) apart from siderophore mediated iron uptake systems. **Figure 1.4.1** shows a schematic outline of the various iron uptake systems of a gram-negative bacteria such as *P. aeruginosa* along with the sub cellular localization of their components. The ferrous iron uptake systems of *P. aeruginosa* are not well studied even though genome sequencing has revealed the occurrence of homologues of known ferrous iron uptake systems of *E. coli* such as *feoAB*.
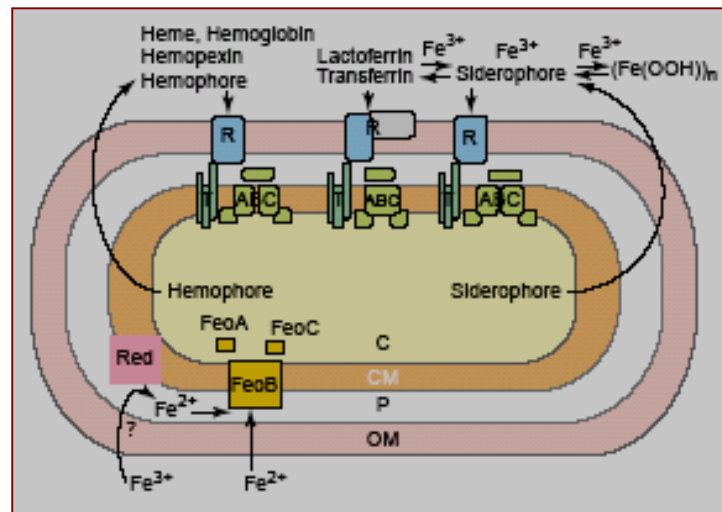
Fig. 1.4.1. Bacterial iron transport. A schematic view of iron uptake systems of Gram-negative bacteria is shown. Under low-iron stress, many bacteria secrete siderophores to bind Fe^{3+} and take it up by specific receptors (R) that are energized by the Ton complex (T). Some pathogenic bacteria are able to use lactoferrin- or transferrin-bound iron either with the help of their siderophores or with specialized receptors in their outer membranes (OM). Often, these bacteria have additional systems to utilize the haem-bound iron of their host either by secreting a special haem-binding protein, a hemophore, or through specific receptors for haem, hemoglobin, or hemopexin, which are able to extract the haem and transport it across the outer membrane. All these different substrates – ferric iron from transferrin, haem, and Fe^{3+}-siderophores – are transported by specialized ABC transporters (ABC) across the cytoplasmic membrane (CM). In the cytoplasm (C), Fe^{3+}-siderophore reductases or haem oxygenases help to mobilize the iron for cell metabolism. FeoB is a transporter, which can either utilize the more-soluble Fe^{2+} or possibly obtain Fe^{2+} from mostly uncharacterized reductive processes (labeled Red in the figure) at the cell surface or in the periplasm (P). FeoA and FeoC might take part in Fe^{2+} transport and mobilization and Fe^{2+} transport is not as well-characterized as Fe^{3+} transport is. (Illustration adopted from Hantke, (2003))

The central role in the control of iron-regulated genes has been assigned to the 'ferric uptake regulator' (Fur) protein, which acts as an iron responsive, DNA binding repressor protein. A widely accepted model of how Fur regulates iron acquisition genes is schematically depicted in **figure1.4.2.** The genetics, biochemistry and biology of Fur and the Fur regulated alternative sigma factor (PvdS) are discussed elsewhere in detail (Escolar *et al.,* 1999;Vasil *et al.,* 1998; Vasil and Ochsner, 1999;Visca *et al.,* 2002; Wilson *et al.,* 2001). These regulatory proteins directly or indirectly regulate a substantial number of other genes encoding proteins with remarkably diverse functions. These genes include: (I) other regulatory genes, (II) genes involved in basic metabolic processes, (III) genes required to survive oxidative stress (e.g. superoxide dismutase), (iv) genes necessary for scavenging iron (e.g. siderophore biosynthesis genes and their cognate receptors) or genes that contribute to virulence (e.g. exotoxin A) of this opportunistic pathogen. Despite a recent expansion of knowledge about the response of *P. aeruginosa* to iron, many

significant biological issues need to be addressed. Virtually nothing is known about which of the distinct iron acquisition mechanisms *P. aeruginosa* deploys outside the laboratory, whether it be in soil, in a pipeline, on plants or in the lungs of the cystic fibrosis patients.
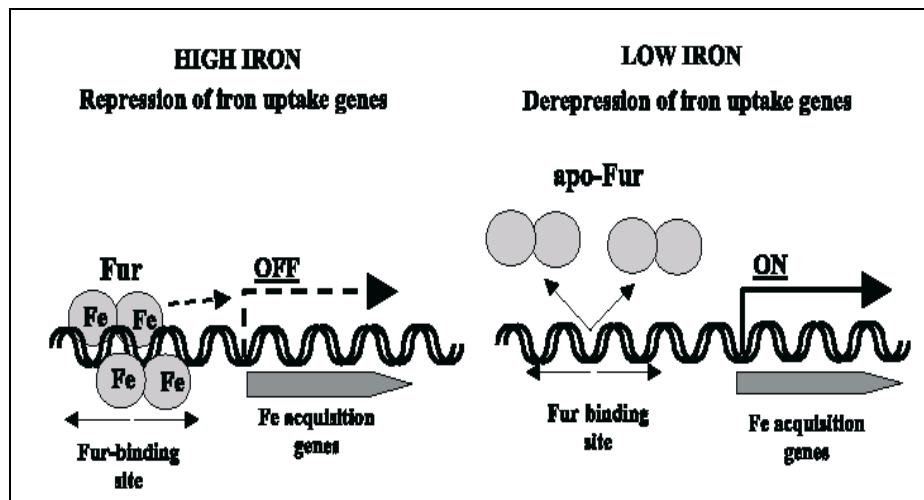
Figure.1.4.2 Schematic representation of the generally accepted model of Fur mediated gene expression of iron uptake genes. Iron acquisition genes are repressed by the binding Fur-Fe during conditions of high iron availability. On the contrary, under low iron conditions, the amount of Fe available for complex formation with Fur is so low that most of the Fur occurs as apo-Fur (unconjugated to Fe). This prevents effective binding of Fur (repressor) to the promoters of the iron acquisition genes. This results in expression of the iron acquisition genes. (Illustration adopted from Andrews et al., (2003))

1.5 Oxidative stress and *Pseudomonas aeruginosa*

Pseudomonas aeruginosa gains its greatest metabolic energy through aerobic respiration. To counter the production of ROIs, the organism possesses two SODs, with either iron (Fe^{2+}; encoded by *sodB* (Hassett *et al.,* 1993; Hassett *et al.,* 1995) or manganese (Mn^{2+}; encoded by *sodA* (Hassett *et al.,* 1993; Hassett *et al.,* 1995)) as cofactor and whose function is to disproportionate $^*O_2$ to H_2O_2 and O_2 (McCord and Fridovich, 1969). To remove H_2O_2, *P. aeruginosa* possesses three catalases, KatA (Brown *et al.,* 1995; Hassett *et al.,* 1992) KatB (Brown *et al.,* 1995; Hassett *et al.,* 1992) and KatC (Pathogenesis Corporation and the Cystic Fibrosis Foundation, 1999). KatA activity is the major catalase activity detected in all phases of growth (Brown *et al.,* 1995; Hassett *et al.,* 1992). In contrast, KatB activity is detectable in bacteria exposed to H_2O_2 or paraquat, the latter of which generates a constant flux of H_2O_2 through SOD-catalyzed dismutation of $^*O_2$ (Brown *et al.,* 1995). Unlike KatA and KatB, little is known of the biological role of KatC in *P. aeruginosa*. In fact, the putative *katC* gene was only recently discovered fortuitously via the *Pseudomonas* Genome Project (Pathogenesis Corporation and the Cystic Fibrosis

Foundation, 1999). Most bacterial catalases are multimers (typically dimers, tetramers, or hexamers) that require heme *b* or heme *d* for catalytic activity. The final step of heme synthesis is catalyzed by ferrochelatase, which condenses Fe^{2+} into protoporphyrin IX. Little is known of the cellular source of iron required for haem assembly. One protein that could provide iron for such a process is bacterioferritin A (BfrA, also known as cytochrome *b*1 or *b*557), the major iron storage protein in *P. aeruginosa* (Moore *et al.,* 1994). Actually, there is evidence in *P. aeruginosa* for two Bfr proteins (BfrA and BfrB), which differ in their N-terminal amino acid sequences (Moore *et al.,* 1994). BfrA is a complex of 24 subunits capable of binding 700 iron atoms (Moore *et al.,* 1994). It also binds 3 to 9 haem groups per 24 subunits in vivo and 24 haem groups in vitro(Kadir and Moore,1990). Recently, a *bfr* gene encoding a bacterioferritin was identified in the related organism *P. putida*; this gene was located downstream of a gene encoding a group III catalase (Kim *et al.,* 1997).

Bacterial aerobic respiration involves a four-electron reduction of molecular oxygen (O_2) to water. Depending upon the environmental conditions, aerobic respiration can be extremely dangerous to the cell. Such is the case when aberrant electron flow from the electron transport chain or cellular redox enzymes to O_2 leads to the production of reactive oxygen intermediates (ROIs). These include superoxide ($^*O_2$), hydrogen peroxide (H_2O_2), and hydroxyl radical HO^*. The unchecked production of each of these species can lead to cell damage, mutations, or death. The production of HO^*, the most destructive of the above compounds, is dependent in part upon the presence of a transition metal, such as iron or copper, and either $^*O_2$ or H_2O_2. Relief from ROIs is provided by various defense systems, including antioxidant enzymes (superoxide dismutase [SOD]), catalase, and peroxidase), DNA repair enzymes and binding protein (e.g., Dps [DNA binding protein from starved cells (Martinez, 1997), and free-radical-scavenging agents (Imlay and Linn, 1987). Although it is clearly important for bacteria to secure the iron supplies required for growth, it is equally important to ensure that their intracellular iron is maintained in a safe, non toxic form (Andrews, 2003). This requires that cellular iron is not allowed to interact with reactive oxygen species in an unrestricted manner. Reactive oxygen species are partially reduced derivatives of molecular oxygen that are produced as a natural consequence of aerobic metabolism (Fridovich, 1995). The one- and two-electron-reduction products of oxygen, namely superoxide and hydrogen peroxide, are only mildly reactive

physiologically. However, iron interacts with these species to generate the highly reactive and extremely damaging hydroxyl radical. The key reactions are shown below:

Iron reduction $\quad\quad\quad O_2^- + Fe^{3+} \longrightarrow Fe^{2+} + O_2 \quad\quad$ (1)

Fenton reaction $\quad\quad\quad Fe^{2+} + H_2O_2 \longrightarrow Fe^{3+} + OH^- + HO^* \quad$ (2)

Haber – Wiess reaction, (1) + (2): $O_2^- + H_2O_2 \xrightarrow{\text{Fe catalysis}} HO^* + OH^- + O_2$
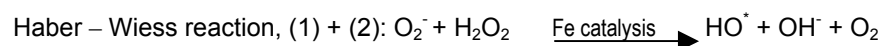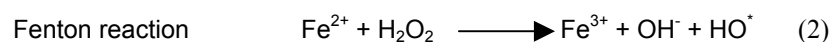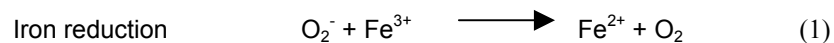
In vivo superoxide concentrations are considered to be too low (at $\sim 10^{-10}$ M) to cause iron reduction, but can be sufficiently high to damage the exposed [4Fe-4S] clusters of dehydratase-lyase family members (e.g. aconitase and α,β-dihydroxyacid dehydratase) which in turn leads to release of free iron. The relevant *in vivo* mediator of iron reduction during iron-induced redox stress appears to be flavins (Woodmansee, 2002). Because of this, redox stress is enhanced by factors that favor the accumulation of reduced flavins (such as inhibition of respiration (Woodmansee, 2002). The role of iron as a major protagonist in redox stress is indicated by the increased sensitivity of bacteria to redox stress agents following growth under iron-rich conditions (Abdul-Tehrani, 1999). In addition, inactivation of the *fur* gene (resulting in deregulation of iron metabolism) increases sensitivity to redox stress, an effect that can be reversed by iron chelation, a *tonB* mutation (blocking iron uptake) or by increasing iron storage capacity through over expression of the ferritin (*ftnA*) gene (Touati, 2000). Also, the impairment of *E.coli* superoxide dismutase mutants can be suppressed by further mutations that raise the intracellular concentrations of the iron chelator, dipicolinate (Maringanti, 1999). It is probable that the enhanced sensitivity of *E. coli* and *P. aeruginosa fur* mutants to redox stress is a direct consequence of increased cellular free iron. This notion is supported by the observation that *fur* mutants, which express iron transport systems constitutively (with respect to iron), have low levels of iron storage proteins and have increased *free* iron levels (Keyer, 1996) (although total cellular iron levels are actually reduced). These findings suggest that Fur regulates the concentration of intracellular free iron through modulation of iron acquisition and iron consumption (e.g. iron storage), and that, in the absence of Fur, iron uptake and consumption are improperly balanced such that free iron levels become excessive.

1.6 Microaerobic/Anaerobic growth of *Pseudomonas aeruginosa*

Most of the known aspects of anaerobic respiration have been extensively reviewed (Moreno-Vivian C, 1999; Stewart, 1998). It should be noted, however, that the well-studied *E. coli* genes and products involved in anaerobic nitrate reduction have not been well studied in *P. aeruginosa*, although many have been identified by homology from the *Pseudomonas* genome project. It is clear that both the metabolic background of *P. aeruginosa* and its denitrification pathway are very different from that of *E. coli* and no general extrapolations should be made without experimental proof. There are also significant differences in the components and metabolic strategies involved in the first rate-limiting step, nitrate reduction, of the denitrification pathway transport of *P. aeruginosa* relative to *E. coli*. Based on microscopic examination of thin sections of airways removed from CF patients that received lung transplants, it has been reported that in contrast to the prevailing surface attachment model of biofilm formation, *P. aeruginosa* is typically seen localized to the epithelial cell surface in CF airway disease where the bacteria are embedded in the thickened, highly inspissated airway mucus. Worlitzsch *et al.,* (2002) have recently shown that there are ''steep hypoxic gradients'' in the mucus lining the CF airways.

P. aeruginosa are seeded onto the mucus surface by inhalation and the bacteria can penetrate the mucus actively (presumably via flagellar, twitching or swarming motility) and/or passively (due to mucus turbulence) into hypoxic zones within the mucus. *P. aeruginosa* adapts to such confines by undergoing a rapid transition from aerobic to anaerobic metabolism, the latter process involving utilization of the alternative electron acceptors, nitrate (NO_3) or nitrite (NO_2), that are present in CF airway mucus. It has been recently shown that nitrate stabilizes the mucoid *P. aeruginosa* form during anaerobic respiration and prevents mucoid-to-nonmucoid conversion under aerobic conditions.

Macro colonies resist secondary defenses, including neutrophils and, to a far lesser extent, macrophages, and many first-tier antibiotics (ceftazidime, tobramycin, ciprofloxacin, etc.), setting the stage for chronic infection. The presence of increased macro colony density and, to a lesser extent, neutrophils, renders the now mucopurulent mass anaerobic. Because of the tendency for CF mucus to become anaerobic, especially during chronic infection, a description of the machinery involved in anaerobic respiration by *P. aeruginosa* and regulation of this process for optimal survival and growth is presented in the following

subsection. Unlike humans, *P. aeruginosa* is capable of luxuriant growth under both aerobic and anaerobic conditions. The latter is either rapid growth via anaerobic respiration, using an inorganic terminal electron acceptor, or very slow growth by substrate level phosphorylation using arginine. Anaerobic respiration requires the presence of NO_3, NO_2, or nitrous oxide (NO) as alternative terminal electron acceptors. The reduction of NO_3 can occur via two routes, through an assimilatory pathway, where NO_3 is reduced to ammonia and subsequently used as a nitrogen source, or by a dissimilatory pathway, where NO_2 is reduced to nitrogen gas for respiration. While assimilation occurs under both aerobic and anaerobic conditions, dissimilatory NO_3 reduction occurs only under anaerobic conditions and involves the sequential reduction of $NO_3 \rightarrow NO_2 \rightarrow$ nitric oxide (NO) $\rightarrow$ nitrogen gas (N_2). Loci important in the first step involving reduction of NO_3 to NO_2 are termed the *nar* (nitrate reduction) genes. Those involved in reduction of NO_2 to NO are termed *nir* (nitrite reductase).
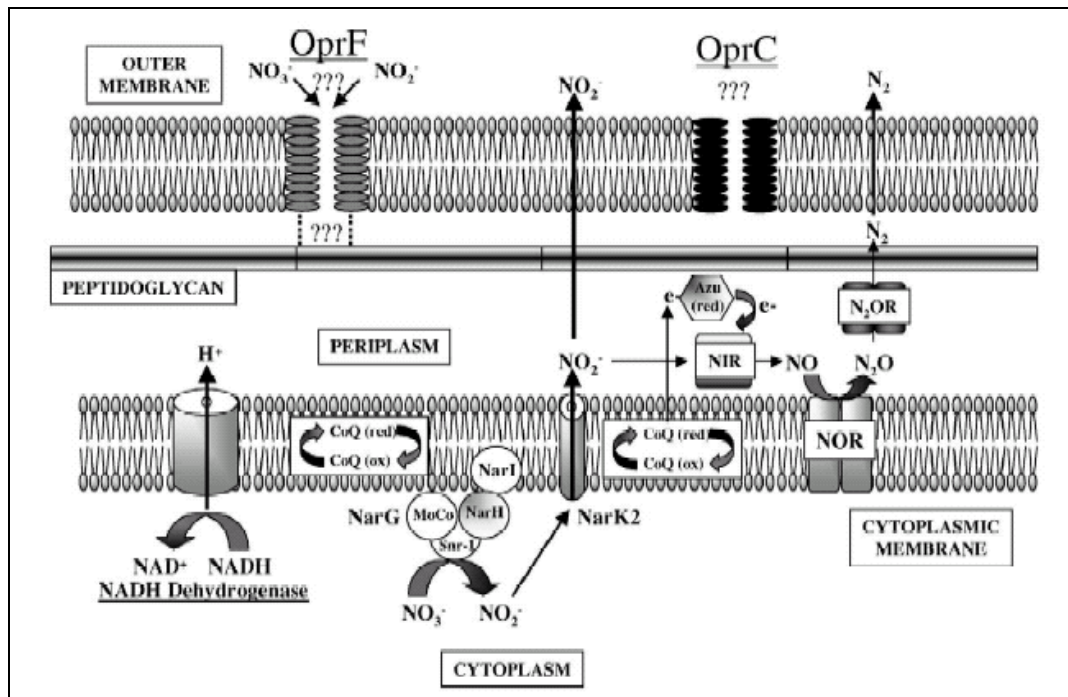
Fig.1.6.1. Model of dissimilatory NO_3 reduction and localization of critical enzymes in *P. aeruginosa*. NAR, NO_3reductase; NIR, NO_2 reductase; NOR, nitric oxide reductase; N OR, nitrous oxide reductase; Azu, azurin blue copper protein; Snr-1, electron donor to NAR; 22 NarK2, NO extrusion protein; MoCo, molybdenum cofactor; NarH and NarI, factors critical for NAR activity. CoQ, coenzmye Q2 (ubiquinone); OprF, outer membrane protein F; OprC, outer membrane protein C (Illustration adopted from Hassett et al., (2002)).

Those involved in removal of NO are termed *nor* (nitric oxide reductase), and finally those involved in removal of NO are termed *nos* (nitrous oxide reductase). Because of the importance of the gene products encoded by the *nar*, *nir*, *nor*, and *nos* loci in respiration

and survival during the denitrification process, it is not surprising that such genes are localized in tightly regulated operons located throughout the genome. A model of how dissimilatory NO_3 reduction works and the cellular localization of enzymes is presented in **figure 1.6.1.**

1.7 Proteomics for analysis of microbial proteomes

The term proteome was first coined to describe the set of proteins encoded by the genome (Wilkins *et al.,* 1996). The study of the proteome, called Proteomics, now evokes not only all the proteins in any given cell, but also the set of all protein isoforms and modifications, the interactions between them, the structural description of proteins and their higher-order complexes, and for that matter almost everything 'post genomic'. In the 1970´s "Proteomics" solely stood for the display of large number of proteins from one organisms on two-dimensional polyacrylamide gels, thereby cataloging the spots to create databases of all expressed proteins (the so-called PROTEOME). During the 1990´s the biological mass spectrometry has emerged as a powerful analytical method, furthermore the complete genome sequences of many organisms got available. Today, "Proteomics" covers the functional analysis of gene products, including large-scale identification, localization and interaction studies of proteins. Proteomics complements other functional genomics approaches, including microarray based expression profiles (Shoemaker *et al.,* 2002) systematic genetics (Tong *et al.,* 2001, Hannon, 2002), systematic phenotypic profiles at the cell and organism level (Giaever *et al.,* 2002, Gerlai, 2002) and small molecule based arrays (Kuruvilla *et al.,* 2002)
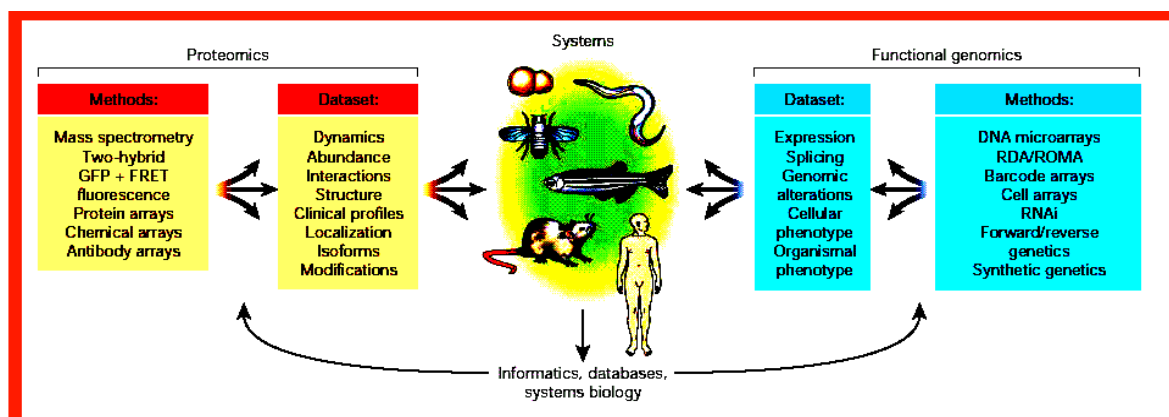
Figure.1.7.1 Schematic representation of the complementing nature of proteomics and functional genomics technologies to the study systems biology. (Illustration adopted from Tyers and Mann, (2003))

Integration of these data sets through bioinformatics will yield a comprehensive database of gene function that will serve as a powerful reference of protein properties and functions, and a useful tool for the individual researcher to both build and test hypotheses. The main reasons for doing proteomics are two folds.

There is no linear relationship between the genome and the proteome of a cell, however proteins are the 'active agents'in cells. Genomics tells us nothing about: post-translational protein modifications, protein isoforms, protein expression levels and the localization of gene products (Görg, 2000). Protein-protein interactions and the molecular composition of cellular structures such as organelles can only be determined at the protein level. The important steps in a typical proteome analysis experiment are explained below briefly.

Sample Preparation

One of the most crucial steps in the 2D-gelelectrophoresis is obtaining and handling the protein sample. The *E. coli* chromosome contains app. 4.000 protein coding genes, but even the best two-dimensional gels can routinely resolve no more than 2.000 proteins. Therefore it is necessary to fractionise cells into organelles, intracellular proteins, membrane proteins or to enrich proteins of interest e.g. by antibody based affinity purification. In addition the multitude of working steps complicates the reproducibility of the method, which makes it essential to optimise and standardize growth conditions and sample preparation.

First Dimension- Isoelectric Focussing

The isoelectric focusing concentrates proteins at their pIs and allows proteins to be separated on the basis of very small charge differences. Under the influence of an electric field a protein moves in a pH gradient until it reaches the position where its net charge = 0 (Isoelectric point). Proteins with a positive net charge will migrate towards the cathode and proteins with a negative net charge will migrate towards the anode. If a protein diffuses away from its pI, it immediately gains charge and migrates back. Today, pre-cast immobilized pH gradient strips (IPG´s) are used because of several advantages: high reproducibility − no drift of the pH gradient, ease in handling, high loading capacity, increase in the useful pH range (different ranges e.g. 3-10, 6-11, 4-7). IEF is performed under strictly denaturing conditions (e.g. 8 M Urea, detergents), which minimizes

aggregation and intermolecular interactions. The use of high voltages (e.g. 8000 V for 3 h) results in a high degree of resolution.

Second Dimension- SDS PAGE

During the second dimension the polypeptides are separated according to their molecular weights. Each spot in the resulting two-dimensional array corresponds to a single protein species in the sample. SDS has to be added for the following reasons: to mask the protein charge by forming an anionic complex with constant net negative charge per mass unit, to disrupt hydrogen bonds, to block hydrophobic interactions and to partially unfold the proteins. Reducing reagents like DTT have to be added for the following reasons: to cleave disulphide bonds between cysteine residues, to completely unfold proteins which results in 'flexible rods' of negative charges with equal charge densities. Today the second dimension is often performed in a vertical electrophoresis system, where no stacking gels are necessary. Normally large gels (for a high resolution) and as many gels as possible per electrophoresis run (for a high reproducibility) are used.

Analysis- Spot identification

2D-gels can be stained by different methods. They include

Autoradiography or phosphor imaging - most sensitive method, but sample must consist of radiolabeled proteins (35S, 14C, 3H or 32P)

Fluorescent staining (e.g. SYPRO Red, Ruthenium Chelate) - rapid, simple and sensitive method, but very expensive dyes and additional equipment

Silver staining - most sensitive non-radioactive method, but time consuming; many variables like reagent, precise timing, and water quality make quantification difficult, not compatible with MS

Coomassie staining - relatively simple and more quantitative method, MS compatible, but 50-fold less sensitive than silver staining.

After the staining procedure patterns containing several hundred spots make image collection hardware and image evaluation necessary. The optical information is first captured with a transmissive scanner (densitometer) and than a software helps to automatically detect the spots, to correct the background, to quantify spot densities and to mach the spots between gels.

Mass spectrometry for protein identification

Mass spectrometry is the cornerstone in Proteomics. Once interesting proteins are selected by differential analysis or other criteria, the proteins can be excised from gels and identified. The ability to precisely determine MW by mass spectrometry and to search databases for peptide mass matches has made high throughput protein identification possible. Peptides are generated by an in-gel digestion of the treated protein spot with enzyme like Trypsin that generates a unique set of peptides for each protein owing to its site-specific cleavage. The peptide mass fingerprinting is usually done with a MALDI-TOF (Matrix Assisted Laser Adsorption/Ionisation Time Of Flight) Mass spectrometry. Proteins that are not identified by MALDI TOF can be identified by sequence tagging or de novo sequencing using Q-TOF (Quadrapole –Time of Flight) Mass Spectrometry, where a single peptide is fragmented and sequenced.

Proteomics approaches have been used to characterize phenotypic changes in *Pseudomonas putida* in response to surface associated growth (Sauer and Camper, 2001). Comparative proteome analysis has been used to compare virulent and avirulent strains of *Brucella melitensis* (Eschenbrenner *et al.,* 2002), antibiotic sensitive and resistant strains of *Staphylococcus aureus* (Cordwell *et al.,* 2002), Mycobacterial strains (Jungblut *et al.,* 1999), to study erythromycin resistance in *Streptococcus pneumoniae* (Cash *et al.,* 1999). Eukaryotic response to *Pseudomonas aeruginosa* quorum sensing signals (AHL) has been investigated using proteomics (Mathesius *et al.,* 2002). Several strategies for analysis of microbial proteomes and data exploitation have been extensively reviewed elsewhere (O'Connor *et al.,* 2000; Washburn and Yates 2000; VanBogelen et al., 1999; Cash, 2000). Cordwell *et al.,* (2001), have extensively reviewed comparative proteomics of bacterial pathogens. A preliminary reference map of the membrane subproteome of *P. aeruginosa* has been generated by gel based proteomic approaches by Nouwens *et al.,* (2000). Proteomics approach has been used for characterizing transitional episodes in *Pseudomonas aeruginosa* biofilm development (Sauer *et al.,* 2002). A detailed account of the application of proteomics to *Pseudomonas aeruginosa* is provided in the reviews by Nowens *et al.,* (2003) and Sherman *et al.,* (2001). The recent completion of the Pseudomonas Genome Project, in conjunction with the Pseudomonas Community Annotation Project (PseudoCAP) has fast-tracked our ability to apply the tools encompassed under the term 'proteomics' to this pathogen. Such global approaches will allow the research community to answer long-standing questions regarding the ability of *P.*

aeruginosa to survive diverse habitats, its high intrinsic resistance to antibiotics and its pathogenic nature towards humans. Proteomics provides an array of tools capable of confirming the expression of Open Reading Frames (ORF), the relative levels of their expression, the environmental conditions required for this expression and the sub-cellular location of the encoded gene-products. Since proteins are important cellular effectors, the biological questions we pose can be defined in terms of changes in protein expression detectable by separation to purity using two-dimensional gel electrophoresis (2-DGE) and relation to gene sequences via mass spectrometry. As such, we can compare strains with well-characterized phenotypic differences, growth under a variety of stresses, protein interactions and complexes and aid in defining proteins of unknown function. More focused approaches that target sub-cellular fractions ('sub-proteomes') prior to 2-DGE can provide further functional information.

Tandem mass spectrometry (MS) has provided proteomics initiatives with highly selective methods for characterizing the dynamic state of protein mixtures responsible for biological function and specificity (Licklider, 2002). The throughput and sensitivity limits of MS-based methods for peptide sequence analyses are tested by comprehensively identifying and characterizing relevant proteins from crude cellular mixtures, thereby setting demanding requirements upon the initial stages of purification and separation. Progress toward meeting these requirements has been maintained by combining relatively large-volume methods developed to selectively isolate or resolve protein and peptide mixtures with low-volume capillary liquid chromatography methods performed on-line with automated MS/MS analyses for maximum sensitivity. Often, excised gel bands from SDS-PAGE are converted to proteolytic mixtures prior to sequence analysis by LC-MS/ MS techniques. Peptide sequence information (MS/MS spectra) is acquired with a high degree of automation via data-dependent software, which provides the ability to sequence five or more peptides independently following a single MS precursor scan to identify peptide parent ions. This highly sophisticated data dependent analysis can provide as many as 60 MS/MS acquisitions per minute for high throughput in mixture analyses where thousands of MS/MS identifications are needed. Matching uninterrupted "raw" MS/MS spectra against protein and EST databases using Sequest or other database search algorithms is a rapid means to unambiguously identify peptide and protein sequences as well as many structural modifications to proteins. However, achieving fully automated analyses is a

challenging endeavor for nanoscale LC-MS/MS, which uses capillary columns of <100μm i.d. that permit flow rates of 150 nL min^{-1}.

1.8 Real Time Polymerase Chain Reaction

Previously, gene quantification has been hindered by the lack of a fast, reliable and accurate method (Freeman *et al.,* 1999). The traditional methods of gene expression quantification like Northern blotting, S1/RNase nuclease protection assay and in situ hybridization often work well but generally require large amount of RNA. The development of PCR and, in particular, reverse transcriptase PCR (RT-PCR) has made gene quantification easier, only a small amount of RNA being required and a large number of samples being analysable in one experiment (Tan and Weis 1992). The subsequent development of real-time PCR has greatly improved quantitative PCR and has several advantages over endpoint quantification. In real-time PCR, the quantification is based on the cycle number at which the PCR product is clearly detected rather than on the amount of PCR product accumulated after a fixed number of cycles. When there is a high starting copy number of the target present in the sample, fewer cycles are required for the production of a signal, and when the target copies are low, more cycles are required. In real-time PCR, accumulation of the product is monitored cycle by cycle.

Figure 1.8.1 LightCycler (real time PCR equipment from Roche) used for the present study. (Illustration adopted from Lightcycler user manual, Roche).

The LightCycler^{TM} (refer **figure1.8.1**) is a real-time PCR machine that allows both rapid PCR cycling and continuous monitoring of product formation (Wittwer *et al.*, 1997). SYBR Green I, an intercalating dye that fluoresces strongly when bound to double stranded DNA (dsDNA), is included in the reactions so that when PCR products are formed, an increase in fluorescence occurs (Ririe *et al.,* 1997). For quantitative PCR, standards of known concentration are included in each run. A standard curve of cycle

number vs. copy number is plotted; samples of unknown concentration are compared with this curve and their concentrations are calculated (Wittwer *et al.,* 1997). The LightCycler instrument basically consists of two different components: a cycler component and a fluorimeter component. These components work together to simplify such complex applications as product analysis, quantification, and mutation analysis. The cycler component has been optimized for rapid PCR applications. Unlike conventional PCR, in which cycling programs take several hours, PCR analyses conducted with the LightCycler take only 20–30 min. Data obtained from fluorimetric analysis can be displayed and directly evaluated with the special LightCycler software. Hence, no additional tedious and time consuming procedures (e.g., agarose gel or Southern blotting analyses) are required to analyze the PCR product. Direct, uncomplicated analysis of results also reduces the number of sample handling steps, thus minimizing the risk of sample contamination. **Figure 1.8.2** shows the comparison of the data output from a conventional PCR and real time PCR.
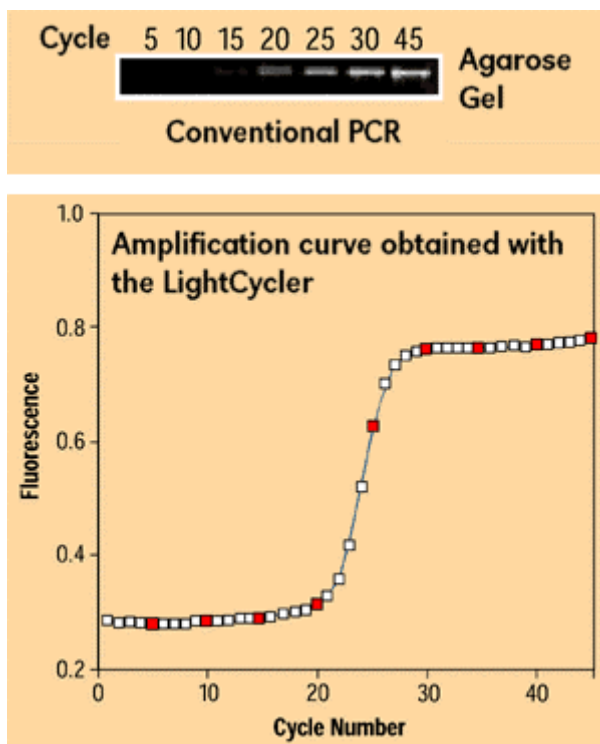
Figure 1.8.2 Comparison of data output from conventional PCR and real time PCR using Lightcycler . (Illustration adopted from Lightcycler user manual, Roche).

One of the greatest advantages the LightCycler instrument offers in comparison to conventional thermal cyclers is that the formation of amplification products can be monitored in real-time. SYBR Green I is a dye that binds specifically to double stranded DNA. Its inherent fluorescence is enhanced when it binds to the minor groove of double-stranded DNA. During PCR, SYBR Green I binds to DNA products as they are synthesized. Thus, the increase in SYBR Green I fluorescence, when measured at the end

21

of each elongation cycle, indicates the amount of PCR product formed during that cycle. To increase the specificity and sensitivity of SYBR Green I detection, a melting curve analysis is performed on the amplification reaction. Together with a melting curve analysis, the SYBR Green I format provides an excellent tool for specific product identification and quantification. Dye staining can detect from approx. 1 to 10^9 copies of a target sequence. Resolution of this amplification-detection method is limited at very low concentrations of template. The LightCycler measures the fluorimetric intensity of SYBR Green I at the end of each elongation phase. The maximum excitation of SYBR Green I dye occurs at 497nm. Maximal emission of DNA stained with SYBR Green I occurs at 521 nm. SYBR Green I is stable at temperatures and pHs that occur during rapid thermal cycling. SYBR Green I is significantly less mutagenic than ethidium bromide.

1.9 Small Colony Variants of *Pseudomonas aeruginosa* – State of the Art

Pseudomonas aeruginosa occur in diverse ecological niches of natural environments as well as in infections of humans, animals and plants. This ubiquitous distribution of *P.aeruginosa* indicates a remarkable degree of physiological and genetic versatility. However there seem to be no genetic or functional differences between environmental and clinical strains (Foght *et al.,* 1996; Romling *et al.,* 1994). The opportunistic pathogen *P. aeruginosa* being a key etiological agent of hospital-acquired infections in the immunocompromised host, is also responsible for chronic lung infection in cystic fibrosis (CF) patients (Gilligan, 1991; Lyczak *et al.,* 2002; Govan and Deretic, 1996; Breitenstein *et al.,* 1997).

| A | B | C |
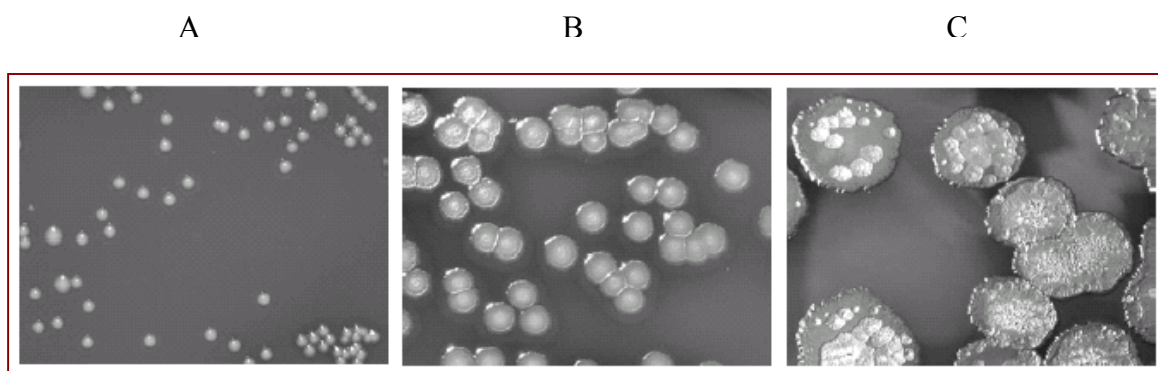
Figure 1.9.1. Morphotypes of strain 20265 grown on Columbia blood agar plates.   Small colony variant -*in vivo* isolated (A), Wildtype -*in vivo* isolated (B), Revertant -*in vitro generated* (C). (Illustration adopted from Haussler et al., (2003))

Despite the fact that chronically infected CF patients harbor only one or few *P. aeruginosa* genotypes (Breitenstein *et al.,* 1997), there is significant phenotypic variation in *P. aeruginosa* isolates from the CF lung, known as 'dissociative' behavior (Zierdt and Schmidt, 1964). The chronically infected CF lung is thought to provide a habitat where *P. aeruginosa* in high cell densities faces a multiplicity of environmental challenges that lead to morphological diversification and the establishment of niche specialists (Oliver *et al.,* 2000). Apart from the best-studied mucoid *P. aeruginosa* phenotype and other colony morphotypes (Govan and Deretic,1996), it has been recognized for many years that dwarf colonies can be isolated from the chronically infected respiratory tract of CF patients (Zierdt and Schmidt, 1964).

Although studies have so far been focused on the most common mucoid phenotype, other phenotypic variants do exist in the chronically infected CF lung, e.g. so-called SCVs, comprising phenotypic variants characterized by slow growth on agar plates and increased antibiotic resistance against a broad range of antipseudomonal agents (Haussler *et al.,* 1999). These dwarf or so-called small-colony variants (SCVs) of *P. aeruginosa* (refer **Figure 1.9.1**) isolated in our laboratory and their recovery of could be correlated with parameters revealing poor lung function and the use of inhaled antibiotics (Haussler *et al.,* 1999). Small colony variants (SCVs), slow growing subpopulations of bacterial pathogens have gained attention in the recent years. *Staphylococcus aureus* SCVs have been found to be associated with persistent and relapsing infections (von. Eiff *et al.,* 2000), increased drug resistance (Schmitz *et al.,* 2001) and altered biochemical profile. There is an increasing body of evidence about their role in exacerbation and persistence of infections.

The recovery of SCVs has a strong correlation with poor lung function and antipseudomonal aerosol therapy. The *P. aeruginosa* SCVs show increased resistance to a broad range of antipseudomonas drugs (Haussler *et. al.,* 1999) apart from the typical SCV traits like small colonial morphology and slow growth as compared to their wildtype counterparts. Another very distinctive feature of *P. aeruginosa* SCVs isolated was their reversion into fast growing phenotypes (revertants) with regained susceptibility patterns after several in vitro passages in antibiotic free medium. Also the SCVs and their revertants did not show any auxotrophy for haemin, menadione or amino acids. Whether the SCVs of *P. aeruginosa* are specially adapted for a hostile environment of the host lung needs to be investigated.

Recently, Deziel *et al.,* (2001) isolated a hyperpiliated and highly adherent small phenotypic variant from a biofilm of *P. aeruginosa* strain 57RP in vitro. It was suggested that the occurrence of this variant within the ecological niche of the biofilm was regulated by a phase-variation mechanism. Similarly, a phase-variation mechanism has been proposed to be the cause of the phenotypic switch of an antibiotic resistant and autoaggregative rough SCV of *P. aeruginosa* strain PA14 to wild-type revertants (Drenkard and Ausubel, 2002).

Haussler *et al.,* (2003) identified a subgroup of hyperpiliated *P. aeruginosa* SCVs isolated from the respiratory tract of CF patients that exhibited similar phenotypic characteristics such as autoaggregative growth behavior in liquid cultures and increased biofilm formation capacity. It was proposed that apart from the antibiotic selection pressure, which might favor the occurrence of SCVs, the diversity of our *P. aeruginosa* morphotypes could be due to adaptive mutations and selection, as had been described for the morphological diversity of *P. fluorescens* phenotypic variants in the heterogeneous environment of a static broth (Rainey and Travisano, 1998).

Wehmhöner *et al.,* (2003) reported that proteome analysis of several clinical *P. aeruginosa* strains including the strain 20265 used in this study, revealed almost identical patterns for the cellular extracts, whereas interclonal diversity and intraclonal diversity were manifested in the secretomes of cultured *P. aeruginosa*. The diversity was even greater for the immunogenic protein patterns expressed in vivo. Proteome analysis of the *P. aeruginosa* morphotypes SCV, revertant and wild type in our laboratory has revealed the differential expression of haemophore HasAp (a haem acquisition protein) among these morphotypes. SCVs express abundant HasAp from an early log phase of growth as compared to the wild type.

von Götz (2003) has carried out an extensive transcriptome analysis of the morphotypes of strain 20265 using DNA microarrays. Overall 309 differentially regulated genes were reported during log and stationary growth phases of growth. As a prominent pathogenicity factor of *P. aeruginosa* the type III protein secretion system and the corresponding effector proteins were found to be upregulated in SCV 20265. The gene expression profiles seemed

to indicate that SCV 20265 was arrested in a physiological state reflecting its adaptation to an anaerobic environment, antibiotic pressure and a biofilm mode of growth.

Till now the molecular causes of the SCV phenotype among the clinical SCVs remains unknown. Even though lots of general functional genomics and proteomics data exist about the clinical SCVs used in this study, very little information on their pathogenic aspects and their specific adaptation to key stress conditions like iron limitation, oxidative stress and anaerobic stress exist. The present study aims to contribute some useful information in this context so as to enable a better understanding of the SCV phenotype, its molecular causes and role in pathogenicity.

1.10 Objectives of the present study

The major objectives of this study were as follows

- To determine if there is any survival or growth advantage for SCV 20265 (a representative of the subgroup of autoaggregative hyperpiliated, cytotoxic SCVs) compared to its clonal wildtype WT 20265 under severe iron limiting conditions, oxidative stress conditions and anaerobic/microaerobic growth conditions.

- To compare the proteome profile of these morphotypes under conditions where they show a differential growth response to iron limitation, oxidative stress and anaerobic stress.

- To look for differentially expressed membrane proteins and supernatant proteins using a subproteomic approach.

- To screen morphotypes of other member strains of the subgroup of hyperpiliated autoaggregative SCVs to assess the distribution of abilities to survive harsh stress conditions.

- To obtain clues about, which selection pressures could be operating in the CF lungs to promote the occurrence of small colony variants.

2. Materials and Methods

2.1 Chemicals and Materials

2.1.1 Chemicals, Reagents and Enzymes

Enzo BioArray Terminal Labeling Kit, Oligonucleotide B2, *P.aeruginosa* GeneChip	Affymetrix
SUPERaseIn (RNase Inhibitor)	Ambion
Immobiline-solution, IPG buffer, IEF (Acrylamide-Bisacrylamide Solution, T = 4%), Deoxynucleotides, Hybond N+ nylon membrane, OnePhorAll-buffer, RNase-free DNase l	Amersham Pharmacia Biotech (Freiburg)
Urea, Thiourea	Baker (Phillipsburg, USA)
DTT; CHAPS; Leupeptin; Pefablock	Biomol (Hamburg)
SeaKem GTG Agarose	Biozym
α-Cyano-4-hydoxy-Cinnamic acid	Bruker Daltonik (Bremen)
Agar, Bacto-Peptone	Difco
Acrylamido Buffer, Tributylphosphine	Fluka (Deisenhofen)
Agarose	Gibco BRL
Bromophenol blue, Bovine serum albumin, MOPS buffer, Random Primers, RNA-standard, Serva Blau G-250, SuperScript II Reverse Transcriptase, Xylene cyanol FF	Invitrogen
Formaldehyde (35%), H_2O_2 (30%) Iodoacetamide, Benzonase (Endonuclease)	Merck (Darmstadt)
Streptavidine-Phycoerythrine, SYBRGreen	Molecular Probes
Sypro ruby Protein Gel Stain	Molecular Probes (Leiden, Netherlands)
Oligodeoxynucleotides, Primers	MWG-Biotech
DNA-ladder standards	New England Biolabs
Streptavidine	Pierce Chemical
RNase Inhibitor, Trypsin (porcine, sequencing grade modified)	Promega
Plasmid Spin Kit, Qia- Mini Prep plasmid kit, QIAquick Gel Extraction Kit, RNeasy Kit,	Qiagen
Lumi Light Chemiluminiscene Substrate	Roche Diagnostics (Mannheim)
RBS 30 (Washing Solution); Rotipherese Gel 30 (Acrylamide / Bis-acrylamide solution, T=40%); SDS; Siliconol M 100, Ethidium bromide, Phenol (Rotiphenol)	Roth (Karlsruhe)
Coomassie Brilliant Blue G-250; Coomassie Brilliant Blue R-250	Serva (Heidelberg)
ASB 14; BSA (Fraction V), Paraquat, Tween 20, H_2SO_4	Sigma (Deisenhofen)
Carrier Ampholyte (Sinulyte)	Sinus (Heidelberg)
Biotin anti-Streptavidine	Vector Laboratories

2.1.2 Equipments and other materials

CCD camera LAS-1000 and intelligent Dark Box	Fujifilm (Raytest)
Electrophoresis Power supply EPS600/EPS 3500 XL	Amersham Pharmacia Biotech (Freiburg)
Flat bed Scanner Powerlook III	Umax Systems (Willich)
Gel Dryer Easy Breeze	Hoefer (Amersham Pharmacia Biotech)
IPGphor Focussing System	Amersham Pharmacia Biotech (Freiburg)
Iso-Dalt Electrophoresis System	Hoefer (Amersham Pharmacia Biotech)
MALDI TOF MS Bruker Ultraflex	Bruker Daltonik (Bremen)
MilliQ water purification system	Millipore (Eschborne)
Optima TLX ultracentrifuge	Beckmann (Gladenbach)
Photometer Spectronic 20 Genesys	Spectronic Instruments (Leeds, Great Britain)
Quadropole – MS QTOF II	Micromass (United Kingdom)
Spectramax 250 Microtiter Photometer	MWG Biotech (Ebersberg)
Trans-Blot SD Semi Dry transfer Cell	Bio-Rad (Munich)
Balance BP3100S and BP210 S	Sartorius
Centrifuge	Hettich Universal
Eppendorf centrifuge 5415C	Eppendorf
Eppendorf centrifuge 5417R	Eppendorf
pH meter 766 Calimatic	Knick
Spectrophotometer U3000	Hitachi
Thermocycler	Landgraf
Thermomixer	Eppendorf
UV- Transilluminator	Bachofer
UV Stratalinker 1800	Stratagene
Vacuum concentrator	Bachofer
Voltage supply power pack 300	Bio-Rad

Biomax Light Film	Kodak (Stuttgart)
Cellophane Sheets 33X38 cm	Amersham Pharmacia Biotech (Freiburg)
Chelex 100 Biotechnology grade	Bio-Rad (Munich)
GelBond-PAG-Film (FMC Bioproducts)	Hoefer (Amersham Pharmacia Biotech)
Immobiline DryStrips	Amersham Pharmacia Biotech (Freiburg)
Molecular weight standard; MW 14.4–94 Kda	Amersham Pharmacia Biotech (Freiburg)
PVDF membrane (Roti-PVDF)	Roth (Karlsruhe)
ReadyStrip IPG Strips	Bio-Rad (Munich)
SERDOLIT MB-1 Ion exchanger	Serva (Heidelberg)
ZipTip$_{c18}$, ZipTip$_{\mu c18}$	Millipore (Eschborn)
Anaerobic chamber Anerocult	Merck
Eppendorf tubes (0.5 ml, 1.5 ml, 2 ml)	Sarstedt
Filter paper GB003	Schleicher and Schuell
Pasteurpipette	Sarstedt
Petri plates 9 cm Ø	Sarstedt
Pipette tips (1 ml, 200 µl, 10 µl)	Sarstedt
Plastic tubes (50 ml, 15 ml)	Greiner
Polaroid film 667	Polaroid
X-ray film Kodak	AGFA

2.1.3 Computer Programmes and Databanks

AIDA advanced image data analyser 2.1	Raytest isotope measuring GmBH (Straubenhardt)
Brucker Data Analysis for TOF 1.6g	Brucker Daltonik (Bremen)
Mascot	Matrix Science Ltd.
Image reader LAS-1000	Fujifilm
Knexus/MS	Proteometrics (Winnipeg, Mannitoba, Canada)
SOFTmax Pro	Molecular Devices (Munich)
Sonar	ProteoMetrics
Jellyfish version 2.1	LabVelocity
ProteomeWeaver	Definiens Imaging GmbH
Microarray Suite	Affymetrix (USA)
Microsoft Access, Excel	Microsoft (USA)

Gene and Protein sequences Annotation data- Databank of the *Pseudomonas aeruginosa* Genome project	http://www.pseudomonas.com
P.aeruginosa genome databank of the Entrez NCBI	http://www.ncbi.nlm.nih.gov/database/index.html
NCBI *P.aeruginosa* complete genome	http://www.ncbi.nlm.nih.gov/cgi-bin/Entrez/framik?db=Genome&gi=163
''SWISS-PROT' (Protein Knowledgebase)''and ''TrEMBL (Computer annotated supplement to SWISS-PROT) ''	http://us.expasy.org/sprot/

2.1.4 Media and Solutions

Vogel Bonner (VB) medium VOGE56

Amount/liter   Component   Final concentration

0.813 g	Magnesium Sulphate ($MgSO_4$)	3.3 mM
2.378 g	Citric acid	10 mM
5.802 g	Sodium ammonium. Hydrogen Phosphate ($NaNH_4PO_2$)	28 mM
8.543 g	Di-pottassium Hydrogen Phosphate(K_2HPO_4)	37 mM
50.13 g	Gluconic acid (Sodium salt)	

Volume made up to 1 liter with double distilled water and pH adjusted to 7.2.

VB Agar
VB medium was solidified by adding 15 g/l agar and autoclaved.

Luria Broth (LB)
Peptone 15 g/l
Yeast Extract 5 g/l
NaCl (10 g/l) 0.17 M

LB Agar
LB medium was solidified by adding 15 g/l agar and autoclaved.

PBS (10X)
NaCl (80 g/l) 1.37 M
KCl (2 g/l) 27 mM
Na_2HPO_4 $7H_2O$ (11.5 g/l) 4.3 mM
KH_2PO_4 (2 g/l) 1.4 mM
pH 7.3

Solutions for DNA work

TBE-Buffer (10X):
Tris (108 g/l) 0.9 M
Boric Acid (55 g/l) 0.9 M
EDTA (7.7 g/l) 0.02 M
pH 8.3-8.5

Loading Buffer (6X):
Ficoll 400 15% (v/v)
Bromophenol Blue 0.25% (w/v)
Xylene cyanol 0.25% (w/v)
EDTA (146 g/l) 0.5 M
pH 8.0

TB Buffer:
PIPES (3 g/l) 10 mM
$CaCl_2$ (1.6 g/l) 15 mM
KCl (18.6 g/l) 250 mM
pH adjusted to 6.7 with KOH, then $MnCl_2$ (50mM-9.58 g/l)
was added, sterilized by filtration and stored at 4°C.

TE Buffer:
Tris-HCl (1.2 g/l) 10 mM
EDTA (0.38 g/l) 1 mM
pH 8.0

Solutions for RNA work

RNA Lysis buffer:
SDS 2 % (w/v)
Sodium acetate 3 mM
EDTA 0.1 % (w/v)
pH 5.5

DNase buffer (10 x):
Sodium acetate 500 mM
$MgCl_2$ $6H_2O$ (20.3 g/l) 100 mM
$CaCl_2$ $2H_2O$ (2.94 g/l) 20 mM
pH 6.5

MOPS buffer (10 x):
MOPS (41.8 g/l) 200 mM
Sodium acetate 100 mM
EDTA (2.9 g/l) 10 mM
pH 7.0

RNA loading buffer:
Glycerol 50 % (v/v)
EDTA (0.29 g/l) 1 mM
Bromophenol blue 0.25% (w/v)
pH 6.0

cDNA Reaction mixture:
1st Strand buffer 5X
DTT 10 mM
dNTPs 0.5 mM
SUPERaseIn 0.5 U/µl
SuperScript II 25 U/µl

2.2 Strains and Culture conditions

2.2.1 Bacterial strains – propagation and maintenance

SCV 20265 and wildtype 20265 isolated from the same CF patient and maintained in our laboratory collection were used for investigation. Also used, were CF isolates Strains 10, 29, 52, 8226 and 231 with respective SCV, revertant and wildtype morphotypes. Stable revertants were generated by repeated culture passage in antibiotic free medium. PAO1**,** a wound isolate, genetic reference strain (Holloway *et al.*, 1994), was also used. TB, a CF strain capable of intracellular survival was also used (Tummler, 1987). For long-term storage the strains were stored as glycerol stocks at − 80 ºC. All bacterial cultures were maintained in LB medium containing 15 % glycerol (v/v) and stored at − 80 °C. For strain propagation, the glycerol stock was streaked on to Columbia Blood agar (sheep blood 5 %) plates to allow effective visual comparison of colony morphology. All plates, eppendorfs and flasks were incubated at 37 ºC.

2.2.2 Depletion of iron from the medium

All glasswares including media storage bottles and funnels were stripped of any traces of iron contamination by treating with 2 M HCl and rinsed clean with double distilled water. Sterile plastic pipettes were used. All the culture experiments were done with plastic tubes so as to avoid free iron contamination. Iron depletion was achieved by treating VB medium, with iron chelating resin Chelex 100 (BIORAD) at 5 g per 100 ml concentration followed by moderate stirring at 4 ºC for 16 hr or longer. The chelex 100 resin was filtered out by using a filter paper and 2,2-Dipyridyl (SIGMA) added to the filtrate to a final concentration of 11 mM or any other specific concentration depending on the experimental needs. The iron-depleted medium was autoclaved before use.

2.2.3 Iron supplementation disc assay

Vogel Bonner (VB) medium was prepared freshly and 2,2-Dipyridyl was added to obtain a final concentration of 1.1 mM. High grade Difco bacto agar was added to 1.5% (w/v) and media autoclaved to pour plates. Iron depleted top agar was prepared containing 0.6 % agar. The following iron sources' stock solutions were freshly prepared: 0.2 M ferrous sulphate (FeSO$_4$), 0.1 M ferric citrate, 10^{-4} M haemoglobin, 10^{-2} M haemin chloride. Bacteria from freshly grown plates were washed vigorously with 0.9% NaCl and 100 μl containing approximately 2 - 5 X 10^{-7} bacteria were suspended in 3 ml of iron depleted top agar, mixed well and spread as a lawn on the iron depleted VB plates. Sterile filter paper discs were placed on dry plates and 8 μl of the iron source was spotted. After a brief period of drying, the plates were incubated at 37 °C for 48 hours. All stock solutions were prepared freshly before use. A 10^{-4}M haemoglobin stock solution was prepared freshly before use by dissolving haemoglobin in suitable quantity of sterile iron depleted medium. 0.2 M ferrous sulphate (FeSO$_4$), stock solution was prepared freshly before use to prevent precipitation of iron as insoluble ferric hydroxide. Ferric chloride (FeCl$_3$) and ferric citrate solutions were also prepared in the same way. All iron salt solutions were filter sterilized and not autoclaved. Haemin chloride stock solution was prepared by dissolving haemin chloride in the presence of NaOH. 10^{-2} M stock solution was prepared and stored at – 20 ºC.

2.2.4 Hydrogen Peroxide (H₂O₂) sensitivity assay

Disc Sensitivity assay

Fresh Luria (L) broth (10.0 g tryptone, 5.0 g yeast extract, 5.0 g NaCl (per liter; pH 7.2)) was prepared and used for making L -agar plates and L- soft agar. For L-agar plates, media was solidified using 1.5 % Bacto Agar and L-soft agar was prepared with 0.6% bacto agar. All morphotypes were grown aerobically at 37 °C in a shaker up to late stationary phase in VB medium. After 48 hr (stationary phase) and 72 hr (late stationary phase) 100 µl of bacteria was removed and diluted in 3 ml of L-soft agar and spread as a lawn over L-agar plates. Sterile filter paper discs were placed on the agar overlay and 8 µl of 30 % H₂O₂ was spotted on the discs. The plates were incubated for 24 hours at 37°C and the diameter of zone of growth inhibition around the discs was measured.

Broth Sensitivity Survival percentage assay

Bacteria were grown aerobically in VB medium until log phase (OD 600 = 0.8) or stationary phase (OD600=2.5) at 37 °C in 20 ml volume in 150 ml culture flasks. Organisms were diluted 1:10 in 3 ml of prewarmed VB medium and incubated with increasing concentrations of H₂O₂ (Merck) for 15 min. The suspensions were serially diluted in 0.9 % saline containing 10 mg of bovine liver catalase (Sigma) per ml, and aliquots were plated on LB agar. CFU were enumerated after incubation at 37°C for 24 to 48 hr. The percentage viability was calculated by comparing the CFU before and after exposure to H₂O₂.

2.2.5 Paraquat and H₂O₂ treatment for Proteome analysis

For proteome analysis of effects of paraquat and H₂O₂ on the morphotypes, SCV and WT 20265 were grown aerobically in 200 ml volume of VB medium in 2 liter culture flasks until stationary phase (OD₆₀₀ 2.0) and cells were harvested quickly by centrifugation .The harvested cells were packed into sterile dialysis bags and suspended in 300 ml fresh VB medium containing 0.03 % H₂O₂. For paraquat treatment, harvested cells were directly resuspended in fresh VB medium of 200 ml volume containing 0.5 mM paraquat (methyl viologen).The bacteria were incubated for 2 hr along with controls that were paralelly grown synchronous cultures treated the same way except for the fact that they lacked any redox agents–H₂O₂ or paraquat. At the end of the incubation the cells were harvested immediately and washed once in 0.9 % NaCl containing bovine liver catalase (Sigma) (10 units /ml) followed by a wash once in normal 0.9 % NaCl. The cells were quickly spun down and frozen for sample preparation for 2D gel analysis.

2.2.6 Anaerobic growth of *Pseudomonas aeruginosa*

Vogel Bonner (VB) medium was prepared freshly containing Potassium Nitrate (KNO_3) supplement at a final concentration of 1 %. Nitrogen gas was bubbled for atleast 1 hr and the container closed immediately. The medium was filter sterilized using Millipore filter (0.22 µ) and always filled the medium into any container to the maximum level possible so as to expel any air in the container 14ml of the medium was quickly aliquoted into 15 ml falcon tubes. Approximately 1×10^8 bacteria were inoculated. The tubes were deposited in the anaerocult (MERCK) or Anerogen (OXOID) anaerobic growth chamber with appropriate oxygen depleting anaerobic pack and indicator strips to monitor anaerobic environment. A negative control having VB medium without KNO_3 was included. The growth in this tube under anaerobic condition is negligible.

2.3 Proteomics

2.3.1 Sample preparation

2.3.1.1 Extraction of cellular proteins

The bacterial culture was centrifuged to pellet the bacterial cells by spinning at 4000 rpm for 5 min in a 50 ml falcon tube. Larger volume cultures were prespun to concentrate the cells to a volume less than 50 ml and subsequently transferred to the 50 ml falcon tube. The pelleted cells were washed 2 times with cold 0.9 % NaCl by spinning quickly at 4500 rpm for 5 min. The pellet was resuspended in an appropriate quantity (usually between 1 - 2 ml) of pre IEF buffer (4 % CHAPS, Protease inhibitor tablet Complete (Roche)) depending on the pellet size. The samples were placed in an ice beaker. The samples were subjected to ultra-sonication with the following sonication parameters: output control 50; duty cycle 5; 3 X for 50 s each. The contaminating polysaccharides and nucleic acids, which are undesirable for a clean IEF were removed by a phenol extraction and purification as described below. Since sonication of the bacterial cells was not satisfactory in the pre IEF buffer having only CHAPS, the heating of the cells in the presence of phenol at 72 °C followed by brief chilling on ice was carried out to lyse the cells completely to release all nucleic acids. 1 ml of the sonicated cells was taken in a 2 ml eppendorf and 1 ml of Tris saturated phenol was added on top and vortexed briefly to mix the contents. The tube was heated to 72 °C for 10 min with simultaneous vortexing on a thermomixer (Eppendorf). The tube was briefly chilled on ice for 3 min followed by centrifugation at 13000 rpm for 10 min at 4 °C. The viscous aqueous phase containing the nucleic acids was removed by pipetting without disturbing the white protein layer at the aqueous: phenol interface and replaced by 1 ml milliQ water and the heating, cooling,

centrifugation steps were repeated again. The nucleic acids were removed by pipetting out the aqueous phase and replaced by 1 ml of milliQ water. The above steps were repeated once more to completely get rid of the nucleic acids along with the aqueous phase.

The proteins were finally precipitated by addition of 1 ml of ice-cold acetone at – 20 °C. After addition of acetone, the tube was briefly inverted few times to mix the contents and incubated in – 20 °C from 1hr to overnight. At the end of the incubation, the tube was centrifuged at 13000 rpm, 4 °C for 15 min to pellet out all the protein. The supernatant containing phenol and acetone was discarded and the pellet air-dried to expel all the acetone. To enhance the purity of the protein powder, it was resuspended in ice-cold acetone and washed by brief vortexing and resuspension followed by centrifugation. This was repeated twice and finally a dried ready-to-use protein powder was obtained by air-drying. This powder was resuspended in about 1 ml of sample solubilization buffer (IEF sample buffer). Unsolubilized debris was removed by ultra centrifugation for 45 min at 50000 rpm at 15 °C. (Low or High temperatures are not good for the urea component of the solubilization buffer). The clear supernatant having the soluble proteins was collected and stored at – 20 °C or – 70 °C until use or immediately used. The concentration of the protein solution was estimated by Bradford Assay.

2.3.1.2 Extraction of Supernatant Proteins

For the preparation of secreted proteins in the culture supernatant, following centrifugation of the cultures (6000 x g, 15 min, 4°C) and passage of the supernatant through a 0.2 μm filter, deoxycholic acid (sodium salt) was added to a final concentration of 0.2 mg/ml [stock-solution: 100 mg/ml, 1:500 dilution]. After 30 min incubation on ice the proteins were precipitated by addition of trichloroacetic acid to 6 % [wt/vol] [stock-solution 30 %, 1:5 dilution] and incubation at 4 °C for 2 hr [or over night]. Following centrifugation at 18,000 g for 30 min the precipitated proteins were resuspended in a small amount of water and 8 volumes acetone (- 20 °C) were added [for example: 5 ml water + 40 ml acetone]. After incubation at – 20 °C for 2 hr followed by centrifugation at 3500 g for 20 min at 4 °C, the pellet was allowed to dry for 5 min and dissolved in an appropriate amount of solubilization buffer. Following centrifugation at 50,000 g for 40 min at 15 °C the protein concentration of the supernatant was determined. Protein extracts were either used immediately for 2D gel electrophoresis or stored at – 70 °C.

2.3.1.3 Sample Solubilization Buffer / IEF sample buffer

Every 100 ml of the IEF sample buffer contained 15 g Thiourea, 4 g CHAPS, 20 mg Tris (170 µl of 1M Tris at preferably alkaline pH), 460 mg DTT, 100 µl Leupeptin (from 1 mg / ml stock), 1 ml Pefablock (from 100 mM stock), 500 µl Pharmalyte 3 – 10 pH. All the above ingredients were dissolved one after another in 9 M Urea solution to make up the final volume to 100 ml. For preparing 100 ml Urea solution 54 g ultrapure Urea was weighed and dissolved in 100 ml MilliQ water to obtain 9 M Urea solution. This urea solution was treated with serdolit and filtered pure with whatmann filterpaper before using it to dissolve the other components of the buffer. This step was essential to deionize Urea in order to free the sample buffer of charged ions, which might interfere in the IEF. Urea and Thiourea took longer time to dissolve and were never heated to temperature above 37 °C. IEF sample buffer was aliquoted into small vials and frozen. Thawed IEF sample buffer was used only once and instantly.

2.3.2 Protein estimation by Bradford Assay

Spectramax 250 microtiter photometer was used in combination with a SOFTMax PRO software to obtain protein concentrations. Bradford assay was performed on 96 well microtiter plates using 10 µl/well of the sample (or its dilution) whose protein concentration is to be determined. 200 µl of 1:5 diluted commercially available Bradford reagent (BIORAD) was dispensed into each well and mixed well with the 10 µl of the unknown sample or the BSA standards of known concentrations (1.0 mg, 0.8 mg, 0.6 mg, 0.4 mg, 0.2 mg, 0.1 mg) used for generating a standard curve. The software generates a table of results with concentration expressed in µg/ml. Using this, the total amount of protein can be estimated.

To measure growth of the bacteria as function of amount of protein, sample pellets were collected in 2 ml eppendorf tubes or any tube of convenient volume. Bacterial pellet was vacuum dried to remove all traces of liquid. The pellet was resuspended in 100 µl of phosphate buffer followed by addition of 50 µl of 2 N NaOH. The tubes were vigorously vortexed followed by a brief centrifugation to concentrate all the liquid to the bottom. The tubes were boiled for 3-5 minutes to solubilise all the proteins before cooling on ice for 5 min. 50 µl of 2.2 N HCl was added to neutralize pH and the volume adjusted to a common value in all the tubes to be analysed. This preparation was used for protein estimation was by Bradford assay on a 96 well microtiter plate format as described above.

2.3.3 I dimension - Isoelectric Focussing (IEF)

The samples to be isoelectric focussed were aliquoted into eppendorf tubes as per the following guidelines depending on the type of detection method to be used to view the proteins after second dimension SDS PAGE and the pH range of the IPG strips to be used.

18 cm IPG strip

pH gradient	Amount of protein	Staining
3-10	400 µg in 360 µl	Colloidal Coomassie
	40 – 60 µg in 360 µl	Silver Staining
4-7	600 µg in 360 µl	Colloidal Coomassie
	60-80 µg in 360 µl	Silver Staining

24 cm IPG strip

pH gradient	Amount of protein	Staining
4-7	800-1000 µg in 420 µl	Colloidal Coomassie
	80 – 100 µg in 420 µl	Silver Staining
5-8	800-1000 µg in 420 µl	Colloidal Coomassie
	80-100 µg in 420 µl	Silver Staining

.

The IPG strip holder was thoroughly cleaned in a solution of detergent and later washed thoroughly in double distilled water to remove trace dirt and detergent completely. A clean tooth brush was used to clean the electrode region. The strip holder was soaked in MilliQ water for a brief period and then dried clean. IPG ampholyte buffer corresponding to the pH gradient of the IPG strip was added to the samples at 0.5 % of the final concentration.   1 µl of Bromophenol blue was added to serve as a tracking dye to monitor the progress of the focussing. The electrodes on the IEF tray were moistened with tiny paper strips soaked in 20 µl SSB. The sample volume was made up to 360 µl or 420 µl with IEF sample buffer. Each sample was applied along the entire length of the ceramic IEF tray without any room for air bubbles.
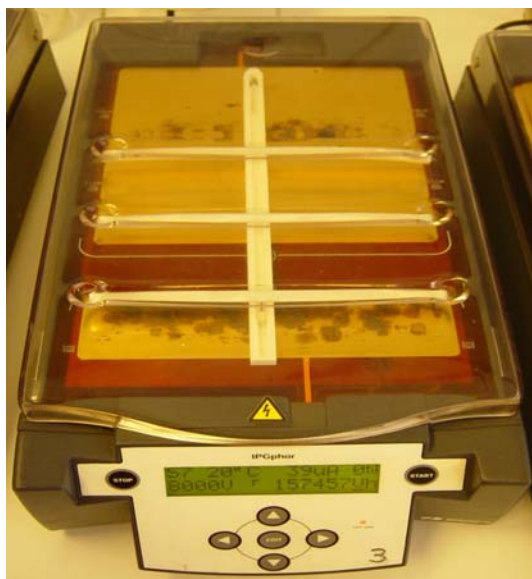
Figure 2.3.1. IPGphor (Amersham Pharmacia) **-** I Dimension isoelectric focussing instrument used for the present study.

The IPG strips stored at – 20 °C were labelled and applied on the IEF tray containing the protein sample, in such a way that the gel side of the strip is in direct contact with the sample liquid. Quickly, silicone oil was applied on top of the strips to prevent dehydration during the run. The focussing was carried out for 2 days until 120000 Voltage Hours were achieved with a maximum applied voltage being 8000 V.

2.3.4 II Dimension SDS PAGE

Large format SDS PAGE gels of 12-15% linear acrylamide gradient were prepared in batches of 23 gels using the special casting system and glass plates supplied by the manufacturer (Hoefer). Typically each gel size was 20.3 x 25.4 x 0.15 cm.To generate a gradient two solutions of 1100ml volume each were prepared and dispensed into the casting chamber using a gradient mixer supplied along with the casting system. 1100 ml of 'Light solution' (38.965 v/v Rotiphorese Gel 30 Acrylamide solution, 375 mM Tris, pH 8.6, 0.1 % SDS) and a 'Heavy solution' (48.70 % v/v Rotiphorese Gel 30 Acrylamide solution, 8 % v/v Glycerine, 375 mM Tris, pH 8.6, 0.1 % SDS) were prepared and cooled at 4 °C for atleast two hours prior to casting. Just before casting, 11ml of 10 % (w/v) APS and 1.57 ml of 10% (v/v) TEMED (for Light Solution) and 5.5 ml 10 % w/v APS and 0.42 ml 10 % v/v TEMED (for Heavy Solution) were mixed well and dispensed into the respective chambers in the gradient mixer. The glass plates were filled with the acrylamide gradient leaving about 2 cm of empty space on the top for embedding the IPG strips later on. To produce a flat uniform layer on top, 1-Butanol was overlaid on the gel surface. The gels were normally solidified overnight. The

gels were later removed and stored in a bath of 375 mM Tris, pH 8.6; 0.1 % SDS in airtight boxes at 4 °C to prevent drying. Prior to II dimension SDS PAGE, equilibration of the isoelectric focussed IPG strips is carried out in order to acquaint the strips to the new buffer system containing SDS that will be used during the II dimension separation.

IEF Strips equilibration buffer (Composition for every 500 ml): Urea 180 g (6 M Urea), Glycerol 150 g (170 ml of 87 % Glycerol; finally 30 % w/v), 10g SDS (100 ml of 10 % SDS stock; finally 2 % w/v), 16.7 ml of 375 mM Tris, pH 8.6. Dissolved in deionised water with final volume made up to 500 ml and aliquoted in vials and stored at – 20 °C.
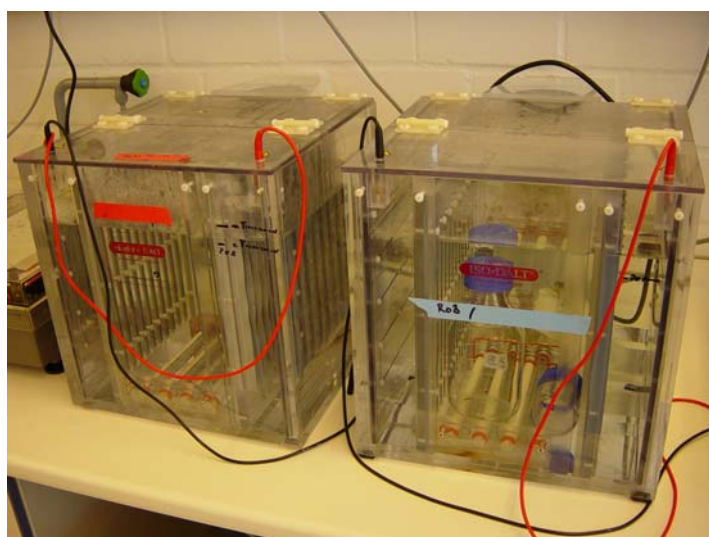
Figure 2.3.2   IsoDalt (Hoefer) – II dimension SDS PAGE apparatus.

Just before 2D SDS PAGE, the IEF strips were equilibrated with 2 solutions A and B consecutively with 15 minutes shaking for each procedure. The strips were equilibrated in special plastic equilibration trays. Normally a volume of 2.5 ml – 3.0 ml was used for each strip. Solution A: 100 mg DTT / 10 ml of IEF equilibration buffer. Solution B: 480 mg Iodoacetamide / 10 ml of IEF equilibration buffer. The iodoacetamide containing solution B was handled with care and discarded safely as a toxic substance.

II Dimension SDS PAGE was carried out on 12 – 15 % linear gradient polyacrylamide gel. The IE focussed strips were embedded in the polyacrylamide gel by using 1.0 % molten agarose (low endosmotic, Biomol)

II dimension running buffer for SDS gel: Tris base 5.8 g, Glycine 299.6 g, and SDS 19.9 g
- all above components were dissolved in a final volume of 20 liters of double distilled water.

2.3.5 Staining and Visualisation of the Protein spots

Colloidal coomassie stain (Neuhoff Stain)

Solution A	Solution B
20 g of 85 % H_3PO_4	5 % w/v CBB-G250
800 ml H_2O	
100 g (NH_4) SO_4	Solution C
H2O ad 980 ml	98 ml solution A and 2 ml Solution B shaken overnight
	Staining solution ready for use: 80 ml C and 20 ml Methanol

Silver staining

	Step	Solution	Time
1	Fixation	40 % ethanol 10 % acetic acid	Minimum1.5 hr optimally 3 hr Maximum overnight
2	Washing	30 % ethanol	3 times 40 min each or 2 times 30 min each
3	Sensitisation	Sodium thiosulphate (0.2 g / l)	1 min
4	Washing	Deionised water	3 times 2 min each
5	Staining	0.2 % Silver nitrate 0.02 % Formaldehyde	20 minutes
6	Washing	Deionised water	3 times 1 min each
7	Developing	3 %Sodium carbonate 0.05 % Formaldehyde Sodium thiosulphate	6- 9 min or even less, needs optimisation and judgement
8	Washing	Deionised water	2 times 2 min each
9	Stopping	0.37 % EDTA	10 min
10	Washing	Deionised water	3 min

Destaining Silver stained gels

In order to prepare Silver stain destaining solution, two stock solutions were prepared.

(A) 30 mM Potassium Ferricyanide $K_3[Fe(CN)_6]$ – 9.87 g/liter and

(B) 100 mM Sodium Thiosulphate – 24.8 g/liter.

(C) Ready to use destainer was prepared by mixing the above two stock solutions just before use in a 1:1 ratio because the destainer is unstable for long-term storage. So it was always prepared and used freshly.

Fluorescence Staining with Ruthenium Chelate

20mM Stock solution of RuBPS stain was prepared and stored in dark at 4°C. Incubation of the gels with the staining solution should be carried out in dark, as the Fluorescence stain is light sensitive. The gels were fixed overnight in 30 % ethanol and 10 % acetic acid (all v/v). The fixation can also be carried out for only 3 - 4 hr. The gels were then rinsed 4 X 30 minutes in 20 % ethanol to facilitate thorough removal of the acetic acid, as the acids if present strongly quench the fluorescence of the chelate. The gels were then stained for 3 - 6 hr in 20 % ethanol containing 100-200 nM of Ruthenium Chelate, i.e. 5–10 µl of the stock solution per liter of staining solution. The Staining can also be carried out overnight. To reduce background, the gels can be washed overnight in 20 % ethanol. Prior to imaging the gels were re-equilibrated in water (2 X 10 min). A comparison between two fluorescent metal chelates for staining proteins separated by electrophoresis has been carried out. One of these chelates is ruthenium II tris (bathophenanthroline disulfonate) and the other is commercial Sypro Ruby. Both can be efficiently detected either with UV tables or with commercial laser fluorescence scanners. The sensitivity and homogeneity of the stains and the interference with mass spectrometry analysis have been investigated. It appears that both stains perform similarly for protein detection, while ruthenium II tris(bathophenanthroline disulfonate) performs better for mass spectrometry analyses and as cost-effectiveness ratio. However, Sypro Ruby is easier to use as a stain.

2.3.6 Mini SDS PAGE gels for Western Blotting

For western blotting and separation of proteins in only one dimension without Isoelectric Focussing on IPG strips, conventional SDS PAGE was employed. The resolving gel and stacking gel were prepared by mixing various components in appropriate volumes as mentioned in the Table below and poured into the glass plates for solidification.

Stacking Gel

Component	Volume
H_2O	5.7 ml
0.5M Tris-Cl pH 6.8	2.5 ml
Rotiphorese Gel 30 (Acrylamide /Bis-acrylamide solution; Roth)	1.7 ml
10 %SDS	100 µl
TEMED	20 µl
25 % APS	30 µl

Resolving Gel

Component	7.5% AA gel	10% AA gel	12% AA gel	15% AA gel
H$_2$O	7.4 ml	6.1 ml	5.1 ml	3.6 ml
1.5 M Tris-Cl pH 8.8	3.8 ml	3.8 ml	3.8 ml	3.8 ml
Rotiphorese Gel 30 (Acrylamide /Bis-acrylamide solution; Roth)	3.8 ml	5.0 ml	6.0 ml	7.5 ml
10 %SDS	150 µl	150 µl	150 µl	150 µl
TEMED	20 µl	20 µl	20 µl	20 µl
25 %APS	10 µl	10 µl	10 µl	10 µl

SDS Running Buffer (10X concentrate)	Sample buffer (2X concentrate)
3.03 % (w/v) Tris-Base 14.04 % (w/v) Glycine 1.00 %(w/v) SDS	0.5 M Tris/HCl, pH- 6.8 20 % (v/v) Glycerine 10 % (w/v) SDS 5 % (v/v) β-mercaptoethanol 0.25 % (w/v) bromophenol blue.

2.3.7 Western Blotting

The transfer of proteins from polyacrylamide gels to the membrane ('Western-Blot') was carried out using a 'semi-dry'-System, employing a TransBlot SD Transfer system from Bio-Rad. Four whatmann papers cut into an appropriate size as that of the membrane itself were soaked in the transfer buffer (25 mM Tris-Base, 190 mM Glycine, 0.1 % w/v SDS, 20 % v/v Methanol, pH 8.5) and applied on the anode plate. A clean PVDF membrane (Roth) of identical size was soaked in methanol and briefly drained for a second and subsequently soaked in transfer buffer and laid on top of the whatmann papers avoiding any air bubbles in between them. The region to be analysed on the SDS-PAGE gels was cut out into an appropriate size as the membrane and incubated in the transfer buffer for 2 minutes and laid on top of the PVDF membrane carefully avoiding any air bubbles between them. Four additional whatmann papers soaked in transfer buffer were quickly placed on top of the gel. A long glass pipette was rolled over the arrangement gently, in order to liberate any trapped air bubbles. The cathode electrode plate was carefully assembled on top and power applied for 90 min such that current flow was 0.9 mA /cm^2 of the membrane area. A higher voltage limit of 25 V was adhered to as per the recommendation of the equipment manufacturer. At the end of the transfer, the membrane was incubated in blocking solution (5% w/v Skimmed milk powder, 1% w/v BSA, 0.02 %v/v Tween 20, 0.02 %v/v gelatin, in TBS solution) for 2 hr on a rocking platform. The primary antibody for detection was stored at –20°C in small aliquots by diluting in blocking solution. After blocking for 2 hr, for detection, the primary antibody was

dispensed at final dilution between 1: 2000 – 1:7500 in the blocking solution. The incubation of the membrane with the antibody was carried out for a minimum of 2 hr at 4°C. Incubation can also be extended over night. At the end of the incubation, the membrane was rinsed in running water once, followed by a sequential wash with a) TBS-T, b) TBS-T + 0.5M NaCl, c) TBS-T + 0.5%v/v TritonX-100, 15 minutes each. At the end of the wash, the secondary antibody (Anti Rabbit IgA) coupled to a peroxidase (Jackson Immuno Research) was used at an effective dilution of 1:8000 in the blocking solution. At the end of 2 hr incubation, the membrane was briefly washed in running water. The membrane was sequentially washed with a) TBS-T, b) TBS-T + 0.5M NaCl, c) TBS-T + 0.5 % v/v TritonX-100, 15 min each.

The detection of the secondary antibody on the membrane was carried out using a commercial kit 'Lumi Light' Chemiluminiscence POD-substrates (Roche Molecular Biochemicals). The underlying principle behind the generation of the chemiluminesence is the coupled disproportionation of the peroxide by peroxidase conjugated to the antibody and simultaneous chemiluminescence generation by the luminol proportional to the peroxidase activity. A 1:1 mixture of the peroxide substrate and luminol/enhancer solutions supplied in the detection kit is poured on to the membrane and the membrane itself sandwiched between two plastic films and incubated for 5 min. The documentation of the signals was accomplished by exposing the membranes to photosensitive film (BiomaxLight Film, Kodak; exposure time 5 s – 45 s depending on the signal intensity) in a dark room or through a video camera (CCD-Camera LAS-1000 and Intelligent Dark Box, Fuji film; exposure time: 10 s – 5 min depending on the signal intensity).

2.3.8 MALDI-TOF MS

2.3.8.1 Excision of protein spots from gels

The gel was rinsed with water. Spots of interest were excised with the help of a clean pipette tip (1ml) cut at the end with a scissors (cutting always close to the bottom edge of the spot to suit the size of the protein spot of interest). The excised spots were chopped into cubes (approx. 1 mm^3) using a sterile scalpel. Gel particles were transferred to an eppendorf tube (1.5 ml). Care was taken not to touch the gel with bare hands in order to avoid keratin contamination from skin and hair. Prior to first use, the latex gloves were washed with water to remove talcum powder and dust entering into the sample tubes.

2.3.8.2 Reduction and Alkylation

Gel pieces were washed with 100-150μl of water for 5 min. The tubes were spun down and the liquid discarded. About 15-50 µl acetonitrile (enough to submerge the gels completely), was added and incubated for 10 to 15 minutes at 37°C in a votexer, until the gel pieces shrunk and became white and stuck together. The gel particles were spun down in a micro centrifuge and all the liquid removed. The gel pieces were swollen in about 50 µl of 10 mM Dithiothreitol / 0.1 M NH_4HCO_3 (with liquid enough to cover the gel and incubated for 15 min at 56 °C to reduce the protein). This in-gel reduction of the proteins is crucial even if proteins were reduced prior to an electrophoresis. This enables better cleavage by Trypsin in the subsequent steps. The gel particles were spun down and excess liquid removed. The gel pieces were dehydrated with acetonitrile as in the previous steps. The acetonitrile was discarded and replaced by 50 µl of 55 mM iodoacetamide / 0.1 M NH_4HCO_3 and incubated for 15min at room temperature in the dark. At the end of the incubation, iodoacetamide solution was removed and the gel particles were washed with 150–200 µl of 0.1 M NH_4HCO_3 for 15 min. The gel particles were spun down and all the liquid discarded. The gel particles were dehydrated with acetonitrile and subsequently all liquid removed and the reduced and alkylated gel particles were dried in a vacuum centrifuge.

2.3.8.3 In gel digestion with Trypsin

The dry, reduced and alkylated gel particles were rehydrated in the Trypsin digestion cocktail containing 50 mM NH_4HCO_3, 5 mM $CaCl_2$ and 12.5 ng/µl of Trypsin at 4 °C (on a ice bucket) for 30 − 45 minutes. (After 15 − 20 minutes, the samples were checked and more enzyme cocktail added if all the liquid was absorbed by the gel pieces). The remaining supernatant was removed and replaced with 5 − 25 µl of the same buffer but without trypsin to just submerge the gel pieces and keep them wet during enzymatic cleavage. The samples were left at 37 °C overnight to completely digest the proteins.

2.3.8.4 Extraction of peptides

15 µl of 25 mM NH_4HCO_3 was added directly to the trypsin digested gel pieces. For Nano ES MS/MS analysis, tryptic peptides were extracted from the gel particles. 10 − 15 µl of 25 mM NH_4HCO_3 was added and incubated at 37 °C for 15 min with vortexing. The gel particles were spun down and 50 µl acetonitrile (1 - 2 times equal to the volume of gel particles) was added and the tubes incubated at 37°C for 15 min with vortexing. The liquid was spun down and the supernatant collected and pooled with the earlier supernatant. 40 − 50 µl of 5 %

Formic acid was added and vortexed for 15 min at 37 °C. The gel particles were spun down and 50 µl of acetonitrile added to the previous mix. The tube was incubated at 37 °C for 15 minutes with vortexing. The gel particles were spun down and the supernatant pooled with previous extracts. The extracted peptide containing pooled supernatant was dried down in a vacuum centrifuge.

2.3.8.5 Guanidination of Lysine residues

Digestion of proteins with Trypsin, generates some peptides with Lysine and some others with arginine as terminal residues. An analysis of the over all MALDI-TOF spectra reveals the under representation of spectral peaks corresponding to peptides with lysine as the end residue and a predominance of the spectral peaks corresponding to arginine containing peptides (Krause *et al.,* 1999). In order to improve the over all spectral quality and representation of lysine containing peptides, chemical modification of lysine residues to homoarginine (Hale *et al.,* 2000; Brancia *et al.,* 2001) has been widely used. The tryptic digests used in this study were also subjected to guanidination of lysine using a modified protocol (Beardsley *et al.,* 2002). The guanidination of lysine with O-methylisourea sulphate imparts a mass shift of 42.02 Da on the peptides. Briefly, for guanidination of the lysine residues, vacuum dried peptides were dissolved in 20µl 50mM NH_4HCO_3 and 20µl 2M O-Methylisourea sulphate (3.2 g / 10ml of 200 mM Na_2CO_3 (pH 10)). The reaction was incubated at 37 °C overnight. The reaction was stopped with 1% TFA in water. The peptide solution was used directly for ZipTip purification before spotting onto the MALDI –TOF target.

2.3.8.6 Ziptipping for MALDI-TOF

For obtaining good quality MALDI-TOF MS spectra, the peptides spotted on the target must be free of hindering impurities and salts that could generate a strong background noise signals. It is therefore imperative to purify and enrich the peptides before placing them on the MALDI – target. ZipTip (Millipore), a pipette tip based chromatographic column of very small volume (1µl) was used for the purification and concentration of the peptides into a very small volume of 1 – 2 µl from a volume of 20-50 µl volume. The column is made of a special material that selectively binds the peptides from a hydrophilic solution (5 % Methanol) and the peptides can be eluted using a hydrophobic solution (65 % Methanol). The following solutions were prepared prior to ZipTipping.

Solution A: Wash solution and Elution solution – 65 % Methanol and 0.5 % HCOOH

Solution B: Equilibration Solution and Peptide Solubilization solution – 5% Methanol and 0.5% HCOOH

The dried peptides were dissolved in 15 – 25µl of solution B. The wall of the eppendorf tube containing the dried peptides was rinsed several times with same solution thoroughly in order to scoop and get all the peptides into solution thoroughly. The ZipTip was washed in solution A by pippetting for 4 – 6 times with approx. 10 – 15 µl volume so as to wash the packed column. The ZipTip was equilibrated in solution B by pipetting a few times with a volume enough to wet the column. The empty equilibrated tip was introduced into the peptide solution. Avoiding air bubbles, the contents of the tube were carefully pipetted in and out of the ZipTip atleast 15 times, simultaneously washing the walls to extract as much peptide as possible into the column in the ZipTip.The ZipTip was washed a few times in fresh equilibration solution (Solution B) to remove dirt and unbound particles. The ZipTip was withdrawn from the tubes with about 15 µl of the equilibration buffer filled in. Gently screwing the pipette suction apparatus, all the liquid was expelled out of the ZipTip leaving behind only 1 - 1.5 µl. Pressing hard this last trace of fluid from the ZipTip was expelled completely and almost instantaneously 1 - 1.5 µl of matrix (α-Cyano-4-Hydroxy Cinnamic acid) dissolved in solution A (65 % Methanol and 0.5 % HCOOH) was aspirated. This liquid was expelled out onto a MALDI-TOF target in order to spot a mixture of concentrated peptide and matrix to crystallize.

2.3.8.7 Spot identification by Mass Spectrometry.

The protein spots were identified by **MALDI-TOF (Matrix assisted Laser Desorption / Ionization Time Of Flight) mass spectrometry**: measurement of peptide masses by MS resulting in a list of measured peptide masses which can be matched against theoretically predicted peptides of proteins in databases (complete protein sequences required!).
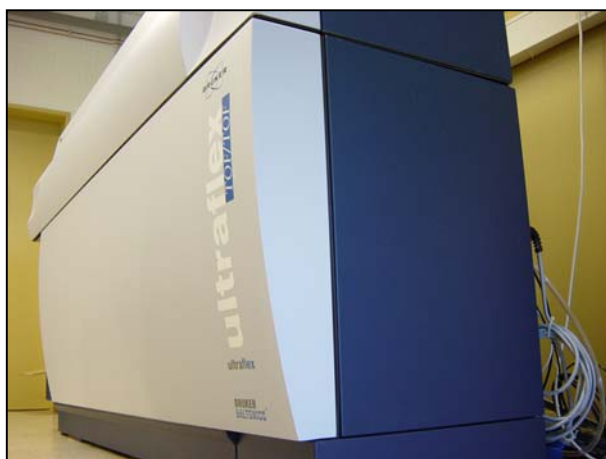
Figure 2.3.3   MALDI-TOF (Ultraflex, Bruker) used for the present study.

The instrument Bruker Ultraflex (figure 2.3.3) was used for the present study. In the standard configuration the instrument is equipped with a gridless pulsed ion extraction ion source and a grid less reflectron that offer high transmission and optimal focusing. The effective flight path in linear mode is 1.2 m and 1.7 m in reflectron mode. The instrument employs a 337 nm laser with a computerised attenuation. Both positive and negative ion analysis are also provided in its standard configuration. All data were acquired in the reflectron mode utilizing peptide standards as internal calibrants. The library searching was fully automated and employed the MASCOT search program (Matrix Science). The searches in these applications were carried out on a local intranet server. A peaklist generated in the XTOF data analysis software was transferred to the BioTools software to be submitted for the library search.

2.3.9 Isolation of Bacterial membranes

The separation of membranes was performed under conditions that stabilize ribosomes using swing bucket ultracentrifuge rotors (Beckman), using 16 ml centrifuge tubes (Beckman). The following stock solutions were prepared: 1.5 M Potassium acetate pH 7.5 (made with acetic acid), 1M Magnesium acetate, 1M HEPES pH 7.5 (made with KOH and prepared freshly and autoclaved), 2.5 M Sucrose. Around 3 g cells were harvested by spinning 3000g for 10 min at 4 °C. The cells were washed once with PBS at 4 °C. The pellet was stored at − 20 °C until further use or used immediately. The cells were lysed in MilliQ water containing

commercially available protease inhibitor tablets Complete (Roche) using a french press (Aminco). The lysis was monitored by observing a drop of the lysate under the microscope to look for any live cells. The lysed cells were stored on ice. A sucrose gradient was set up in the centrifuge tubes by overlaying increasing concentrations of sucrose solutions one on top of the other. The individual components of the gradient themselves were prepared by mixing the various components from the stock solutions above and diluting the 2.5 M sucrose stock as per the scheme below.

To obtain 10 ml of individual components of the gradient, water and 2.5 M sucrose were mixed as follows.

	0 M Sucrose	1.5 M Sucrose	2 M Sucrose
H₂O (with protease inhibitor)	**8.8 ml**	**2.8 ml**	**0.8 ml**
2.5 M Sucrose	**0 ml**	**6 ml**	**8 ml**

To 10 ml preparation of each concentration the following volume of the other components were added from their respective stock solutions in order to obtain a complete gradient onto which the sample can be overlayed.

Final concentration   Volume from stock solution

5 mM	Mg acetate	50 µl
100 mM	K acetate	666 µl
50 mM	HEPES	500 µl
1/2000 volume	β-mercaptoethanol	5 µl

The sample itself was prepared as an 8 ml volume sucrose solution with effective concentration of sucrose being 0.5 M.

3 ml of 2 M sucrose was laid on the bottom of the centrifuge tube, gently. On top of this another 3 ml of 1.5 M sucrose was laid on top carefully avoiding any intermixing. The lysed cells (sample) itself representing the 0.5 M sucrose component of the gradient was gently overlaid. 2 ml of 0 M sucrose (containing all components except 2.5 M Sucrose) was laid on top to complete the gradient (refer **figure 2.3.4**). All operations were performed on ice. The set up was placed on prechilled rotors and centrifuged in an ultracentrifuge at 27000 rpm (at least 50000 g) for 45 min at 4 °C.
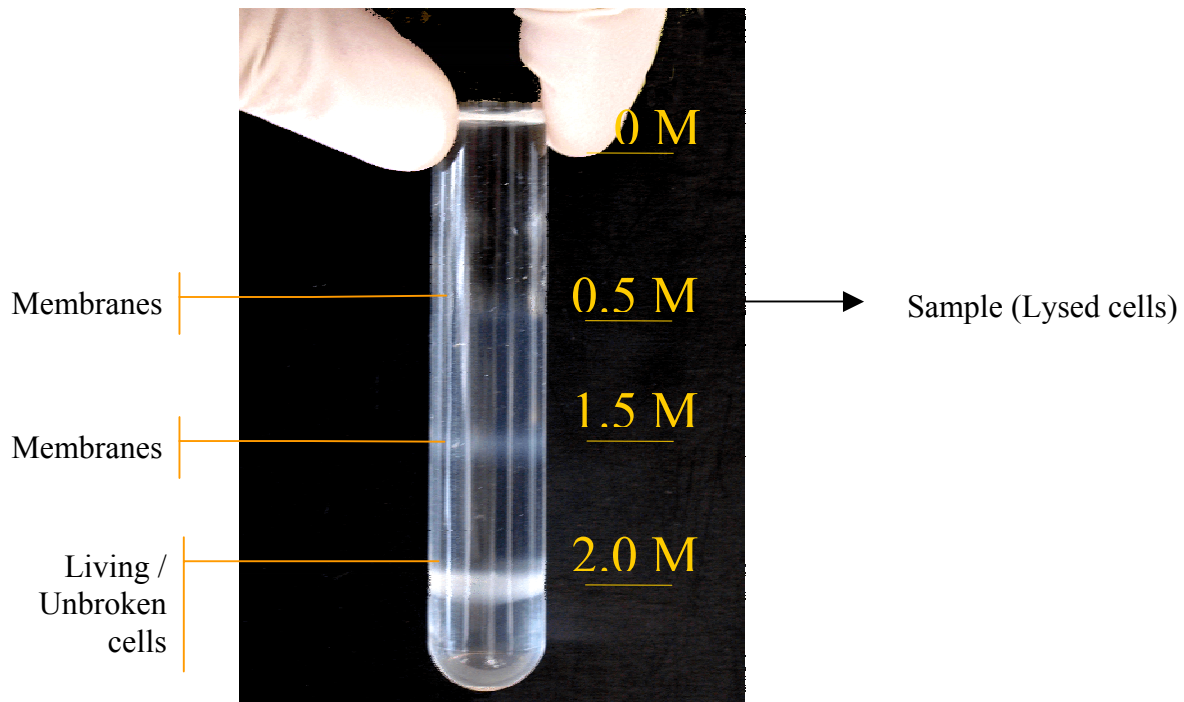
Figure 2.3.4 Setting up a sucrose gradient and embedding the French pressed cells in the gradient for ultra centrifugation to isolate membranes. (Illustration courtesy, Maja Baumgärtner, GBF, Braunschweig).

At the end of the ultra centrifugation, using a long tipped glass pasteur pipette, the membrane fraction seen as a white hazy ring at the interface between the 1.5 M sucrose layer and 0.5 M sucrose layer was collected. The isolated membrane fraction was mixed well with MilliQ water containing protease inhibitors (1:1) and centrifuged in an ultracentrifuge for 1 hr at 27000 rpm at 4 °C. At the end of the centrifugation, the membrane pellet was washed with 3 ml volume of ice cold 1M Tris (pH 7.5) for 30 min at 50000 rpm, 4 °C in a table top mini-ultracentrifuge, in order to get rid of soluble cytoplasmic protein contaminants. The pellet was dispersed and treated with ice-cold 0.1M sodium carbonate solution of pH 11 by shaking in a rocking platform for 1 hour in order to break up any membrane vesicles. The membrane pellet was recovered by ultra centrifugation at 50000 rpm for 30 min at 4 °C. The pellet was subsequently washed with ice-cold MilliQ water twice in order to remove any traces of sodium carbonate remaining from the previous treatment. All the wash solutions contained protease inhibitors and were ice-cold solutions. The final pure membrane pellet was either directly dissolved in suitable sample buffers for 16 BAC separation or directly treated with Trypsin in case of nano flow LC/MS identification of the various membrane protein species.

2.3.10 16 BAC gel analysis

16 BAC - I Dimension

7.5 % separation gel (40 ml)

7.2 g	Urea
10 ml	30 % AA / 0.8 % Bis AA
10 ml	300 mM KH_2PO_4 / 1 % H_3PO_4 (pH 2.1)
10 ml	Milli Q water
1.4 ml	1.7 % Bis AA
2 ml	80 mM Ascorbic acid
64 µl	5 mM $FeSO_4$
1.6 ml	1 : 1200 Hydrogen peroxide H_2O_2 (made from 30 % stock)

16 BAC Overlay

75 mM KH_2PO_4 / 1 % H_3PO_4 (pH 2.1)

Electrode buffers

Anode Buffer
22.52 g   Glycine
7.6 ml   85% H_3PO_4
and volume made up to 2 liters with double distilled water.

From this 2 liters, 500 ml was taken away and 0.57 g of BAC detergent was added in order to be used as cathode buffer.

4% Stacking gel (10 ml)

1g	Urea
1.33 ml	30 % AA / 0.8 % BisAA
2.5 ml	0.5M KH_2PO_4 (pH 4.1)
3 ml	H_2O
1.38 ml	1.7 % BisAA
0.5 ml	80 mM Ascorbic acid
8.5 µl	5 mM $FeSO_4$
0.5 ml	1:750 H_2O_2 (30 % stock solution)

Note: 10 ml of Ascorbic acid and $FeSO_4$ stock were always freshly prepared just before use.

Sample buffer

4.5 g	Urea
1 gram	16 BAC (approx 250 mM)
1 ml	Glycerine
4 ml	H_2O
1.5 ml	1.5 M DTT

volume made up to 10 ml with milliQ water.

Sample buffer may have to be gently heated up in a microwave oven for a very brief time 1-3s to dissolve the 16 BAC detergent. Ideally tiny 20 ml or 10 ml glass beakers were used for preparing the buffer.

Note: The gel was poured and stored at 4°C overnight before use.

The gels were run overnight with orange red dye and reversed current lead directions.
The gels were then stained with Coomassie - R 250 containing fixative in itself.
The gels were briefly destained in normal fixative for few hours to view the bands.
The gels were then cut to isolate the strips of independent samples and destained fully.

II dimension of the BAC

Sample gel
3.2 ml	Acrylamide / Bisacrylamide (normal solution used for making gels)
6.2 ml	Gel buffer
16.8 ml	H_2O
200 µl	10 % APS
20 µl	TEMED

Anode buffer
0.2 M   Tris (36.34 grams) pH 8.9 (with HCl)
volume was made up to 1.5 liters

Cathode buffer
0.1 M	Tris
0.1 M	Tricine
0.1 %	SDS

pH 8.25, Volume was made up to 1 liter, the pH is usually 8.25 and need not be tested.

Tricine gel

Seperation gel
48 ml	Acrylamide / Bisacrylamide
30 ml	Gel buffer
12 ml	Glycerine
300 µl	10 % APS
30 µl	TEMED

Spacer gel
10.1 ml	Acrylamide / Bisacrlyamide
10 ml	Gel buffer
9.9 ml	Distilled water
100 µl	10 % APS
10 µl	TEMED

Stock solutions for Tricine gels
Gel buffer
3 M   Tris
%   SDS
pH 8.45 (adjust with HCl) at 25° C

Overlay solution
1M   Tris
%   SDS
pH 8.45 (with HCl)

3 X sample buffer
15 %   SDS
30 %   Glycerine
150 mM   Tris
6 %   Mercaptoethanol
0.006 %   Bromophenol blue
pH 6.8 (with HCl)

2.3.11 Carbonate extraction of Integral membrane proteins

Approximately 40 mg (dry weight) of cells were lysed using a sonicator of 10 Watts power for 3 X 30 s on ice in 5ml PBS with 150 units of endonuclease and complete mini (Roche). 20 mg of cellular protein (as determined by Bradford analysis) was diluted to 6ml with 50 mM Tris/HCl, pH 7.3 containing 0.7 mg of DNase I (Sigma). The cells were ruptured in an Aminco French press with two presses at 9.65×10^7 Pascals and the unbroken cells removed by centrifugation at 2500 g for 10 min. The supernatant was diluted with ice-cold 0.1 M sodium carbonate (pH 11) to a final volume of 60 ml and stirred slowly on ice for 1 hr. The carbonate treated membranes were collected by ultra centrifugation in a Beckman 55.2 Ti rotor at an average of 115000 g for 1 hr at 4°C. The supernatant was discarded and the membrane pellet resuspended and washed in 2 ml of 50 mM Tris/HCl, pH 7.3. The pellet was collected by centrifugation at an average of 115 000 g for 20 min (Beckman 55.2 Ti rotor) and solubilized for 2D electrophoresis with 1.5 ml of IEF solution [7 M urea, 2 M thiourea, 1% (w/v) ASB14, 40 mM Tris, 2 mM tributyl phosphine (TBP) and 0.5% (v/v) Biolytes 3-10 (Bio-Rad, CA, USA)].

2.3.12 Nano flow LC/MS

Reverse phase (RP) chromatography is the most common form of chromatography used in LC/MS applications of complex peptide mixtures. The basic principle of reverse phase HPLC is that the peptides stick to the reverse phase HPLC columns in high aqueous mobile phase and are eluted from RP HPLC columns with high organic mobile phase. In RP HPLC peptides are separated based on their hydrophobic character by running a linear gradient of the organic solvent (acetonitrile). Typically, 60/60 gradient is used to resolve an unknown mixture. 60/60 gradient means that the gradient starts near 100 % aqueous and ramps to 60 % organic solvent in 60 min. The majority of the peptides (10 to 30 amino acids in length) elute by the time the gradient reaches 30 % organic. However, for our analysis, 80/120 gradient was used.

Column specifications

Bonded phase: C18
Column dimension: 15 cm X 75µm (Pepmap, LC packing, Holland Dionex,USA)
Particle size: 3 µm
Pore size: 100 A°

Preferred solvent system for ESI LC/MS

A: HPLC grade water, 0.1 % formic acid
B: HPLC grade Acetonitrile, 0.1 % formic acid
(0.1 % acid is usually included in order to improve the peak shape and sever as a proton source in the reverse phase LC/MS).

Flow rate: a flow rate of 200 nanolitres/ min was used.

Sample preparation for LC/MS

The pellet of protein to be analysed was digested over night with 35 - 50 µl of Trypsin (20 µg/ml) in 50 mM NH_4HCO_3 at 37 °C. This solution of Trypsin is approximately 10 times more concentrated than the solution of Trypsin used for digestion of the proteins spots picked from the gels for subsequent MALDI-TOF MS. At the end of digestion, the tryptic digests were centrifuged in a mini-ultracentrifuge at 50000 rpm for 45 min at 4 °C. The debris free supernatant having the peptides was collected and dilutions of the peptide mixture were made in solvent A (HPLC grade water, 0.1% formic acid). Usually a 1: 20 dilution was found to be appropriate to yield an optimal loading.

2.4 Real time Polymerase Chain Reaction

2.4.1 RNA-Preparation from *P. aeruginosa*

Care was taken to carryout all the operations as quickly as possible in order to minimise RNA degradation and also changes in the gene expression introduced by handling of the cells. While working with Phenol and Chloroform the fume hood was used. Only fresh and autoclaved (twice) pipette tips and eppendorf cups were used. Different pipettes were used for RNA work and DEPC-treated solutions.

- 2,5 ml lysis-buffer (2 % SDS, 30 mM Na-Acetate, 3 mM EDTA; pH 5.5) and 5 ml Phenol (pH 5.5; *Roth*) was pre-incubated in 14 ml Falcon-Tubes at 65 °C in a water-bath.

- The bacterial cells from 12 ml of fresh culture ($OD_{600} \approx 0.8$ (approx. 9.6 x 10^9 cells; inoculated with $OD_{600} \approx 0.05$ using pre-inoculum grown over night; yielding approx. 120 µg RNA) was recovered from the culture flasks and harvested by centrifugation at 3500 rpm for 5 min at 4 °C (Hettich-centrifuge in the cold-room) in 14 ml Falcons and resuspended quickly in 0.5 ml 0.9 % NaCl or water.

- The lysis-mixture was quickly added to the harvested cells and the tubes shaken 10 min vigorously followed by 5min incubation on ice. The tubes were centrifuged at 20 min at 3500 rpm, 4°C.

- The supernatant was collected and mixed with 3 ml Phenol/CHCl$_3$/Isoamylalkohol (25:24:1), shaken for 5 min vigorously followed by 5 min incubation on ice. The tubes were centrifuged for 10 min at 3500 rpm, 4°C.

- The supernatant was collected and mixed with 3 ml CHCl$_3$/Isoamylalkohol (24:1), shaken for 2 min, followed by 5 min incubation on ice. The tubes were centrifuged for 10 min at 3500 rpm, 4 °C.

- The supernatant was collected and mixed with
  0.1 Volume 3 M Na-Acetate (pH 5.5)
  2.5 Volume 99 % EtOH (- 20 °C)

- The contents of the tubes were let to precipitate for 2 hr to over night at − 20 °C followed by centrifugation for 30 min at 3500 rpm, 4 °C.

- The pellet was washed with 5 ml 70 % EtOH (- 20 °C) and transferred to an eppendorf cup containing 70 % EtOH followed by centrifugation for 10 min at 14000 rpm, 4 °C (Eppendorf-cooled centrifuge).

- EtOH was removed as much as possible by pipetting, and pellet was subsequently dissolved in 174.2 µl H_2O (mixed well, followed by 5 min incubation on ice). To digest

the contaminating DNA the following were added followed by 30 min incubation at 37 °C on a Thermo mixer (*Eppendorf*).

+ 20 µl DNase-buffer (10X (500 mM Na-Acetate (pH 6.5); 100 mM MgCl$_2$, 20 mM CaCl$_2$))

+ 4,8 µl DNase (10 U/µl) *Roche* (5 U DNaseI per 1x10^9 cells)

+ 1 µl RNasin *Promega* or SUPERaseIn *Ambion*

- The RNA was purified using RNeasy-columns (*Qiagen, Hilden, Germany)* as described in the handbook, eluted with 2 times 30 µl RNAse free water supplied with the kit (and incubated briefly for 5 min on ice).

- The concentration was estimated with UV-absorption on a Spectrophotometer (*Eppendorf*) and quality determined with a MOPS/Formaldehyde Agarose-gel. The total yield was 250 - 100 µg.

2.4.2 cDNA synthesis

2 µg of total RNA was taken in a 1.5 ml eppendorf. The volume was adjusted to 9 µl using RNAse free water. 2 µl of the random primer was added to the tube. The contents were mixed well with a pipette and incubated at 65 °C for 10 min followed by chilling on ice for two minutes and brief spin for 15 s to concentrate the contents at the bottom of the reaction tube. Following components were added to complete the reaction mixture: 4 µl of 5X concentrated first strand buffer of expand RT; 2 µl of 10 mM DTT; 2 µl of 10 mM dNTPs; 1 µl of Expand Reverse Transcriptase.

The reaction tube was incubated at 43 °C for 60 min, chilled on ice briefly for 2 minutes and spun down to concentrate the contents and stored at − 20 °C until further use. Second strand synthesis and PCR amplification were done to check the cDNA synthesis and specificity of primers for the target sequence. To 3 µl of the previous reaction mixture, the following components were added

Component	Volume
10 X PCR buffer	2 µl
2 mM dNTP (dATP, dGTP, dTTP, dCTP)	2 µl
5pM Forward primer	2 µl
5pM Reverse primer	2 µl
Expand Hifi	1 µl
DdH$_2$O	8 µl

Contents were mixed well and PCR amplified.

2.4.3 Lightcycler

Reactions of 10 µl volume were setup and found to be optimal. The various components of the reaction mix are as follows.

Component	Volume
Primer (Forward)	1 µl
Primer (Reverse)	1 µl
SYBR GREEN: ENZYME: dNTPS Mix	1 µl
DMSO	0.5 µl
$MgCl_2$	0.4 µl
H_2O	4.1 µl
cDNA Template	2 µl

The reaction mix was dispensed into the special glass capillary tube that fit in the sample carousel of the lightcycler instrument. Further operations were performed as described in the the LightCycler manual.

2.5. GeneChip® *P.aeruginosa* Genome Array Analysis

2.5.1 cDNA Synthesis

10 µg of total RNA per sample was used. The incubation was performed in a Thermocycler (Landgraf). The following mixture was prepared for primer annealing.

Primer Hybridisation Mix

Components	Volume or Amount	Final Concentrations
Total RNA	10 µg	0.33 µg/µl
Random Primers (75 ng /µl) or Oligo (dT) primer (75 µg/µl)	10 µl	25 ng/µl
Spike Transcript (130 pM) (Optional)	2 µl	8.67 pM
Nuclease-free H_2O	Up to 30 µl	
Total Volume	**30µl**	

Spike transcripts are sense RNA controls from *Bacillus subtilis* genes that can serve as control transcripts and be spiked into *P. aeruginosa* total RNA used for target preparation at a predetermined concentration in order to monitor labelling, hybridisation and staining efficiency. The contents were mixed and centrifuged and about 50 µl of RNase free paraffin was laid on top. RNA primer mix was placed at 70 °C for 10 min followed by 25 °C for 10 min and then chilled on to 4 °C. The following reaction mix for cDNA synthesis was prepared and added to the primer hybridisation mix.

cDNA Synthesis Components

Components	Volume or Amount	Final Concentrations
5X 1st Strand Buffer	12 µl	1 X
100mM DTT	6 µl	10 mM
10mM dNTPs	3 µl	0.5 mM
SUPERase•In (20U/µl)	1.5 µl	0.5 U/µl
SuperScript II (200U/µl)	7.5 µl	25 U/µl
Total Volume	**30 µl**	

The contents were mixed well by pipetting and centrifuged quickly in order to concentrate all the contents of the tube to the bottom. The reaction was carried out by incubating, at 25 °C for 10 min, 37 °C for 60 min and 42 °C for 60 min. The enzyme was inactivated at 70 °C for 10 min and held at 4 °C. 20 µl of 1N NaOH was added and incubated at 65 °C for 30 min followed by addition of 20 µl of 1N HCl for the neutralization. The reaction mix was transferred to a 1.5 ml eppendorf tube. cDNA synthesis products were purified using QIAquick Column (Qiagen). Paraffin and contents of the cDNA reaction mix can be run through the QIAquick Column together without any problem. Detailed protocols are stated in the QIAquick PCR Purification Kit Protocols provided by the supplier. The product was eluted with 40 µl of EB Buffer (supplied with QIAquick kit). The purified cDNA product was quantified by 260 nm absorbance (1.0 A_{260} unit = 33 µg/mL of single strand DNA). Typical yields of cDNA are 2.5 – 4.0 µg for reactions primed with random primers. However the yields of cDNA for reactions primed with Oligo (dT) primers were often low, around 500 – 1 µg / 10 µg of total RNA used or variable depending on the polyadenylation levels in the specific RNA sample.

2.5.2 cDNA Fragmentation

The following Fragmentation reaction mix was prepared.

Fragmentation Reaction

Components	Volume/Amount	Concentration
10X One Phor-All Buffer	5 µl	1 X
CDNA	40 µl	3-7 µg
DNase I (0.6U/µl in1X One Phor-All Buffer)	X µl	0.6 U/µg of cDNA
Nuclease –free H₂O	**Upto 50µl.**	

The reaction was incubated at 37 °C for 10 min. The enzyme was incubated at 98 °C for 10 min. The fragmented cDNA was added directly to the terminal labelling reaction or stored at – 20 °C until further use. To examine the fragmentation result, about ~200ng of the product was loaded on 2 % agarose gel and stained with SYBR green for 1 hr.

2.5.3 Terminal Labeling

Enzo BioArray^{TM} Terminal Labeling Kit with Biotin-ddUTP (Affymetrix) was used to label the 3' termini of the fragmentation products. The following Terminal Label Reaction mix was prepared.

Terminal Label Reaction

Components	Volume/Amount
5X Reaction Buffer	12 µl
10X CoCl$_2$	6 µl
Biotin ddUTP	1 µl
Terminal Deoxynucleotide Transferase	2 µl
Fragmentation Product (1.5 – 6 µg)	39 µl
Total Volume	60 µl

The reaction was incubated at 37 °C for 20 – 60 min. The reaction was stopped by adding 2 µl of 0.5 M EDTA. The target was hybridised onto the probe arrays as quickly as possible on the same day.

2.5.4 Target Hybridisation; Washing, Staining, Scanning; Data Analysis

Target Hybridisation, Washing Staining and Scanning of the hybridised chips were performed as per the GeneChip Expression Analysis Protocols recommended by the user manual accompanying the GeneChip consignment from Affymetrix. These procedures were performed by the DNA Microarray facility at the Gesellschaft für Biotechnologische Forschung (GBF), Braunschweig. Primary Data Analysis was performed using Microarray Suite (MAS) Software 5.0 supplied by Affymetrix. Subsequent analysis was performed using Microsoft Access and Microsoft Excel. When primary data was analyzed, a signal for every gene was considered to be present only if there was strong presence (P) and/or marginal presence (M) of signals (as computed by Affymetrix, MAS 5.0, using default parameters) on both replicate chips hybridized with the same cDNA. When there was absence (A) of signal in only one of the replicate chips, the gene itself was considered to be undetected. The annotations of the genes were based on the most recent annotations available from the PseudoCAP website www.pseudomonas.com.

3. Results and Discussion

3.1 Differential growth response of morphotypes to iron limitation

3.1.1 Differential growth under iron limitation

Severe iron limiting conditions are likely to be encountered *in vivo* in the CF lung habitat colonized by *Pseudomonas aeruginosa*. In order to determine whether there existed any inter-morphotype differential growth response to iron limiting growth conditions, SCV 20265 and WT 20265 were grown in Vogel Bonner medium that was pre treated with a divalent cation chelator resin Chelex 100 (BioRad). Ferrous (Fe^{2+}) ions are chelated and removed along with the resin. However the efficiency of chelation of iron from the medium is debatable. The comparison of growth under chelex 100 treated vogel bonner medium and normal vogel bonner (untreated) medium revealed only a slight difference in growth pertaining to the lag phase. During log phases of growth no significant inter morphotype growth differences between the SCV 20265 and WT 20265 could be recorded (data not shown). So it was important to achieve a complete depletion of iron. After a thorough search in the literature regarding iron depletion from the medium, use of other iron specific chelators was pursued to achieve satisfactory iron depletion.

2,2-dipyridyl is an iron specific chelator widely used for chelating iron from the medium to achieve iron depletion or iron limitation. A range of concentrations of the chelator 2,2-Dipyridyl was tested. At 1.1mM concentration of 2,2-Dipyridyl in the medium, a crucial difference in the growth of SCV 20265 and WT 20265 was reproducibly detectable. Bacteria were grown in 50 ml falcon tubes with 10 ml volume of Vogel Bonner (VB) medium (untreated) or VB medium containing 1.1mM 2,2-Dipyridyl (iron limiting). Typically, the WT 20265 grows slightly faster in the normal VB medium as compared to the SCV 20265 during the early and mid log phases, but eventually both reach the same optical density towards the stationary and late stationary phase (refer **Figure 3.1.1**). This slight difference in the doubling time is typical and consistent with the slow growing nature of the SCV in comparison to the WT. But there was a completely altered pattern of growth in the presence of 1.1mM 2,2-Dipyridyl. The SCV 20265 showed an early onset of growth while the WT 20265 was still in an extended lag phase (refer **Figure 3.1.2**). This clear ready adaptation of the SCV 20265 to iron limitation stress imposed by the presence of iron chelator 2,2-Dipyridyl was further investigated to demonstrate that the observed growth differences were indeed in response to iron limitation and not due to 2,2-dipyridyl toxicity.
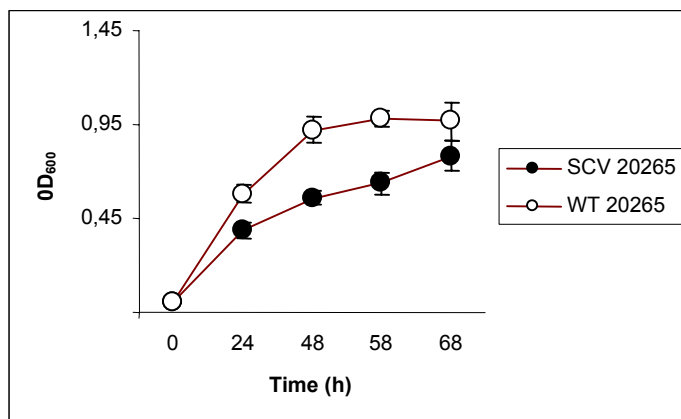
Figure 3.1.1 Growth of SCV 20265 and WT 20265 in the normal Vogel Bonner medium (untreated for iron depletion). The WT 20265 grows faster than SCV 20265 during log phase but both reach the similar optical densities (OD_{600}) towards the stationary phase.
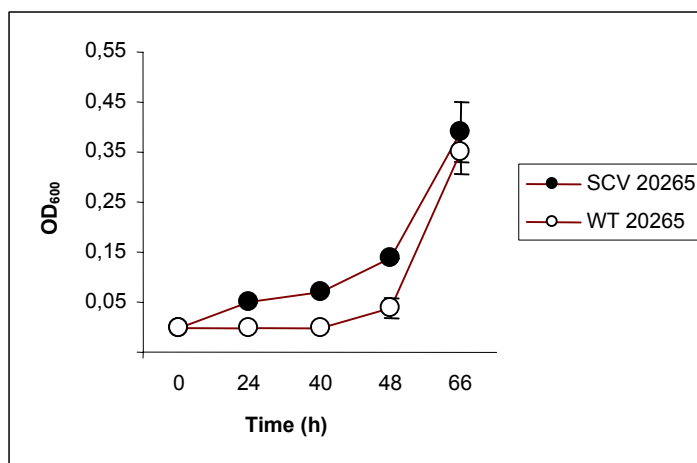
Figure 3.1.2 Growth of SCV20265 and WT 20265 under iron limiting conditions in the presence of 1.1mMDipyridyl in the medium. An early onset of growth of SCV 20265 between 0 and 48 hours is in sharp contrast with the extended lag phase of WT 20265.

It was interesting to note that although an early onset of growth of SCV 20265 was detectable, WT 20265 eventually grew after an extended lag phase of about 48 hours in the presence of 1.1mM 2,2-Dipyridyl. Thus the iron chelation in the presence of 1.1mM dipyridyl was not potent enough to restrict the growth of even the poorly adapted morphotype. Therefore iron limitation by 2,2-Dipyridyl was tested over a range of concentrations starting from 0.1mM to 11mM, in order to determine the most appropriate concentration for our experiments to study the inter-morphotype differential response to iron limitation. Accordingly, at 11mM of the chelator concentration in the medium, it was possible to achieve a complete iron depletion indicated by a complete inhibition of growth of both the morphotypes. Using this concentration of chelator in the medium as an ideal negative control, a range of concentrations of Ferrous iron salt, $FeSO_4$ was supplemented in order to revive the growth of the bacteria.

2,2-dipyridyl is an iron chelator with selectivity for Fe^{2+} ions. It chelates Fe^{2+} ions in a 3:1 ratio. Therefore, a 11mM concentration of dipyridyl can be expected to chelate approximately 3.6mM Fe^{2+}. It is likely that between 3.5mM to 3.0mM $FeSO_4$ supplementation there exists a near perfect iron depletion condition. Accordingly, at around 3.3mM of $FeSO_4$ supplement in the medium containing 11mM 2,2-dipyridyl would present a situation where the iron chelation is in a dynamic equilibrium with scarce amount of ferrous available for the bacteria to utilize, which in turn would mimic an iron limited condition.

A range of concentrations of $FeSO_4$ starting from 3.0mM to 10mM was supplemented in the presence of fixed amount of 11mM of 2,2-dipyridyl and bacteria inoculated into 1 ml of medium in 2ml eppendorf tubes. 2 ml eppendorf tubes were used in order to device a high-throughput screening system where several conditions with varying concentrations of chelator and iron supplement could be tested in parallel for both the morphotypes with greater ease of handling as compared to using vessels of higher volume. To provide exchange of gases a tiny hole of 0.5mm radius was punched on top of the eppendorfs using a sterile needle. The results of the growth pattern of the morphotypes of 20265 are shown in the **figure 3.1.3**. The cells grew in thick non-dispersible clumps in the small volume of 1ml and so growth could not be quantified by conventional CFU counting or by measuring the optical density at 600nm, because representative sampling was difficult to obtain. Therefore, total protein concentration was estimated by Bradford method and the protein concentration was used a measure of growth. Most important observation was the ability of SCV 20265 to grow even at the least supplemented levels of $FeSO_4$, i.e.3.3mM, while there was no growth of the WT at this iron limiting concentration of supplement. There was no growth of any of the morphotypes at 3.0mM concentrations of $FeSO_4$ supplement because the chelator outnumbers the ferrous ions. There was no growth of any of the morphotypes in the unsupplemented tubes, which served as a negative control (refer **2 in Fig. 3.1.3**). However at higher concentrations of supplemented $FeSO_4$ (3.5mM, 4.0mM and 5.0mM FeSO4; refer **4,5,6 in Fig 3.1.3**) the WT grew, as did the SCV. In a normal medium lacking iron chelator (refer **1 in Fig 3.1.3**), the WT outgrew the SCV. This clearly demonstrates the ability of SCV to survive and thrive under iron limiting conditions as compared to WT 20265. Growth of SCV needed a minimum supplementation of 3mM in the presence of 11mM dipyridyl.
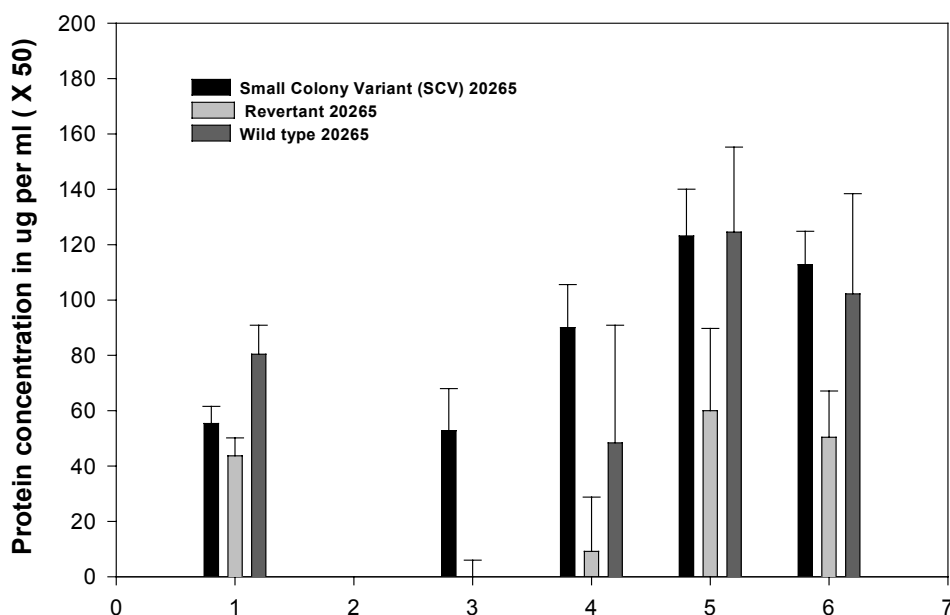
Figure 3.1.3 Growth of *P. aeruginosa* 20265 morphotypes - SCV, wildtype and revertant under iron limitation and supplementation, measured as a function of protein concentration after 96 hours of growth. Shown here are values representing the average mean and calculated standard deviation of protein concentrations from three independent experiments carried out with triplets for each experimental condition. **1)** Normal Vogel Bonner (VB) medium (+Control), **2)** Iron depleted VB (IDVB) Medium (-ve control), **3)** IDVB +3.0mM FeSO4, 4**)** IDVB + 3.5 mM FeSO$_4$, **5)** IDVB + 4.0 mM FeSO$_4$, **6)** IDVB + 5.0mM FeSO$_4$.

Notably, SCV alone were able to grow at 3mM FeSO$_4$ while revertant and wildtype, even after incubation for 96 hours did not grow up to any significant level as compared to the SCVs (refer **3 in Fig 3.1.3**). However, all the three morphotypes grew in the presence of FeSO$_4$ at concentrations of 3.5mM onwards. Optimal growth (comparable to growth in iron rich condition) occurred upon supplementing the media with 4.0mM to 5.0mM FeSO$_4$.

Morphotypes of two other strains, namely 10 and 29 were tested for their ability to grow under the iron limiting conditions described above. The results are presented in the **table 3.1.1** below. The 10 WT and 29 SCV were found to grow with 3.0mM FeSO$_4$ supplement (i.e. iron limiting condition) much like the SCV 20265. Other iron sources such as Ferric citrate, haemoglobin and haemin chloride were also supplemented instead of FeSO$_4$ in order to check if there was any differential preference for certain iron sources. But observable growth was detected only with the FeSO$_4$ supplementation.

Table 3.1.1. **Summary of growth patterns of the different morphotypes tested for growth under iron limiting and iron replete conditions with different sources of iron.** 'Yes' indicates growth 'No' indicates absence of growth and 'Part Yes' indicates partial growth or poor growth. (SCV- Small colony variant, REV-Revertant, WT – Wildtype)

Strain / morphotype	FeSO$_4$		Ferric citrate	Porphyrin	
	10mM (iron rich)	3mM (iron deplete)	10^{-4}M	Haemoglobin (10^{-4}M-10^{-6}M)	Hemin Chloride (10^{-4}M-10^{-6}M)
20265 SCV	Yes	Yes	No	No	No
20265 REV	Yes	No	No	No	No
20265 WT	Yes	No	No	No	No
10 SCV	Yes	No	No	No	No
10 REV	Yes	No	No	No	No
10 WT	Yes	Yes	No	No	No
29 SCV	Yes	Yes	No	No	No
29 REV	Yes	Part Yes	No	No	No
29 WT	Yes	No	No	No	No

3.1.2   Differential growth response to different iron sources

Even though the initial approach to study the inter-morphotypic differential responses encompassed the investigations of *in vitro* generated revertant too, it was becoming increasingly evident from iron limitation assays and other phenotypic traits and experiments of Wehmhöner (2003) and Götz (2003) that the revertant itself was not a genuine reversion of the SCV back to its clonal Wildtype phenotype. This was evident from the fact that the revertant was different from the wildtype and SCV and so it was reasonable to assume that the revertant could be the product of a mutation or genetic switch mechanism that is independent of the ones that lead to the occurrence of SCV from the Wildtype. So further analysis of inter-morphotype studies were restricted to only the clonal SCV and wildtype pairs of any stain used. This was done partially to simplify the problem and to enable easier and efficient handling of the experiments. Therefore any results of the present study must be experimentally verified in the revertant also in order to make the picture complete. As the results of the experiments presented in the previous **section 3.1.1**, indicated a greater preference for iron in the form of Fe^{2+}, differential preference of SCV and WT for different iron sources was tested using an agar plate assay. For details about how the assay was performed refer to the relevant section in the Materials and Methods section. After testing a range of concentrations of the chelator 2,2-Dipyridyl suitable for bringing about complete iron

limitation and inhibition of growth in this plate assay, it was found that 1.1mM 2,2-Dipyridyl was optimal. This is only one tenth the concentration of chelator used in the liquid assays described in **section 3.1.1**. The results of this assay performed with strain 20265 morphotpes is presented in **figure 3.1.4**.Colonies of SCV 20265 appeared around the discs of all the different iron supplements while no WT 20265 grew around any of the discs in spite of prolonged incubation. An interesting observation was that when the chelator 2,2-Dipyridyl concentration was lowered to about half (i.e. from 1.1mM to 0.5 mM) substantial number of colonies of WT 20265 also began to appear around $FeSO_4$ (source of Fe^{2+}) and haemoglobin supplemented discs. This is clearly suggestive of the ability of SCV 20265 to mobilize different sources of iron efficiently in the presence of iron chelators. A negative control included in the experiment had only sterile deionised water spotted on the discs and showed no growth of colonies of neither SCV nor WT. This clearly showed that the observed growth was dependent only on iron availability and not due to 2,2-Dipyridyl toxicity.

Another interesting observation was that relatively more bacterial colonies appeared around the Ferrous (Fe^{2+}) supplemented discs as compared to the number of colonies growing around the other sources of iron. The colonies also appeared much earlier than the colonies around the other iron sources. This indicates the greater preference for iron in the form of Ferrous ions as compared to the other sources like ferric or haem or haemin.

| | Deionised water (-ve control) | Ferrous Fe(II) | Ferric Fe(III) | Haemoglobin | Haemin |
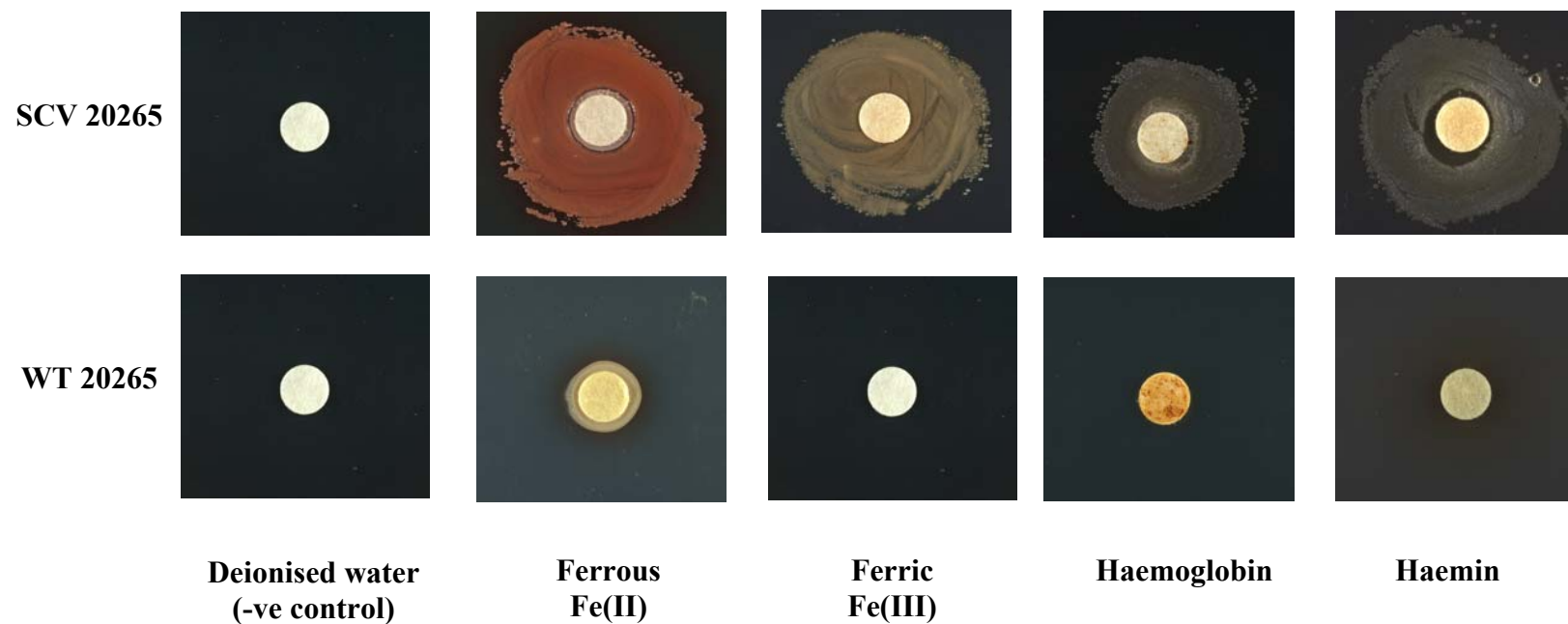
Figure. 3.1.4 Iron supplementation assay. Bacteria were spread as a lawn on an iron depleted VB agar plate containing 1.1mM 2,2-dipyridyl by diluting 100μL bacterial suspension in 3.0ml of 0.6% VB agar containing 1.1mM of 2,2-dipyridyl. Sterile filter paper discs were laid on the lawn of bacteria and 8μl of different iron sources were spotted. Shown here are the appearance of colonies around the discs for SCV 20265 and complete absence of growth for WT 20265. (Note: the small ring around the Fe(II) disc of WT 20265 is not because of bacterial growth and is due to the precipitated iron salt.)

Table 3.1.2. Differential response of morphotypes to iron supplementation under two different iron depletion conditions. A plus indicates appearance of growing colonies around the sterile filter paper discs spotted with the different iron sources mentioned, while a minus indicates the absence of any growth in the 2,2-dipyridyl containing iron limiting plates. (+ + + growth in all triplicates; - - - absence of growth in all triplicates)

Strain / Morphotype	1.1mM Dipyridyl				0.5 mM Dipyridyl			
	Ferrous Fe (II) 0.2M	Ferric Fe (III) 0.1M	Haemin Chloride 2mM	Haemo-globin 10^{-4}M	Ferrous Fe (II) 0.2M	Ferric Fe (III) 0.1M	Haemin Chloride 2mM	Haemo-globin 10^{-4}M
SCV 20265	+ + +	+ + +	+ + +	+ + +	+ + +	+ + +	+ + +	+ + +
WT 20265	- - -	- - -	- - -	- - -	+ + +	- - -	- - -	+ + +
SCV 231	- - -	- - -	- - -	- - -	- - -	- - -	- - -	- - -
WT 231	- - -	- - -	- - -	- - -	+ + +	+ + +	+ + +	+ + +
SCV 52	+ + +	+ + +	- - -	- - -	+ + +	+ + +	+ + +	+ + +
WT 52	- - -	- - -	- - -	- - -	+ + +	+ + +	+ + +	+ + +
SCV 8226	- - -	- - -	- - -	- - -	+ + +	+ + +	+ + +	+ + +
WT 8226	+ + +	+ + +	+ + +	+ + +	+ + +	+ + +	+ + +	+ + +

This iron supplementation assay was performed with clonal SCV and WT pairs of three more strains that were members of the subgroup having hyperpiliated, cytotoxic, autoaggregative SCVs of which the strain 20265 is a representative member. The distribution of the ability to adapt and survive iron limitation conditions in the above-described assay, among the members of this subgroup, was tested and the results presented in the **table 3.1.2**.

It can be inferred from the results of the table that the SCV 231 was not as well adapted to iron limitation and couldn't mobilise the iron as well as its clonal wildtype WT 231. This is clear from the complete absence of colonies of SCV 231 around the iron supplemented discs of both the concentrations of the chelator i.e. 1.1mM and 0.5mM. So the SCV 231 was not able to withstand the iron limitation in the first place to be able to subsequently mobilise iron from the discs and utilize it for survival and growth, as did the clonal WT 231.

In the case of strains 52 and 8226, SCV 52 and WT 8226 were found to be fitter than their respective other clonal morphotype, in surviving the iron limitation and subsequently mobilizing the iron for growth. In this respect the WT 8226 and SCV 52 behaved like the SCV 20265. Overall picture presented by the results of experiments in **section 3.1.1** and **3.1.2** can be summarised as below.

SCV 20265 represents a clonal variant that is clearly well adapted to iron limitation in its vicinity. It is also capable of mobilizing the micronutrient, iron from different iron sources and different forms (Fe^{2+}, Fe^{3+}, Haem, Haemin) using its versatile arsenal of iron uptake systems. The distribution of adaptive/survival ability to iron limitation among the clonal morphotypic variants of different strains isolated from the CF lung habitat is variable i.e. not all SCVs are better adapted to iron limitation or mobilization of iron in the presence of a chelator. Thus the iron limitation is perhaps one of the many selection forces operating in various niches of a CF lung, leading to the occurrence of SCVs.

A detailed proteomic analysis of the proteins relevant to the above observations of the SCV 20265 and its clonal WT 20265 under iron limitation stress is discussed in the following **sections 3.1.4 – 3.1.6**.

3.1.3 Western Blot analysis of Fur protein

Ferric uptake regulator (*fur*) is the global regulator of many genes with iron dependent gene expression in *Pseudomonas aeruginosa* (Vasil et al., 2000) and many bacteria including *E.coli* (Escolar et al., 1999). fur acts a positive repressor, i.e. it represses transcription upon interaction in the absence of Fe^{2+}. Binding of Fe^{2+} to fur increases its affinity for its DNA binding site. Hassett et al., (1996) have demonstrated that mutations in the *P. aeruginosa* fur locus affect aerobic growth and SOD and catalase activities in *P. aeruginosa*. *fur* mutants showed increased manganese superoxide dismutase (Mn-SOD) and decreased catalase activities. Sensitivity to both the redox-cycling agent paraquat and hydrogen peroxide was greater in each mutant than in the wild type strain.

Since the present study was aimed at studying the differential response of SCV and WT to iron limitation and oxidative stress, the expression of fur protein in strain 20265 morphotypes was analyzed using western blotting. However, it must be mentioned here that only polyclonal sera raised against *E. coli* fur protein was available and made use of. The *E.coli* anti-fur antibody was received as a gift from Dr.Jose L.Martinez, CNB, Spain.

The blots in **figure 3.1.5** reveal that the anti *fur* antibody locates the *fur* homologue of *P. aeruginosa* of nearly same size (16Kda), but also seems to show some cross reactivity (in few higher molecular weight bands) upon long exposures of 10 min (data not shown). The detection of the specific binding was accomplished by using chemiluminescence reaction of the enzyme coupled secondary antibody using chemiluminescence substrate.
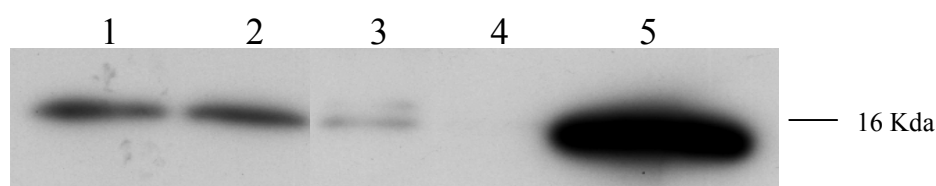
Figure 3.1.5. Western blotting using anti-*fur* antibody (polyclonal) for probing *fur* expression levels in *Pseudomonas aeruginosa* 20265 (Chemiluminescence detection with Photographic film) 1) SCV20265 normal 2) WT20265 normal 3) SCV20265 iron deplete 4) WT iron deplete 5) *E.coli* log phase + ve Control

An *E.coli* log phase (OD_{600} = 0.6; LB medium) total cellular extract was used as a positive control (refer **Lane 5 in fig 3.1.5**). Strongest signals were detected in this lane because the *fur* expression is maximum in a log phase of growth owing to the abundance of iron in a complex medium such as LB. **Lanes 1 and 2** show the fur levels in SCV 20265 and WT 20265 log phase cellular extracts from VB medium. The intensities of signals are relatively low as

compared to the control. One reason for this is attributable to the lesser iron content in the VB medium itself. However in the presence of 1.1mM 2,2-Dipyridyl in the VB medium, the fur expression falls down. This is clearly seen in the signal intensities of **Lanes 3 and 4**. However the faint signal in **Lane 3** (SCV 20265) in contrast with the complete absence of signal in **Lane 4** (WT 20265) is somewhat indicative of the lesser need for iron relative to the lower levels that can be tolerated by WT 20265. The SCV perhaps shuts down the *fur* expression completely only in response to even lower iron limitation than the level used in the above experiment. However the results were only suggestive and not conclusive and warranted the use of *P. aeruginosa* fur specific antibodies to further analyse *fur* expression. This approach needs further investigation. Although attempts were made to locate fur protein on the 2D gels, fur protein still remains elusive. One reason for this could be the possible low levels in which fur might be produced considering its nature of being a transcriptional regulator. The other abundant proteins could be masking the fur preventing its detection in the normal staining methods. Since *fur* is widely acknowledged to play a decisive role in iron metabolism, more focussed approach must be adopted in future studies to determine the dynamics of its expression among the various morphotypes in response to iron limitation.

3.1.4 Proteome analysis of iron limitation stress response

Extensive proteome analysis of strain 20265 was carried out in order to identify the differences in their global gene expression at a protein level. This was important in order to identify candidate gene products that might provide insight into the molecular basis of the differential adaptation observed in the growth experiments discussed in section 3.1.1 and 3.1.2 and to understand the overall behavior and possible causes for the occurrence of SCV phenotype. Cells were grown in VB medium in 1liter culture flasks and harvested at log phase (OD_{600}=0.6) and stationary phase (OD_{600} =1.5). Supernatants were prepared as described in the materials and methods section before. Vogel Bonner medium was an ideal choice because of the minimal salts defining it and the compatibility of its components to sample preparation for proteome analysis.
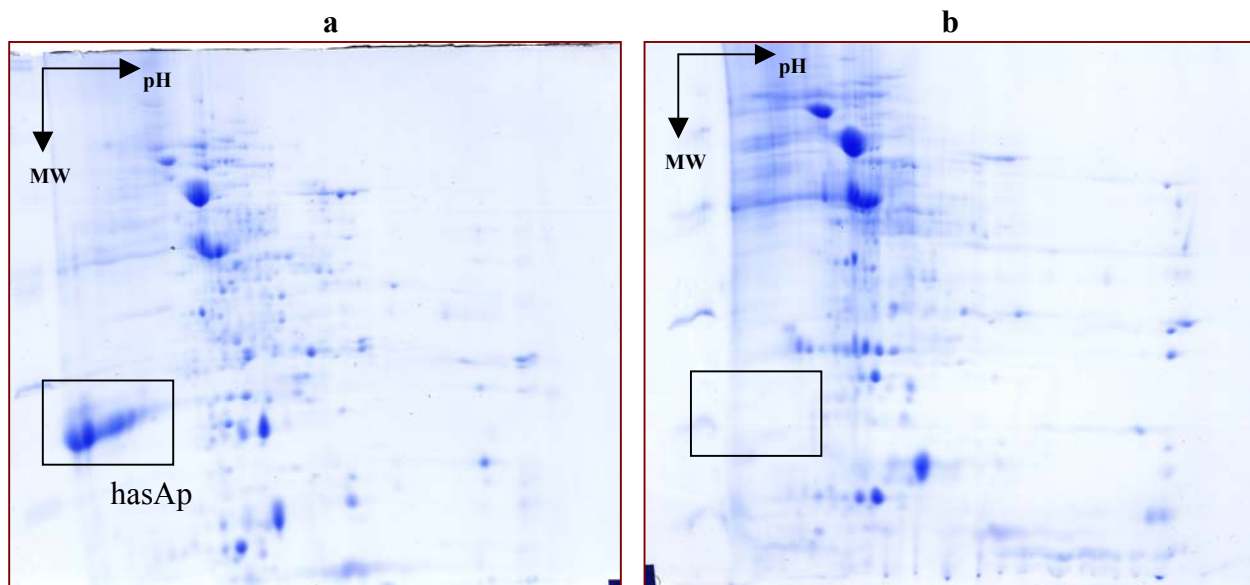
Figure 3.1.6. Supernatant proteins of log phase cultures (OD$_{600}$=0.6) of morphotypes of strain 20265 grown in normal Vogel Bonner medium. Secreted proteins (Secretome) were resolved on an IPG strip of pH range 3-10 and 12-15% linear gradient gel. Abundant secretion of HasAp (hemophore) can be seen in SCV 20265(a), which is hardly detectable in WT 20265 (b) during early log phase of growth.

The log phase supernatants analyzed (refer **figure 3.1.6**) showed the higher expression of *hasAp* (a haemophore) PA3407 in SCV 20265 as compared to the WT 20265.
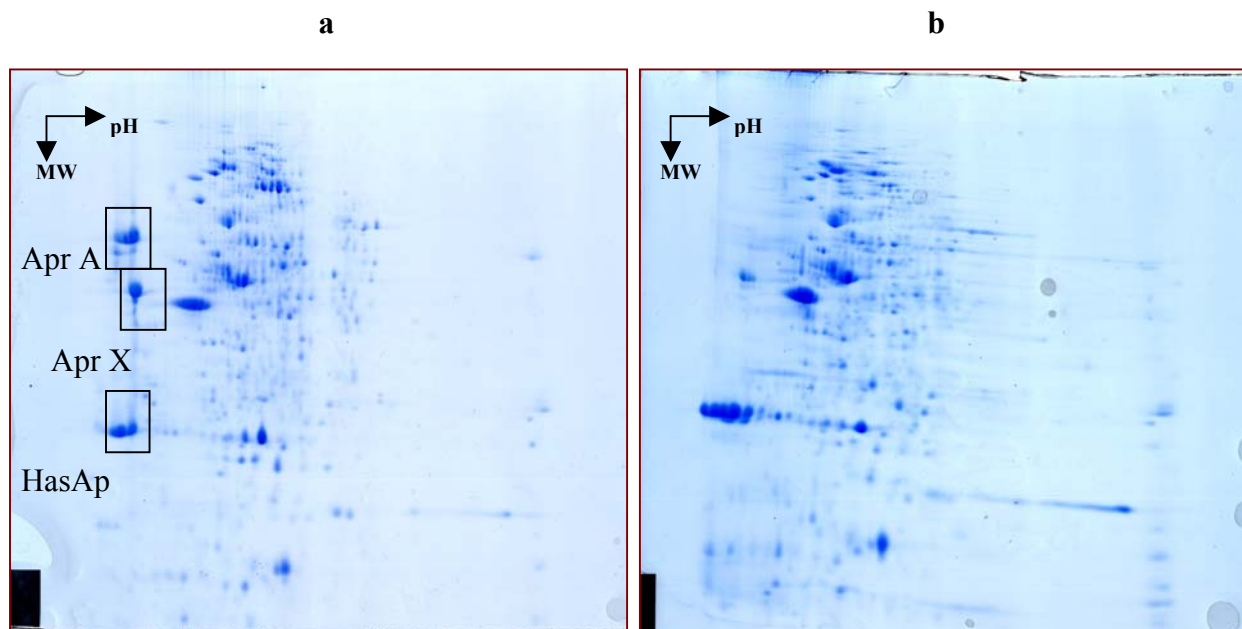
Figure 3.1.7. Supernatant proteins of stationary phase cultures (OD$_{600}$=1.5) of morphotypes of strain 20265 grown in normal Vogel Bonner medium. Secreted proteins (Secretome) were resolved on an IPG strip of pH range 3-10 and 12-15% linear gradient gel. HasAp (hemophore) is detectable as an abundant protein species in both supernatants. SCV 20265 (a) secretes Alkaline metalloproteinase precursor AprA and AprX also in much higher levels compared to WT 20265 (b).

2D gel analysis of late supernatants obtained from stationary phase cultures shown in **figure 3.1.7** revealed that the alkaline metalloproteinase precursor (AprA) was also differentially

69

expressed. Notably, its is widely known that low iron levels induce *AprA* expression. The *hasAp* is also expressed in WT 20265 in significant amounts during stationary phase of growth.

In order to investigate the effect of the iron chelator 2,2-Dipyridyl on the proteome of the morphotypes of strain 20265, SCV and WT were grown aerobically up to a log phase (OD_{600} 0.6) in the normal Vogel Bonner medium. 2,2-Dipyridyl was introduced into the cultures at a final effective concentration of 1.1mM and incubated again for 4 hours along with synchronous cultures lacking 2,2-Dipyridyl. At the end of 4 hours incubation, the cells were harvested from both the 2,2-Dipyridyl treated and untreated cultures, washed and total cellular protein extracted and analysed on a 2D gel. Comparison of the treated and untreated cultures of SCV and WT revealed the effect of 2,2-Dipyridyl on several iron acquisition and oxidative stress related proteins. The **figure 3.1.8** shows the 2D gels prepared from cultures of the morphotypes of strain 20265 with and without iron chelation by 2,2-Dipyridyl. It was interesting to note that although the resolution of a large number of proteins on the 2D gels was achieved, the specific iron-depletion responsive proteome was far from complete. Several proteins that were previously known to be iron regulated were also identified by MALDI TOF/ MS. **Table 3.1.3 and 3.1.4** show a selected list of proteins that were differentially expressed under iron limitation imposed by the presence of 1.1mM of 2,2 Dipyridyl.

Table 3.1.3. Selected list of iron regulated proteins expressed higher in SCV 20265 during growth in the presence of 2,2-Dipyridyl.

PA Number	Protein Name	Gene Name	Function	Class
PA4236	Catalase	katA	Adaptation, protection	Class 1
PA4366	superoxide dismutase	sodB	Adaptation, protection	Class 1
PA3901	Fe(III) dicitrate transport protein FecA	fecA	Transport of small molecules	Class 2
PA4221	Fe(III)-pyochelin outer membrane receptor precursor	fptA	Transport of small molecules	Class 1
PA2398	ferripyoverdine receptor	fpvA	Transport of small molecules	Class 1
PA4470	fumarate hydratase	fumC1	Energy metabolism	Class 1
PA4468	superoxide dismutase	sodM	Adaptation, protection	Class 1
PA4880	probable bacterioferritin		Central intermediary metabolism	Class 3
PA3529	probable peroxidase		Putative enzymes	Class 3
PA2399	pyoverdine synthetase D	pvdD	Adaptation, protection	Class 1

Table 3.1.4. Selected list of proteins expressed higher in WT 20265 during growth in the presence of 2,2-Dipyridyl.

PA4067	Outer membrane protein G precursor	oprG	Membrane proteins	Class 1
PA2476	thiol:disulfide interchange protein	dsbG	Chaperones & heat shock proteins	Class 2
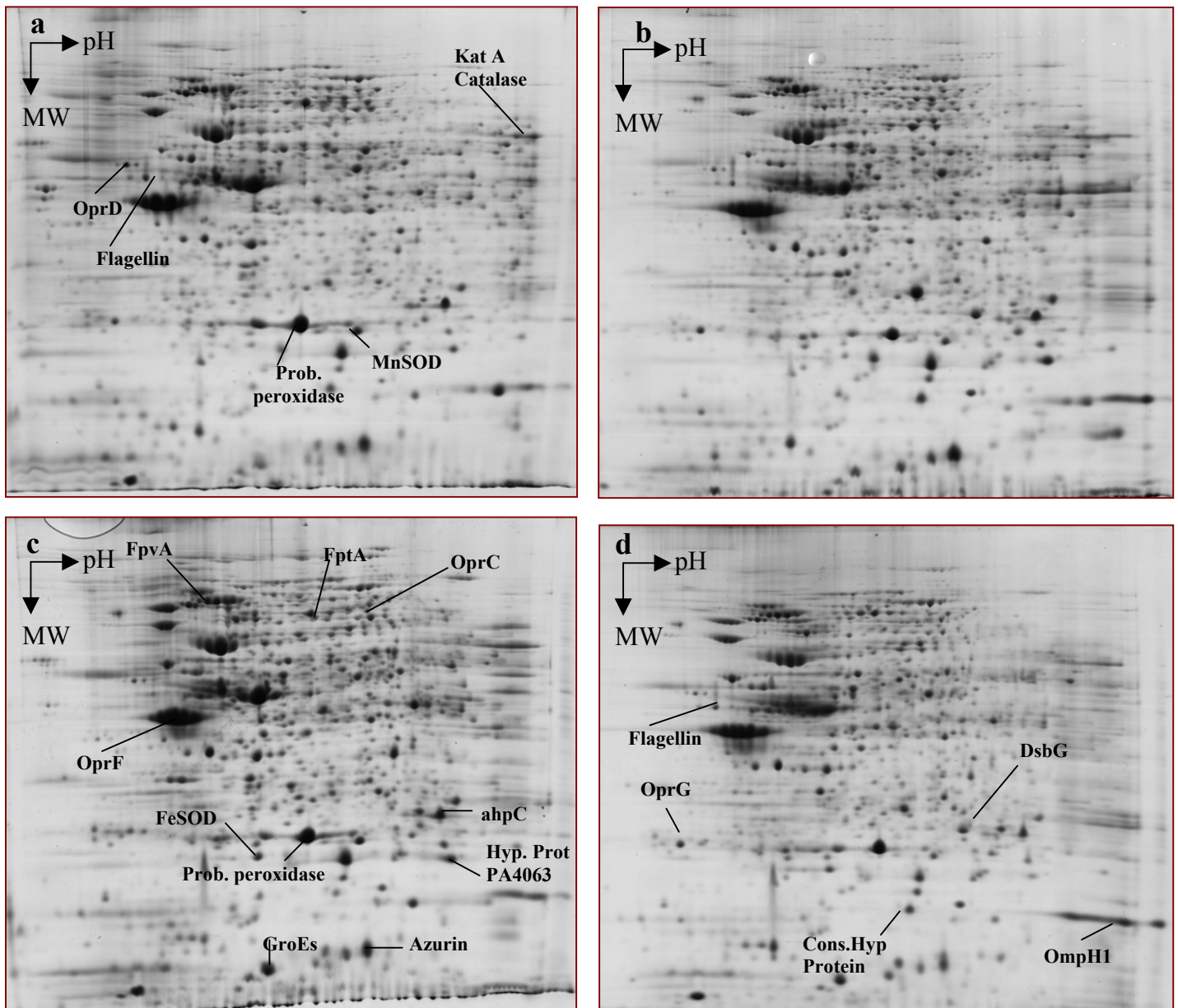
Figure 3.1.8. Cellular protein extracts of SCV 20265 and WT 20265 from 2,2-Dipyridyl treated cultures. Total Cellular protein extracts were resolved on IPG strips of pH range 4-7; 12-15% linear gradient gel. SCV 20265 cellular extract without 2,2-Dipyridyl treatment (a), WT 20265 cellular extract without 2,2-Dipyridyl treatment (b), SCV 20265 cellular extract from 2,2-Dipyridyl treated culture (c), WT 20265 cellular extract from 2,2-Dipyridyl treated culture (d).

The total supernatant proteins from the above cultures were also resolved on the 2D gels and the results are shown in **figure 3.1.8**. The effect of iron chelation on the supernatants was readily detectable as some readily observable protein patterns on the 2D gel.
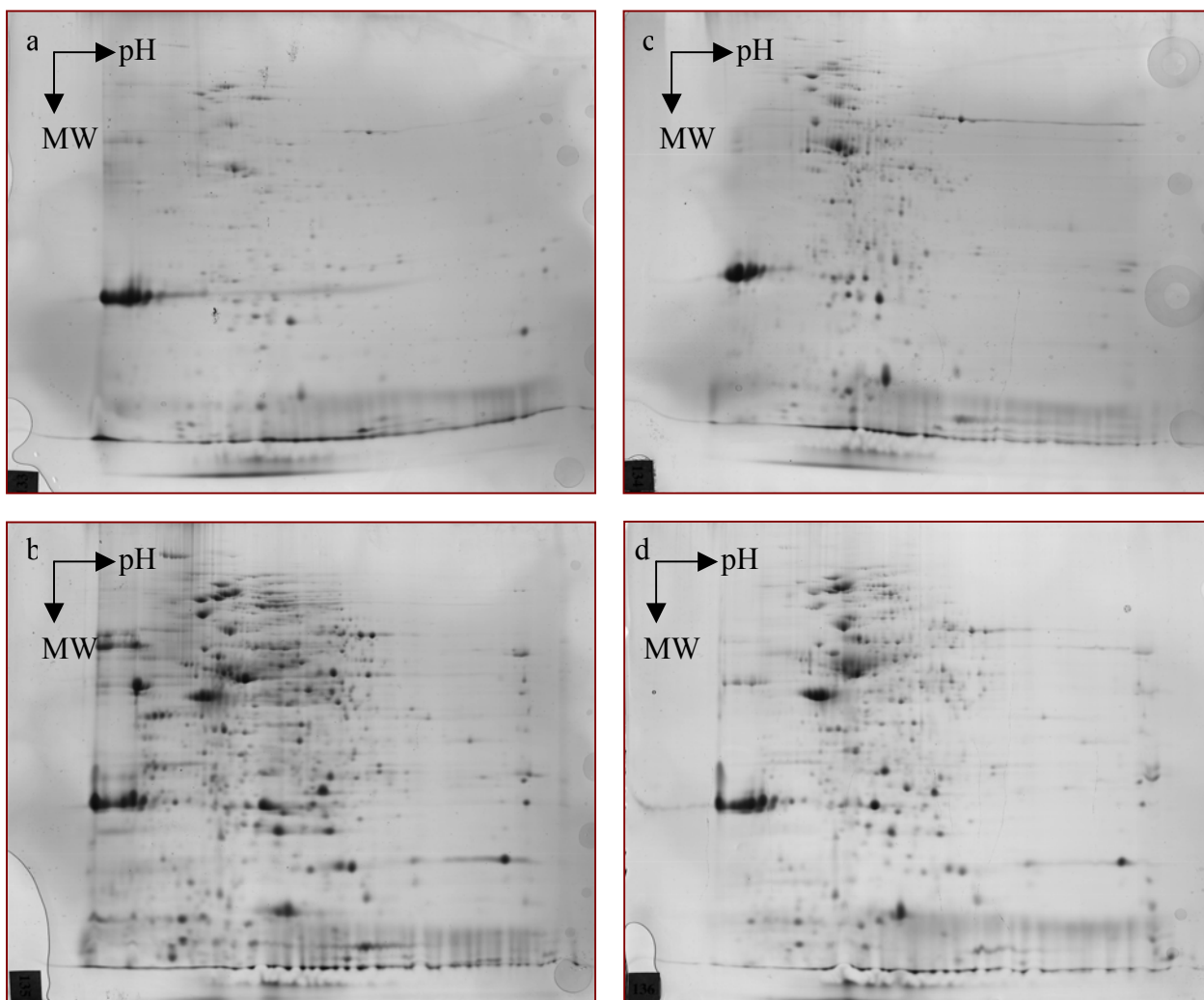
Figure 3.1.9. Supernatant protein extracts of SCV 20265 and WT 20265 from 2,2-Dipyridyl treated cultures. Secretome was resolved on IPG strips of pH range 3-10; 12-15% linear gradient gel. SCV 20265 supernatant from normal VB cultures (a), SCV 20265 supernatant from 1.1mM 2,2-Dipyridyl treated cultures (b), WT 20265 supernatant from normal VB cultures (c), WT 20265 supernatant from 1.1mM 2,2-Dipyridyl treated cultures (d).

However upon identification by peptide mass fingerprinting with MALDI TOF, many of the proteins identified were typical ribosomal proteins and house keeping cellular proteins that were released upon cell lysis. Some typically iron regulated proteins like the Hemophore HasAp and alkaline protease were also detected readily owing to their high abundance.

As most part of the protein profile of soluble cellular proteome, remained the same for both the morphotypes, it became important to adopt subproteome analysis. The membrane subproteome and the secreted supernatant subproteome (secretome) were the most obvious candidates for such analysis. The membrane proteins owing to their relative low abundance and high hydrophobicity mediated poor solubility in conventional IEF buffers, were grossly underrepresented in the 2D gels made from total cellular extract. The supernatants were too

not detected in the cellular extracts. A close look at the secretome was important as many of the virulence determinants such as hemophores, Type III secreted effectors, exotoxins etc. are often a part of the secretome.

3.1.5   Membrane subproteome analysis by 16 BAC system

As with any other subproteomic approach, obtaining the membrane subproteome and secretome involved prefractionation and enrichment of these protein subsets from the whole cell extracts. Details of the seperation and enrichments are available in the materials and methods section. Briefly, the membrane proteins were obtained by subjecting the lysed cells on a sucrose gradient stabilized ultra centrifugation in the presence of protease inhibitors. The harvested cells were lysed by French pressing and subsequently overlayed on to the sucrose gradient as indicated in the materials and methods. Under these conditions of centrifugation, the ribosomal proteins which are the most predominant species of proteins were stabilized and their undesirable dispersal was avoided as much as possible. Membrane proteins obtained this way are not devoid of membrane associated proteins and the structural components of the membrane like the lipid bilayer. Resolution of membrane proteins by 2D gel electrophoresis is a challenging task owing to their hydrophobic nature and precipitation at their pI during isoelectric focusing step. Integral membrane proteins, particularly those with more than one transmembrane domain, have traditionally been difficult to separate by two dimensional electrophoresis methods. In a 16 BAC based separation, the first dimension involves discontinuous gel electrophoresis in an acid buffer system using the cationic detergent 16 BAC (Benzyldimethyl-n-hexadecylammonium chloride). The second dimension consists of discontinuous SDS-PAGE.

Figure 3.1.10 shows the resolution of the membrane enriched protein fractions visualized at the end of first and second dimensional linear separation on gels using 16 BAC detergent.

I - Dimension   II - Dimension
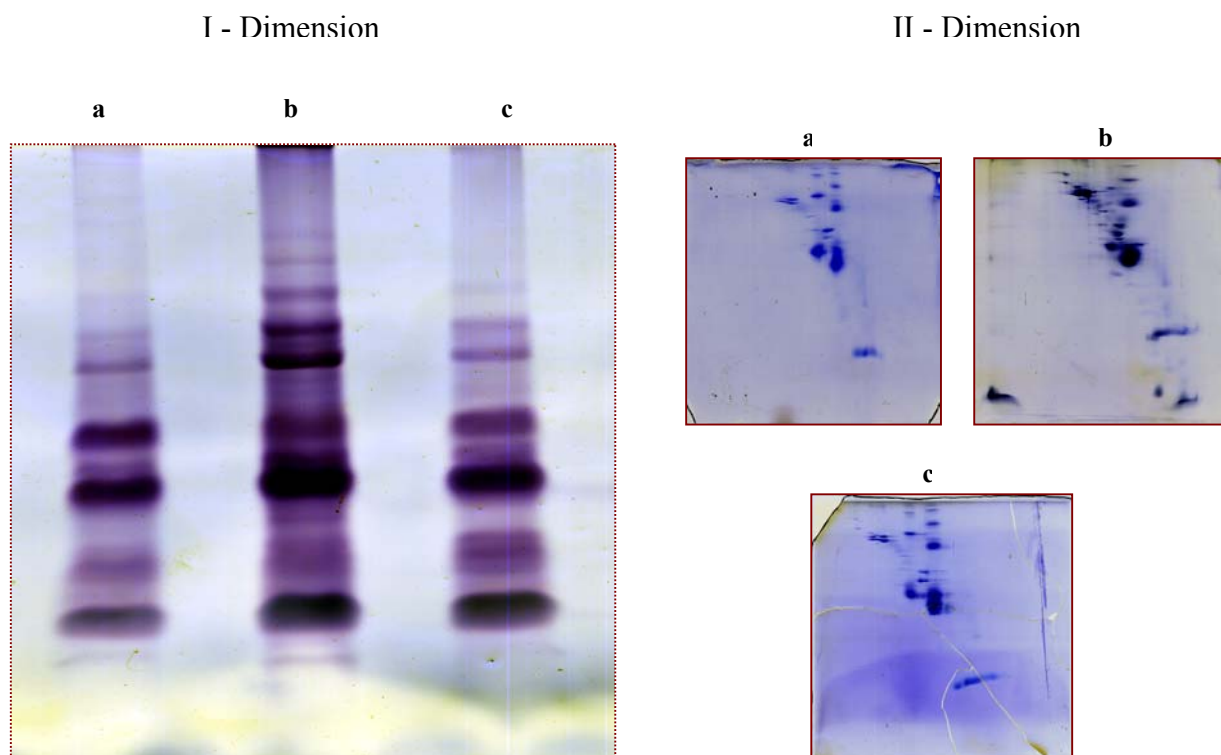
Figure 3.1.10. 16 BAC isolation of membrane protein fraction. Stained and Visualized at the end of I dimension and II dimension. SCV 20265 grown in the presence of 1.1mM Dipyridyl (a), WT 20265 grown in normal VB medium (b), SCV 20265 grown in normal VB medium (c). It can be noted that only few membrane proteins could be resolved on the gels representing a fraction of the total membrane subproteome.

The number of proteins that could be resolved, was arguably less making it difficult to analyze expression levels among different morphotypes. Additionally, the 16 BAC system of resolving membrane proteins was cumbersome and tedious. This made it unfit for handling many samples at a time. It was interesting to know that among the many proteins identified by subsequent MALDI-TOF, haemophore receptor HasR was one among them. HasR is a typical membrane protein with membrane spanning domains and involved in the haemophore (HasAp) mediated haem uptake. A list of membrane proteins identified by MALDI-TOF after resolving on a 16 BAC gel is given in **Table 3.1.5**. **Figure 3.1.11** shows the positions of some of the membrane proteins identified on the 16 BAC gel
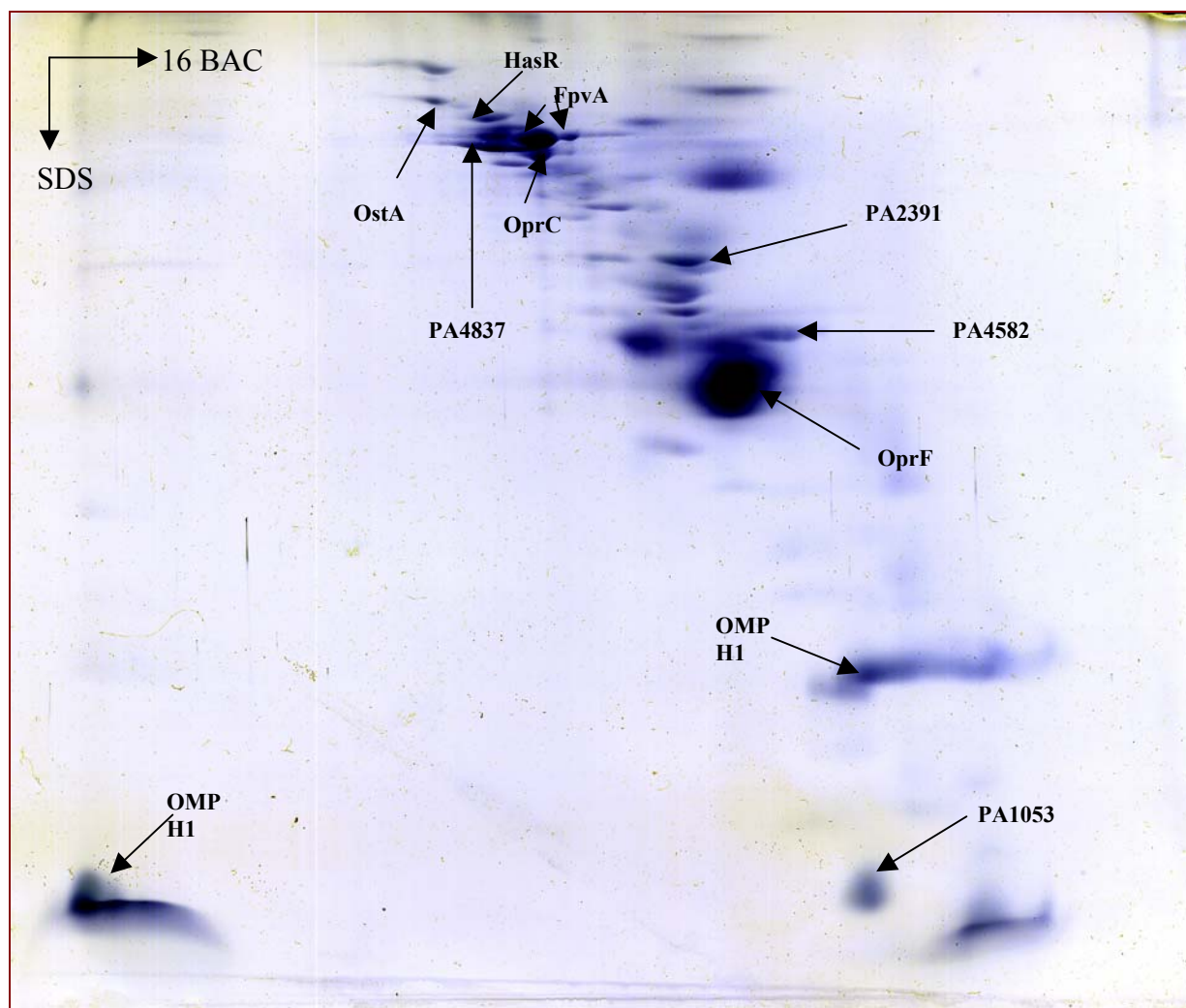
Figure 3.1.11. **Membrane proteins identified by MALDI-TOF** after a resolution on a gel using a 16 BAC system. The gels were stained with colloidal coomassie.

Table 3.1.5. Selected list of membrane proteins resolved using 16 BAC and identified by MALDI-TOF/MS

PA Number	Protein Name	Gene Name	Function	Class
PA3408	Haem uptake outer membrane receptor HasR precursor	hasR	Transport of small molecules	Class 2
PA3790	Putative copper transport outer membrane porin OprC precursor	oprC	Transport of small molecules	Class 1
PA4837	probable outer membrane protein precursor		Membrane proteins	Class 3
PA2391	probable outer membrane protein precursor	opmQ	Membrane proteins;Transport of small molecules	Class 3
PA4582	conserved hypothetical protein		Hypothetical, unclassified, unknown	Class 4
PA1777	Major porin and structural outer membrane porin OprF precursor	oprF	Membrane proteins;Transport of small molecules	Class 1
PA1053	conserved hypothetical protein		Hypothetical, unclassified, unknown;Membrane proteins	Class 4
PA2398	ferripyoverdine receptor	fpvA	Transport of small molecules	Class 1
PA0595	organic solvent tolerance protein OstA precursor	ostA	Adaptation, protection	Class 2
PA1178	PhoP/Q and low Mg2+ inducible outer membrane protein H1 precursor	oprH	Transport of small molecules/Outer membrane protein	Class 1
PA4624	hypothetical protein		Hypothetical, unclassified, unknown	Class 4

Enrichment and prefractionation of membrane proteins and subsequent resolution of the membrane proteins on a 2D gel, was attempted, applying the method described in Nouwens et al., (2000), as an alternative to the cumbersome 16 BAC system and sucrose gradient centrifugation. Briefly, the membrane proteins were obtained by ultra centrifugation of sodium carbonate treated membranes and membrane proteins solubilized in a conventional IPG buffer that has CHAPS replaced by ASB-14 and DTT replaced by Tributyl phosphine. More detailed protocol is available in the materials and methods section. ASB-14 is a zwitterionic detergent like CHAPS (used for solubilising cytosolic proteins during IEF) with a better ability to solubilize many of the hydrophobic integral membrane that are often not solublized by CHAPS proteins. Results (data not shown) revealed that the carbonate extraction of integral membrane proteins seemed to be not as efficient as the sucrose gradient strategy and henceforth the method had to be abandoned. Further analysis of the membrane subproteome was all restricted to sucrose gradient prefractionated membranes.

3.1.6 Nano flow LC/MS analysis of membrane and supernatant subproteomes

 Special gel based seperation of membrane proteins using the 16 BAC system or using special detergents like ASB14 were highly challenging and cumbersome. The number of proteins resolved was a far cry from the number of proteins that would represent a subproteome at any give time. Therefore, the outputs from these conventional strategies were less informative. So, a sophisticated gel less nano flow LC/MS based identification of proteins in membrane enriched fractions and later supernatants, was adopted owing to its ease and power of identifying many more proteins than one would identify with the gel based approaches. However, in order to be able to weigh the pros and cons of the gel based resolution and gel less nano flow LC/MS based approach to analyze complex subproteomes like membrane proteins and supernatant proteins (secretome), an attempt was made to first resolve the membrane fractions with a 16 BAC system using BAC detergent for solubilising the membrane proteins of the morphotypes of strain 20265.

Nano flow LC/MS was used to investigate the membrane and supernatant protein patterns which are likely to be affected most by the presence of 2,2-Dipyridyl in the medium than the cyosolic proteins. Majority of the membrane proteins are not amenable for 2D gel analysis using conventional buffers owing to their hydrophobicity and hence poor solubility. Nanoflow LC/MS based gel free analysis proved to be a much more efficient strategy. It was ideal for

handling many samples at any one time. **Figure 3.1.12** shows the schematic representation of the nanoflow LC/MS to analyze subproteomes.
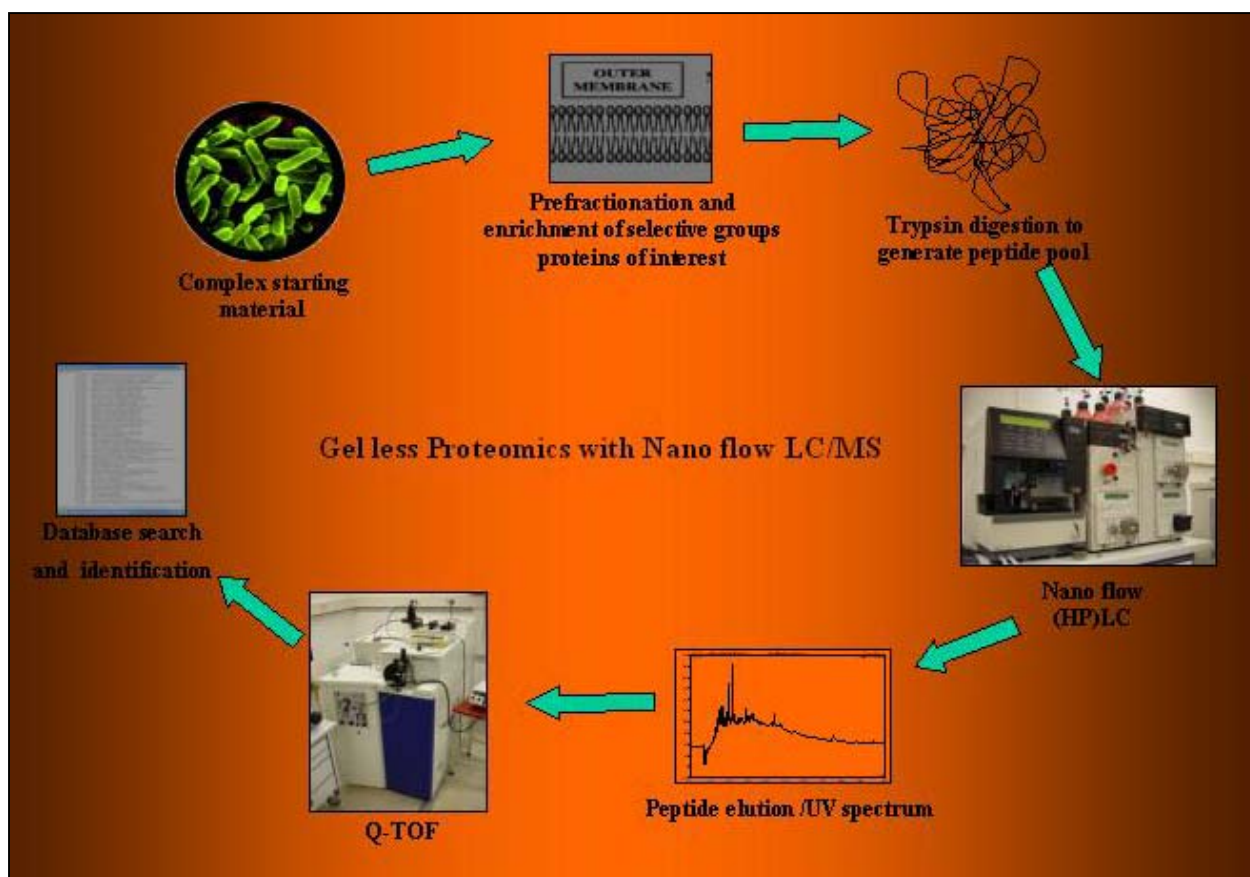
Figure 3.1.12. Schematic representation of a subproteome analysis by nanoflow LC/MS approach.

During a nano flow LC/MS analysis the HPLC generates UV spectra of the various peptides eluted from the complex tryptic digest based on their hydophobicity into the steady flowing stream of a solvent gradient over the entire period of flow through the separation column. These spectra are particularly useful for assessing the concentration of peptides eluted. Even though these spectra are by themselves not informative about protein patterns in the samples, they are useful in normalization of the peptide loads for different samples being compared. **Figure 3.1.13** reveals the nearly equal amounts of protein digests from different samples of SCV and WT 20265 used. **Figure 3.1.14** gives an overview of the number of proteins identified by LC/MS approach from membrane and supernatant proteins-enriched fraction of SCV 20265 and WT 20265 grown under normal and iron limited conditions. In response to iron limitation, the number of detected secreted proteins increased while the number of detected membrane proteins detected. Overall, more iron responsive proteins could be detected in SCV 20265 fractions as compared to WT 20265 fractions.
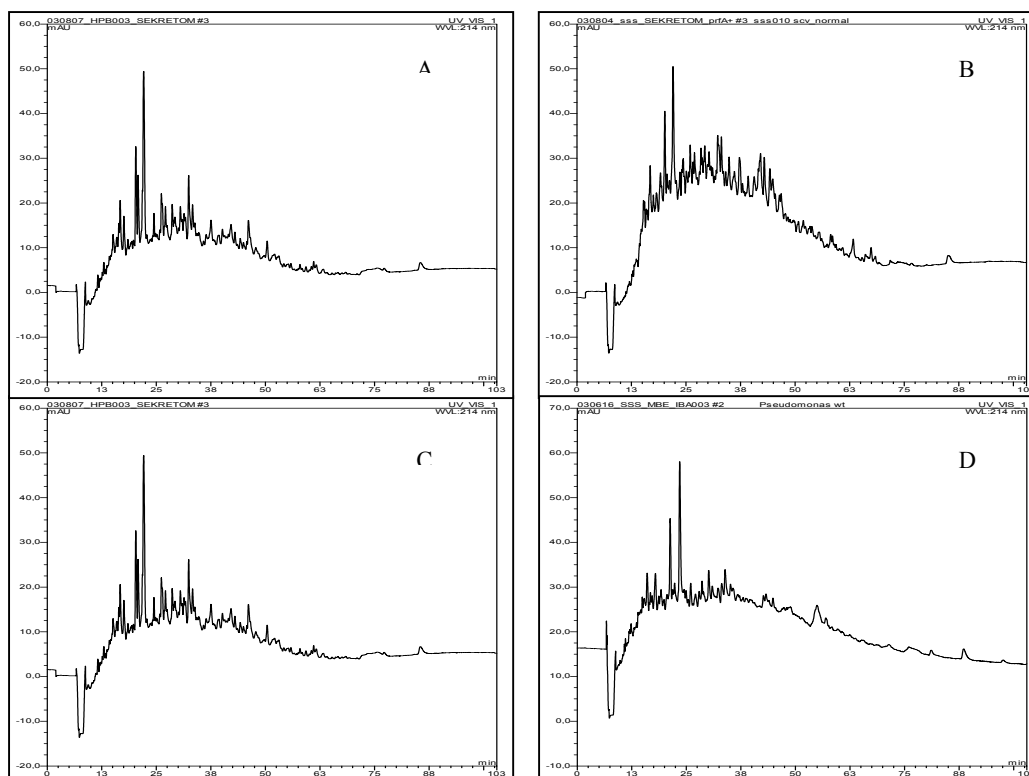
Figure 3.1.13. UV spectra of the various protein digests of membrane proteins of SCV 20265 and WT 20265 used for analysis with nano flow LC/MS. SCV 20265 iron limited membrane subproteome (A), SCV 20265 normal membrane subproteome (B), WT 20265 iron limited membrane subproteome (C), WT 20265 normal membrane subproteome (D). Peaks correspond to the eluted peptides.
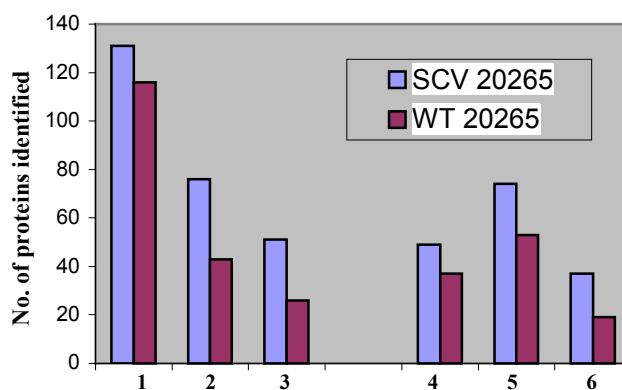
Figure 3.1.14 Overview of the LC/MS analysis of supernatant proteins and membrane proteins of SCV 20265 and WT 20265 under normal and iron limiting growth conditions. **Membrane proteins (1-3):** Membrane proteins detected after growth in normal VB medium (1); Membrane proteins detected after growth iron limited VB medium (2); morphotype specific iron limited membrane proteins (3). **Supernatant proteins (4-6):** supernatant proteins detected after growth in normal VB medium (4); supernatant proteins detected after growth in iron limited VB medium (5); morphotype specific iron limited supernatant proteins (6).

The results of the significant hits of proteins, identified from the membrane fractions and supernatants of SCV 20265 and WT 20265 grown under normal and iron limiting conditions are listed in the **tables 3.1.6–3.1.17**.

Table 3.1.6. List of proteins detected in the membrane enriched fraction of iron starved SCV20265 grown in the presence of 1.1mM 2,2-Dipyridyl in the Vogel Bonner medium. These proteins were not detected in the SCV 20265 in the absence of 2,2-Dipyridyl in the medium.

PA Number	Gene Name	Protein Name	Function	Class	Mass	Score	Peptides matched
PA0595	OstA	organic solvent tolerance protein OstA precursor	Adaptation, protection	Class 2	104207	31	3
PA0962		probable dna-binding stress protein	Adaptation, protection	Class 3	17482	57	1
PA2386	PvdA	L-ornithine N5-oxygenase	Adaptation, protection	Class 1	49447	311	6
PA2424		probable non-ribosomal peptide synthetase	Adaptation, protection	Class 3	479998	29	9
PA4290		probable chemotaxis transducer	Adaptation, protection;Chemotaxis	Class 3	58368	53	1
PA2399	PvdD	pyoverdine synthetase D	Adaptation, protection;Secreted Factors (toxins, enzymes, alginate)	Class 1	273510	83	1
PA4671		probable ribosomal protein L25	Adaptation, protection;Translation, post-translational modification, degradation	Class 3	21949	96	4
PA1927	MetE	5-methyltetrahydropteroyltriglutamate-homocysteine S-methyltransferase	Amino acid biosynthesis and metabolism	Class 2	86157	40	3
PA3068	GdhB	NAD-dependent glutamate dehydrogenase	Amino acid biosynthesis and metabolism	Class 2	182525	70	3
PA5323	ArgB	acetylglutamate kinase	Amino acid biosynthesis and metabolism	Class 2	31829	62	1
PA3108	PurF	Amidophosphoribosyltransferase	Amino acid biosynthesis and metabolism;Nucleotide biosynthesis and metabolism	Class 2	55335	59	2
PA2261		probable 2-ketogluconate kinase	Carbon compound catabolism	Class 3	34020	31	2
PA4412	MurG	UDP-N-acetylglucosamine--N-acetylmuramyl-(pentapeptide) pyrophosphoryl-undecaprenol N-acetylglucosamine transferase	Carbon compound catabolism;Cell wall / LPS / capsule	Class 2	37775	54	1
PA1528	ZipA	cell division protein ZipA	Cell division	Class 2	32217	143	2
PA4407	FtsZ	cell division protein FtsZ	Cell division	Class 2	41192	49	1
PA4408	FtsA	cell division protein FtsA	Cell division	Class 2	44618	63	2
PA2393		probable dipeptidase precursor	Central intermediary metabolism	Class 3	49330	347	9
PA3126	IbpA	heat-shock protein IbpA	Chaperones & heat shock proteins	Class 2	16573	194	6
PA3617	RecA	RecA protein	DNA replication, recombination, modification and repair	Class 1	36856	82	2
PA1552		probable cytochrome c	Energy metabolism	Class 3	34622	96	2
PA1553		probable cytochrome c oxidase subunit	Energy metabolism	Class 3	22744	51	3
PA1787	AcnB	aconitate hydratase 2	Energy metabolism	Class 2	93569	27	2
PA2994	NqrF	Na+-translocating NADH:quinone oxidoreductase, subunit Nqr6	Energy metabolism	Class 2	45441	55	1
PA5490	Cc4	cytochrome c4 precursor	Energy metabolism	Class 2	20721	170	3
PA5554	AtpD	ATP synthase beta chain	Energy metabolism	Class 2	49469	54	1
PA5556	AtpA	ATP synthase alpha chain	Energy metabolism	Class 2	55359	154	4
PA5558	AtpF	ATP synthase B chain	Energy metabolism	Class 2	16946	233	6
PA0946		hypothetical protein	Hypothetical, unclassified, unknown	Class 4	36754	56	1
PA1323		hypothetical protein	Hypothetical, unclassified, unknown	Class 4	11579	38	1
PA2361		hypothetical protein	Hypothetical, unclassified, unknown	Class 4	141260	40	3
PA2392		hypothetical protein	Hypothetical, unclassified, unknown	Class 4	62255	102	3
PA2548		hypothetical protein	Hypothetical, unclassified, unknown	Class 4	51000	28	1
PA2754		conserved hypothetical protein	Hypothetical, unclassified, unknown	Class 4	11867	30	1
PA3481		conserved hypothetical protein	Hypothetical, unclassified, unknown	Class 4	38864	104	1
PA3797		conserved hypothetical protein	Hypothetical, unclassified, unknown	Class 4	29977	25	2

PA3804		hypothetical protein	Hypothetical, unclassified, unknown	Class 4	36081	121	2
PA3848		hypothetical protein	Hypothetical, unclassified, unknown	Class 4	50516	42	2
PA3988		hypothetical protein	Hypothetical, unclassified, unknown	Class 4	22870	40	1
PA4372		hypothetical protein	Hypothetical, unclassified, unknown	Class 4	38300	118	2
PA4452		conserved hypothetical protein	Hypothetical, unclassified, unknown	Class 4	10771	29	1
PA4656		conserved hypothetical protein	Hypothetical, unclassified, unknown	Class 4	33831	57	1
PA5037		hypothetical protein	Hypothetical, unclassified, unknown	Class 4	57412	52	1
PA1245		hypothetical protein	Hypothetical, unclassified, unknown;Membrane proteins	Class 4	41392	439	6
PA5473		conserved hypothetical protein	Hypothetical, unclassified, unknown;Membrane proteins	Class 4	63222	76	1
PA5568		conserved hypothetical protein	Hypothetical, unclassified, unknown;Membrane proteins	Class 4	64034	73	2
PA2853	OprI	Outer membrane lipoprotein OprI precursor	Membrane proteins	Class 1	8829	56	1
PA4370	IcmP	Insulin-cleaving metalloproteinase outer membrane protein precursor	Membrane proteins	Class 1	47202	301	7
PA0969	TolQ	TolQ protein	Membrane proteins;Transport of small molecules	Class 1	25266	117	2
PA0973	OprL	Peptidoglycan associated lipoprotein OprL precursor	Membrane proteins;Transport of small molecules	Class 1	17914	78	3
PA2520	CzcA	RND divalent metal cation efflux transporter CzcA	Membrane proteins;Transport of small molecules	Class 2	113805	34	6
PA3901	FecA	Fe(III) dicitrate transport protein FecA	Membrane proteins;Transport of small molecules	Class 2	85415	69	3
PA4224	PchG	pyochelin biosynthetic protein PchG	Membrane proteins;Transport of small molecules	Class 1	37673	197	4
PA3050	PyrD	Dihydroorotate dehydrogenase	Nucleotide biosynthesis and metabolism	Class 2	36106	48	1
PA4756	CarB	Carbamoylphosphate synthetase large subunit	Nucleotide biosynthesis and metabolism;Amino acid biosynthesis and metabolism	Class 1	117257	40	2
PA3820	SecF	secretion protein SecF	Protein secretion/export apparatus	Class 2	33021	27	2
PA0953		probable thioredoxin	Putative enzymes	Class 3	16885	89	2
PA2815		probable acyl-CoA dehydrogenase	Putative enzymes	Class 3	88707	72	1
PA0641		probable bacteriophage protein	Related to phage, transposon, or plasmid	Class 3	130710	33	7
PA1249	AprA	alkaline metalloproteinase precursor	Secreted Factors (toxins, enzymes, alginate)	Class 1	50402	248	5
PA1246	AprD	alkaline protease secretion protein AprD	Secreted Factors (toxins, enzymes, alginate);Protein secretion/export apparatus	Class 1	63631	41	1
PA0963	AspS	aspartyl-tRNA synthetase	Transcription, RNA processing and degradation	Class 2	66166	68	4
PA2976	Rne	ribonuclease E	Transcription, RNA processing and degradation	Class 2	117395	158	4
PA4269	RpoC	DNA-directed RNA polymerase beta* chain	Transcription, RNA processing and degradation	Class 2	154287	86	3
PA3656	RpsB	30S ribosomal protein S2	Translation, post-translational modification, degradation	Class 2	27319	126	2
PA4272	RplJ	50S ribosomal protein L10	Translation, post-translational modification, degradation	Class 2	17623	55	1
PA4273	RplA	50S ribosomal protein L1	Translation, post-translational modification, degradation	Class 2	24219	26	1
PA4432	RpsI	30S ribosomal protein S9	Translation, post-translational modification, degradation	Class 2	14606	27	1
PA4808	SelA	L-seryl-tRNA(ser) selenium transferase	Translation, post-translational modification, degradation	Class 2	50261	56	1
PA3745	RpsP	30S ribosomal protein S16	Translation, post-translational modification, degradation;DNA replication, recombination, modification and repair	Class 2	9199	29	1
PA2408		probable ATP-binding component of ABC transporter	Transport of small molecules	Class 3	27048	44	2
PA4222		probable ATP-binding component of ABC transporter	Transport of small molecules	Class 3	61355	92	2
PA0425	mexA	RND multidrug efflux membrane fusion protein MexA precursor	Transport of small molecules;Antibiotic resistance and susceptibility	Class 1	40945	337	9
PA0971	TolA	TolA protein	Transport of small molecules;Membrane proteins	Class 2	37912	89	1
PA4225	PchF	pyochelin synthetase	Transport of small molecules;Secreted Factors (toxins, enzymes, alginate)	Class 1	196962	79	4
PA4226	PchE	dihydroaeruginoic acid synthetase	Transport of small molecules;Secreted Factors (toxins, enzymes, alginate)	Class 1	156325	67	3
PA3271		probable two-component sensor	Two-component regulatory systems	Class 3	127373	107	3

Table 3.1.7 List of proteins detected in the membrane enriched fraction of SCV20265 grown in normal Vogel Bonner medium without any iron chelator 2,2-Dipyridyl.

PA Number	Gene name	Protein name	Function	Class	Mass	Score	Peptides matched
PA0139	AhpC	alkyl hydroperoxide reductase subunit C	Adaptation, protection	Class 2	20529	153	3
PA4761	DnaK	DnaK protein	Adaptation, protection;Chaperones & heat shock proteins;DNA replication, recombination, modification and repair	Class 2	68361	380	11
PA1561	Aer	aerotaxis receptor Aer	Adaptation, protection;Chemotaxis	Class 2	57144	40	3
PA3529	PA3529	probable peroxidase	Adaptation, protection;Putative enzymes	Class 3	21808	196	5
PA4235	BfrA	Bacterioferritin	Adaptation, protection;Transport of small molecules	Class 1	17929	33	1
PA0316	Sera	D-3-phosphoglycerate dehydrogenase	Amino acid biosynthesis and metabolism	Class 2	44189	195	6
PA0895	AruC	N-succinylglutamate 5-semialdehyde dehydrogenase	Amino acid biosynthesis and metabolism	Class 1	43720	55	1
PA1685	MasA	enolase-phosphatase E-1	Amino acid biosynthesis and metabolism	Class 2	26455	54	1
PA1750	PA1750	phospho-2-dehydro-3-deoxyheptonate aldolase	Amino acid biosynthesis and metabolism	Class 2	39108	55	1
PA3164	PA3164	still frameshift 3-PHOSPHOSHIKIMATE 1-CARBOXYVINYLTRANSFERASE prephenate dehydr	Amino acid biosynthesis and metabolism	Class 2	79271	85	1
PA4402	Arg	Glutamate N-acetyltransferase	Amino acid biosynthesis and metabolism	Class 2	41736	42	1
PA5171	ArcA	arginine deiminase	Amino acid biosynthesis and metabolism	Class 1	46407	48	2
PA5429	AspA	Aspartate ammonia-lyase	Amino acid biosynthesis and metabolism	Class 2	51038	33	1
PA4696	Ilv	acetolactate synthase large subunit	Amino acid biosynthesis and metabolism;Biosynthesis of cofactors, prosthetic groups and carriers	Class 2	62978	45	3
PA2623	Icd	isocitrate dehydrogenase	Amino acid biosynthesis and metabolism;Carbon compound catabolism;Energy metabolism	Class 2	45548	155	3
PA5015	AceE	pyruvate dehydrogenase	Amino acid biosynthesis and metabolism;Energy metabolism	Class 1	99501	312	9
PA2744	ThrS	threonyl-tRNA synthetase	Amino acid biosynthesis and metabolism;Translation, post-translational modification, degradation	Class 2	73034	46	3
PA2019	PA2019	RND multidrug efflux membrane fusion protein precursor	Antibiotic resistance and susceptibility;Transport of small molecules; inner membrane	Class 2	42061	69	2
PA4054	Rib	GTP cyclohydrolase II / 3,4-dihydroxy-2-butanone 4-phosphate synthase	Biosynthesis of cofactors, prosthetic groups and carriers	Class 2	39413	52	2
PA2323	PA2323	probable glyceraldehyde-3-phosphate dehydrogenase	Carbon compound catabolism	Class 3	59923	92	3
PA3636	KdsA	2-dehydro-3-deoxyphosphooctonate aldolase	Carbon compound catabolism;Cell wall / LPS / capsule	Class 1	31123	41	1
PA0482	GlcB	malate synthase G	Carbon compound catabolism;Central intermediary metabolism	Class 2	78611	139	5
PA0552	Pgk	phosphoglycerate kinase	Carbon compound catabolism;Energy metabolism	Class 2	40379	47	2
PA5427	AdhA	alcohol dehydrogenase	Carbon compound catabolism;Energy metabolism;cytoplasmic	Class 2	35889	112	2
PA4481	MreB	rod shape-determining protein MreB	Cell division;Cell wall / LPS / capsule	Class 2	36953	85	4
PA1800	Tig	trigger factor	Cell division;Chaperones & heat shock proteins	Class 2	48552	66	2
PA4751	FtsH	cell division protein FtsH	Cell division;inner membrane	Class 2	69911	103	2
PA3244	Mind	cell division inhibitor MinD	Cell division;'Inner membrane-associated	Class 2	29617	74	1
PA4941	HflC	protease subunit HflC	Cell division;Translation, post-translational modification, degradation	Class 2	33095	42	3
PA4942	HflK	protease subunit HflK	Cell division;Translation, post-translational modification, degradation	Class 2	44018	130	3
PA3643	LpxB	lipid A-disaccharide synthase	Cell wall / LPS / capsule	Class 2	41268	63	4
PA4406	LpxC	UDP-3-O-acyl-N-acetylglucosamine deacetylase	Cell wall / LPS / capsule	Class 1	33414	75	2
PA4450	MurA	UDP-N-acetylglucosamine 1-carboxyvinyltransferase	Cell wall / LPS / capsule	Class 2	44617	47	2

PA4545	ComL.	competence protein ComL	Cell wall / LPS / capsule	Class 2	38591	73	2
PA3999	DacC	D-ala-D-ala-carboxypeptidase;'penicillin-binding protein 6 precursor	Cell wall / LPS / capsule;Periplasm	Class 2	42431	113	3
PA2023	GalU	UTP--glucose-1-phosphate uridylyltransferase	Central intermediary metabolism	Class 2	31216	58	2
PA3182	Pgl	6-phosphogluconolactonase	Central intermediary metabolism	Class 1	25556	101	1
PA3471	PA3471	probable malic enzyme	Central intermediary metabolism	Class 3	62381	61	1
PA3452	MqoA	malate:quinone oxidoreductase	Central intermediary metabolism;Energy metabolism	Class 2	57174	31	3
PA1596	HtpG	heat shock protein HtpG	Chaperones & heat shock proteins	Class 2	71624	146	4
PA4572	FklB	peptidyl-prolyl cis-trans isomerase FklB	Chaperones & heat shock proteins;Translation, post-translational modification, degradation;Outer membrane	Class 2	21782	51	2
PA3002	Mfd	transcription-repair coupling protein Mfd	DNA replication, recombination, modification and repair	Class 2	128716	34	1
PA0669	PA0669	probable DNA polymerase alpha chain	DNA replication, recombination, modification and repair;Putative enzymes	Class 3	115697	38	2
PA1555	PA1555	probable cytochrome c	Energy metabolism	Class 3	33791	111	2
PA1562	AcnA	aconitate hydratase 1	Energy metabolism	Class 2	99086	80	2
PA1583	SdhA	Succinate dehydrogenase (A subunit)]	Energy metabolism	Class 2	63492	245	5
PA1588	SucC	succinyl-CoA synthetase beta chain	Energy metabolism	Class 2	41517	222	5
PA1589	SucD	succinyl-CoA synthetase alpha chain	Energy metabolism	Class 2	30247	228	5
PA2951	EtfA	electron transfer flavoprotein alpha-subunit	Energy metabolism	Class 2	31404	183	5
PA2952	EtfB	electron transfer flavoprotein beta-subunit	Energy metabolism	Class 2	26360	139	4
PA4429	PA4429	probable cytochrome c1 precursor	Energy metabolism	Class 3	28975	53	2
PA5490	Cc4	cytochrome c4 precursor	Energy metabolism	Class 2	20721	38	2
PA5555	AtpG	ATP synthase gamma chain	Energy metabolism	Class 2	31533	32	1
PA5558	AtpF	ATP synthase B chain	Energy metabolism	Class 2	16946	115	2
PA4329	PykA	pyruvate kinase II	Energy metabolism;Carbon compound catabolism	Class 2	52220	168	5
PA4587	CcpR	cytochrome c551 peroxidase precursor	Energy metabolism;Periplasmic	Class 1	37380	90	3
PA2968	FabD	malonyl-CoA-[acyl-carrier-protein] transacylase	Fatty acid and phospholipid metabolism	Class 1	32424	42	1
PA3112	AccD	acetyl-CoA carboxylase beta subunit	Fatty acid and phospholipid metabolism	Class 2	31822	37	1
PA3639	AccA	acetyl-coenzyme A carboxylase carboxyl transferase (alpha subunit)	Fatty acid and phospholipid metabolism	Class 2	34925	56	2
PA0141	PA0141	conserved hypothetical protein	Hypothetical, unclassified, unknown	Class 4	34441	114	3
PA0588	PA0588	conserved hypothetical protein	Hypothetical, unclassified, unknown	Class 4	73676	170	3
PA0833	PA0833	hypothetical protein	Hypothetical, unclassified, unknown	Class 4	24698	262	6
PA1011	PA1011	hypothetical protein	Hypothetical, unclassified, unknown	Class 4	43030	359	8
PA1767	PA1767	hypothetical protein	Hypothetical, unclassified, unknown	Class 4	56777	82	1
PA1789	PA1789	hypothetical protein	Hypothetical, unclassified, unknown	Class 4	31254	112	3
PA2078	PA2078	hypothetical protein	Hypothetical, unclassified, unknown	Class 4	67255	25	4
PA2831	PA2831	conserved hypothetical protein	Hypothetical, unclassified, unknown	Class 4	42906	47	1
PA3031	PA3031	hypothetical protein	Hypothetical, unclassified, unknown	Class 4	8007	25	1
PA3214	PA3214	hypothetical protein	Hypothetical, unclassified, unknown	Class 4	23200	54	1
PA3309	PA3309	conserved hypothetical protein	Hypothetical, unclassified, unknown	Class 4	16486	131	3
PA3613	PA3613	hypothetical protein	Hypothetical, unclassified, unknown	Class 4	88324	60	4
PA3691	PA3691	hypothetical protein	Hypothetical, unclassified, unknown	Class 4	14459	114	2
PA3800	PA3800	conserved hypothetical protein	Hypothetical, unclassified, unknown	Class 4	40372	164	4
PA4308	PA4308	conserved hypothetical protein	Hypothetical, unclassified, unknown	Class 4	53214	87	2

PA4328	PA4328	hypothetical protein	Hypothetical, unclassified, unknown	Class 4	34398	53	1
PA4352	PA4352	conserved hypothetical protein	Hypothetical, unclassified, unknown	Class 4	30953	196	8
PA4372	PA4372	hypothetical protein	Hypothetical, unclassified, unknown	Class 4	38300	38	1
PA4423	PA4423	conserved hypothetical protein	Hypothetical, unclassified, unknown	Class 4	65589	112	3
PA4426	PA4426	conserved hypothetical protein	Hypothetical, unclassified, unknown	Class 4	20607	160	5
PA4441	PA4441	hypothetical protein	Hypothetical, unclassified, unknown	Class 4	16408	60	2
PA4465	PA4465	conserved hypothetical protein	Hypothetical, unclassified, unknown	Class 4	32199	50	1
PA4639	PA4639	hypothetical protein	Hypothetical, unclassified, unknown	Class 4	20723	205	5
PA4699	PA4699	hypothetical protein	Hypothetical, unclassified, unknown	Class 4	25986	46	1
PA5506	PA5506	hypothetical protein	Hypothetical, unclassified, unknown	Class 4	32124	36	1
PA4016	PA4016	hypothetical protein	Hypothetical, unclassified, unknown;Membrane proteins	Class 4	62565	36	2
PA2462	PA2462	hypothetical protein	Hypothetical, unclassified, unknown;outermembrane	Class 4	572832	45	12
PA3372	PA3372	conserved hypothetical protein	Hypothetical, unclassified, unknown;Transport of small molecules	Class 4	27882	26	2
PA1041	PA1041	Probable outer membrane protein precursor	Membrane proteins	Class 3	21734	87	1
PA1119	PA1119	Probable outer membrane protein precursor	Membrane proteins	Class 3	18399	57	4
PA2900	PA2900	Probable outer membrane protein precursor	Membrane proteins	Class 3	29835	118	1
PA3648	PA3648	Probable outer membrane protein precursor	Membrane proteins	Class 3	88233	161	3
PA3692	PA3692	Probable outer membrane protein precursor	Membrane proteins	Class 3	28497	464	9
PA4876	OsmE	osmotically inducible lipoprotein OsmE	Membrane proteins;Adaptation, protection	Class 2	12515	73	2
PA2853	OprI	outer membrane lipoprotein OprI precursor	Membrane proteins;Outer membrane	Class 1	8829	53	1
PA4370	PA4370	Insulin-cleaving metalloproteinase outer membrane protein precursor	Membrane proteins;Outer membrane	Class 1	47202	55	3
PA3821	SecD	Secretion protein SecD	Membrane proteins;Protein secretion/export apparatus;'Inner membrane protein	Class 2	67632	126	1
PA1777	OprF	outer membrane protein OprF precursor	Membrane proteins;Transport of small molecules	Class 1	37616	350	12
PA0427	OprM	outer membrane protein OprM precursor	Membrane proteins;Transport of small molecules;Antibiotic resistance and susceptibility	Class 1	52566	25	1
PA4358	PA4358	Probable ferrous iron transport protein	Membrane proteins;Transport of small molecules;Inner membrane protein	Class 3	82459	52	2
PA0413	PA0413	still frameshift probable component of chemotactic signal transduction system	Motility & Attachment;Chemotaxis;Two-component regulatory systems	Class 3	268412	82	5
PA3115	FimV	motility protein FimV	Motility & Attachment;Membrane proteins	Class 1	96871	52	3
PA3637	PyrG	CTP synthase	Nucleotide biosynthesis and metabolism	Class 2	59581	129	2
PA3686	Adk	Adenylate kinase	Nucleotide biosynthesis and metabolism	Class 2	23093	43	1
PA0299	SpuC	putrescine aminotransferase	Putative enzymes	Class 1	50421	52	1
PA0744	PA0744	Probable enoyl-CoA hydratase/isomerase	Putative enzymes	Class 3	40564	36	1
PA2491	PA2491	Probable oxidoreductase	Putative enzymes	Class 3	36809	58	2
PA3972	PA3972	Probable acyl-CoA dehydrogenase	Putative enzymes	Class 3	60300	47	2
PA4128	PA4128	conserved hypothetical protein	Putative enzymes	Class 4	28186	33	2
PA4434	PA4434	Probable oxidoreductase	Putative enzymes	Class 3	38620	75	3
PA3841	ExoS	exoenzyme S – ADP-ribosyltransferase	Secreted Factors (toxins, enzymes, alginate);'Type III Secretion	Class 1	48273	115	2
PA4238	RpoA	DNA-directed RNA polymerase alpha chain	Transcription, RNA processing and degradation	Class 2	36627	32	1
PA4745	NusA	N utilization substance protein A	Transcription, RNA processing and degradation	Class 2	54625	128	3
PA5239	Rho	transcription termination factor Rho	Transcription, RNA processing and degradation	Class 2	47040	85	5
PA0576	RpoD	sigma factor RpoD	Transcriptional regulators	Class 1	69600	41	3
PA2834	PA2834	Probable transcriptional regulator	Transcriptional regulators;'Cytoplasmic	Class 3	36098	30	2
PA0459	PA0459	Probable ClpA/B protease ATP binding subunit	Translation, post-translational modification, degradation	Class 3	94118	96	3

PA2071	fusA2	elongation factor G	Translation, post-translational modification, degradation	Class 2	77525	106	3
PA3162	RpsA	30S ribosomal protein S1	Translation, post-translational modification, degradation	Class 2	61832	241	5
PA4240	RpsK	30S ribosomal protein S11	Translation, post-translational modification, degradation	Class 2	13621	30	1
PA4257	RpsC	30S ribosomal protein S3	Translation, post-translational modification, degradation	Class 2	25822	26	2
PA4271	RplL	50S ribosomal protein L7 / L12	Translation, post-translational modification, degradation	Class 2	12472	27	5
PA4542	ClpB	ClpB protein	Translation, post-translational modification, degradation	Class 2	94947	289	6
PA4744	InfB	translation initiation factor IF-2	Translation, post-translational modification, degradation	Class 2	90857	69	3
PA5051	ArgS	arginyl-tRNA synthetase	Translation, post-translational modification, degradation	Class 2	65158	355	8
PA4265	TufA	elongation factor Tu	Translation, post-translational modification, degradation;'Cytoplasmic	Class 2	43342	516	12
PA4266	FusA1	elongation factor G	Translation, post-translational modification, degradation;'Cytoplasmic	Class 2	77735	336	8
PA4264	RpsJ	30S ribosomal protein S10	Translation, post-translational modification, degradation;Transcription, RNA processing and degradation	Class 2	11759	55	1
PA2987	PA2987	probable ATP-binding component of ABC transporter	Transport of small molecules	Class 3	24635	52	2
PA4595	PA4595	probable ATP-binding component of ABC transporter	Transport of small molecules	Class 3	61283	32	2
PA3891	PA3891	probable ATP-binding component of ABC transporter	Transport of small molecules;Inner membrane associated	Class 3	43276	36	2
PA0972	TolB	TolB protein	Transport of small molecules;Periplasmic	Class 2	47722	28	1

Table 3.1.8. List of proteins detected in the membrane enriched fraction of iron starved WT 20265 grown in the presence of 1.1mM 2,2-Dipyridyl in the Vogel Bonner medium. These proteins were not detected in the absence of 2,2-Dipyridyl in the growth medium of WT 20265.

PA Number	Gene Name	Protein Name	Function	Class	Mass	Score	Peptides matched
PA0962		probable dna-binding stress protein	Adaptation, protection	Class 3	17482	72	1
PA4307	pctC	chemotactic transducer PctC	Adaptation, protection;Chemotaxis	Class 1	68266	54	1
PA3529		probable peroxidase	Adaptation, protection;Putative enzymes	Class 3	21808	89	3
PA2623	icd	isocitrate dehydrogenase	Amino acid biosynthesis and metabolism;Carbon compound catabolism;Energy metabolism	Class 2	45548	36	3
PA2494	mexF	RND multidrug efflux transporter MexF	Antibiotic resistance and susceptibility;Membrane proteins;Transport of small molecules	Class 1	115437	803	19
PA2019		RND multidrug efflux membrane fusion protein precursor	Antibiotic resistance and susceptibility;Transport of small molecules	Class 2	42061	54	2
PA2493	mexE	RND multidrug efflux membrane fusion protein MexE precursor	Antibiotic resistance and susceptibility;Transport of small molecules	Class 1	45004	268	8
PA2009	hmgA	homogentisate 1,2-dioxygenase	Carbon compound catabolism	Class 2	47811	31	2
PA3244	minD	cell division inhibitor MinD	Cell division	Class 2	29617	29	2
PA2813		probable glutathione S-transferase	Central intermediary metabolism	Class 3	23390	46	1
PA1805	ppiD	peptidyl-prolyl cis-trans isomerase D	Chaperones & heat shock proteins;Translation, post-translational modification, degradation	Class 2	68699	92	3
PA1552		probable cytochrome c	Energy metabolism	Class 3	34622	32	3
PA1584	sdhB	succinate dehydrogenase (B subunit)	Energy metabolism	Class 2	26138	58	1
PA1586	sucB	dihydrolipoamide succinyltransferase (E2 subunit)	Energy metabolism	Class 2	42861	104	2
PA2999	nqrA	Na+-translocating NADH:ubiquinone oxidoreductase subunit Nrq1	Energy metabolism	Class 2	48051	32	1
PA3639	accA	acetyl-coenzyme A carboxylase carboxyl transferase (alpha subunit)	Fatty acid and phospholipid metabolism	Class 2	34925	72	1
PA0588		conserved hypothetical protein	Hypothetical, unclassified, unknown	Class 4	73676	211	4
PA0759		conserved hypothetical protein	Hypothetical, unclassified, unknown	Class 4	33647	32	1
PA0807		conserved hypothetical protein	Hypothetical, unclassified, unknown	Class 4	28703	29	3
PA0946		hypothetical protein	Hypothetical, unclassified, unknown	Class 4	36754	48	1
PA3804		hypothetical protein	Hypothetical, unclassified, unknown	Class 4	36081	109	1
PA3909		hypothetical protein	Hypothetical, unclassified, unknown	Class 4	83029	27	5
PA4372		hypothetical protein	Hypothetical, unclassified, unknown	Class 4	38300	91	2
PA4394		conserved hypothetical protein	Hypothetical, unclassified, unknown	Class 4	29799	81	1
PA4423		conserved hypothetical protein	Hypothetical, unclassified, unknown	Class 4	65589	250	6
PA4459		conserved hypothetical protein	Hypothetical, unclassified, unknown	Class 4	21340	35	2
PA4016		hypothetical protein	Hypothetical, unclassified, unknown;Membrane proteins	Class 4	62565	29	1
PA0973	oprL	Peptidoglycan associated lipoprotein OprL precursor	Membrane proteins;Transport of small molecules	Class 1	17914	163	2
PA3920		probable metal transporting P-type ATPase	Membrane proteins;Transport of small molecules	Class 3	83386	71	2
PA1860		hypothetical protein	Putative enzymes	Class 4	32016	29	2
PA2491		probable oxidoreductase	Putative enzymes	Class 3	36809	142	3
PA3593		probable acyl-CoA dehydrogenase	Putative enzymes	Class 3	64115	56	5

PA2478		probable thiol:disulfide interchange protein	Putative enzymes;Membrane proteins	Class 3	62054	104	2
PA4270	rpoB	DNA-directed RNA polymerase beta chain	Transcription, RNA processing and degradation	Class 2	150744	27	5
PA1490		probable transcriptional regulator	Transcriptional regulators	Class 3	28365	30	2
PA3656	rpsB	30S ribosomal protein S2	Translation, post-translational modification, degradation	Class 2	27319	61	1
PA4265	tufA	elongation factor Tu	Translation, post-translational modification, degradation	Class 2	43342	183	6
PA4267	rpsG	30S ribosomal protein S7	Translation, post-translational modification, degradation	Class 2	17493	36	1
PA3745	rpsP	30S ribosomal protein S16	Translation, post-translational modification, degradation;DNA replication, recombination, modification and repair	Class 2	9199	71	1
PA1922		probable TonB-dependent receptor	Transport of small molecules	Class 3	72218	50	5
PA2812		probable ATP-binding component of ABC transporter	Transport of small molecules	Class 3	34519	171	5
PA4461		probable ATP-binding component of ABC transporter	Transport of small molecules	Class 3	26434	66	2
PA4595		probable ATP-binding component of ABC transporter	Transport of small molecules	Class 3	61283	96	3

Table 3.1.9 List of proteins detected in the membrane enriched fraction of WT 20265 grown in normal Vogel Bonner medium without any iron chelator 2,2-Dipyridyl.

PA Number	Gene Name	Product Name	Function	Class	Mass	Score	Peptides matched
PA3327		probable non-ribosomal peptide synthetase	Adaptation, protection	Class 3	259246	38	8
PA1561	aer	aerotaxis receptor Aer	Adaptation, protection;Chemotaxis	Class 2	57144	105	2
PA1608		probable chemotaxis transducer	Adaptation, protection;Chemotaxis	Class 3	58202	61	2
PA1646		probable chemotaxis transducer	Adaptation, protection;Chemotaxis	Class 3	69781	115	3
PA1930		probable chemotaxis transducer	Adaptation, protection;Chemotaxis	Class 3	47772	68	2
PA2573		probable chemotaxis transducer	Adaptation, protection;Chemotaxis	Class 3	57669	64	2
PA2652		probable chemotaxis transducer	Adaptation, protection;Chemotaxis	Class 3	60307	158	5
PA2654		probable chemotaxis transducer	Adaptation, protection;Chemotaxis	Class 3	77078	122	4
PA2788		probable chemotaxis transducer	Adaptation, protection;Chemotaxis	Class 3	56354	92	2
PA2867		probable chemotaxis transducer	Adaptation, protection;Chemotaxis	Class 3	51425	59	2
PA3708		probable chemotaxis transducer	Adaptation, protection;Chemotaxis	Class 3	59023	132	4
PA4309	pctA	chemotactic transducer PctA	Adaptation, protection;Chemotaxis	Class 1	67975	257	7
PA4633		probable chemotaxis transducer	Adaptation, protection;Chemotaxis	Class 3	76576	59	2
PA4844		probable chemotaxis transducer	Adaptation, protection;Chemotaxis	Class 3	70740	102	2
PA5072		probable chemotaxis transducer	Adaptation, protection;Chemotaxis	Class 3	69659	125	3
PA2018		RND multidrug efflux transporter	Antibiotic resistance and susceptibility;Membrane proteins;Transport of small molecules	Class 2	112626	127	4
PA4598	mexD	RND multidrug efflux transporter MexD	Antibiotic resistance and susceptibility;Membrane proteins;Transport of small molecules	Class 1	111525	39	2
PA2019		RND multidrug efflux membrane fusion protein precursor	Antibiotic resistance and susceptibility;Transport of small molecules	Class 2	42061	140	5
PA5427	adhA	alcohol dehydrogenase	Carbon compound catabolism;Energy metabolism	Class 2	35889	63	3
PA1528	zipA	cell division protein ZipA	Cell division	Class 2	32217	118	2
PA4407	ftsZ	cell division protein FtsZ	Cell division	Class 2	41192	72	4
PA4408	ftsA	cell division protein FtsA	Cell division	Class 2	44618	118	4
PA4751	ftsH	cell division protein FtsH	Cell division	Class 2	69911	239	8
PA4481	mreB	rod shape-determining protein MreB	Cell division;Cell wall / LPS / capsule	Class 2	36953	86	5
PA4941	hflC	protease subunit HflC	Cell division;Translation, post-translational modification, degradation	Class 2	33095	72	2
PA4942	hflK	protease subunit HflK	Cell division;Translation, post-translational modification, degradation	Class 2	44018	323	8
PA3999	dacC	D-ala-D-ala-carboxypeptidase	Cell wall / LPS / capsule	Class 2	42431	251	8
PA4545	comL	competence protein ComL	Cell wall / LPS / capsule	Class 2	38591	61	1
PA4700	mrcB	penicillin-binding protein 1B	Cell wall / LPS / capsule	Class 2	85434	27	1
PA4997	msbA	transport protein MsbA	Cell wall / LPS / capsule;Fatty acid and phospholipid metabolism;Transport of small molecules	Class 2	66390	98	2
PA4385	groEL	GroEL protein	Chaperones & heat shock proteins	Class 1	57050	64	4
PA1805	ppiD	peptidyl-prolyl cis-trans isomerase D	Chaperones & heat shock proteins;Translation, post-translational modification, degradation	Class 2	68699	107	3
PA2476	dsbG	thiol:disulfide interchange protein DsbG	Chaperones & heat shock proteins;Translation, post-translational modification, degradation	Class 2	28035	31	1
PA0004	gyrB	DNA gyrase subunit B	DNA replication, recombination, modification and repair	Class 2	90133	31	3

PA3617	recA	RecA protein	DNA replication, recombination, modification and repair	Class 1	36856	28	1
PA3640	dnaE	DNA polymerase III, alpha chain	DNA replication, recombination, modification and repair	Class 2	130822	69	4
PA1555		probable cytochrome c	Energy metabolism	Class 3	33791	132	2
PA1583	sdhA	succinate dehydrogenase (A subunit)	Energy metabolism	Class 2	63492	28	2
PA4429		probable cytochrome c1 precursor	Energy metabolism	Class 3	28975	90	2
PA5490	cc4	cytochrome c4 precursor	Energy metabolism	Class 2	20721	26	1
PA5554	atpD	ATP synthase beta chain	Energy metabolism	Class 2	49469	56	1
PA5555	atpG	ATP synthase gamma chain	Energy metabolism	Class 2	31533	74	3
PA5556	atpA	ATP synthase alpha chain	Energy metabolism	Class 2	55359	141	5
PA5558	atpF	ATP synthase B chain	Energy metabolism	Class 2	16946	152	5
PA0541		hypothetical protein	Hypothetical, unclassified, unknown	Class 4	17112	35	1
PA0788		hypothetical protein	Hypothetical, unclassified, unknown	Class 4	116374	39	4
PA0946		hypothetical protein	Hypothetical, unclassified, unknown	Class 4	36754	68	3
PA1011		hypothetical protein	Hypothetical, unclassified, unknown	Class 4	43030	348	11
PA1064		hypothetical protein	Hypothetical, unclassified, unknown	Class 4	24157	81	1
PA1198		conserved hypothetical protein	Hypothetical, unclassified, unknown	Class 4	22273	65	2
PA1293		hypothetical protein	Hypothetical, unclassified, unknown	Class 4	38770	35	1
PA1324		hypothetical protein	Hypothetical, unclassified, unknown	Class 4	18292	90	2
PA2163		hypothetical protein	Hypothetical, unclassified, unknown	Class 4	74710	32	4
PA2462		hypothetical protein	Hypothetical, unclassified, unknown	Class 4	572832	34	9
PA2548		hypothetical protein	Hypothetical, unclassified, unknown	Class 4	51000	26	2
PA2883		hypothetical protein	Hypothetical, unclassified, unknown	Class 4	6265	42	1
PA2901		hypothetical protein	Hypothetical, unclassified, unknown	Class 4	12928	73	1
PA3674		hypothetical protein	Hypothetical, unclassified, unknown	Class 4	14385	100	2
PA3691		hypothetical protein	Hypothetical, unclassified, unknown	Class 4	14459	155	6
PA3800		conserved hypothetical protein	Hypothetical, unclassified, unknown	Class 4	40372	228	4
PA3848		hypothetical protein	Hypothetical, unclassified, unknown	Class 4	50516	40	2
PA3988		hypothetical protein	Hypothetical, unclassified, unknown	Class 4	22870	44	2
PA4352		conserved hypothetical protein	Hypothetical, unclassified, unknown	Class 4	30953	51	4
PA4372		hypothetical protein	Hypothetical, unclassified, unknown	Class 4	38300	82	3
PA4426		conserved hypothetical protein	Hypothetical, unclassified, unknown	Class 4	20607	77	2
PA4441		hypothetical protein	Hypothetical, unclassified, unknown	Class 4	16408	122	5
PA4639		hypothetical protein	Hypothetical, unclassified, unknown	Class 4	20723	90	2
PA4699		hypothetical protein	Hypothetical, unclassified, unknown	Class 4	25986	41	2
PA4735		hypothetical protein	Hypothetical, unclassified, unknown	Class 4	118518	58	2
PA4842		hypothetical protein	Hypothetical, unclassified, unknown	Class 4	39964	176	5
PA5006		hypothetical protein	Hypothetical, unclassified, unknown	Class 4	54811	47	1
PA5037		hypothetical protein	Hypothetical, unclassified, unknown	Class 4	57412	174	3
PA5258		hypothetical protein	Hypothetical, unclassified, unknown	Class 4	40767	237	5
PA5506		hypothetical protein	Hypothetical, unclassified, unknown	Class 4	32124	37	1
PA0070		hypothetical protein	Hypothetical, unclassified, unknown;Membrane proteins	Class 4	31697	32	2
PA0833		hypothetical protein	Hypothetical, unclassified, unknown;Membrane proteins	Class 4	24698	57	1
PA1767		hypothetical protein	Hypothetical, unclassified, unknown;Membrane proteins	Class 4	56777	56	1
PA4961		hypothetical protein	Hypothetical, unclassified, unknown;Membrane proteins	Class 4	56732	33	2

PA number	Gene	Description	Category	Class			
PA5568		conserved hypothetical protein	Hypothetical, unclassified, unknown;Membrane proteins	Class 4	64034	70	3
PA1041		probable outer membrane protein precursor	Membrane proteins	Class 3	21734	75	3
PA1119		probable outer membrane protein precursor	Membrane proteins	Class 3	18399	31	1
PA2853	oprI	Outer membrane lipoprotein OprI precursor	Membrane proteins	Class 1	8829	85	1
PA2900		probable outer membrane protein precursor	Membrane proteins	Class 3	29835	104	1
PA3648		probable outer membrane protein precursor	Membrane proteins	Class 3	88233	101	2
PA3692		probable outer membrane protein precursor	Membrane proteins	Class 3	28497	694	14
PA4370	icmP	Insulin-cleaving metalloproteinase outer membrane protein precursor	Membrane proteins	Class 1	47202	186	11
PA4765	omlA	Outer membrane lipoprotein OmlA precursor	Membrane proteins	Class 1	19383	35	2
PA4876	osmE	osmotically inducible lipoprotein OsmE	Membrane proteins;Adaptation, protection	Class 2	12515	121	3
PA0260		hypothetical protein	Membrane proteins;Hypothetical, unclassified, unknown	Class 4	78154	33	4
PA3821	secD	secretion protein SecD	Membrane proteins;Protein secretion/export apparatus	Class 2	67632	116	2
PA0969	tolQ	TolQ protein	Membrane proteins;Transport of small molecules	Class 1	25266	94	1
PA1777	oprF	Major porin and structural outer membrane porin OprF precursor	Membrane proteins;Transport of small molecules	Class 1	37616	477	31
PA5291		probable choline transporter	Membrane proteins;Transport of small molecules	Class 3	73408	65	1
PA1092	fliC	flagellin type B	Motility & Attachment	Class 1	49213	48	2
PA0411	pilJ	twitching motility protein PilJ	Motility & Attachment;Chemotaxis	Class 1	72484	87	3
PA3115	fimV	Motility protein FimV	Motility & Attachment;Membrane proteins	Class 1	96871	37	1
PA3805	pilF	type 4 fimbrial biogenesis protein PilF	Motility & Attachment;Protein secretion/export apparatus	Class 1	28520	105	3
PA1013	purC	phosphoribosylaminoimidazole-succinocarboxamide synthase	Nucleotide biosynthesis and metabolism	Class 2	26814	31	1
PA2815		probable acyl-CoA dehydrogenase	Putative enzymes	Class 3	88707	131	6
PA3324		probable short-chain dehydrogenase	Putative enzymes	Class 3	65729	32	3
PA3896		probable 2-hydroxyacid dehydrogenase	Putative enzymes	Class 3	35610	29	2
PA4431		probable iron-sulfur protein	Putative enzymes	Class 3	20815	57	1
PA4819		probable glycosyl transferase	Putative enzymes	Class 3	35670	26	3
PA5008		hypothetical protein	Putative enzymes;Hypothetical, unclassified, unknown	Class 4	29041	29	18
PA2477		probable thiol:disulfide interchange protein	Putative enzymes;Membrane proteins	Class 3	30144	81	3
PA2976	rne	ribonuclease E	Transcription, RNA processing and degradation	Class 2	117395	164	4
PA4271	rplL	50S ribosomal protein L7 / L12	Translation, post-translational modification, degradation	Class 2	12472	34	1
PA3262		probable peptidyl-prolyl cis-trans isomerase, FkbP-type	Translation, post-translational modification, degradation;Chaperones & heat shock proteins	Class 3	26829	135	5
PA0972	tolB	TolB protein	Transport of small molecules	Class 2	47722	36	2
PA1435		probable RND efflux membrane fusion protein precursor	Transport of small molecules	Class 3	41171	45	2
PA2857		probable ATP-binding component of ABC transporter	Transport of small molecules	Class 3	24570	50	2
PA2987		probable ATP-binding component of ABC transporter	Transport of small molecules	Class 3	24635	30	2
PA0425	mexA	RND multidrug efflux membrane fusion protein MexA precursor	Transport of small molecules;Antibiotic resistance and susceptibility	Class 1	40945	38	1
PA1180	phoQ	two-component sensor PhoQ	Two-component regulatory systems	Class 1	50249	122	2
PA2480		probable two-component sensor	Two-component regulatory systems	Class 3	47663	51	3
PA4982		probable two-component sensor	Two-component regulatory systems	Class 3	109071	27	2

89

Table 3.1.10. List of iron limitation specific proteins detected in the membrane enriched fraction of only SCV 20265 under iron-limited growth. These proteins were not detected in the WT 20265 samples from either normal or iron limited cultures. These proteins were also not detected in the SCV 20265 grown in normal Vogel bonner medium in the absence of 2,2-Dipyridyl.

PA Number	Gene Name	Protein Name	Function	Class	Mass	Score	Peptides matched
PA0595	ostA	organic solvent tolerance protein OstA precursor	Adaptation, protection	Class 2	104207	31	3
PA2386	pvdA	L-ornithine N5-oxygenase	Adaptation, protection	Class 1	49447	311	6
PA2424		probable non-ribosomal peptide synthetase	Adaptation, protection	Class 3	479998	29	9
PA4290		probable chemotaxis transducer	Adaptation, protection;Chemotaxis	Class 3	58368	53	1
PA2399	pvdD	pyoverdine synthetase D	Adaptation, protection;Secreted Factors (toxins, enzymes, alginate)	Class 1	273510	83	1
PA4671		probable ribosomal protein L25	Adaptation, protection;Translation, post-translational modification, degradation	Class 3	21949	96	4
PA1927	metE	5-methyltetrahydropteroyltriglutamate-homocysteine S-methyltransferase	Amino acid biosynthesis and metabolism	Class 2	86157	40	3
PA3068	gdhB	NAD-dependent glutamate dehydrogenase	Amino acid biosynthesis and metabolism	Class 2	182525	70	3
PA5323	argB	Acetylglutamate kinase	Amino acid biosynthesis and metabolism	Class 2	31829	62	1
PA3108	purF	amidophosphoribosyltransferase	Amino acid biosynthesis and metabolism;Nucleotide biosynthesis and metabolism	Class 2	55335	59	2
PA2261		probable 2-ketogluconate kinase	Carbon compound catabolism	Class 3	34020	31	2
PA4412	murG	UDP-N-acetylglucosamine--N-acetylmuramyl-(pentapeptide) pyrophosphoryl-undecaprenol N-acetylglucosamine transferase	Carbon compound catabolism;Cell wall / LPS / capsule	Class 2	37775	54	1
PA2393		probable dipeptidase precursor	Central intermediary metabolism	Class 3	49330	347	9
PA3126	ibpA	heat-shock protein IbpA	Chaperones & heat shock proteins	Class 2	16573	194	6
PA3617	recA	RecA protein	DNA replication, recombination, modification and repair	Class 1	36856	82	2
PA1552		probable cytochrome c	Energy metabolism	Class 3	34622	96	2
PA1553		probable cytochrome c oxidase subunit	Energy metabolism	Class 3	22744	51	3
PA1787	acnB	aconitate hydratase 2	Energy metabolism	Class 2	93569	27	2
PA2994	nqrF	Na+-translocating NADH:quinone oxidoreductase, subunit Nqr6	Energy metabolism	Class 2	45441	55	1
PA1323		hypothetical protein	Hypothetical, unclassified, unknown	Class 4	11579	38	1
PA2361		hypothetical protein	Hypothetical, unclassified, unknown	Class 4	141260	40	3
PA2392		hypothetical protein	Hypothetical, unclassified, unknown	Class 4	62255	102	3
PA2754		conserved hypothetical protein	Hypothetical, unclassified, unknown	Class 4	11867	30	1
PA3481		conserved hypothetical protein	Hypothetical, unclassified, unknown	Class 4	38864	104	1
PA3797		conserved hypothetical protein	Hypothetical, unclassified, unknown	Class 4	29977	25	2
PA4452		conserved hypothetical protein	Hypothetical, unclassified, unknown	Class 4	10771	29	1
PA4656		conserved hypothetical protein	Hypothetical, unclassified, unknown	Class 4	33831	57	1

PA1245		hypothetical protein	Hypothetical, unclassified, unknown;Membrane proteins	Class 4	41392	439	6
PA5473		conserved hypothetical protein	Hypothetical, unclassified, unknown;Membrane proteins	Class 4	63222	76	1
PA2520	czcA	RND divalent metal cation efflux transporter CzcA	Membrane proteins;Transport of small molecules	Class 2	113805	34	6
PA3901	fecA	Fe(III) dicitrate transport protein FecA	Membrane proteins;Transport of small molecules	Class 2	85415	69	3
PA4224	pchG	pyochelin biosynthetic protein PchG	Membrane proteins;Transport of small molecules	Class 1	37673	197	4
PA3050	pyrD	Dihydroorotate dehydrogenase	Nucleotide biosynthesis and metabolism	Class 2	36106	48	1
PA4756	carB	carbamoylphosphate synthetase large subunit	Nucleotide biosynthesis and metabolism;Amino acid biosynthesis and metabolism	Class 1	117257	40	2
PA3820	secF	secretion protein SecF	Protein secretion/export apparatus	Class 2	33021	27	2
PA0953		probable thioredoxin	Putative enzymes	Class 3	16885	89	2
PA0641		probable bacteriophage protein	Related to phage, transposon, or plasmid	Class 3	130710	33	7
PA1249	aprA	alkaline metalloproteinase precursor	Secreted Factors (toxins, enzymes, alginate)	Class 1	50402	248	5
PA1246	aprD	alkaline protease secretion protein AprD	Secreted Factors (toxins, enzymes, alginate);Protein secretion/export apparatus	Class 1	63631	41	1
PA0963	aspS	aspartyl-tRNA synthetase	Transcription, RNA processing and degradation	Class 2	66166	68	4
PA4269	rpoC	DNA-directed RNA polymerase beta* chain	Transcription, RNA processing and degradation	Class 2	154287	86	3
PA4272	rplJ	50S ribosomal protein L10	Translation, post-translational modification, degradation	Class 2	17623	55	1
PA4273	rplA	50S ribosomal protein L1	Translation, post-translational modification, degradation	Class 2	24219	26	1
PA4432	rpsI	30S ribosomal protein S9	Translation, post-translational modification, degradation	Class 2	14606	27	1
PA4808	selA	L-seryl-tRNA(ser) selenium transferase	Translation, post-translational modification, degradation	Class 2	50261	56	1
PA2408		probable ATP-binding component of ABC transporter	Transport of small molecules	Class 3	27048	44	2
PA4222		probable ATP-binding component of ABC transporter	Transport of small molecules	Class 3	61355	92	2
PA0971	tolA	TolA protein	Transport of small molecules;Membrane proteins	Class 2	37912	89	1
PA4225	pchF	pyochelin synthetase	Transport of small molecules;Secreted Factors (toxins, enzymes, alginate)	Class 1	196962	79	4
PA4226	pchE	dihydroaeruginoic acid synthetase	Transport of small molecules;Secreted Factors (toxins, enzymes, alginate)	Class 1	156325	67	3
PA3271		probable two-component sensor	Two-component regulatory systems	Class 3	127373	107	3

Table 3.1.11. List of iron limitation specific proteins detected in the membrane enriched fraction of only WT 20265 under iron-limited growth. These proteins were not detected in the SCV 20265 samples from both normal and iron limited cultures. These proteins were also not detected in the WT 20265 cultures grown in the absence of 2,2-Dipyridyl.

PA Number	Gene Name	Protein Name	Function	Class	Mass	Score	Peptides matched
PA4307	pctC	chemotactic transducer PctC	Adaptation, protection;Chemotaxis	Class 1	68266	54	1
PA2494	mexF	RND multidrug efflux transporter MexF	Antibiotic resistance and susceptibility;Membrane proteins;Transport of small molecules	Class 1	115437	803	19
PA2493	mexE	RND multidrug efflux membrane fusion protein MexE precursor	Antibiotic resistance and susceptibility;Transport of small molecules	Class 1	45004	268	8
PA2009	hmgA	Homogentisate 1,2-dioxygenase	Carbon compound catabolism	Class 2	47811	31	2
PA3244	minD	cell division inhibitor MinD	Cell division	Class 2	29617	29	2
PA2813		probable glutathione S-transferase	Central intermediary metabolism	Class 3	23390	46	1
PA1805	ppiD	peptidyl-prolyl cis-trans isomerase D	Chaperones & heat shock proteins;Translation, post-translational modification, degradation	Class 2	68699	92	3
PA1584	sdhB	succinate dehydrogenase (B subunit)	Energy metabolism	Class 2	26138	58	1
PA1586	sucB	dihydrolipoamide succinyltransferase (E2 subunit)	Energy metabolism	Class 2	42861	104	2
PA2999	nqrA	Na+-translocating NADH:ubiquinone oxidoreductase subunit Nrq1	Energy metabolism	Class 2	48051	32	1
PA0759		conserved hypothetical protein	Hypothetical, unclassified, unknown	Class 4	33647	32	1
PA0807		conserved hypothetical protein	Hypothetical, unclassified, unknown	Class 4	28703	29	3
PA3909		hypothetical protein	Hypothetical, unclassified, unknown	Class 4	83029	27	5
PA4394		conserved hypothetical protein	Hypothetical, unclassified, unknown	Class 4	29799	81	1
PA4459		conserved hypothetical protein	Hypothetical, unclassified, unknown	Class 4	21340	35	2
PA3920		probable metal transporting P-type ATPase	Membrane proteins;Transport of small molecules	Class 3	83386	71	2
PA1860		hypothetical protein	Putative enzymes	Class 4	32016	29	2
PA3593		probable acyl-CoA dehydrogenase	Putative enzymes	Class 3	64115	56	5
PA2478		probable thiol:disulfide interchange protein	Putative enzymes;Membrane proteins	Class 3	62054	104	2
PA4270	rpoB	DNA-directed RNA polymerase beta chain	Transcription, RNA processing and degradation	Class 2	150744	27	5
PA1490		probable transcriptional regulator	Transcriptional regulators	Class 3	28365	30	2
PA4267	rpsG	30S ribosomal protein S7	Translation, post-translational modification, degradation	Class 2	17493	36	1
PA3745	rpsP	30S ribosomal protein S16	Translation, post-translational modification, degradation;DNA replication, recombination, modification and repair	Class 2	9199	71	1
PA1922		probable TonB-dependent receptor	Transport of small molecules	Class 3	72218	50	5
PA2812		probable ATP-binding component of ABC transporter	Transport of small molecules	Class 3	34519	171	5
PA4461		probable ATP-binding component of ABC transporter	Transport of small molecules	Class 3	26434	66	2

Table 3.1.12. List of proteins detected in the secreted proteins(secretome) enriched fraction of SCV 20265 grown in normal Vogel Bonner medium.

PA Number	Gene Name	Protein Name	Function	Class	Mass	Score	Peptides matched
PA0139	ahpC	alkyl hydroperoxide reductase subunit C	Adaptation, protection	Class 2	20529	37	1
PA4366	sodB	superoxide dismutase	Adaptation, protection	Class 1	21337	43	1
PA4761	dnaK	DnaK protein	Adaptation, protection;Chaperones & heat shock proteins;DNA replication, recombination, modification and repair	Class 2	68361	491	13
PA1178	oprH	PhoP/Q and low Mg2+ inducible outer membrane protein H1 precursor	Adaptation, protection;Membrane proteins	Class 1	21561	242	8
PA3529		Probable peroxidase	Adaptation, protection;Putative enzymes	Class 3	21808	201	6
PA0456		Probable cold-shock protein	Adaptation, protection;Transcriptional regulators	Class 3	7702	28	1
PA5015	aceE	Pyruvate dehydrogenase	Amino acid biosynthesis and metabolism;Energy metabolism	Class 1	99501	41	3
PA0854	fumC2	Fumarate hydratase	Carbon compound catabolism;Energy metabolism	Class 2	49091	27	2
PA4385	groEL	GroEL protein	Chaperones & heat shock proteins	Class 1	57050	557	19
PA4386	groES	GroES protein	Chaperones & heat shock proteins	Class 1	10260	83	2
PA1804	hupB	DNA-binding protein HU	DNA replication, recombination, modification and repair	Class 1	9081	120	2
PA1588	sucC	succinyl-CoA synthetase beta chain	Energy metabolism	Class 2	41517	83	3
PA2951	etfA	electron transfer flavoprotein alpha-subunit	Energy metabolism	Class 2	31404	54	3
PA2952	etfB	electron transfer flavoprotein beta-subunit	Energy metabolism	Class 2	26360	30	1
PA4922	azu	azurin precursor	Energy metabolism	Class 1	15998	122	7
PA5300	cycB	cytochrome c5	Energy metabolism	Class 2	13450	51	1
PA0423		conserved hypothetical protein	Hypothetical, unclassified, unknown	Class 4	20764	78	3
PA0460		hypothetical protein	Hypothetical, unclassified, unknown	Class 4	18716	64	1
PA0542		conserved hypothetical protein	Hypothetical, unclassified, unknown	Class 4	14758	81	1
PA1711		hypothetical protein	Hypothetical, unclassified, unknown	Class 4	8691	64	1
PA1830		hypothetical protein	Hypothetical, unclassified, unknown	Class 4	11102	26	1
PA2453		hypothetical protein	Hypothetical, unclassified, unknown	Class 4	8112	83	3
PA2462		hypothetical protein	Hypothetical, unclassified, unknown	Class 4	572832	34	6
PA3031		hypothetical protein	Hypothetical, unclassified, unknown	Class 4	8007	57	2
PA3611		hypothetical protein	Hypothetical, unclassified, unknown	Class 4	14977	55	2
PA3836		hypothetical protein	Hypothetical, unclassified, unknown	Class 4	34199	27	1
PA4063		hypothetical protein	Hypothetical, unclassified, unknown	Class 4	21222	37	3
PA4453		conserved hypothetical protein	Hypothetical, unclassified, unknown	Class 4	23745	50	4
PA4625		hypothetical protein	Hypothetical, unclassified, unknown	Class 4	219625	91	3
PA4739		conserved hypothetical protein	Hypothetical, unclassified, unknown	Class 4	11753	177	5
PA3647		Probable outer membrane protein precursor	Membrane proteins	Class 3	19078	30	1
PA3692		Probable outer membrane protein precursor	Membrane proteins	Class 3	28497	46	1
PA1777	oprF	Major porin and structural outer membrane porin OprF precursor	Membrane proteins;Transport of small molecules	Class 1	37616	58	1
PA5505		Probable TonB-dependent receptor	Membrane proteins;Transport of small molecules	Class 3	28048	90	4
PA1092	fliC	flagellin type B	Motility & Attachment	Class 1	49213	165	3
PA1706	pcrV	type III secretion protein PcrV	Protein secretion/export apparatus	Class 1	32264	61	2
PA1708	popB	translocator protein PopB	Protein secretion/export apparatus	Class 1	40036	177	5

PA1709	popD	Translocator outer membrane protein PopD precursor	Protein secretion/export apparatus	Class 1	31290	256	7
PA4128		conserved hypothetical protein	Putative enzymes	Class 4	28186	24	2
PA0044	exoT	exoenzyme T	Secreted Factors (toxins, enzymes, alginate)	Class 1	48485	783	21
PA3841	exoS	exoenzyme S	Secreted Factors (toxins, enzymes, alginate)	Class 1	48273	1391	33
PA5483	algB	two-component response regulator AlgB	Transcriptional regulators;Two-component regulatory systems	Class 1	49292	31	2
PA2851	efp	translation elongation factor P	Translation, post-translational modification, degradation	Class 2	20972	43	1
PA4265	tufA	elongation factor Tu	Translation, post-translational modification, degradation	Class 2	43342	239	6
PA4266	fusA1	elongation factor G	Translation, post-translational modification, degradation	Class 2	77735	239	9
PA4273	rplA	50S ribosomal protein L1	Translation, post-translational modification, degradation	Class 2	24219	50	1
PA4542	clpB	ClpB protein	Translation, post-translational modification, degradation	Class 2	94947	92	4
PA0300	spuD	polyamine transport protein	Transport of small molecules	Class 1	40604	30	3
PA0888	aotJ	arginine/ornithine binding protein AotJ	Transport of small molecules	Class 1	27992	35	1

Table 3.1.13. List of proteins detected in the secreted proteins (secretome) enriched fraction of SCV 20265 grown in vogel bonner medium containing 1.1mM of 2,2-Dipyridyl.

PA Number	Gene Name	Protein Name	Function	Class	Mass	Score	Peptides matched
PA4366	sodB	superoxide dismutase	Adaptation, protection	Class 1	21337	43	1
PA4761	dnaK	DnaK protein	Adaptation, protection;Chaperones & heat shock proteins;DNA replication, recombination, modification and repair	Class 2	68361	494	12
PA1178	oprH	PhoP/Q and low Mg2+ inducible outer membrane protein H1 precursor	Adaptation, protection;Membrane proteins	Class 1	21561	426	13
PA3529		probable peroxidase	Adaptation, protection;Putative enzymes	Class 3	21808	226	6
PA0456		probable cold-shock protein	Adaptation, protection;Transcriptional regulators	Class 3	7702	85	2
PA4694	ilvC	ketol-acid reductoisomerase	Amino acid biosynthesis and metabolism;Biosynthesis of cofactors, prosthetic groups and carriers	Class 2	36401	39	2
PA2623	icd	isocitrate dehydrogenase	Amino acid biosynthesis and metabolism;Carbon compound catabolism;Energy metabolism	Class 2	45548	127	6
PA1587	lpdG	lipoamide dehydrogenase-glc	Amino acid biosynthesis and metabolism;Energy metabolism	Class 2	50134	52	2
PA3181		2-keto-3-deoxy-6-phosphogluconate aldolase	Carbon compound catabolism;Central intermediary metabolism	Class 2	23939	34	1
PA4385	groEL	GroEL protein	Chaperones & heat shock proteins	Class 1	57050	696	17
PA4386	groES	GroES protein	Chaperones & heat shock proteins	Class 1	10260	84	2
PA3227	ppiA	peptidyl-prolyl cis-trans isomerase A	Chaperones & heat shock proteins;Translation, post-translational modification, degradation	Class 2	20092	135	3
PA5489	dsbA	thiol:disulfide interchange protein DsbA	Chaperones & heat shock proteins;Translation, post-translational modification, degradation	Class 2	23360	177	6
PA1804	hupB	DNA-binding protein HU	DNA replication, recombination, modification and repair	Class 1	9081	121	3
PA4762	grpE	heat shock protein GrpE	DNA replication, recombination, modification and repair;Chaperones & heat shock proteins	Class 2	20689	40	1
PA1588	sucC	succinyl-CoA synthetase beta chain	Energy metabolism	Class 2	41517	362	10
PA1589	sucD	succinyl-CoA synthetase alpha chain	Energy metabolism	Class 2	30247	136	4
PA2951	etfA	electron transfer flavoprotein alpha-subunit	Energy metabolism	Class 2	31404	99	3
PA2952	etfB	electron transfer flavoprotein beta-subunit	Energy metabolism	Class 2	26360	131	3
PA4470	fumC1	fumarate hydratase	Energy metabolism	Class 1	48665	31	1
PA4922	azu	azurin precursor	Energy metabolism	Class 1	15998	204	7
PA0315		hypothetical protein	Hypothetical, unclassified, unknown	Class 4	15453	72	2
PA0388		hypothetical protein	Hypothetical, unclassified, unknown	Class 4	15293	60	3
PA0423		conserved hypothetical protein	Hypothetical, unclassified, unknown	Class 4	20764	481	10
PA0460		hypothetical protein	Hypothetical, unclassified, unknown	Class 4	18716	32	2
PA0542		conserved hypothetical protein	Hypothetical, unclassified, unknown	Class 4	14758	83	1
PA0549		hypothetical protein	Hypothetical, unclassified, unknown	Class 4	41061	25	2
PA0754		hypothetical protein	Hypothetical, unclassified, unknown	Class 4	34896	44	1
PA0856		hypothetical protein	Hypothetical, unclassified, unknown	Class 4	19986	80	1
PA0943		hypothetical protein	Hypothetical, unclassified, unknown	Class 4	27166	114	4
PA1221		hypothetical protein	Hypothetical, unclassified, unknown	Class 4	67540	34	1
PA1830		hypothetical protein	Hypothetical, unclassified, unknown	Class 4	11102	55	1
PA2451		hypothetical protein	Hypothetical, unclassified, unknown	Class 4	21957	29	1
PA2453		hypothetical protein	Hypothetical, unclassified, unknown	Class 4	8112	45	2

PA2474		**hypothetical protein**	Hypothetical, unclassified, unknown	Class 4	34191	30	1
PA3031		**hypothetical protein**	Hypothetical, unclassified, unknown	Class 4	8007	90	2
PA3435		**conserved hypothetical protein**	Hypothetical, unclassified, unknown	Class 4	15861	35	1
PA3598		**conserved hypothetical protein**	Hypothetical, unclassified, unknown	Class 4	29572	27	1
PA3931		**conserved hypothetical protein**	Hypothetical, unclassified, unknown	Class 4	28084	114	4
PA4063		**hypothetical protein**	Hypothetical, unclassified, unknown	Class 4	21222	94	4
PA4395		**conserved hypothetical protein**	Hypothetical, unclassified, unknown	Class 4	18033	25	1
PA4453		**conserved hypothetical protein**	Hypothetical, unclassified, unknown	Class 4	23745	117	3
PA4625		**hypothetical protein**	Hypothetical, unclassified, unknown	Class 4	219625	65	2
PA4708		**hypothetical protein**	Hypothetical, unclassified, unknown	Class 4	31019	159	5
PA4738		**conserved hypothetical protein**	Hypothetical, unclassified, unknown	Class 4	7607	89	3
PA4739		**conserved hypothetical protein**	Hypothetical, unclassified, unknown	Class 4	11753	283	9
PA5305		**conserved hypothetical protein**	Hypothetical, unclassified, unknown	Class 4	11520	45	1
PA5359		**hypothetical protein**	Hypothetical, unclassified, unknown	Class 4	16461	27	1
PA5481		**hypothetical protein**	Hypothetical, unclassified, unknown	Class 4	17355	56	3
PA1245		**hypothetical protein**	Hypothetical, unclassified, unknown;Membrane proteins	Class 4	41392	54	2
PA3647		**probable outer membrane protein precursor**	Membrane proteins	Class 3	19078	76	1
PA1777	**oprF**	**Major porin and structural outer membrane porin OprF precursor**	Membrane proteins;Transport of small molecules	Class 1	37616	131	3
PA5505		**probable TonB-dependent receptor**	Membrane proteins;Transport of small molecules	Class 3	28048	78	3
PA3807	**ndk**	**nucleoside diphosphate kinase**	Nucleotide biosynthesis and metabolism	Class 1	15582	50	2
PA5240	**trxA**	**thioredoxin**	Nucleotide biosynthesis and metabolism;Translation, post-translational modification, degradation;Energy metabolism	Class 2	11862	74	3
PA1249	**aprA**	**alkaline metalloproteinase precursor**	Secreted Factors (toxins, enzymes, alginate)	Class 1	50402	209	6
PA3743	**trmD**	**tRNA (guanine-N1)-methyltransferase**	Transcription, RNA processing and degradation	Class 2	28341	25	1
PA4755	**greA**	**transcription elongation factor GreA**	Transcription, RNA processing and degradation	Class 2	17148	206	5
PA5483	**algB**	**two-component response regulator AlgB**	Transcriptional regulators;Two-component regulatory systems	Class 1	49292	27	1
PA3162	**rpsA**	**30S ribosomal protein S1**	Translation, post-translational modification, degradation	Class 2	61832	40	3
PA3653	**frr**	**ribosome recycling factor**	Translation, post-translational modification, degradation	Class 1	20473	52	4
PA4265	**tufA**	**elongation factor Tu**	Translation, post-translational modification, degradation	Class 2	43342	180	4
PA4266	**fusA1**	**elongation factor G**	Translation, post-translational modification, degradation	Class 2	77735	432	14
PA5051	**argS**	**arginyl-tRNA synthetase**	Translation, post-translational modification, degradation	Class 2	65158	25	1
PA0283	**sbp**	**sulfate-binding protein precursor**	Transport of small molecules	Class 2	36411	127	3
PA0300	**spuD**	**polyamine transport protein**	Transport of small molecules	Class 1	40604	110	3
PA0888	**aotJ**	**arginine/ornithine binding protein AotJ**	Transport of small molecules	Class 1	27992	188	5
PA0958	**oprD**	**Basic amino acid, basic peptide and imipenem outer membrane porin OprD precursor**	Transport of small molecules	Class 1	48331	78	1
PA1074	**braC**	**branched-chain amino acid transport protein BraC**	Transport of small molecules	Class 1	39744	107	4
PA1342		**probable binding protein component of ABC transporter**	Transport of small molecules	Class 3	33033	173	6
PA3190		**probable binding protein component of ABC sugar transporter**	Transport of small molecules	Class 3	45103	68	3
PA3313		**hypothetical protein**	Transport of small molecules	Class 4	36516	93	4
PA3407	**hasAp**	**heme acquisition protein HasAp**	Transport of small molecules	Class 1	20890	62	4

Table 3.1.14. List of proteins detected in the secreted proteins (secretome) enriched fraction of WT 20265 grown in normal Vogel Bonner medium.

PA Number	Gene Name	Protein Name	Function	Class	Mass	Score	Peptides Matched
PA0139	ahpC	alkyl hydroperoxide reductase subunit C	Adaptation, protection	Class 2	20529	122	3
PA4366	sodB	superoxide dismutase	Adaptation, protection	Class 1	21337	71	2
PA4761	dnaK	DnaK protein	Adaptation, protection;Chaperones & heat shock proteins;DNA replication, recombination, modification and repair	Class 2	68361	329	10
PA1178	oprH	PhoP/Q and low Mg2+ inducible outer membrane protein H1 precursor	Adaptation, protection;Membrane proteins	Class 1	21561	392	10
PA3529		probable peroxidase	Adaptation, protection;Putative enzymes	Class 3	21808	156	3
PA0456		probable cold-shock protein	Adaptation, protection;Transcriptional regulators	Class 3	7702	74	2
PA1159		probable cold-shock protein	Adaptation, protection;Transcriptional regulators	Class 3	7720	69	1
PA2623	icd	isocitrate dehydrogenase	Amino acid biosynthesis and metabolism;Carbon compound catabolism;Energy metabolism	Class 2	45548	92	4
PA4385	groEL	GroEL protein	Chaperones & heat shock proteins	Class 1	57050	845	21
PA4386	groES	GroES protein	Chaperones & heat shock proteins	Class 1	10260	149	4
PA2476	dsbG	thiol:disulfide interchange protein DsbG	Chaperones & heat shock proteins;Translation, post-translational	Class 2	28035	34	1
PA1804	hupB	DNA-binding protein HU	DNA replication, recombination, modification and repair	Class 1	9081	133	2
PA1588	sucC	succinyl-CoA synthetase beta chain	Energy metabolism	Class 2	41517	52	2
PA1589	sucD	succinyl-CoA synthetase alpha chain	Energy metabolism	Class 2	30247	101	4
PA4922	azu	azurin precursor	Energy metabolism	Class 1	15998	64	2
PA2966	acpP	acyl carrier protein	Fatty acid and phospholipid metabolism	Class 1	8735	36	1
PA0312		conserved hypothetical protein	Hypothetical, unclassified, unknown	Class 4	17403	32	2
PA0315		hypothetical protein	Hypothetical, unclassified, unknown	Class 4	15453	27	1
PA0423		conserved hypothetical protein	Hypothetical, unclassified, unknown	Class 4	20764	179	6
PA0505		hypothetical protein	Hypothetical, unclassified, unknown	Class 4	7866	174	3
PA0587		conserved hypothetical protein	Hypothetical, unclassified, unknown	Class 4	48712	37	2
PA0807		conserved hypothetical protein	Hypothetical, unclassified, unknown	Class 4	28703	62	2
PA1093		hypothetical protein	Hypothetical, unclassified, unknown	Class 4	13026	37	1
PA1198		conserved hypothetical protein	Hypothetical, unclassified, unknown	Class 4	22273	42	1
PA2506		hypothetical protein	Hypothetical, unclassified, unknown	Class 4	8042	28	1
PA2567		hypothetical protein	Hypothetical, unclassified, unknown	Class 4	65577	26	2
PA3351		hypothetical protein	Hypothetical, unclassified, unknown	Class 4	11244	252	5
PA4739		conserved hypothetical protein	Hypothetical, unclassified, unknown	Class 4	11753	159	3
PA3819		conserved hypothetical protein	Hypothetical, unclassified, unknown;Membrane proteins	Class 4	18961	29	1
PA1092	fliC	flagellin type B	Motility & Attachment	Class 1	49213	174	4
PA1086	flgK	flagellar hook-associated protein 1 FlgK	Motility & Attachment;Cell wall / LPS / capsule	Class 2	71690	172	4
PA2071	fusA2	elongation factor G	Translation, post-translational modification, degradation	Class 2	77525	45	4
PA4254	rpsQ	30S ribosomal protein S17	Translation, post-translational modification, degradation	Class 2	10080	26	1
PA4265	tufA	elongation factor Tu	Translation, post-translational modification, degradation	Class 2	43342	375	10
PA4266	fusA1	elongation factor G	Translation, post-translational modification, degradation	Class 2	77735	248	11
PA4273	rplA	50S ribosomal protein L1	Translation, post-translational modification, degradation	Class 2	24219	85	2
PA4274	rplK	50S ribosomal protein L11	Translation, post-translational modification, degradation	Class 2	14898	34	1

Table 3.1.15. List of proteins detected in the secreted proteins (secretome) enriched fraction of WT 20265 grown in Vogel Bonner medium containing 1.1mM of 2,2-Dipyridyl.

PA Number	Gene Name	Protein Name	Function	Class	Mass	Score	Peptides matched
PA0139	ahpC	alkyl hydroperoxide reductase subunit C	Adaptation, protection	Class 2	20529	36	1
PA0300	spuD	polyamine transport protein	Transport of small molecules	Class 1	40604	37	2
PA0329		conserved hypothetical protein	Hypothetical, unclassified, unknown	Class 4	11766	41	1
PA0423		conserved hypothetical protein	Hypothetical, unclassified, unknown	Class 4	20764	73	3
PA0542		conserved hypothetical protein	Hypothetical, unclassified, unknown	Class 4	14758	64	2
PA0856		hypothetical protein	Hypothetical, unclassified, unknown	Class 4	19986	70	1
PA0938		hypothetical protein	Hypothetical, unclassified, unknown	Class 4	49236	30	1
PA1092	fliC	flagellin type B	Motility & Attachment	Class 1	49213	48	1
PA1178	oprH	PhoP/Q and low Mg2+ inducible outer membrane protein H1 precursor	Adaptation, protection;Membrane proteins	Class 1	21561	146	5
PA1221		hypothetical protein	Hypothetical, unclassified, unknown	Class 4	67540	24	3
PA1342		probable binding protein component of ABC transporter	Transport of small molecules	Class 3	33033	46	1
PA1588	sucC	succinyl-CoA synthetase beta chain	Energy metabolism	Class 2	41517	47	2
PA1777	oprF	Major porin and structural outer membrane porin OprF precursor	Membrane proteins;Transport of small molecules	Class 1	37616	164	4
PA1804	hupB	DNA-binding protein HU	DNA replication, recombination, modification and repair	Class 1	9081	67	2
PA1830		hypothetical protein	Hypothetical, unclassified, unknown	Class 4	11102	25	1
PA2302		probable non-ribosomal peptide synthetase	Putative enzymes	Class 3	228903	31	2
PA2453		hypothetical protein	Hypothetical, unclassified, unknown	Class 4	8112	36	1
PA2476	dsbG	thiol:disulfide interchange protein DsbG	Chaperones & heat shock proteins;Translation, post-translational modification, degradation	Class 2	28035	100	5
PA2851	efp	translation elongation factor P	Translation, post-translational modification, degradation	Class 2	20972	40	1
PA2853	oprI	Outer membrane lipoprotein OprI precursor	Membrane proteins	Class 1	8829	46	1
PA2951	etfA	electron transfer flavoprotein alpha-subunit	Energy metabolism	Class 2	31404	45	2
PA2952	etfB	electron transfer flavoprotein beta-subunit	Energy metabolism	Class 2	26360	25	1
PA2970	rpmF	50S ribosomal protein L32	Translation, post-translational modification, degradation	Class 2	6787	51	2
PA3229		hypothetical protein	Hypothetical, unclassified, unknown	Class 4	9621	72	2
PA3529		probable peroxidase	Adaptation, protection;Putative enzymes	Class 3	21808	171	5
PA3647		probable outer membrane protein precursor	Membrane proteins	Class 3	19078	30	3
PA3692		probable outer membrane protein precursor	Membrane proteins	Class 3	28497	182	5
PA3745	rpsP	30S ribosomal protein S16	Translation, post-translational modification, degradation;DNA replication, recombination, modification and repair	Class 2	9199	30	2
PA3819		conserved hypothetical protein	Hypothetical, unclassified, unknown;Membrane proteins	Class 4	18961	28	1
PA3836		hypothetical protein	Hypothetical, unclassified, unknown	Class 4	34199	31	1
PA3848		hypothetical protein	Hypothetical, unclassified, unknown	Class 4	50516	29	1
PA4240	rpsK	30S ribosomal protein S11	Translation, post-translational modification, degradation	Class 2	13621	58	1
PA4244	rplO	50S ribosomal protein L15	Translation, post-translational modification, degradation	Class 2	15165	39	1
PA4247	rplR	50S ribosomal protein L18	Translation, post-translational modification, degradation	Class 2	12654	66	1

PA4249	rpsH	30S ribosomal protein S8	Translation, post-translational modification, degradation	Class 2	14162	33	2
PA4264	rpsJ	30S ribosomal protein S10	Translation, post-translational modification, degradation;Transcription, RNA processing and degradation	Class 2	11759	50	1
PA4265	tufA	elongation factor Tu	Translation, post-translational modification, degradation	Class 2	43342	151	4
PA4266	fusA1	elongation factor G	Translation, post-translational modification, degradation	Class 2	77735	224	10
PA4273	rplA	50S ribosomal protein L1	Translation, post-translational modification, degradation	Class 2	24219	53	2
PA4274	rplK	50S ribosomal protein L11	Translation, post-translational modification, degradation	Class 2	14898	55	1
PA4385	groEL	GroEL protein	Chaperones & heat shock proteins	Class 1	57050	275	9
PA4386	groES	GroES protein	Chaperones & heat shock proteins	Class 1	10260	60	2
PA4563	rpsT	30S ribosomal protein S20	Translation, post-translational modification, degradation;Central intermediary metabolism	Class 2	9911	64	1
PA4611		hypothetical protein	Hypothetical, unclassified, unknown	Class 4	9710	71	2
PA4694	ilvC	ketol-acid reductoisomerase	Amino acid biosynthesis and metabolism;Biosynthesis of cofactors, prosthetic groups and carriers	Class 2	36401	32	1
PA4739		conserved hypothetical protein	Hypothetical, unclassified, unknown	Class 4	11753	65	3
PA4755	greA	transcription elongation factor GreA	Transcription, RNA processing and degradation	Class 2	17148	27	1
PA4761	dnaK	DnaK protein	Adaptation, protection;Chaperones & heat shock proteins;DNA replication, recombination, modification and repair	Class 2	68361	97	6
PA4814	fadH2	2,4-dienoyl-CoA reductase FadH2	Fatty acid and phospholipid metabolism	Class 2	74586	25	1
PA4932	rplI	50S ribosomal protein L9	Translation, post-translational modification, degradation	Class 2	15522	47	1
PA5167		probable c4-dicarboxylate-binding protein	Membrane proteins;Transport of small molecules	Class 3	37027	60	1
PA5505		probable TonB-dependent receptor	Membrane proteins;Transport of small molecules	Class 3	28048	29	1
PA5506		hypothetical protein	Hypothetical, unclassified, unknown	Class 4	32124	34	2

Table 3.1.16. List of iron limitation specific proteins detected in the secreted proteins (secretome) enriched fraction of only SCV 20265 under iron-limited growth. These proteins were not detected in the WT 20265 supernatant samples from both normal and iron limited cultures.

PA Number	Gene Name	Product Name	Function	Class	Mass	Score	Peptides matched
PA4694	ilvC	ketol-acid reductoisomerase	Amino acid biosynthesis and metabolism;Biosynthesis of cofactors, prosthetic groups and carriers	Class 2	36401	39	2
PA1587	lpdG	lipoamide dehydrogenase-glc	Amino acid biosynthesis and metabolism;Energy metabolism	Class 2	50134	52	2
PA3181		2-keto-3-deoxy-6-phosphogluconate aldolase	Carbon compound catabolism;Central intermediary metabolism	Class 2	23939	34	1
PA3227	ppiA	peptidyl-prolyl cis-trans isomerase A	Chaperones & heat shock proteins;Translation, post-translational modification, degradation	Class 2	20092	135	3
PA5489	dsbA	thiol:disulfide interchange protein DsbA	Chaperones & heat shock proteins;Translation, post-translational modification, degradation	Class 2	23360	177	6
PA4762	grpE	heat shock protein GrpE	DNA replication, recombination, modification and repair;Chaperones & heat shock proteins	Class 2	20689	40	1
PA4470	fumC1	Fumarate hydratase	Energy metabolism	Class 1	48665	31	1
PA0388		hypothetical protein	Hypothetical, unclassified, unknown	Class 4	15293	60	3
PA0549		hypothetical protein	Hypothetical, unclassified, unknown	Class 4	41061	25	2
PA0754		hypothetical protein	Hypothetical, unclassified, unknown	Class 4	34896	44	1
PA0943		hypothetical protein	Hypothetical, unclassified, unknown	Class 4	27166	114	4
PA2451		hypothetical protein	Hypothetical, unclassified, unknown	Class 4	21957	29	1
PA2474		hypothetical protein	Hypothetical, unclassified, unknown	Class 4	34191	30	1
PA3435		conserved hypothetical protein	Hypothetical, unclassified, unknown	Class 4	15861	35	1
PA3598		conserved hypothetical protein	Hypothetical, unclassified, unknown	Class 4	29572	27	1
PA3691		hypothetical protein	Hypothetical, unclassified, unknown	Class 4	14459	86	2
PA3931		conserved hypothetical protein	Hypothetical, unclassified, unknown	Class 4	28084	114	4
PA4395		conserved hypothetical protein	Hypothetical, unclassified, unknown	Class 4	18033	25	1
PA4708		hypothetical protein	Hypothetical, unclassified, unknown	Class 4	31019	159	5
PA4738		conserved hypothetical protein	Hypothetical, unclassified, unknown	Class 4	7607	89	3
PA5305		conserved hypothetical protein	Hypothetical, unclassified, unknown	Class 4	11520	45	1
PA5359		hypothetical protein	Hypothetical, unclassified, unknown	Class 4	16461	27	1
PA5481		hypothetical protein	Hypothetical, unclassified, unknown	Class 4	17355	56	3
PA1245		hypothetical protein	Hypothetical, unclassified, unknown;Membrane proteins	Class 4	41392	54	2
PA3807	ndk	nucleoside diphosphate kinase	Nucleotide biosynthesis and metabolism	Class 1	15582	50	2
PA5240	trxA	Thioredoxin	Nucleotide biosynthesis and metabolism;Translation, post-translational modification, degradation;Energy metabolism	Class 2	11862	74	3
PA1249	aprA	alkaline metalloproteinase precursor	Secreted Factors (toxins, enzymes, alginate)	Class 1	50402	209	6
PA3743	trmD	tRNA (guanine-N1)-methyltransferase	Transcription, RNA processing and degradation	Class 2	28341	25	1
PA3162	rpsA	30S ribosomal protein S1	Translation, post-translational modification, degradation	Class 2	61832	40	3
PA3653	frr	ribosome recycling factor	Translation, post-translational modification, degradation	Class 1	20473	52	4
PA5051	argS	arginyl-tRNA synthetase	Translation, post-translational modification, degradation	Class 2	65158	25	1
PA0283	sbp	sulfate-binding protein precursor	Transport of small molecules	Class 2	36411	127	3
PA0958	oprD	Basic amino acid, basic peptide and imipenem outer membrane porin OprD precursor	Transport of small molecules	Class 1	48331	78	1
PA1074	braC	branched-chain amino acid transport protein	Transport of small molecules	Class 1	39744	107	4

PA3190		**BraC** **Probable binding protein component of ABC sugar transporter**	Transport of small molecules		Class 3	45103	68	3
PA3313		**hypothetical protein**	Transport of small molecules	Class 4	36516	93	4
PA3407	**hasAp**	**heme acquisition protein HasAp**	Transport of small molecules	Class 1	20890	62	4

Table 3.1.17. List of iron limitation specific proteins detected in the secreted proteins (secretome) enriched fraction of only WT 20265 under iron-limited growth. These proteins were not detected in the SCV 20265 supernatant samples from both normal and iron limited cultures.

PA Number	Gene Name	Product Name	Function	Class	Mass	Score	Peptides matched
PA0329		conserved hypothetical protein	Hypothetical, unclassified, unknown	Class 4	11766	41	1
PA0938		hypothetical protein	Hypothetical, unclassified, unknown	Class 4	49236	30	1
PA2302		probable non-ribosomal peptide synthetase	Putative enzymes	Class 3	228903	31	2
PA2853	oprl	Outer membrane lipoprotein Oprl precursor	Membrane proteins	Class 1	8829	46	1
PA2970	rpmF	50S ribosomal protein L32	Translation, post-translational modification, degradation	Class 2	6787	51	2
PA3229		hypothetical protein	Hypothetical, unclassified, unknown	Class 4	9621	72	2
PA3745	rpsP	30S ribosomal protein S16	Translation, post-translational modification, degradation;DNA replication, recombination, modification and repair	Class 2	9199	30	2
PA3848		hypothetical protein	Hypothetical, unclassified, unknown	Class 4	50516	29	1
PA4240	rpsK	30S ribosomal protein S11	Translation, post-translational modification, degradation	Class 2	13621	58	1
PA4244	rplO	50S ribosomal protein L15	Translation, post-translational modification, degradation	Class 2	15165	39	1
PA4247	rplR	50S ribosomal protein L18	Translation, post-translational modification, degradation	Class 2	12654	66	1
PA4249	rpsH	30S ribosomal protein S8	Translation, post-translational modification, degradation	Class 2	14162	33	2
PA4264	rpsJ	30S ribosomal protein S10	Translation, post-translational modification, degradation;Transcription, RNA processing and degradation	Class 2	11759	50	1
PA4563	rpsT	30S ribosomal protein S20	Translation, post-translational modification, degradation;Central intermediary metabolism	Class 2	9911	64	1
PA4611		hypothetical protein	Hypothetical, unclassified, unknown	Class 4	9710	71	2
PA4814	fadH2	2,4-dienoyl-CoA reductase FadH2	Fatty acid and phospholipid metabolism	Class 2	74586	25	1
PA4932	rplI	50S ribosomal protein L9	Translation, post-translational modification, degradation	Class 2	15522	47	1
PA5167		probable c4-dicarboxylate-binding protein	Membrane proteins;Transport of small molecules	Class 3	37027	60	1
PA5506		hypothetical protein	Hypothetical, unclassified, unknown	Class 4	32124	34	2

A brief summary of the data presented in the above tables (**3.1.6-3.1.17**) is as follows. From the membrane enriched fractions of SCV 20265 grown under iron limitation in the presence of 1.1mM of 2,2-Dipyridyl, 76 proteins were identified (refer **table 3.1.6**). These proteins were not detected in the normally grown SCV 20265. From the membrane enriched fractions of SCV 20265 grown under normal VB medium, about 131 proteins were identified (refer **table 3.1.7**). In case of the WT 20265, 43 proteins were identified from the membrane enriched fraction of WT 20265 grown in the presence of iron chelator (refer **Table 3.1.8**) and 116 proteins (refer **Table 3.1.9**), from the membrane enriched fraction of WT 20265 grown in normal VB medium in the absence of any iron chelator.

About 51 proteins (refer **Table 3.1.10**), were found to be exclusively detected in the SCV 20265 membrane fraction of iron starved cells while 26 proteins (refer **Table 3.1.11**) were detected in the membrane enriched fractions of only iron starved WT 20265. It is reasonable to expect that many, if not all of these short listed proteins are truly iron responsive and have the potential to explain some of the observed differential responses to iron limitation and preferences for certain iron supplementation, that were seen in the assays described in the previous sections. Significance of the possible differential expression of some of these proteins is discussed in the Discussions **section 3.1.8**.

The supernatant enriched fractions of normal and iron limited SCV 20265 and WT 20265 were also analysed by LC/MS. The results of protein identifications from these fractions are enlisted in the tables **3.1.12-3.1.17**. In summary, a total of 49 proteins were detected in the normal supernatant of SCV 20265 (refer **Table 3.1.12**) while a total of 74 proteins were detected in the iron limited culture supernatants in the presence of 2,2-Dipyridyl (refer **Table 3.1.13**). In case of WT 20265, 37 proteins (refer **Table 3.1.4**) were detected in the culture supernatant of bacteria grown in normal VB medium while 53 proteins (refer **Table 3.1.5**) were detected in the iron limited culture supernatants. About 37 proteins (refer **Table 3.1.16**) were detected exclusively in the SCV 20265 supernatants in response to iron limitation caused by the presence of 1.1mM of 2,2-Dipyridyl in the medium while 19 proteins (refer T**able 3.1.17**) were detected exclusively in the WT 20265 supernatant in response to iron limitation.

One interesting observation was that, in response to the presence of 2,2-Dipyridyl (and therefore iron limitation in the medium) the number of proteins detectable in the membrane enriched fractions of both the morphotypes (SCV 20265 and WT 20265) was less than the

number of proteins detected in membrane fractions of normal (2,2-Dipyridyl absent) cultures. On the other hand the number of proteins detectable in the supernatants of iron-limited cultures of both the morphotypes was more than the number of proteins detectable in the normal supernatants of both the morphotypes.

3.1.7 Real Time PCR analysis of PA 4358 (feoB)

The polytopic membrane protein feoB, which is essential for Fe (II) uptake in bacteria, contains a guanine-nucleotide-specific nucleotide binding site (Marlovits *et al.*, 2002). G proteins are critical for the regulation of membrane protein function and signal transduction. Nevertheless, coupling between G proteins and membrane proteins with multiple membrane-spanning domains has so far been observed only in higher organisms. Using real time PCR, the levels of mRNA transcripts of probable ferrous iron transporter PA4358 with 78 % similarity to feoB (ferrous iron transport protein B) of *E. coli*, was quantified in cultures of SCV 20265 and WT 20265 during the log phase of growth (OD_{600} 0.80). The differential expression of the feoB protein detected in the membrane sub proteome during nano flow LC/MS analysis (refer LC/MS results **tables 3.1.5 and 3.1.6**), was indicative of possible differences at the level of transcription of this gene. *feoB* homologue in *Pseudomonas aeruginosa*, PA4358 was repeatedly detected in SCV 20265 membrane fractions but never detected in the WT 20265. Apart from this, it was also important to monitor the expression levels of *feoB* transcripts using a sensitive and accurate gene expression method like real time PCR in order to quantitatively document the expression differences which was not readily possible at a protein level with the LC/MS technique.

The house keeping gene *rpoD* (PA0576) (sigma 70 factor) whose expression levels are constant during the log phase was chosen as the external standard and internal reference. *rpoD* is the choice of similar real time and reverse transcriptase PCR analysis of gene expression in *Pseudomonas aeruginosa*. The levels of *feoB* transcripts were therefore quantified relative to the levels of *rpoD* transcripts.

The higher preference for Ferrous (Fe^{2+}) as a source of iron for growth as revealed by the appearance of more colonies around ferrous sulphate spotted discs on the plate assays described in **Fig 3.1.4.** in section 3.1.2 and liquid assays under microaerobic conditions in 2ml eppendorf assays in **Figure 3.1.3** in section 3.1.2, were indicative of the involvement of a specialized ferrous iron transporter which might very well be the hitherto not so well studied

or described PA4358 annotated as a probable ferrous iron transporter on account of its very high similarity to its well studied counterpart in *E.coli*.

Briefly, six independent cultures (volume 15 ml) of SCV 20265 and WT 20265 were grown up to log phase (OD_{600} 0.8) in 150 ml flasks with continuous shaking at 37 °C. Total RNA was prepared from the cultures independently and after DNAse treatment, quality control on formaldehyde agarose gels followed by quantification, the RNAs were pooled in 2 pools each comprising RNA samples from 3 independent cultures in a 1:1:1 ratio. Each of these pools representing an average of three independent cultures was used for real time PCR analysis independently. The rationale behind such a strategy was to exclude the variations that may occur between independent cultures. The real time PCR was performed with LightCycler (Roche) with SYBR Green-I fluorescence based detection of amplified products. The results are summarized in the figures and tables below.

Table 3.1.18   Lightcycler Quantification report. The quantification of transcript units and the calculated ratio of *feoB/rpoD* transcripts expressed as fold difference in gene expression is presented below for two different pools of samples of SCV 20265 and WT 20265 each comprising total RNA preparation from three independent cultures in total.

Pool A

S No.	WT 20265 A			SCV 20265 A		
	RpoD Transcript units	FeoB Transcript Units	Calculated ratio (Fold Difference)	RpoD Transcript units	FeoB Transcript Units	Calculated ratio (Fold Difference)
1	0.0000810	0.00000270	3.3	0.0000138	0.00000329	23.8
2	0.0000835	0.00000244	2.9	0.0000130	0.00000454	34.9
(1)	0.0000810	0.00000244	3.1	0.0000138	0.00000454	32.89
(2)	0.0000835	0.00000270	3.2	0.0000130	0.00000329	25.30

Pool B

S No.	WT 20265 B			SCV 20265 B		
	RpoD Transcript units	FeoB Transcript Units	Calculated ratio (Fold Difference)	RpoD Transcript units	FeoB Transcript Units	Calculated ratio (Fold Difference)
1	0.0000376	0.00000156	4.1	0.0000195	0.00000466	23.89
2	0.0000313	0.00000180	5.7	0.0000184	0.00000466	25.32
(1)	0.0000376	0.00000180	4.7	0.0000195	0.00000466	23.89
(2)	0.0000313	0.00000156	4.9	0.0000184	0.00000466	25.32

The table **3.1.18** is a summary of the relative abundance of mRNA transcripts of FeoB with respect to the house keeping gene sigma factor rpoD in SCV20265 and WT20625.
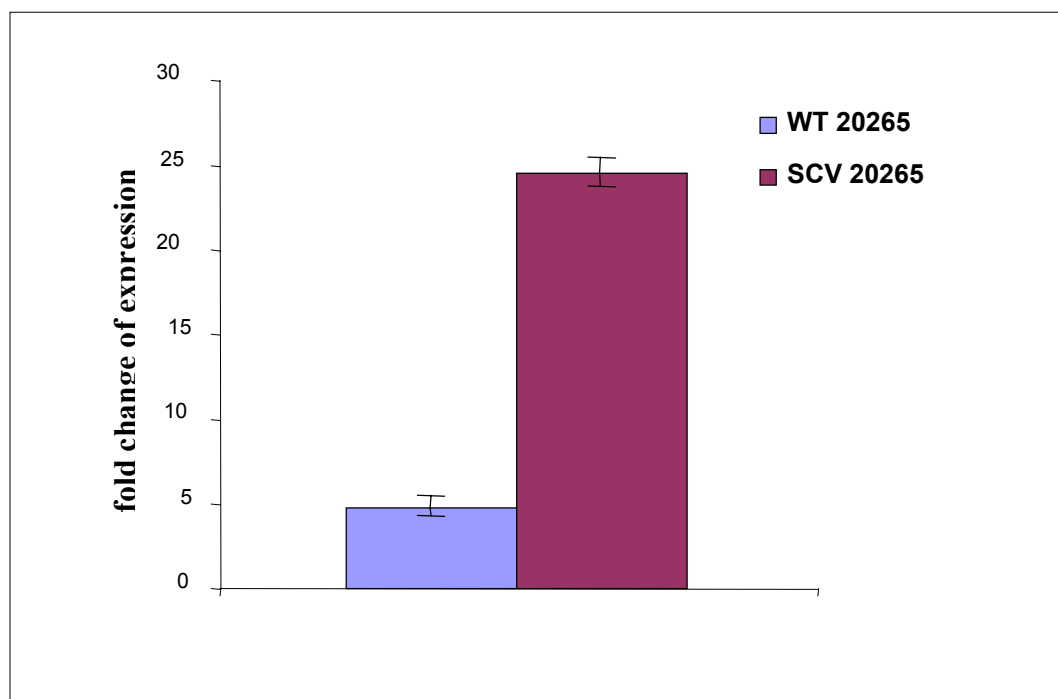
Figure 3.1.15. Expression of PA 4358 (probable ferrous iron transporter) in SCV 20265 and WT 20265. The fold change in gene expression of PA4358 in the morphotypes of 20265 revealed a significant differential regulation. The SCV 20265 shows about 20 folds higher expression as compared to WT 20265 under log phase. The error bars represent the standard deviation of the values obtained from two independent experiments and a total of four independent cross comparisons.

The whole procedure of using lightcycler SYBR green I system as above was to obtain a semi quantification of the relative abundance of the PA4358 transcripts in SCV and WT 20265 relative to the rpoD transcripts which is considering it to be expressed to its fullest capacity, being an important house keeping gene. Thus absolute quantification of the specific transcripts was not the goal of the above analysis.

The pattern of higher expression of the *feoB* homologue in SCV 20265 (about 20 folds higher than WT 20265) as compared to its WT 20265 at a mRNA level as revealed by the real time PCR analysis (**figure 3.1.15**) was found to correlate well with the observations at the protein level determined using nano flow LC/MS of membrane protein. *feoB* homolog in *P. aeruginosa,* PA4358 might have a greater role in the iron uptake in *P. aeruginosa* than previously thought. Further investigations are needed to decipher the role of *feoB* in virulence and adaptation of *P. aeruginosa* diverse morphotypic variants in the CF lung.

3.1.8   Discussion

In the human body iron is present in growth-limiting amounts for any invading bacteria (Braun, 2001). *P. aeruginosa* is found in a remarkable variety of environments, which furnish a variety of exigencies, both in terms of how to obtain iron from its surroundings and how to deal with potentially toxic levels once it starts to increase its uptake. Consequently, in comparison with many other frank pathogens that need to acquire iron only from the limited ecological niches to which they are restricted, i.e. a human host (Vasil and Ochsner, 1999), *P. aeruginosa* has to use an assortment of strategies for accessing iron and for regulating its intake (**Table 1.4.1**). On the other hand, iron deficiency has been shown to be directly, related to the increased severity of suppurative lung disease in CF patients. It has been speculated that iron loss into the airway may, contribute to iron deficiency and may facilitate PA infection (Reid *et al.,* 2002). Chelation of iron to iron-binding proteins is a strategy of host defense. Some pathogens counter this via the secretion of low-molecular-weight iron-chelating agents (siderophores), human phagocytes possess a high-capacity mechanism for iron acquisition from low-molecular-weight iron chelates, in vivo, this process could serve as an additional mechanism of host defense to limit iron availability to invading siderophore-producing microbes (Britigan *et al.*, 2000).

Because of the high insolubility of iron (III) in aerobic conditions, many gram-negative bacteria produce, under iron limitation, small iron-chelating compounds called siderophores, together with new outer-membrane proteins, which function as receptors for the ferrisiderophores (Dao *et al.*, 1999; Folschweiller *et al.*, 2000). It has been shown that by chelating iron, lactoferrin stimulates twitching, a specialized form of surface motility, causing the bacteria to wander across the surface instead of forming cell clusters and biofilms. These findings reveal a specific anti-biofilm defence mechanism acting at a critical juncture in biofilm development, the time bacteria stop roaming as individuals and aggregate into durable communities (Singh *et al.*, 2002). However, it is well known that *Pseudomonas aeruginosa* like many other bacteria prefers to grow as a biofilm and does form robust biofilms in the CF lung. Thus it has several efficient iron uptake systems to obtain this precious micronutrient.

Proteome analysis of the SCV 20265 supernatants in an earlier work form our laboratory (Wehmhöner, 2003) also revealed a higher expression of hemophore HasAp in SCV 20265 as compared to the WT 20265 as observed in this study (**figure 3.1.6**). This led us to speculate that iron limitation, could be an important selection pressure among other stress conditions,

for the occurrence of Small Colony Variant phenotype in the CF lung. Diverse morphotypes of *Pseudomonas aeruginosa* are a common occurrence in the CF lung habitat, which offers a plethora of niches each with a unique of combination of stress conditions ranging from iron limitation to anaerobic stress. This study began to test the hypothesis that SCV 20265 was one such morphotype or clonal variant that was specialized for surviving under iron limitation stress.

Accordingly, the iron limitation was studied using various assays on liquid broth and agar plates using 2,2-Dipyridyl as an iron chelator to mimic an iron-limiting environment of the lung. Several chelators are used to achieve chelation of iron. The selectivity and affinity of chelators is a crucial criterion to be considered. 2,2-Dipyridyl is not metabolized and is considered a selective chelator of Ferrous (Fe^{2+}) iron, which is the biologically useful and soluble form of iron. 2,2-Dipyridyl has been extensively used for iron limitation studies in many bacteria including *Pseudomonas aeruginosa* (Ochsner *et al.*, 2002; Ochsner, Johnson, and Vasil, 2000).

Observations on the ability of SCV 20265 to mobilize and utilize iron from haemoglobin supplemented on discs, discussed in the **section 3.1.2** can be correlated well with the higher expression of hemophore HasAp. Although an alternative haem uptake system (phu) exists in *Pseudomonas aeruginosa,* its affinity and role in haem uptake is much lesser compared to the Has system encoding the haemophore HasAp (Ochsner, Johnson, and Vasil, 2000). The secretion of haemophore is certainly inducible by iron limitation such as the presence of 2,2-dipyridyl in the medium. When HasAp secretion in SCV 20265 could be induced even in the absence of an iron limiting stress under log phase of growth, it is reasonable to expect that the expression of HasAp in SCV 20265 under conditions of iron limitation would be even more prolific. The likely existence of a survival advantage for SCVs as compared to the wildtype in an iron limiting environment of the cystic fibrosis lung with haemoglobin (released by spontaneous or bacterial haemolysin induced lysis of RBCs), as a prominent source of iron, can also be expected.
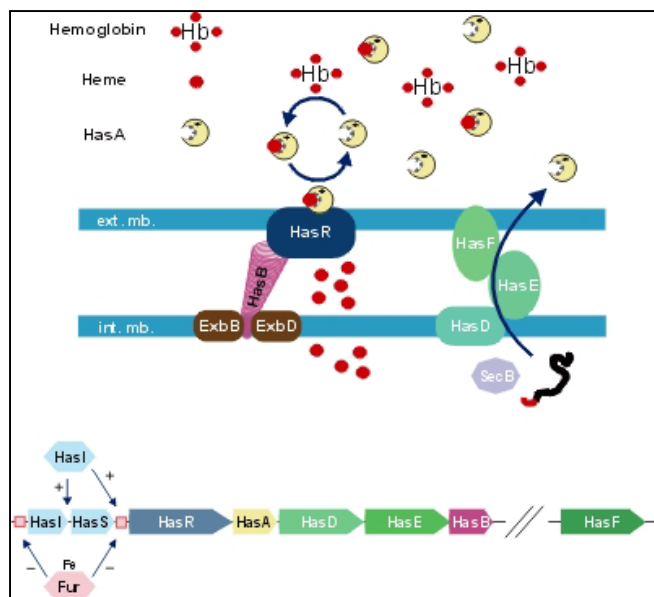
Figure 3.1.16. Schematic representation of HasAp export by an ABC transporter system and its ability to chelate haem as a source of iron. Also shown is the genetic organization of the genes of the Has operon.

HasAp is required for *P. aeruginosa* utilization of haemoglobin iron. It can replace HasA for HasR-dependent haemoblobin acquisition in a system reconstituted in *Escherichia coli*. HasAp, like HasA, lacks a signal peptide and is secreted by an ABC transporter (Letoffe, Redeker, and Wandersman, 1998). Functional iron deficiency (defined by transferrin saturation <16%) was found in 44 (62%) of 71 adult cystic fibrosis (CF) patients and haemoglobin concentration and mean cell volume were lower in iron-deficient patients, in whom there was a non-significant trend for lower serum ferritin (Palma, Worgall, and Quadri, 2003; Pond, Morton, and Conway, 1996). This study indicates that haemoglobin might be available in abundance as an iron source in the airway.

The results of the iron limitation assays and iron sources supplementation assays clearly indicated that the adaptation to iron limitation was not common to all the small colony variants. This was evident from the fact that the strain 10 wildtype was found to be better adapted to iron limitation as compared to its clonal SCV. Similarly the 8226 Wildtype was able to mobilize iron from the different sources better than its clonal SCV (refer **table 3.1.2**). In this respect it was better adapted to iron stress much like the SCV 20265. Thus, it is not fitting to say that SCV phenotype is purely an outcome of iron limitation stress. But SCV 20265 did indeed have a clear adaptation to iron limitation as revealed by the protein expression pattern in the proteome analysis.

Fur repressor regulates the expression of a range of genes in an intracellular Fe^{2+} concentration dependant fashion in many gram negative bacteria including *P. aeruginosa* (Ochsner and Vasil, 1996). Thus it was of interest to analyse its expression levels in the SCV 20265 that was well adapted to iron limitation. Accordingly, a western blot analysis with anti-fur raised against *E.coli* fur was performed. Since the *E.coli fur* and Pseudomonas *fur* are closely related, we expected to see some signals. The Pseudomonas fur protein was detected with negligible noise signals caused by cross reactivity. But the analysis revealed not so significant differences in the fur levels as seen in **figure 3.1.5**. Even though *fur* is the chief gobal regulator of iron-regulated genes in *P. aeruginosa*, there are several other extra cytoplasmic factors and sigma factors like the *pvdS*, which are also crucial in the context of iron regulation. Venturi *et al.,* (1995) have suggested that gene regulation of siderophore mediated iron uptake in *P. aeruginosa* involves several regulatory elements apart from Fur repressor, owing to possibility of *P. aeruginosa* being able to utilise heterologous siderophores.

A recent global analysis of iron–dependent gene expression in *P. aeruginosa* (Ochsner *et al.*, 2002) has revealed 205 iron regulated genes (118 were induced by iron starvation, and 87 were repressed), many of which *fur* dependent. This number represents a high proportion (4%) of *P. aeruginosa* genes and confirms that iron availability can have a major influence on gene expression in bacteria. Genes induced by low iron included those encoding: iron acquisition systems (~30), proteases, exotoxin A, fumarase C, SodA, ferridoxin, ferridoxin reductase, and several oxidoreductases and dehydrogenases. The activities of fumarase- and manganese-cofactored superoxide dismutase (SOD), encoded by the fumC and sodA genes in *P. aeruginosa*, are known to be elevated in mucoid, alginate-producing bacteria and in response to iron deprivation (Hassett *et al.*, 1997). Bacteria exposed to the iron chelator 2,2-Dipyridyl, but not ferric chloride, have demonstrated an increase in fumarase activity. Mucoid bacteria either are in an iron-starved state relative to nonmucoid bacteria or simply require more iron for the process of alginate biosynthesis. In addition, the iron-regulated, tricarboxylic acid cycle enzyme fumarase C is essential for optimal alginate production by *P. aeruginosa* (Hassett *et al.*, 1997). In our 2D gel analysis of the SCV 20265 and WT 20265 under iron limitation, we could identify differential expression of many of these proteins. However it must be admitted that unlike the DNA microarray approach where almost all the expressed transcripts can be analysed, the Proteomics approach is hindered with the its inherent inability to resolve only a thousand protein spots on a single gel. The relative

abundances of different protein species is also a crucial factor to be considered because abundant protein spots can mask the low abundant protein spots.

Proteome analysis of the isogenic mophotypes of *P. aeruginosa* 20265 by Wehmhoner *et al.*, (2003) has revealed that cellular extracts gave very similar protein patterns in two-dimensional gels, suggesting that the conserved species-specific core genome encodes proteins that are expressed under standard culture conditions in vitro. In contrast, the protein profiles of extracts of culture supernatants were dependent on the growth phase, and there were significant differences between clones. In this study the secretome expression was concluded to be a sensitive measure of *P. aeruginosa* strain variation. This was more or less the case with the present study too. Not so many differences were seen in the cellular extracts. So a subproteome approach was adopted exploiting gel less proteomics a strategy of nanoflow LC/MS. The supernatant proteome (secretome) and membrane subproteome were the focus of this study.

Hanna *et. al,* (2000) have compared proteins expressed by isogenic mucoid and non mucoid CF strains using 2D gel electrophoresis and mass spectrometry similar to the approach used in this study. Their results included proteins such as the OprH, OprF, Fe-SOD, DNAK, AhpC, catalase, Ornithine carbamolyase that were also detected in our study. This suggests that these proteins are common to many CF isolates. Their work has also emphasizes the need to focus attention on the membrane proteins.

The extensive subproteome analysis of the secretome and membrane subproteome was carried out using gel-less LC/MS approach with some focus on the dynamics of expression of these subproteomes in response to the presence of 2,2-Dipyridyl in the medium. The results of the protein identifications presented in the **tables 3.1.6-3.1.17**, included several iron uptake related proteins such as the HasAp, genes of Pyoverdine gene cluster *pvd*. On the other hand in the normal supernatants of SCV 20265, several Type III secretion components like popB and type III toxins exoS and exoT were detected (refer **table 3.1.12**). These were exclusively detected in the SCV 20265 supernatants. *dsbA* was yet another protein detected exclusively in SCV 20265 supernatants. *dsbA* is induced during mucoid conversion and is important for protease production and twitching motility (Malhotra *et al.,* 2000). Also *dsbA* has been known to be important for virulence. The differential expression of these proteins correlates well with

enhanced cytotoxicity of SCV 20265 compared to the WT 20265 that has been observed in other works from our laboratory.

Pyoverdin is capable of iron acquisition from lactoferrin and transferrin (Xiao and Kisaalita, 1997). Pyoverdines have also been demonstrated to bind and oxidize ferrous ions and it has been suggested that iron exchange and reduction mechanisms in fluorescent pseudomonads is interrelated (Xiao and Kisaalita, 1998). Pyoverdin has been demonstrated to be involved in signalling its own production and also some virulence factors like exotoxin A and endoprotease (Lamont *et al.,* 2002). An enhanced expression of ferripyoverdine receptors and pvd genes in SCV 20265 can thus have enormous consequences for the SCV 20265 adaptation to iron limitation or mobilization of iron from a variety of iron sources.

The PhoP-PhoQ has been implicated in the resistance of *P. aeruginosa* to aminoglycosides and the polycationic antibiotic polymyxin B and the expression of outer membrane protein OprH (Macfarlane *et al.,* 2000). OprG has been shown to be involved in low affinity iron uptake (Yates, Morris, and Brown, 1989). These were also some candidates that have been identified as being possibly differentially expressed.

Outer membrane proteins (OMPs) of Gram-negative bacteria have diverse functions and are directly involved in the interaction with various environments encountered by pathogenic organisms. Thus, OMPs represent important virulence factors and play essential roles in bacterial adaptation to host niches, which are usually hostile to invading pathogens. OMPs contribute to bacterial adaptive responses including iron uptake, antimicrobial peptide resistance, serum resistance, and drug/bile resistance (Lin, Huang, and Zhang, 2002).

The LC/MS approach presented in the present study must be viewed as a crude screening strategy to shortlist the proteins of interest for subsequent study with conventional, more informative but cumbersome, gel based proteomics. However, the data from the LC/MS analysis of membrane subproteomes and supernatants were in good correlation with the observations on the plate and growth assays under iron limitation described in the sections 3.1.1 and 3.1.2. Thus, we could say that these differentially expressed proteins to some extent, contributed for the relative fitness of the SCV 20265 under iron limitation. It was also possible to use the LC/MS approach to pick up a candidate protein from a broad analysis of the membrane subproteome study its expression level further at the transcription level using

real time PCR. PA 4358 was consistently detected only in the SCV 20265 membrane fraction but not in that of the WT 20265 (**table 3.1.7**). So gene specific primers were designed for this gene and its expression was studied using real time PCR. Interestingly, the higher expression of this probable ferrous iron transporter in the SCV 20265 at a protein level was found to be the case even at the level of transcription. This finding has an important implication in being able to explain the higher preference for ferrous iron as a source of iron.

The involvement of selective ferrous iron transporter like the *feoB* may explain this observation. It is important to recall here that $FeSO_4$ was found to be the most potent iron source capable of permitting growth of bacteria in the presence of 11mM Dipyridyl in the experiments discussed in **section 3.1.1**. The role of *feoB* homologue in *P. aeruginosa* has not been studied well so far. The annotation of this gene and assignment of function have been purely based on sequence similarities to the somewhat well studied counterpart in *E. coli.* However a vital role for *feoB* in pathogenicity has been demonstrated in *Helicobacter pylori* (Velayudhan *et al.,* 2000) and *Legionella pneumophila* (Robey and Cianciotto, 2002) using *feoB* mutants. Thus it is possible that a similar role might exist for the *P. aeruginosa* feoB. This remains to be demonstrated using knockouts in the future.

3.2   Differential response of morphotypes to oxidative stress

3.2.1   Sensitivity of the morphotypes to hydrogen peroxide induced oxidative stress

Sensitivity to hydrogen peroxide, a major source of oxidative stress was measured using a plate assay adopted from a similar assay described by Brown. *et. al.,* (1995). Briefly, bacteria were grown in liquid medium up to log phase or stationary phase and spread on solidified LB agar plates uniformly as a lawn. Sterile discs saturated with hydrogen peroxide (3 % or 30 %) were placed on each plate and allowed to dry followed by incubation at 37 °C overnight. The following day, diameter of zone of inhibition of growth around the discs was measured for both morphotypes. A large ZOI indicated the high sensitivity to the hydrogen peroxide. **Figure 3.2.1** shows the differential sensitivity SCV 20265 and WT 20265 to hydrogen peroxide. SCV 20265 had a relatively small zone of inhibition as compared to the WT 20265 during stationary phase of growth and iron depleted growth. The differences were not so pronounced during log phases of growth (data not shown).

a   b
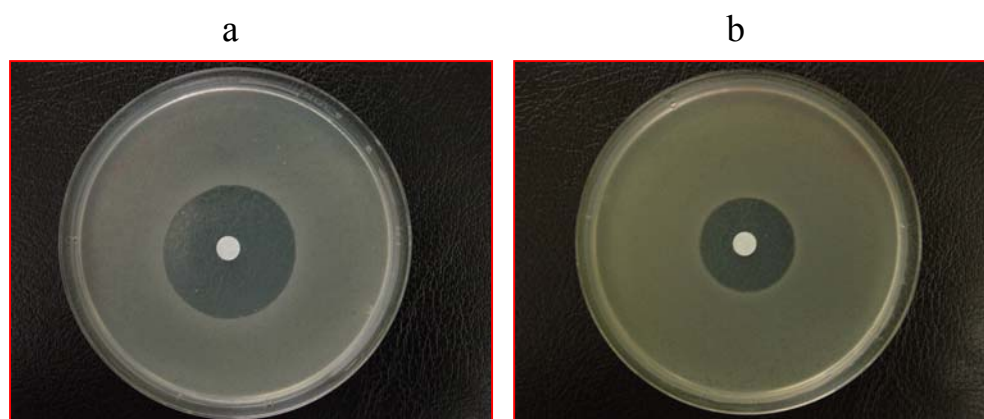
Figure 3.2.1. Sensitivity of morphotypes of strain 20265 to hydrogen peroxide induced oxidative stress. Note the larger diameter of the zone of inhibition around the hydrogen peroxide (30%) impregnated discs in Wild type 20265 (a) as compared to that of SCV 20265 (b).

The disc assays were also performed using the morphotypes of three other strains namely 8226, 231 and 52 to see if this differential sensitivity was prevalent among the morphotypes of these strains which are too members of the hyperpiliated, cytotoxic subgroup of SCVs of which 20265 is the representative strain. It was observed that the resistance of SCV to hydrogen peroxide compared to its clonal wildtype counterpart was not a widespread occurrence among all members of the subgroup of hyperpiliated and cytotoxic SCVs tested. Instead, WT 52, WT 8226, WT 231 were more resistant (having less diameter of ZOI) as compared to their respective SCVs (refer **figure 3.2.2**). This is indicative of the fact that

114

oxidative stress is only one of the many stress conditions that might select for the occurrence SCVs in the lung.
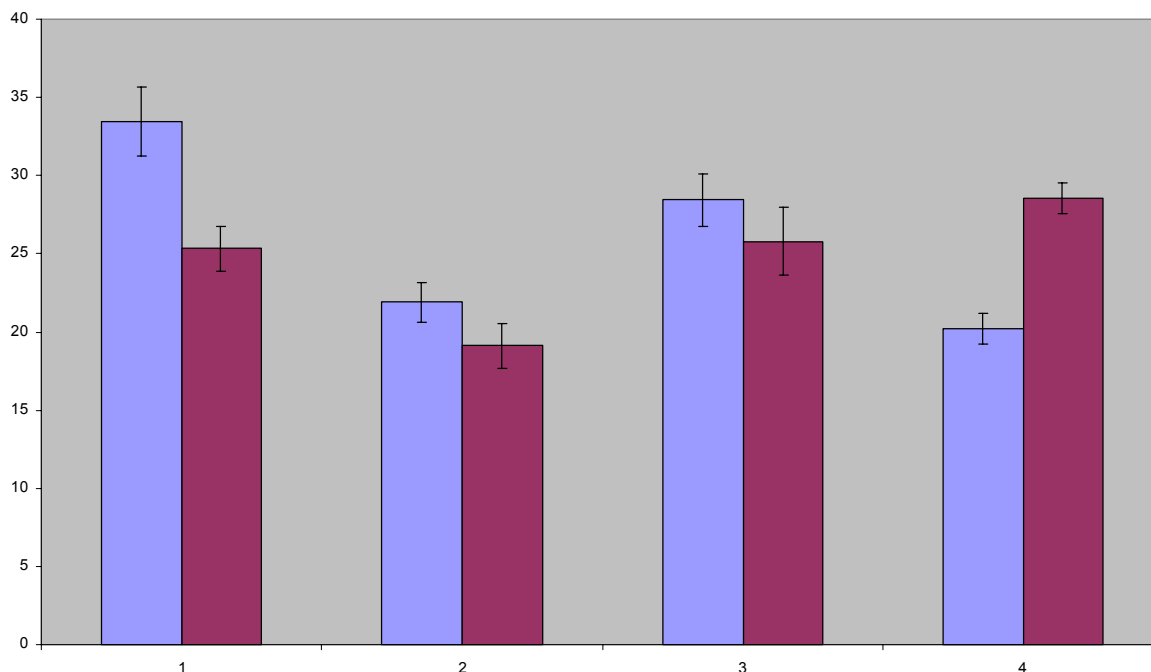
Figure 3.2.2. Sensitivity of SCV and wildtype bacteria of the four strains of *P.aeruginosa* to hydrogen peroxide. Sensitivity was recorded as the mean SE (n=9) of the diameter of growth inhibition in millimeters. 9 plates from three independent experiments were tested. Strain 231(1), Strain 52 (2), Strain 8226 (3), Strain 20265 (4). (Blue bars represent SCV and Red bars represent Wildtype)

In order to further demonstrate differential sensitivity of the morphotypes of strain 20265 to hydrogen peroxide more precisely, survival percentage of the bacteria was estimated following a brief exposure of known number of bacteria to a known concentration of hydrogen peroxide. The procedure described by Ma *et al.,* (1999) was modified and adopted. Briefly, about $6 - 8 \times 10^7$ bacteria of each morphotype was diluted in a final volume of 3 ml of fresh Vogel Bonner medium (pre incubated at 37°C) containing 0.03 % or 0.003 % hydrogen peroxide, followed by an incubation of the tubes for 15 min at 37 °C in a shaker. After the exposure to hydrogen peroxide, 100 µl of the bacteria was withdrawn and immediately serial diluted in 0.9 % NaCl solution containing bovine catalase and plated. The plates were counted the following day to assess the percentage of bacteria that survived the exposure to hydrogen peroxide. The results are presented in the **table 3.2.1** below.

Concentration of H_2O_2	SCV 20265 survival %	WT 20265 survival %
0.03 %	81 % 72 %	60% 58%
0.003%	125% 133%	81% 88%

Table 3.2.1 Hydrogen peroxide survival percentage assay. Survival percentages of SCV and WT of strain 20265 from two independent experiments are shown in the table. Note the high survival % of SCV 20265 following an H_2O_2 insult.

The results of the survival percentage assay summarized in the table above clearly established that the SCV 20265 did indeed survive better an H_2O_2 insult as compared to the WT 20265. The average survival of 76% for SCV 20265 as compared to the 59% for the WT 20265 during exposure to 0.03% hydrogen peroxide is in accordance with the observations in the disc assays discussed earlier. More impressive was the ability of SCV 20265 to begin dividing (125 % survival) upon exposure to 0.003% H_2O_2 while only 80 % of the WT 20265 could survive.

3.2.2 Proteome analysis of oxidative stress response

3.2.2.1 Response to Hydrogen peroxide

Bacteria were grown up to stationary phase(OD$_{600}$ 2.0 - 2.5) as with the above experiments. As *P. aeruginosa* has endogenous catalase activity, most of the hydrogen peroxide is removed by action of these catalases readily. *KatA, KatB* are the major catalases of *P. aeruginosa*. The cells were filled in a dialysis bag and and suspended in fresh medium containing 0.03 % hydrogen peroxide for 2 hr with shaking. During the period of incubation, the dialysis bag regulates diffusion of hydrogen peroxide and prevents rapid depletion of the same, thus ensuring a steady flow of hydrogen peroxide throughout the incubation period providing the stress to the bacteria.
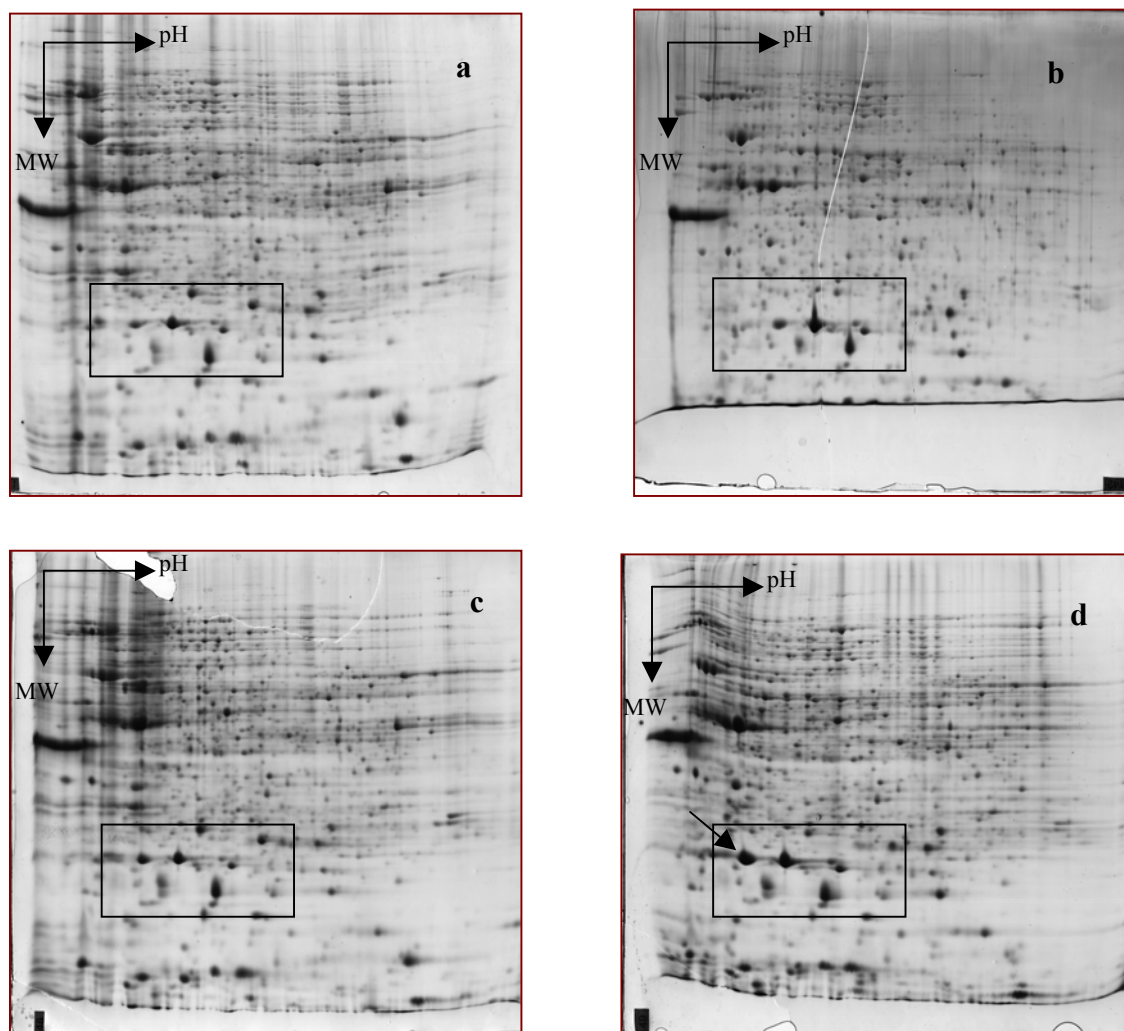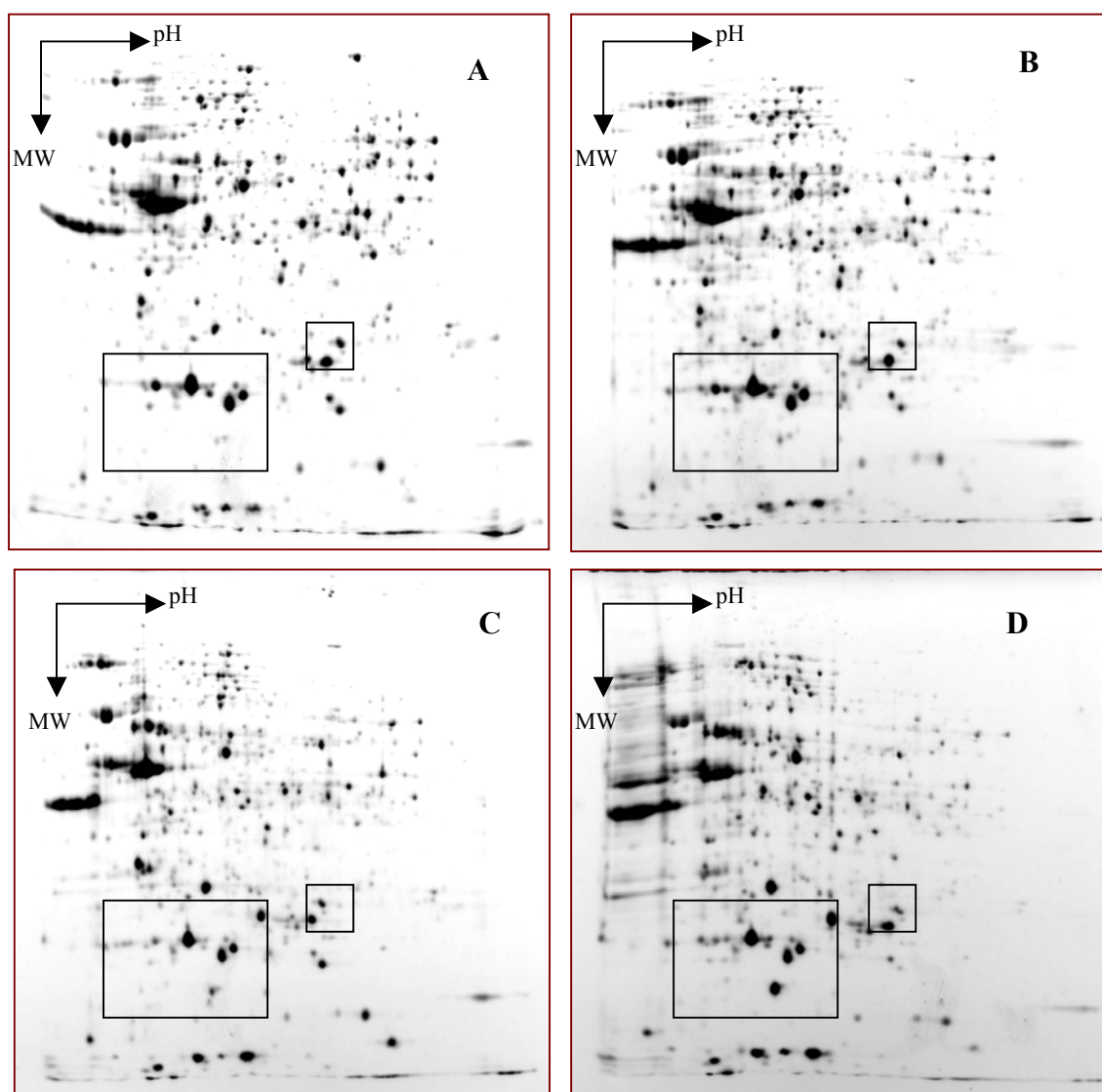

Figure 3.2.3 Proteome analysis of hydrogen peroxide induced stress (IPG strips of pH range 5-8 and gels of 12-15% linear gradient) WT 20265 untreated (a), SCV 20265 untreated (b), WT 20265 after 2 hours exposure to H$_2$O$_2$ (c), SCV 20265 after 2 hours exposure to H$_2$O$_2$ (d). Inset boxes show regions of differential expression.

117

In the previous section 3.2.1, the resistance of SCV 20265 to hydrogen peroxide has been demonstrated on two modes. The important objective of the proteome analysis was to look for some key differences at a proteome level that might explain the differential sensitivity of the SCV 20265 to hydrogen peroxide on the plate assays and survival percentage assays. Following separation of the total cellular extract made from hydrogen peroxide treated and untreated bacteria on 2D gels, Proteome Weaver, an image analysis program was used to locate differentially expressed proteins.
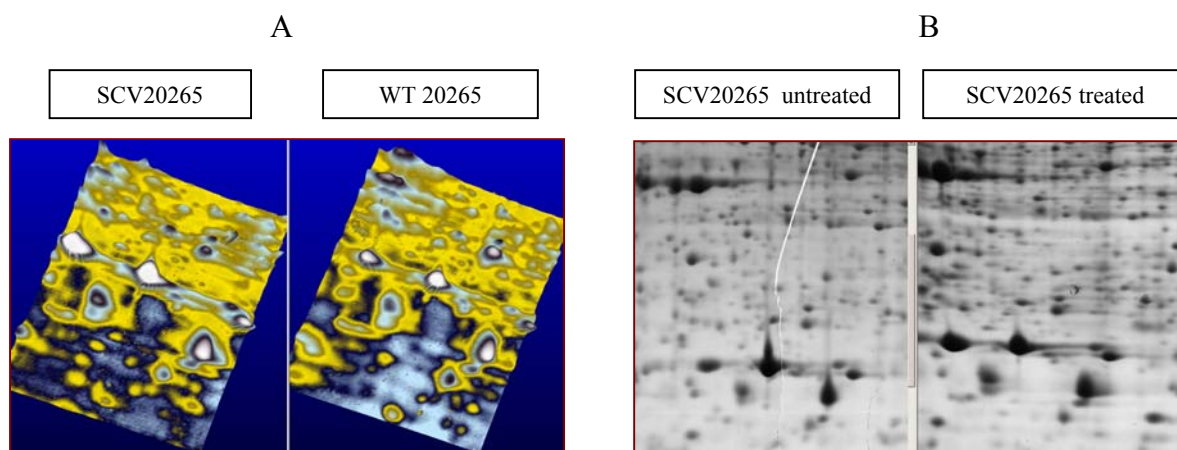
Figure 3.2.4. Expression of PA3529 (probable peroxidase) and Mn-SOD following hydrogen peroxide treatment. Image analysis using proteome weaver. False colouring for better visualisation of expression differences (A), Normal View of the corresponding region of the gels (B).

PA3529, a probable peroxidase was a notable protein that had a differential expression in response to hydrogen peroxide treatment (refer **Figure 3.2.4**). Interestingly this probable peroxidase also was found to be differentially expressed in response to iron limitation (refer **figure 3.1.7**). The MnSOD was also found to be slightly more in the SCV 20265 cellular extracts treated with hydrogen peroxide compared to similar extract of the WT 20265. Although it has been described in the literature that KatB is a key protein that is highly expressed in response to a hydrogen peroxide insult, KatB was not identified among the spots selected for MS identification. This only hints at the need to optimise the assay and IPG strips used for resolving the protein extracts. The widely used 4-7 pH range IPG strips were not optimal to detect these key genes. Henceforth, the analysis and discussions are restricted to those proteins with relevance to oxidative stress, identified from the present analysis.

3.2.2.2 Response to Paraquat treatment

Response to paraquat was measured. Unlike hydrogen peroxide used for oxidative stress in the previous approach, paraquat generates a constant supply of hydrogen peroxide, which ensures an induction of a sustained oxidative stress response during the whole period of incubation. Accordingly, the two morphotypes from strain 20265 were exposed to paraquat (methyl viologen) at a final concentration of 0.25 mM for 2 hr after growing them both to an OD_{600} of 2.0 (Stationary phase). As a control, parallely grown bacteria were incubated for 2 hours without any paraquat treatment. Total cellular extracts were made from both treated and untreated cells and resolved on a 12-15 % linear gradient 2D gel with pH range of 5-8.

Figure 3.2.5 Proteome analysis of paraquat induced oxidative stress. (IPG strips of pH range 5-8 and gels of 12-15% linear gradient) SCV 20265 untreated (A), SCV 20265 treated (B), WT 20265 untreated(C), WT 20265 treated (D). Inset boxes show proteins of differential expression

Table 3.2.2 List of proteins identified by MALDI TOF that are related to oxidative stress resistance.

PA Number	Protein Name	Gene name	Function	Class
PA4922	azurin precursor	Azu	Energy metabolism	Class 1
PA4236	catalase	KatA	Adaptation, protection	Class 1
PA3529	probable peroxidase		Putative enzymes	Class 3
PA4366	superoxide dismutase	SodB	Adaptation, protection	Class 1
PA4468	superoxide dismutase	SodM	Adaptation, protection	Class 1
PA0139	alkyl hydroperoxide reductase subunit C	AhpC	Adaptation, protection	Class 2

Figure 3.2.5 and **Table 3.2.2** summarize the results of the proteome analysis of paraquat induced oxidative stress. It was interesting to note that several key oxidative stress related proteins were detected. The expression of the probable peroxidase PA3529 was markedly high as in was the case in the hydrogen peroxide treatments. ahpC was yet another candidate that showed an up regulation in response to paraquat treatment. It can be clearly seen from the figure 3.2.4 that, in SCV 20265, both these proteins were expressed in levels higher than the WT 20265

3.2.3 Discussion

Neutrophils form superoxide anion ($^*O_2$) and hydrogen peroxide (H_2O_2) and release myeloperoxidase (MPO) during ingestion of microbial pathogens (Britigan *et al.*, 1996). Biofilm bacteria show marked resistance to oxidizing agents (e.g., H_2O_2, HOCl) relative to planktonic cells (Hassett *et al.*, 1999). Superoxide promotes hydroxyl-radical formation and consequent DNA damage in cells of all types. Superoxide may accelerate oxidative DNA damage by leaching iron from storage proteins or enzymic [4Fe-4S] clusters. The released iron might then deposit on the surface of the DNA, where it could catalyze the formation of DNA oxidants using other electron donors (Keyer and Imlay, 1996). The leading cause of mortality in patients with cystic fibrosis (CF) is respiratory failure due in large part to chronic lung infection with *P. aeruginosa* strains that undergo mucoid conversion, display a biofilm mode of growth in vivo and resist the infiltration of polymorphonuclear leukocytes (PMNs), which release free oxygen radicals such as H_2O_2.The mucoid phenotype among the strains infecting CF patients indicates overproduction of a linear polysaccharide called alginate. Mucoid conversion is a response to oxygen radical exposure and that this response is a mechanism of defense by the bacteria. PMNs and their oxygen radicals can cause this phenotypic and genotypic change which is so typical of the intractable form of *P. aeruginosa* in the CF lung (Mathee *et al.*, 1999).

It has been shown that PAO1 can create microaerobic/anaerobic growth conditions by at least two mechanisms: (i) blockage of the transfer of oxygen and (ii) formation of a polysaccharide capsule on the cell surface. It has been also postulated that the blockage of oxygen transfer may play an important role in the defense of this pathogen against reactive oxygen intermediates (Sabra, Kim, and Zeng, 2002). This might be very well the case with SCV 20265's better resistance to hydrogen peroxide induced oxidative stress as revealed by oxidative stress assays described in **figure 3.2.1** and **Table 3.2.1**. In the subsequent section the better growth of SCV 20265 under microaerobic/anaerobic conditions has been demonstrated to support this view.

Improved oxidative-stress-sustaining properties have been observed when the flavohemoglobins from *E. coli, Klebsiella pneumoniae, Deinococcus radiodurans*, and *P. aeruginosa* were expressed in *E. coli* (Frey *et al.,* 2002). If we recall **figure 3.1.6**, SCV 20265 shows a higher expression of haemoglobin scavenging Haemophore HasAp. This could be correlated with its ability to acquire external haemoglobin for incorporation into its falvihaemoglobin or use it directly by some unknown mechanism to resist oxidative stress apart from its direct use as a source of iron. Additionally the haem from haemoglobin scavenged by the haemophore hasAp might be used in the synthesis of catalases. Thus it is intriguing to think that the iron related phenotypes of SCV 20265 might also have some implications to the oxidative stress related phenotypes. However the direct links to these two phenotypic traits need further experimental proof.

P. aeruginosa bfrA may be required as one source of iron for the haem prosthetic group of katA and thus for protection against H_2O_2 (Ma *et al.,* 1999). Iron availability, but not oxygen availability, has been shown to be a major factor affecting catalase expression in biofilms (Frederick *et al.,* 2001). Thus there occurs a strong relationship between iron metabolism and the management of oxidative stress.

Proteome analysis of the cellular extracts of the 20265 SCV and WT treated with hydrogen peroxide and paraquat showed no gross changes in the protein pattern. The expression differences of some of the key oxidative stress proteins were not as prolific as was the case with the iron acquisition related proteins discussed in the previous section on response of the morphotypes to iron. However, the plate assays and broth H_2O_2 sensitivity assays (**figure 3.2.1 and table 3.2.1**) have revealed a significantly higher resistance of SCV 20265 to H_2O_2.

KatB is not produced during the normal *P. aeruginosa* growth cycle, and catalase activity is considered to be greater in nonmucoid than in mucoid, alginate-producing organisms. When exposed to hydrogen peroxide and, to a greater extent, paraquat, total catalase activity is also elevated. In addition, an increase in *katB* activity causes a marked increase in resistance to hydrogen peroxide. *katB* was localized to the cytoplasm, while *katA*, the "housekeeping" enzyme, can be detected in both cytoplasmic and periplasmic extracts. A *P. aeruginosa katB* mutant has been shown to demonstrate 50 % greater sensitivity to hydrogen peroxide than wildtype bacteria, suggesting that *katB* is essential for optimal resistance of *P. aeruginosa* to exogenous hydrogen peroxide (Brown *et al.*, 1995). However, no *katB* was detected using 2D gel analysis of paraquat treated and H_2O_2 treated samples. Perhaps the pH range of the IPG strips used was not optimal for resolving the *katB* spots. A more focussed proteome analysis might help in the detection of *katB* and analysis of its expression.

Sensitivity to both the redox-cycling agent paraquat and hydrogen peroxide has been shown to be greater in *fur* mutants. Mutations in the *P. aeruginosa fur* locus affect aerobic growth and SOD and catalase activities in *P. aeruginosa* and reduced siderophore-mediated iron uptake, especially that by pyoverdin, may be one possible mechanism contributing to such effect (Hassett *et al.*, 1996). Accordingly, the differences in pyoverdin synthesis genes and its cognate receptors expression, and the expression of several oxidative stress resistance related thioredoxins, elaborated in the **tables 3.1.6 – 3.1.17**, can be correlated with the sensitivity of WT 20265 to exogenous hydrogen peroxide.

In general, fur protein is autoregulated by fur and by Fe^{2+} and linked to the metabolism of the cell via cAMP signaling. Additionally, in *E.coli*, regulation of *fur* by oxidative stress response via *soxRS* and *oxyR* has also been reported (Zeng *et al.,* 1999). It is possible such a mechanism could also operate in *P. aeruginosa* given the high similarities in their metabolic pathways. Though *fur* is traditionally known as a global repressor, *fur* also has been suspected to positively regulate some genes. Recently, the positive regulation of *sodB* by *fur* by a posttranscriptional mechanism has been reported in *E. coli* (Dubrac and Touati, 2000).

Iron SOD is more important than manganese SOD for aerobic growth, resistance to paraquat, and optimal pyocyanin biosynthesis in *P. aeruginosa* (Hassett, Schweizer, and Ohman, 1995). However, in biofilm studies, Hassett *et al.,* (1999) have shown that catalase activity in wild-type bacteria was significantly reduced relative to planktonic bacteria; catalase activity in the

PAI (Pseudomonas Autoinducer) mutants was reduced even further and consistent with relative differences observed between each strain grown planktonically. While wildtype and mutant biofilms contained less catalase activity, they were more resistant to hydrogen peroxide treatment than their respective planktonic counterparts. Also, while catalase was implicated as an important factor in biofilm resistance to hydrogen peroxide insult, other unknown factors seemed potentially important, as PAI mutant biofilm sensitivity appeared not to be incrementally correlated to catalase levels (Hassett *et al.*, 1999). In this connection, it is important to recall the highly autoaggegative and biofilm forming nature of the SCV 20265 as compared to the free-living planktonic nature of WT 20265. Thus independent of the levels of catalase activities and its expression, SCV 20265 could still be more resistant to hydrogen peroxide compared to the Wildtype employing some unknown factors one of which could be the probable peroxidase PA3529 whose expression was markedly increased in response to H_2O_2 treatment. There are also host of other peroxidases like the a*hpC* whose role in oxidative stress resistance is not to be undermined.

It has been described Britigan *et al.*, (2001), that clinical *P. aeruginosa* isolates vary little in FeSOD and catalase expression. Some strains produce a newly described MnSOD variant, whereas some deficient in MnSOD production. The absence of MnSOD expression in a *P. aeruginosa* strain causing invasive human disease indicates that MnSOD is probably not essential for *P. aeruginosa* virulence (Britigan *et al.*, 2001). From the proteome analysis of hydrogen peroxide treated cells, the FeSOD expression was not found to be significantly different between the WT and SCV. But a differential expression of MnSOD was observable. This is in good correlation with the observations of Britigan *et al.,* (2001). Also since both the SCV and WT 20265 come from the same habitat, namely the CF lung, it's possible that the expression of their basic core enzymes is more or less the same.

Polack et al., (1996) have shown that MnSOD may participate in the adaptation of mucoid strains of *P. aeruginosa* to the stationary phase of growth in the lungs of CF patients. The sodA mutant exhibited an increased sensitivity to oxidative stress generated by paraquat and was less resistant to oxidative stress in the stationary phase of growth compared with its parental strain (Polack *et al.*, 1996). So it is possible that there might be some mutations in the key enzymes that render them functionally in active even though their expression levels might not be affected. These mutations are difficult to be detected in a proteome analysis.

Salunkhe *et al.,* (2003) have shown that one operon encoding four proteins of previously unknown function (PA0939–PA0942) was 20–200-fold up-regulated in all three analyzed strains in response to paraquat induced oxidative stress in their study. This operon, the constitutively highly expressed manganese-dependent superoxide dismutase SodA, the catalase KatA, and the alkylhydroperoxide reductase AhpC were speculated to confer the most resistance to paraquat-induced stress in *P. aeruginosa* (Salunkhe *et al.,* 2003). The resistance to paraquat induced oxidative stress is also greatly influenced by many regulatory proteins like the OxyR and SoxRS. One inherent disadvantage of the Proteomics approach is its difficulty to resolve more than a thousand spots each representing a gene product. Even among these, most of the prominent spots are often house keeping enzymes. The low abundant regulatory proteins such as the transcriptional regulators are often masked or not detectable in a complex mixture and hence need several rounds of enrichment before they can be detected.

The role of the blue copper protein azurin and cytochrome c(551) as the possible electron donors to nitrite reductase in the dissimilatory nitrate reduction pathway *in Pseudomonas aeruginosa* have been investigated by Vijgenboom *et al.,* (1997). It was shown by an in vivo approach with mutant strains of *P. aeruginosa* deficient in one or both of these electron-transfer proteins, that cytochrome c(551), but not azurin, is functional in this pathway. Expression studies demonstrated the presence of azurin in both aerobic and anaerobic cultures. A sharp increase in azurin expression was observed when cultures were shifted from exponential to stationary phase. The stationary-phase sigma factor, sigma(s), was shown to be responsible for this induction. In addition, one of the two promoters transcribing the azu gene was regulated by the anaerobic transcriptional regulator ANR. An azurin deficient mutant was more sensitive to hydrogen peroxide and paraquat than the wild-type P. aeruginosa. These results suggest a physiological role of azurin in stress situations like those encountered in the transition to the stationary phase (Vijgenboom, Busch, and Canters, 1997). In SCV 20265 and WT 20265 azurin has been shown to be differentially expressed (**refer figure 3.1.8**). Thus we may speculate that azurin levels could also contribute for the observed differences in sensitivities of SCV 20265 and WT 20265 to hydrogen peroxide induced oxidative stress on plates. OxyR-recG locus is essential for the oxidative stress defense and for DNA repair (Ochsner *et al.,* 2000). Therefore it is important to analyze the expression of this locus in the future studies.

Even though the precise molecular causes for the observed differences in sensitivities of the SCV and WT 20265 to oxidative stress, is yet to be determined, the present investigation with proteome analysis and functional assays on plates and broth has clearly confirmed the occurrence of intraclonal variation in response to oxidative stress. Secondly, this throws some light on the complex interactions of the different metabolic labyrinths pertaining to iron homeostasis, anerobiosis and oxidative stress. Oxidative stress in the CF lungs, like iron limitation might also be speculated to select for clonal variants like the SCV 20265, which shows enhanced resistance to the oxidative stress compared to its wildtype.

3.3   Differential response of morphotypes to anaerobic growth conditions

3.3.1   Differential growth of morphotypes under anaerobic conditions

Recent evidence suggests the occurrence of anaerobic/microaerobic conditions within the CF lung habitat and the ability of *P.aeruginosa* to grow and form robust biofilms in the hypoxic mucous (Yoon *et al.*, 2002). The fitness and differential growth of the clonal morphotypes was tested under anaerobic growth conditions in the presence of potassium nitrate as a source of nitrate. To achieve maximum oxygen depletion from the medium, vogel bonner medium was bubbled with nitrogen gas for two hours. The medium was quickly filled up to brim in culture tubes. It is known that in the presence of nitrate in the medium, the bacterial ability to sense oxygen gradient is paralysed and therefore they take to an anaerobic mode of growth utilizing nitrate as the terminal electron acceptor instead of oxygen.

To achieve optimal anaerobic environment during incubation, the culture tubes were left unshaken in a commercially available anaerobic jar (Merck). Special oxygen depletion packs obtained from the manufacturer were put inside the jars to deplete the oxygen within and to ensure the availability of an anaerobic environment. Special colour indicator strips provided by the manufacturer were placed in the jars in order to visualize and monitor the depletion of oxygen within, during the entire period of incubation.
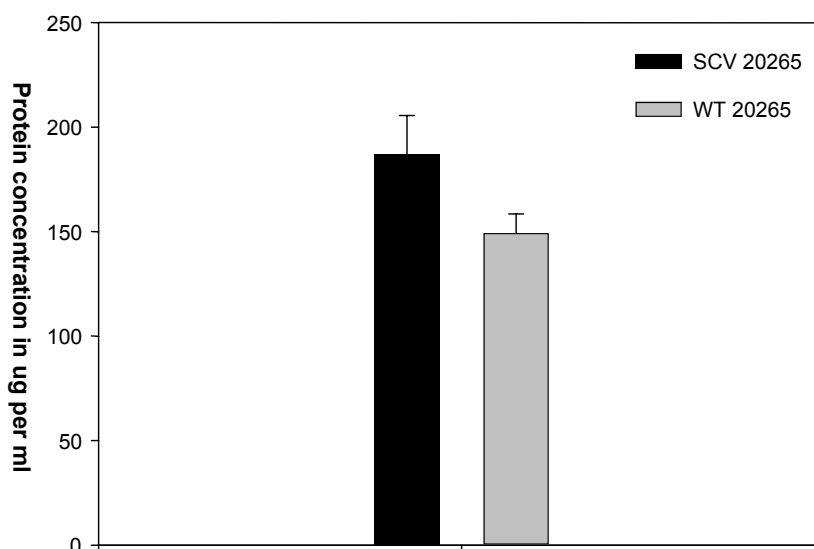
Figure 3.3.1 Aanerobic growth of morphotypes of 20265 in Vogel Bonner (VB) medium bubbled with N_2 gas and tubes incubated at 37° C in <u>Anerocult (Merck)</u> anaerobic jar after 96 hours of growth. Note the higher growth (as seen by high protein concentration) of SCV 20265. Error bars represent standard deviations of three independent cultures.

1% KNO_3 was used as described in as a source of nitrate Yoon *et al.*, (2002). A negative control of Vogel Bonner medium without any nitrate supplementation was also included.

Figure 3.3.1 shows the growth of the SCV and WT of strain 20265 measured as the function of protein concentration. Protein concentration of the medium was chosen as a measure of growth because of the growth of the bacteria as aggregates and any representative sampling for Optical density measurement or serial dilution for CFU counting was not possible. Additionally, in order to avoid any aeration during sampling, several parallel cultures were grown and whole culture tubes were used for sampling at various time points. The SCV 20265 shows clearly more growth than WT 20265 under these anaerobic growth conditions utilizing nitrate.
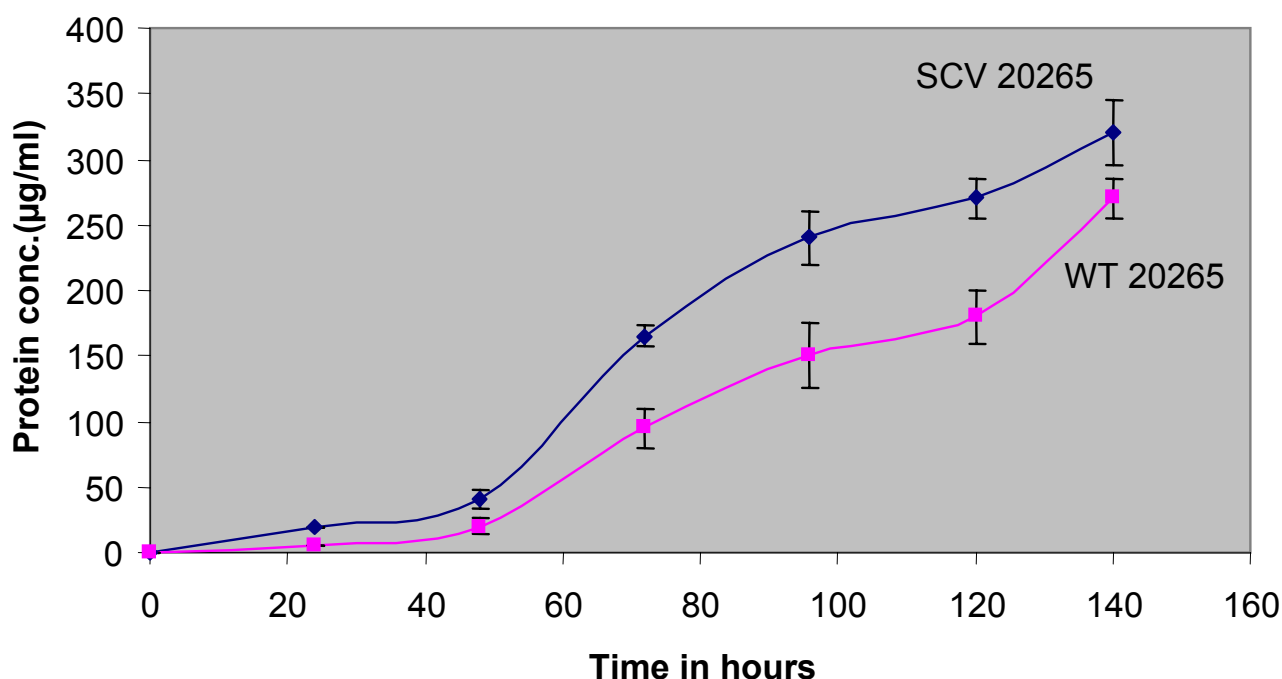
Figure 3.3.2 Growth of morphotypes of strain 20265 under microaerobic growth in the presence of 1% KNO₃ followed over a period of time. Growth has been measured as a function of protein concentration in the culture. The error bars represent strandard deviation of three independent experiments.

The growth of the SCV 20265 and WT 20265 was followed from the time of inoculation over a period of 150 hours (refer **Fig. 3.3.2**). Interestingly, the SCV 20265 was growing much better and faster than the Wildtype 20265. A comparison of the growth curve under normal vogel bonner medium (refer **Fig. 3.1.1**) shows the marked difference in the pattern of growth of the SCV and WT under these two different conditions of growth**.**

The slow growing SCV grows faster than the WT under this specialized growth condition in the dearth of oxygen and availability of an alternative electron acceptor. The proteome profile of the morphotypes under these conditions have been investigated to gain insight into the possible differences at a protein level. These are discussed in **section 3.3.2**. The ability of

these morphotypes to form biofilms under these conditions must be investigated further to see if these growth differences under anaerobic conditions are also translated as differences in nature and size of the biofilms they form under such conditions. These results are consistent with our working hypothesis of the small colony variants being a clonal variant specially adapted to specific niches in the CF lung that have specific stresses such as the redox stress, iron limitation, anaerobic stress or a combination of these.

3.3.2 Proteome analysis of anaerobically grown bacteria

SCV 20265 and WT 20265 were grown for 48 to 72 hours in the presence of 1 % KNO_3 in nitrogen bubbled VB medium in special anaerobic jars (Merck) with culture vessels filled up to the brim without any shaking as described above. The cells were quickly harvested and lysed for extraction of cellular proteins. **Figure 3.3.3** shows the cellular extracts of SCV 20265 and WT 20265 grown anaerobically.
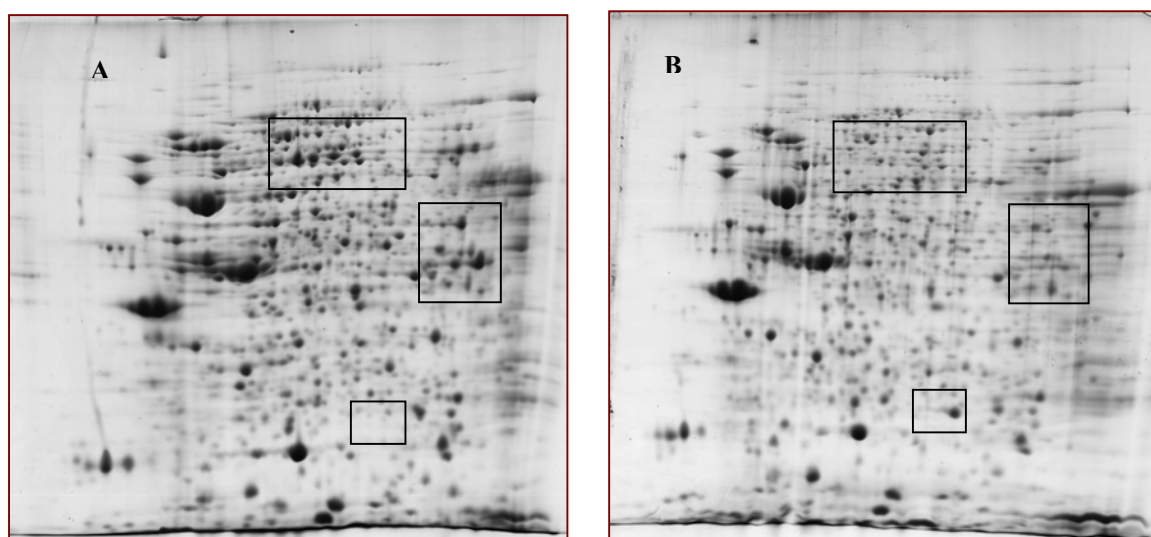
Figure 3.3.3 Proteome analysis of anaerobically grown SCV 20265 and WT 20265 in the presence of 1% KNO₃ supplement in VB medium. Total cellular extract of the cells were resolved on a 12- 15% linear gradient gel and IPG strips with pH 4–7 and stained with Colloidal Coomassie. SCV 20265 (A) and WT 20265 (B). Inset boxes show regions of differential expression**.**

Some of the differentially expressed proteins detected include Chain A *Pseudomonas aeruginosa* Cd1 Nitrite reductase reduced cyanide complex, Ferripyochelin receptor FptA, Catalase (Kat A), Chain A Catabolic ornithine carbamyl transferase, D-3-Phosphoglycerate dehydrogenase. Anaerobically induced low affinity iron transporter OprG was also expressed in slightly higher levels in the SCV. **Figure 3.3.4** shows the positions of some of these differentially expressed spots and other major protein spots that were detected on 2D gels that were used to resolve the total cellular extract of anaerobically grown SCV 20265. **Figure**

3.3.5 shows the 3D visualisation of the differential expression of a particular protein spot identified as a DsbG (PA2476) - a thiol: disulfide interchange protein using image analysis software ProteomeWeaver. DsbG has a Thioredoxin family active site and belongs to the DsbC subfamily of chaperones. DsbG was one of the few proteins that were consistently expressed in high levels by WT 20265 while its expression was hardly detectable in the SCV 20265 cultures. Under anaerobic conditions of growth also DsbG was consistently expressed only in the WT 20265 in levels much higher than that of the SCV 20265.
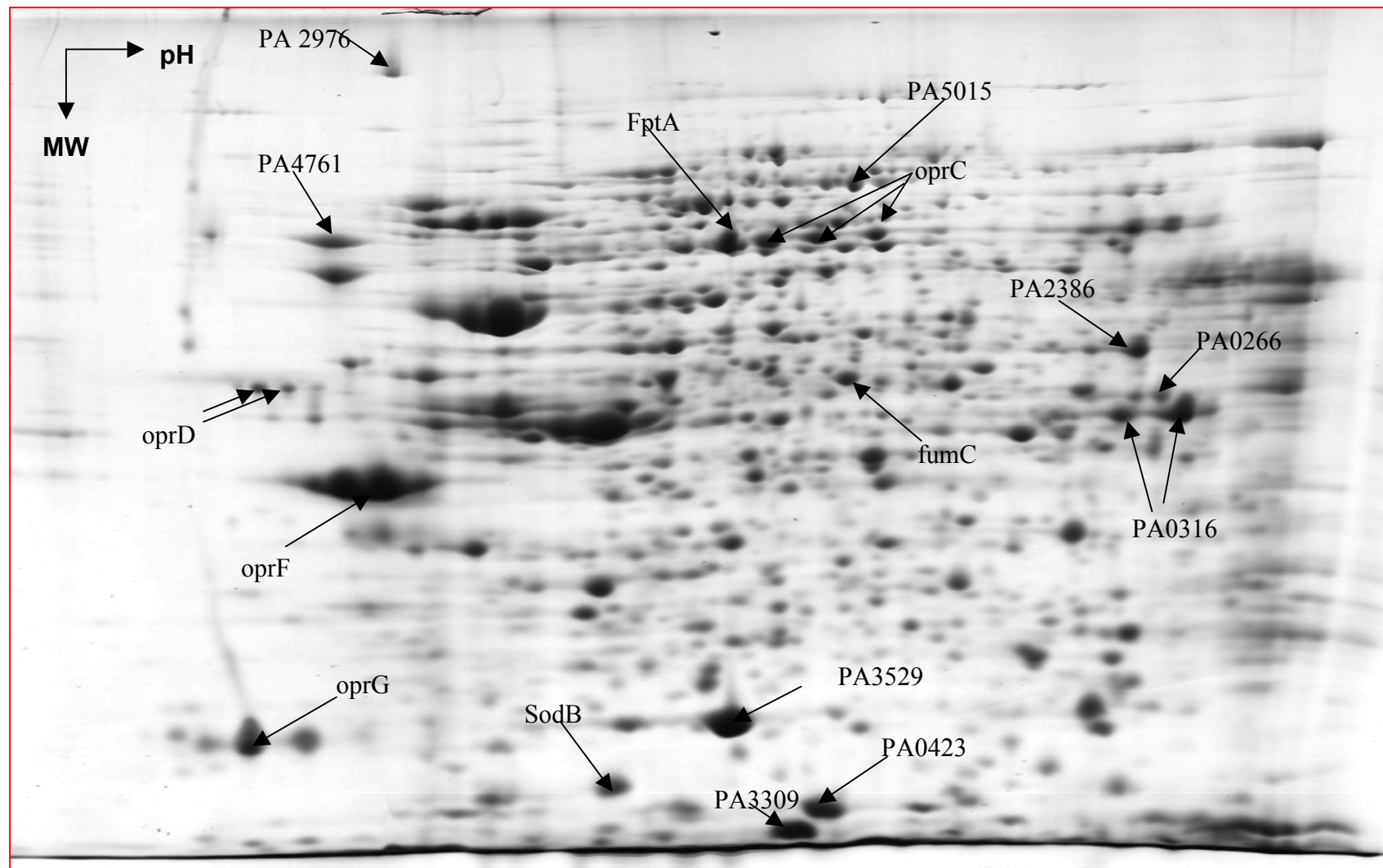
Figure 3.3.4. 2D gel prepared from SCV 20265 anaerobically grown in the presence of 1% KNO$_3$ supplement in VB medium. Total cellular protein extract of the bacterial cells was resolved on a 12-15% linear gradient gel with pH 4–7. Some of the differentially expressed proteins include those that are involved in iron uptake and nitrate respiration.

Monocolour

False Colour
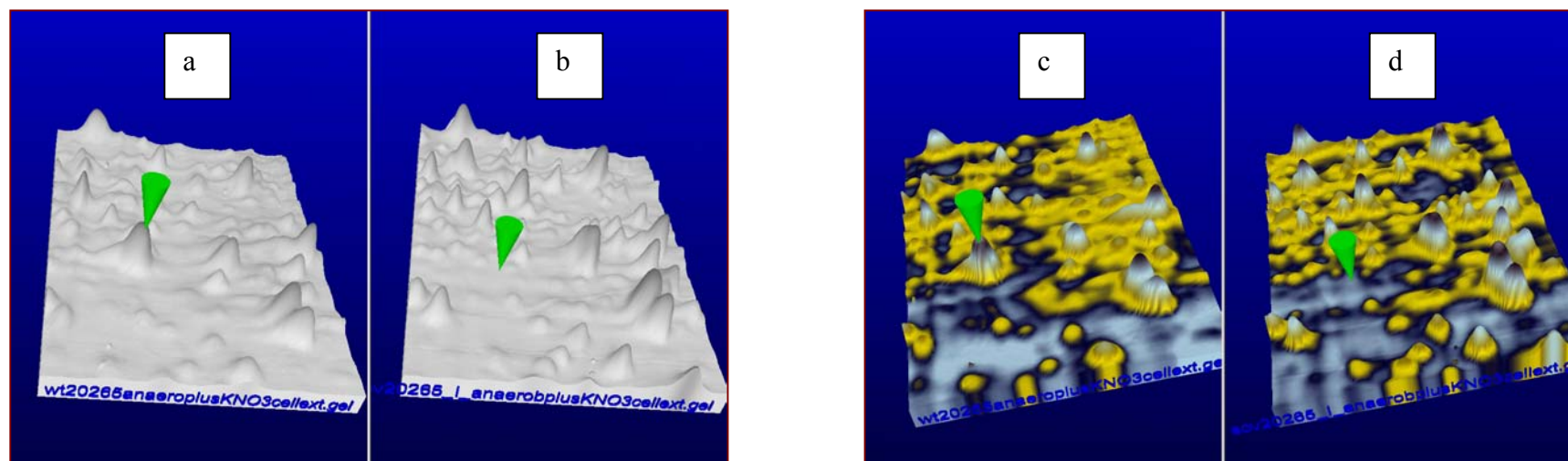
Fig 3.3.5. 3D visualization of differential expression of DsbG in WT 20265 (a&c) and SCV 20265 (b&d) using Proteome weaver image analysis software. DsbG is one of the few proteins that was consistently expressed only by the WT 20265 cultures but absent in the SCV 20265 irrespective of the growing conditions. This differential expression was observable in the anaerobically grown cultures too.

3.3.3 Discussion

Recent evidence indicates that *Pseudomonas aeruginosa* residing as biofilms in airway mucus of cystic fibrosis (CF) patients is undergoing anaerobic metabolism, a form of growth requiring gene products that are not utilized during aerobic growth. The outer membrane protein, OprF, and the rhl quorum sensing circuit are two previously unrecognized cellular factors that are now known to be required for optimal anaerobic biofilm viability. Without OprF, bacteria grow extremely poorly because they lack nitrite reductase activity while lacking rhlR or rhlI forces bacteria to undergo metabolic suicide by overproduction of nitric oxide. Furthermore, anaerobic growth seems to favor maintenance of the mucoid, alginate-overproducing phenotype. Thus, with increasing age of CF patients, mucoid populations predominate, indicating that anaerobic bacteria reside in the inspissated airway mucus. The role of anaerobic respiration in Pseudomonas pathogenesis in CF lungs is gaining so much importance that it has recently been proposed to develop of new drugs to combat anaerobic metabolism by *P. aeruginosa* for more effective treatment of chronic CF lung infections (Hassett *et al.,* 2002).

The major components of nitrate respiration apparatus in *Pseudomonas aeruginosa* are presented in the **figure1.6.1.** Cd-1 nitrite reductase catalyzes the conversion of nitrite to NO in denitrifying bacteria (Cutruzzola *et al.,* 2001). Interestingly, there was a significantly higher expression of the Cd1- nitrite reductase in SCV 20265 anaerobically grown cultures. One other component of the anaerobic respiration machinery namely the OprC was also found to be expressed higher in the SCV 20265 compared to the WT 20265. These observations together with the better growth of SCV 20265 under anaerobic growth conditions (refer **Figure 3.3.1 and 3.3.2**) lead us to speculate the better adaptation of SCV 20265 in the anaerobic mucous of the CF lung.

Additionally, in all the conditions of growth analysed so far, it has been a general observation that OprF, whose crucial role in anaerobic respiration has been emphasised repeatedly by several workers (Hassett *et al.,* 2002, Yoon *et al.,* 2002), was produced in very high levels by both the morphotypes. This reconfirms the ability of both these morphotypes to survive anaerobically. Thus the differential growth of SCV and WT 20265 under anaerobic conditions in the presence of nitrate supplement can be explained on the basis of differential expression of other components of the nitrate metabolism such as the nitrite reductase and OprC, which have been identified in the proteome analysis. However, these represent only a small piece of

a complex puzzle and therefore these observations can be interpreted as mere starting points for further experiments and cannot be claimed as anything conclusive. Since the role of quorum sensing system rhl is also known to be vital for optimal anaerobic growth, further investigations of the expression of the components of this system are also needed.

3.4 Polyadenylation of mRNA in *Pseudomonas aeruginosa*

3.4.1 Polyadenylation of mRNA in *Pseudomonas aeruginosa*

During the synthesis of cDNA from *P. aeruginosa* 20265 morphotypes, for the real time PCR analysis of *feoB* described in section 3.1.6, an attempt was made to prepare cDNA of the total mRNA using oligo (dT) primed reverse transcription. Generally the cDNAs of bacterial mRNA complement are generated with random hexamer primers. The use of oligo (dT) primers are largely restricted to the preparation of cDNA from eukaryotic mRNAs which are known to invariably have long poly (A) tracts at their 3'end. It is widely believed that such poly (A) tails are rare in the prokaryotic world whose RNAs undergo little or no processing after transcription. However, there is growing evidence about the occurrence of polyadenylated mRNAs in a variety of prokaryotes (Sarkar, 1997).

Total RNA was isolated as described in the relevant materials and methods section. DNAse was used to remove any traces of genomic DNA. The quality of the mRNA was checked on the formaldehyde agarose gel. **Figure 3.4.1** shows the purity of the total RNA isolation used for the study from *P. aeruginosa* 20265 morphotypes on a 1.5 % (w/v) agarose gel.
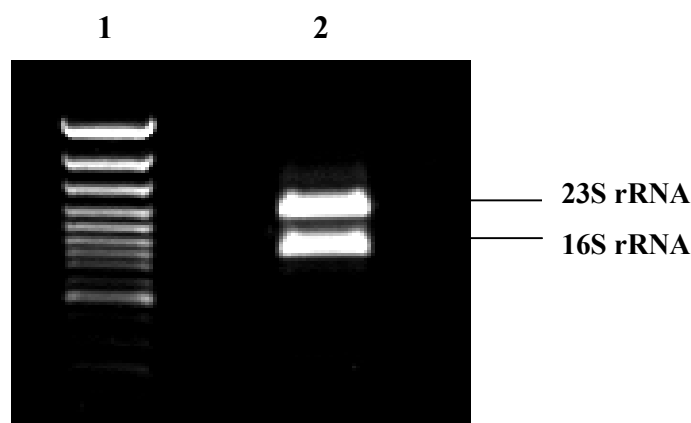
Fig 3.4.1 Total RNA from *P. aeruginosa* 20265 separated by non denaturing agarose gel electrophoresis (1.5 % w/v) and stained with 0.5 μg ethidium bromide per ml. 100 bp DNA ladder (1); RNA (2 μg) purified from *P. aeruginosa* PAO1 (2).

cDNA was prepared in the presence and absence of oligo (dT). A cDNA preparation with random hexamer primers was used as a positive control and a cDNA reaction mix without mRNA was used as a negative control. The cDNA was then analyzed on 0.8 % agarose gel and visualized under UV light after staining with ethidium bromide. A continuous smear of cDNA could be observed and no bands were observed in the negative controls.

Specific mRNA transcripts of *rpoD* were amplified with gene specific primers (refer Appendix) using cDNA of the morphotypes of 20265 *P. aeruginosa.* As expected, a 359 bp sequence corresponding to the *rpoD* product was observed (refer **figure 3.4.2, lanes 3,4,5**). It was confirmed that the amplification of *rpoD* using cDNA prepared in presence of oligo (dT) was identical to that obtained with genomic DNA amplification and the random hexamer primer generated cDNA. This was done by sequencing the eluted PCR products from these three reactions (data not shown).
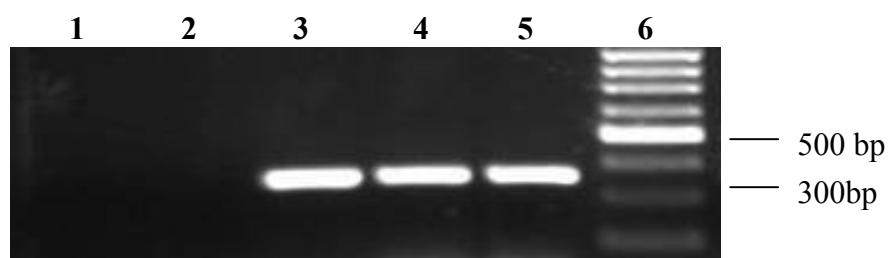
Figure 3.4.2. Electrophoresis of cDNA corresponding to rpoD mRNA transcript amplified by RT-PCR with gene specific primers from WT 20265 *Pseudomonas aeruginosa*. cDNA preparation without RT (1); cDNA preparation without oligo(dT) or random primers (2); Genomic DNA amplified rpoD (3); cDNA preparation with random primers (4); cDNA preparation with oligo(dT) (5); Standard 3000 -100bp size (6).

Further, mRNA transcript of *feoB* homologue in *P. aeruginosa,* namely PA4358 was amplified by RT-PCR (data not shown) using the gene specific primers shown in Appendix I, and transcripts could be detected in cDNA preparations made in presence of oligo (dT). Again, the size and sequence identity of the RT-PCR product was found to match that amplified from the genomic DNA. Thus the ability to synthesize cDNA using oligo (dT) primers was clearly demonstrated which confirmed the occurrence of polyadenylation in mRNAs of *P. aeruginosa.*
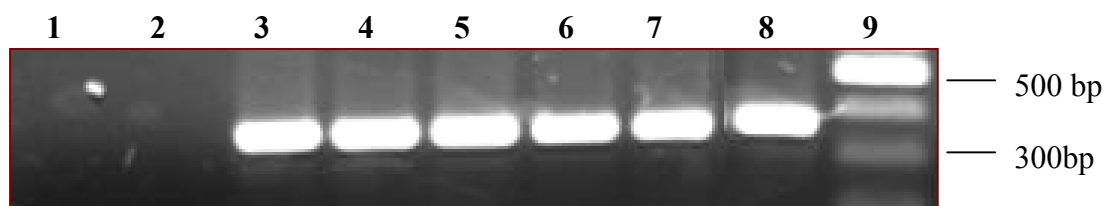

Figure 3.4.3. Electrophoresis of cDNA corresponding to rpoD mRNA transcript amplified by RT-PCR with gene specific primers from *Pseudomonas aeruginosa* PAO1 and TB. cDNA preparation without RT (1); cDNA preparation without oligo (dT) or random primers (2); Genomic DNA amplified rpoD from strain TB (3); cDNA preparation with random primers for strain TB (4); cDNA preparation with oligo (dT) for strain TB (5);Genomic DNA amplified rpoD from strain PAO1 (6); cDNA preparation with random primers for strain PAO1 (7); cDNA preparation with oligo (dT) for strain PAO1 (8); Standard (3000bp – 100 bp) (9).

In order to determine if the phenomenon of polyadenylation itself was widespread among the different isolates of *P. aeruginosa* or if it was restricted only to the clinical isolate 20265 used in this study, rpoD was amplified from cDNA synthesised with oligo (dT) primers from

strains PAO1 (Genome sequenced strain) and a clinical isolate TB. The results are presented in **figure 3.4.3**. The amplification of a similar gene product corresponding to rpoD, which was identical to the amplification products amplified from strain 20265, clearly demonstrated the occurrence of polyadenylation in these isolates of *Pseudomonas aeruginosa* too.

In order to confirm and evaluate the extent of polyadenylation of *P. aeruginosa* mRNA, *P. aeruginosa* PAO1 (genome sequenced strain) RNA isolated from cells (in exponential phase of growth) grown in Vogel Bonner (VB) medium, was reverse transcribed with either the oligo (dT) primer or the random hexamer primers. As shown in **figure 3.4.4**, a continuous smear of *P. aeruginosa* PAO1 cDNA could be observed with oligo (dT) primers as well as with random hexamer primers whereas no bands were observed in the negative controls lacking RNA or oligo (dT) primers. The yield of cDNA prepared using oligo (dT) primed reaction was approximately five times less than that prepared using random primed reactions for the same amount of RNA used, as determined by UV absorption using a spectrophotometer. Both the resultant cDNAs were separately hybridized to *P. aeruginosa* PAO1 GeneChip (Affymetrix).
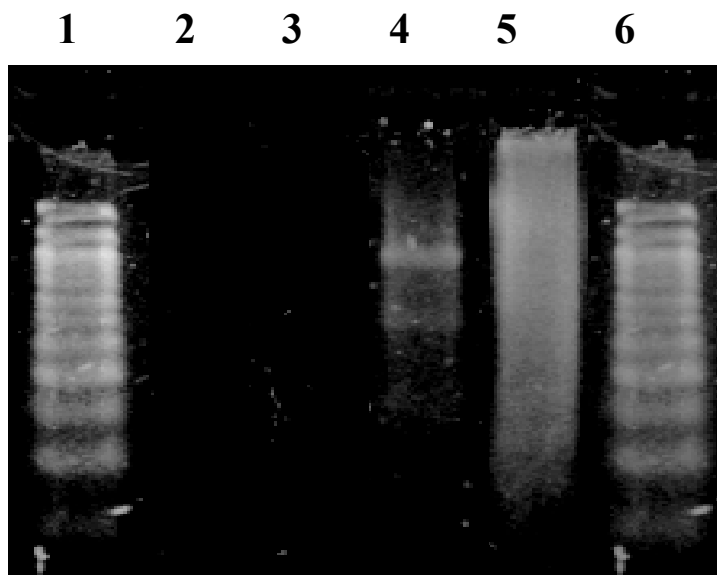

Figure 3.4.4 cDNA synthesis in the presence of oligo (dT) primers or random hexamer primers using RNA isolated from PAO1. Marker 100 bp DNA ladder (1); cDNA mix without RNA (negative control) (2); cDNA mix without oligo (dT) primers (negative control) (3); cDNA preparation using oligo (dT) primers (4); cDNA preparation with random hexamer primers (positive control) (5); Marker 100 bp DNA ladder (6). The gel was run on 2 % agarose gel and stained with sybr green.

This DNA oligonucleotide array comprises of oligonucleotide probes for 5549 coding sequences (CDS), 18 tRNA genes, one rRNA operon and 199 probe sets corresponding to all

intergenic regions selected from the annotated genome of strain PAO1, as well as 117 genes found in other *P. aeruginosa* strains. The comparative DNA microarray analysis was used to identify the specific genes whose RNA transcripts were polyadenylated giving some estimates about the extent of polyadenylation and the type of transcripts that were polyadenylated. Accordingly, a total of 2739 genes were detected with significant (according to statistical algorithms of MAS 5.0) signal intensities using random primed cDNA synthesis. This represents 49.3 % of the total 5549 *P. aeruginosa* PAO1 CDS on the chip (**Table 3.4.1**). Out of these 2739, 1199 genes representing 21.6 % of the 5549 CDS, were found to have polyadenylation of their mRNA transcripts because they were also detected in cDNA preparations made from oligo (dT) primed reactions (**Table 3.4.1)**.

Table 3.4.1 Number of genes and the respective percentages for which signals could be detected on a *P. aeruginosa* GeneChip using cDNAs prepared from either oligo (dT) primers or random hexamer primers.

	Number of genes	Percentage
Total number of genes (CDS) on the GeneChip	**5549**	**100%**
Total number of genes detected in the GeneChip	**2755**	**49.6%**
Genes detected **using random primers**	**2739**	**49.3%**
using oligo (dT) primers	**1215**	**21.8%**
using oligo (dT) primers and not with random primers	**16**	**0.1%**
using random primers and not with oligo (dT) primers	**1540**	**27.7%**
by both random primers and oligo (dT) primers	**1199**	**21.6%**
Genes not detected	**2794**	**50.3%**

Thus, 43.7 % of the genes detected using random primed cDNA synthesis showed polyadenylation of their corresponding mRNAs. 16S rRNA, 23S rRNA and several tRNA species were polyadenylated too. Signals for only 16 genes were detected exclusively using oligo (dT) primed cDNA. All these 16 genes were not detected in random primed cDNA preparations in the present study and interestingly almost all of them belonged to the functional class of hypothetical proteins. However, the DNA microarray results of two earlier works which used random primed cDNA of strain 20265 (von Götz *et al.,* 2004) and strain PAO1 (Salunkhe *et al.*, 2003) were compared to the results of the present study. The detection

of the 16 genes (that were detected exclusively using the oligo (dT) primed cDNA in the present study) was found to be highly variable. Detection of signals for these genes was scrutinized in several independent GeneChips hybridized with random primed cDNA prepared from strain 20265 RNA, harvested under similar culture conditions (data not shown) and several independent GeneChips hybridized with random primed cDNA prepared from strain PAO1 RNA, harvested under different culture conditions (data not shown). None of the 16 genes in question were absent in all the hybridisations indicating that cDNAs for these genes were not exclusively primed by oligo (dT) only as revealed by the present study.

Figure 3.4.5 gives a comparison of numbers of genes whose mRNA transcripts were polyadenylated, non-polyadenylated and total number of genes detected by random primed cDNA synthesis belonging to different functional classes. mRNAs of genes belonging to almost all the 26 major functional classes enlisted in **figure 3.4.5** were polyadenylated. Little or no polyadenylation was observed in the mRNAs corresponding to genes belonging to two component regulatory systems, phage related proteins and putative enzymes. A high proportion of polyadenylated mRNAs corresponded to genes belonging to the functional classes of translation and posttranslational modification, energy metabolism and genes coding hypothetical protein. The proportion of polyadenylated mRNAs exceeded the non-polyadenylated mRNAs in the functional classes of motility and attachment, protein secretion and export and nucleotide biosynthesis genes, adaptation and protection, amino acid biosynthesis, cell division, cell wall / capsule / LPS, chaperones and heat shock, energy metabolism, transcription and translation and post-translational processing.

rpoD and *feoB,* whose transcripts were found to be polyadenylated in the RT PCR, were also were detected as polyadenylated genes in the DNA microarray analysis. As a further evidence for the occurrence of polyadenylation in *P. aeruginosa,* expression signals of *pnp* (PA4740), *rne* (PA2976) and *pcnB* (PA4727), putative enzymes involved in the mRNA degradation and polyadenylation could be detected in the array analysis. In addition the putative poly (A) binding protein PA3162 (ribosomal protein S1) was also detected in high levels. PA4944 (*hfq*) was yet another gene with a possible involvement in polyadenylation, whose transcripts were detected with significant signal intensities (data not shown).
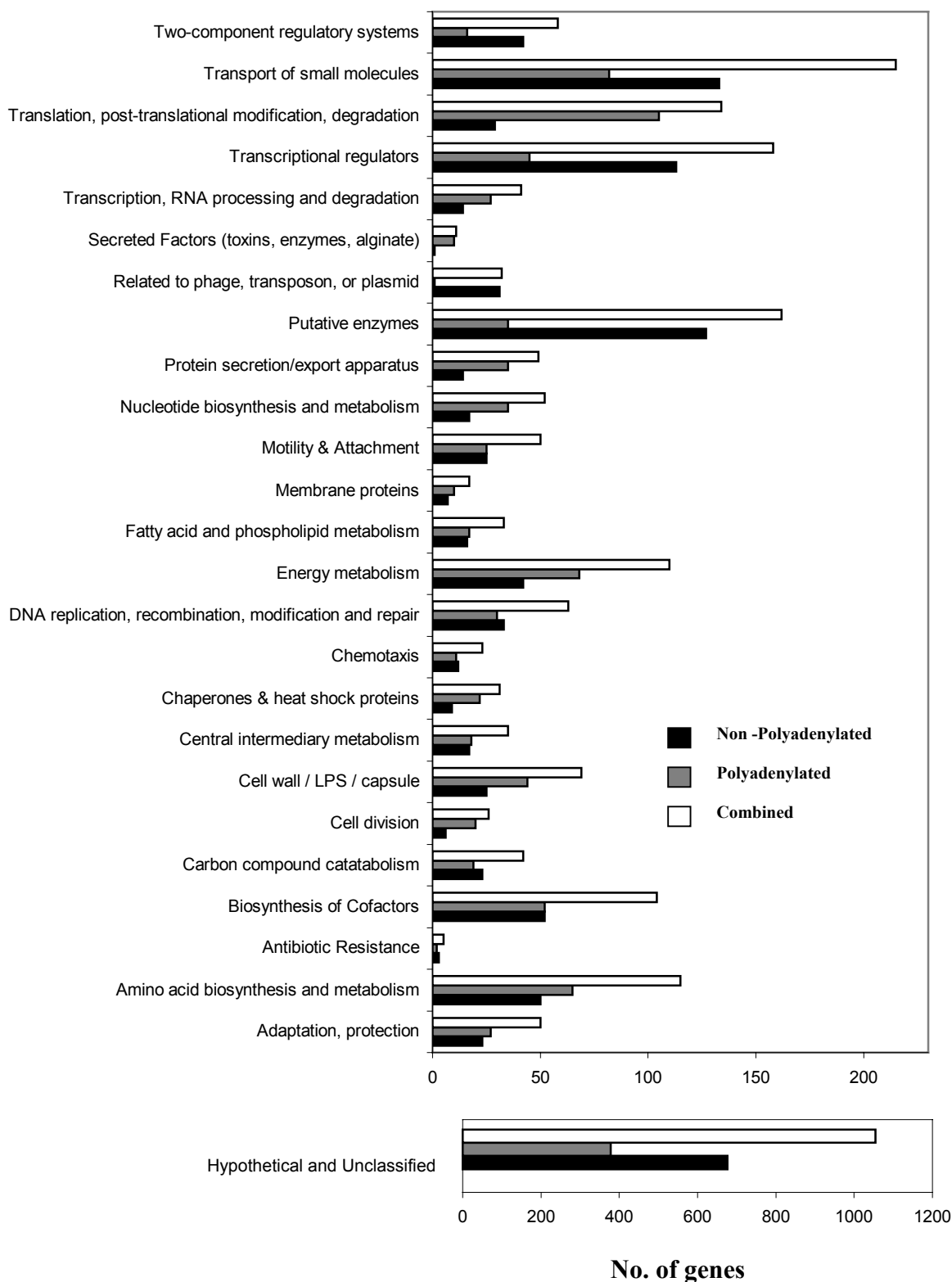
Figure 3.4.5. Comparison of numbers of genes whose mRNA transcripts were polyadenylated or non-polyadenylated as detected by GeneChip analysis. The genes analysed are categorized into functional classes based on the annotation available from the *Pseudomonas* genome sequence. Inset bar graph shows shows the relative number of genes for the functional class Hypothetical, unclassified proteins. Category 'Combined' in the figure legend represents the combined total of polyadenylated and non-polyadenylated transcripts identified in each functional class.

3.4.2 Discussion

mRNA polyadenylation now appears to be a common property of all living cells, but until recently it had been extensively studied only in eukaryotes (Colgan *et al.,* 1997; Sachs *et al.,* 1997; Wickens *et al.,* 1997). In eubacteria mRNAs have been detected in both gram positive and gram-negative organisms (Sarkar, 1996; Sarkar, 1997). In Mycobacteria, the oligo(dT) primed synthesis of cDNA by reverse transcriptase has been reported (Rindi *et al.,* 1998; Adilakshmi *et al.,* 2000). Unlike the poly (A) tracts in eukaryotic mRNA which range from 80 to 200 nucleotides, poly (A) tracts in prokaryotes range between 14 and 60 nucleotides and, moreover, polyadenylation occurs at all unprotected RNA 3'termini irrespective of their secondary structure. The functions of bacterial RNA polyadenylation are quiet diverse, ranging from the control of plasmid replication to the modulation of mRNA stability, as well as a possible role in mRNA translation (Sarkar, 1997). Polyadenylation of transcripts in bacteria is believed to be involved in the regulation of gene expression by influencing the efficiency of mRNA degradation (Jasiecki, *et al.,* 2003). Polyadenylation is now emerging as a process that plays an important role in maintaining the momentum of exonucleolytic degradation by adding single-stranded extensions to the 3' ends of mRNAs and their decay intermediates, thereby facilitating further exonuclease digestion (Steege, 2000). Much of our knowledge about bacterial polyadenylation has been derived from works in *E. coli* (Sarkar, 1996). To the best of our knowledge there has been no report demonstrating the occurrence of polyadenylation in any Pseudomonad. DNA microarray analysis had been used to demonstrate the extent of polyadenylation of mycobacterial mRNAs (Lakey, *et al.,* 2002). A similar DNA microarray approach was employed in this study to confirm and evaluate the extent of polyadenylation in *P. aeruginosa*. The GeneChip hybridisation revealed the oligo (dT) primed cDNA synthesis for only 1215 genes, whereas the priming with random primers yielded hybridisation signals for 2739 genes. It is possible that the number of mRNAs primed by oligo (dT) was underestimated because the large amounts of polyadenylated rRNA may depress cDNA synthesis from mRNA templates. Indeed there were intense signals for the rRNA genes too when the GeneChips were hybridized with oligo (dT) primed cDNAs (data not shown). Priming efficiency of the random hexamer primers to generate representative cDNAs was unrivalled by the oligo (dT) primers. Therefore use of oligo (dT) primers to generate representative cDNA of total RNA preparation is largely relevant in the context of detecting the polyadenylated species of RNAs among a heterogenous mixture of total RNA preparation and not to complement detection using random hexamer primed cDNA.

The chief enzymes that are responsible for the polyadenylation are poly (A) polymerases. Even though the poly (A) polymerases of *E. coli* have been well studied, their counterparts in *P. aeruginosa* have been annotated purely based on their sequence homologies. *pcnB* encodes the major poly (A) polymerase (PAP I) in *E. coli*. Poly (A) polymerase (ATP: polyribonucleotide adenylyltransferase) catalyzes the template–independent sequential addition of adenylate residues to the 3'hydroxyl termini of RNA molecules. *pnp* encodes a 3'-exonuclease, polynucleotide phosphorylase (PNPase) and *rne* encodes an endonuclease RNase E, both of which are implicated in the turnover of poly(A) tracts and the in vivo modulation of polyadenylation in *E. coli* (Mohanty, *et al.,* 2000). It is known that S1 ribosomal protein is a poly (A) binding protein in *E. coli* (Kalapos, *et al.,* 1997). *hfq* is known to stimulate elongation of poly (A) tails by poly (A) polymerase I in *E. coli* (Hajnsdorf, et al., 2000). Detection of signals, for the putative counterparts of these poly (A) tail-related genes in our array analysis is an additional evidence for the occurrence of polyadenylation in *P. aeruginosa.* Our study also indicates that polyadenylation seems to occur in the mRNAs of all the major functional classes of genes and is not restricted to any one or few of them.

Polyadenylation depends on growth rate (Jasiecki, *et al.,* 2003) and growth phase (Cao, *et al.,* 1997) in *E. coli* with increased polyadenylation observed in slowly growing cells. Levels of poly (A) polymerase, PAP I, was reported to be higher in slowly growing cells cultivated in media supporting high growth rates (Jasiecki, *et al.,* 2003). It remains to be investigated whether there exist any differences in polyadenylation with respect to growth phases in *P. aeruginosa* also and if the polyadenylation in *P. aeruginosa* has the same functions as described in *E. coli* i.e. marking mRNA transcripts for degradation by ribonucleases, which is important for maintaining an equilibrium of the normal RNA turnover, or if it has some novel functions.

The experimental demonstration of the occurrence of polyadenylation to an appreciable extent in the *P. aeruginosa* transcripts is significant in many respects. Firstly, it proves the occurrence of a basic biological phenomenon in *P. aeruginosa*, which has only been speculative so far. Secondly, it opens our views to possible new means of post-transcriptional regulation of gene expression in *P. aeruginosa.* It also underlines the importance of the need to further study polyadenylation and therefore mRNA stability in the biology of *P. aeruginosa.* It might be reasonable to speculate that the polyadenylation might be even more widespread and may be found in other species of *Pseudomonas* too. To our knowledge,

nothing is known about the post-transcriptional processing through polyadenylation in *Pseudomonas aeruginosa*. In this context, understanding the role of this phenomenon and the enzymes involved in these processes and their impact on the overall gene expression will be important.

4.   Summary and Conclusion

The role of SCVs isolated from chronically infected CF lungs, in pathogenesis is still unclear. The objectives of the present study were to determine if the SCV 20265 and WT 20265 (the paradigm strain of a subgroup of hyperpiliated, autoaggregative and cytotoxic SCVs) displayed a differential growth response to some typical stress conditions like iron limitation, oxidative stress and anaerobic/microaerobic mode of growth and follow up the possible molecular causes of such differentially responses at a proteome level using Proteomics technologies encompassing mass spectrometry, as major investigation tool.

Previous works in our laboratory have accomplished some Transcriptome analysis (von Götz 2003) and Proteome analysis (Wehmhöner, 2002) of the strain 20265 with no specific attention to these stress conditions. Additionally, other SCV related works from our laboratory have demonstrated the enhanced virulence of SCV 20265 and some other hyperpiliated and autoaggregative SCVs using killing assays in mice and worm (*C.elegans*) models. It is in this context that the present study began with testing the hypothesis that SCV 20265 may represent a clonal variant that is better adapted than its clonal wildtype WT 20265 to cope up with stresses like iron limitation stress, oxidative stress and anaerobic stress which are likely to be encountered in the various niches of the CF lung that they colonise. Several functional assays to demonstrate the relative fitness of these morphotypes and morphotypes of the few other strains, to the above mentioned stress conditions were standardized. It was clearly demonstrated on plate assays and liquid assays that the SCV 20265 was indeed better adapted to cope up with 2,2-Dipyridyl induced iron limitation. The distribution of this special trait was variable. Not all SCVs are well adapted to iron stress better than their clonal WT and vice versa. This was also true of the response of the morphotypes to oxidative stress induced by hydrogen peroxide. Not all SCVs were fitter than their corresponding clonal wildtypes to survive an oxidative insult. SCV 20265 was however unique in its ability to adapt to these diverse stress consitions better than its clonal WT.

The ability to grow well under an anaerobic/microaerobic mode of growth was tested in the SCV 20265 and WT 20265. The results revealed that SCV 20265 was indeed outgrowing the WT 20265 under anaerobic mode of growth using a supplemented nitrate source. Extensive proteome analysis was also performed on the morphotypes of 20265 grown under the different stress conditions. The differential expression of several iron acquisition related proteins, oxidative stress combat proteins and proteins involved in nitrate respiration could be

detected and correlated well with the differential responses of SCV 20265 on functional assays. One interesting aspect of this study was the detailed investigation of the membrane and supernatant subproteome using a gel-less nanoflow LC/MS approach. The challenges of analysing the membrane subproteome with conventional gel based systems like the 16-BAC separation have been done away with the greater ease, precision and high-throughput of LC/MS approach. These were some areas that were not well explored before in the previous studies. Careful analysis of the LC/MS protein identifications revealed the reproducible differential expression of one probable ferrous iron transporter – a *feoB* homolog (PA4358). Using real time PCR, expression level of the probable Ferrous iron transporter (*feoB*), PA4358 was followed at an mRNA level and its higher expression by SCV 20265 was confirmed. The role of *feoB* in pathogenesis or iron acquisition of *P. aeruginosa* is hitherto unknown. This offers a good prospect for future investigations in this line. This clearly illustrated that one could apply gel-less LC/MS approach for a initial round of screening for candidates of differential expression in a comparative proteome analysis such as this study and subsequently identify potential genes whose expression can be followed with other sensitive specific approaches. This approach is particularly useful for analysing challenging subproteomes such as that of the membrane subproteome. Also the greater ease in handling several samples and the number of significant protein identifications obtained are unrivalled by the cumbersome gel based conventional approaches. However, one sure disadvantage of this LC/MS approach was that the inability to provide quantitative information on the relative abundance of any protein between the subjects compared.

One unexpected outcome of the present study was the discovery of the phenomenon of polyadenylation of mRNAs in *P. aeruginosa*. Even though, genome sequencing and annotation of the genome sequence has hinted at existence of Poly (A) polymerase enzyme, the chief enzyme responsible for polyadenylation of mRNA transcripts, there has been no experimental proof for the occurrence of polyadenylation in *P. aeruginosa* so far. Much of what we know about polyadenylation in bacteria is from the studies undertaken in *E.coli*. Since any extrapolation of observations in *E.coli* to *P. aeruginosa* must be backed by strong experimental proof, the present study investigated the phenomenon of polyadenylation in *P. aeruginosa*. During the real time PCR analysis of *feoB* transcripts an attempt was made to synthesise cDNA using oligo (dT) primer (that binds only to Poly (A) sequences on mRNA). Surprisingly, it was possible to prepare cDNA using oligo (dT) primer. Subsequently, the occurrence of polyadenylation was confirmed using independent approaches on several

strains of *P.aeruginosa*. Using RT PCR specific transcripts of rpoD were amplified from cDNA synthesised using both random primers and oligo (dT) primers. Additionally the specific amplification products from the different cDNA sources were compared with the PCR products of *rpoD* amplified using genomic DNA as template. All the products were found to match. To gain broader understanding of the type of genes and the number of genes that were polyadenylated, a genome wide analysis of PAO1 genome was undertaken using DNA microarrays. Interestingly, as high as 43% of the expressed genes of PAO1 were found to be polyadenylated during log phase. The discovery of polyadenylation in *P. aeruginosa* and the high level of polyadenylation among the transcripts, surely hint at the possible role for post transcriptional processing in the control of gene expression in *P. aeruginosa*. Future studies in this direction must be able to provide more insight into role of polyadenylation in Pseudomonas gene expression and its biology in general.

The present study has to a large extent accomplished many of its fore set goals. The study has clearly answered that SCV 20265 is fitter than its clonal WT in surviving harsher stress conditions like those of iron limitation, oxidative stress and ability to grow under anaerobic condition using nitrate. Proteomics provided a great deal of information on several proteins of the iron acquisition systems, Superoxide dismutases and other oxidative stress combat proteins, membrane proteins, nitrate utilization and anaerobic respiration proteins. In many cases the differential expression of these proteins could be correlated with the observed differential responses of the morphotypes to the various stress conditions. However, the picture obtained with the proteome data was far from complete because of the inherent difficulty of the proteomics approach to look at all of the expressed proteins in a single experiment unlike the DNA microarray approach. Henceforth, it is important that in order to gain a complete picture, both the approaches must be used in parallel to complement the findings from each other. It is therefore worth investigating the iron limitation stress response, oxidative stress response and anaerobic mode of growth using nitrate supplements, of the SCV and WT pairs of strain 20265 using DNA microarrays to obtain some trancriptome analysis of these responses in order to evolve well directed future proteomics studies. Once a short list of proteins to be investigated, has been generated using the transcriptome analysis, it is much easier to follow the protein level expression of these genes on 2D gels using special enrichment and prefractionation strategies and a combination of different pH IPG strips.

From the present study, there are some candidates that can be suggested for further focussed investigation and it might be even worth generating isogenic mutants of these genes in order

to ascertain their role in the pathogenicity of *Pseudomonas aeruginosa* and perhaps even in the inter clonal variations. These include the *feoB* homologue (PA4358), *dsbG* (PA2476), *dsbA* (PA5489), *hasAp* (PA 3407), *minD* (PA3244), *mexE* (PA2493), *czaA* (PA2520) and *ostA* (PA0595). Many of these proteins have been differentially expressed in the SCV or WT and might have some role to play in pathogenicity or basic biology. But for most of these the functions have been assigned purely using *in silico* bioinformatic analysis based on sequence similarity to homologues in *E. coli* or other related bacteria. Therefore, any functional demonstration of the accuracy of their present annotations is lacking at the moment. It must be emphasised here that this list is not exhaustive and more such candidates could be picked upon careful data analysis in combination with other future experiments like the ones proposed above.

In conclusion, SCV 20265 represents a highly adapted clonal variant with a slow growing phenotype that can tackle iron limitation, oxidative stress and anaerobic stress better than its clonal wildtype. This exemplifies clonal variation as a means of adaptation to the harsh CF lung habitat where such stress conditions are likely to occur. It is possible that similar adaptation occurs in variants of other isolates too even though it may not necessarily be the rule for very SCV. Overall the situation represents a complex bacterial adaptation to the plethora of changing niches of a complex habitat such as the CF lung. Studies such as this will surely help in understanding the basic mechanisms of adaptation of this versatile pathogenic bacteria and help in evolving novel therapeutic strategies and diagnostic methods that can improve the conditions of patients suffereing from infections.

5.   Literature

Abdul-Tehrani,H., Hudson,A.J., Chang,Y.S., Timms,A.R., Hawkins,C., Williams,J.M., Harrison,P.M., Guest,J.R., and Andrews,S.C. (1999) Ferritin mutants of *Escherichia coli* are iron deficient and growth impaired, and fur mutants are iron deficient *J.Bacteriol.* **181**: 1415-1428.

Adilakshmi,T., Ayling,P.D., and Ratledge,C. (2000) Polyadenylylation in mycobacteria: evidence for oligo(dT)-primed cDNA synthesis *Microbiology* **146 (Pt 3)**: 633-638.

Andrews,S.C., Robinson,A.K., and Rodriguez-Quinones,F. (2003) Bacterial iron homeostasis *FEMS Microbiol.Rev.* **27**: 215-237.

Ankenbauer,R.G. (1992) Cloning of the outer membrane high-affinity Fe(III)-pyochelin receptor of *Pseudomonas aeruginosa J.Bacteriol.* **174**: 4401-4409.

Beardsley,R.L., Reilly,J.P. (2002) Optimization of guanidination procedures for MALDI mass mapping *Anal.Chem.* **74**: 1884-1890.

Bernal,A., Ear,U., and Kyrpides,N. (2001) Genomes OnLine Database (GOLD): a monitor of genome projects world-wide *Nucleic Acids Res.* **29**: 126-127.

Bodey,G.P. (1983) Infectious diseases update: 1982. Summary of a symposium *Rev.Infect.Dis.* **5**: 232-234.

Bodey,G.P., Bolivar,R., Fainstein,V., and Jadeja,L. (1983) Infections caused by *Pseudomonas aeruginosa Rev.Infect.Dis.* **5**: 279-313.

Brancia,F.L., Butt,A., Beynon,R.J., Hubbard,S.J., Gaskell,S.J., and Oliver,S.G. (2001) A combination of chemical derivatisation and improved bioinformatic tools optimises protein identification for proteomics *Electrophoresis* **22**: 552-559.

Braun,V. (2001) Iron uptake mechanisms and their regulation in pathogenic bacteria *International Journal of Medical Microbiology* **291**: 67-79.

Breitenstein,S., Walter,S., Bosshammer,J., Romling,U., and Tummler,B. (1997) Direct sputum analysis of *Pseudomonas aeruginosa* macrorestriction fragment genotypes in patients with cystic fibrosis *Med.Microbiol.Immunol.(Berl)* **186**: 93-99.

Britigan,B.E., Ratcliffe,H.R., Buettner,G.R., and Rosen,G.M. (1996) Binding of myeloperoxidase to bacteria: Effect on hydroxyl radical formation and susceptibility to oxidant-mediated killing *Biochimica et Biophysica Acta-General Subjects* **1290**: 231-240.

Britigan,B.E., Miller,R.A., Hassett,D.J., Pfaller,M.A., McCormick,M.L., and Rasmussen,G.T. (2001) Antioxidant enzyme expression in clinical isolates of *Pseudomonas aeruginosa*: Identification of an atypical form of manganese superoxide dismutase *Infection and Immunity* **69**: 7396-7401.

Brown,S.M., Howell,M.L., Vasil,M.L., Anderson,A.J., and Hassett,D.J. (1995) Cloning and characterization of the katB gene of *Pseudomonas aeruginosa* encoding a hydrogen peroxide-inducible catalase: purification of KatB, cellular localization, and demonstration that it is essential for optimal resistance to hydrogen peroxide *J.Bacteriol.* **177**: 6536-6544.

Cao, G. J., and Sarkar, N. (1997) Stationary phase-specific mRNAs in *Escherichia coli* are polyadenylated. *Biochem.Biophys.Res.Commun.* **239:**46-50.

Cash,P., Argo,E., Ford,L., Lawrie,L., and McKenzie,H. (1999) A proteomic analysis of erythromycin resistance in *Streptococcus pneumoniae Electrophoresis* **20**: 2259-2268.

Cash,P. (2000) Proteomics in medical microbiology *Electrophoresis* **21**: 1187-1201.

Colgan,D.F., and Manley,J.L. (1997) Mechanism and regulation of mRNA polyadenylation *Genes Dev.* **11**: 2755-2766.

Cordwell,S.J., Nouwens,A.S., and Walsh,B.J. (2001) Comparative proteomics of bacterial pathogens *Proteomics.* **1**: 461-472.

Cordwell,S.J., Larsen,M.R., Cole,R.T., and Walsh,B.J. (2002) Comparative proteomics of *Staphylococcus aureus* and the response of methicillin-resistant and methicillin-sensitive strains to Triton X-100 *Microbiology* **148**: 2765-2781.

Cutruzzola,F., Brown,K., Wilson,E.K., Bellelli,A., Arese,M., Tegoni,M., Cambillau,C., and Brunori,M. (2001) The nitrite reductase from *Pseudomonas aeruginosa*: Essential role of two active-site histidines in the catalytic and structural properties *Proceedings of the National Academy of Sciences of the United States of America* **98**: 2232-2237.

Dao,K.H.T., Hamer,K.E., Clark,C.L., and Harshman,L.G. (1999) Pyoverdine production by *Pseudomonas aeruginosa* exposed to metals or an oxidative stress agent *Ecological Applications* **9**: 441-448.

de Bentzmann,S., Roger,P., and Puchelle,E. (1996) *Pseudomonas aeruginosa* adherence to remodelling respiratory epithelium *Eur.Respir.J.* **9**: 2145-2150.

de Bentzmann,S., Plotkowski,C., and Puchelle,E. (1996) Receptors in the *Pseudomonas aeruginosa* adherence to injured and repairing airway epithelium *Am.J.Respir.Crit Care Med.* **154** : S155-S162.

de Bentzmann,S., Roger,P., Dupuit,F., Bajolet-Laudinat,O., Fuchey,C., Plotkowski,M.C., and Puchelle,E. (1996) Asialo GM1 is a receptor for *Pseudomonas aeruginosa* adherence to regenerating respiratory epithelial cells *Infect.Immun.* **64**: 1582-1588.

Dean,C.R., Poole,K. (1993) Cloning and characterization of the ferric enterobactin receptor gene (pfeA) of *Pseudomonas aeruginosa J.Bacteriol.* **175**: 317-324.

DeWitte,J.J., Cox,C.D., Rasmussen,G.T., and Britigan,B.E. (2001) Assessment of structural features of the pseudomonas siderophore pyochelin required for its ability to promote oxidant-mediated endothelial cell injury *Archives of Biochemistry and Biophysics* **393**: 236-244.

Deziel,E., Comeau,Y., and Villemur,R. (2001) Initiation of biofilm formation by *Pseudomonas aeruginosa* 57RP correlates with emergence of hyperpiliated and highly adherent phenotypic variants deficient in swimming, swarming, and twitching motilities *J.Bacteriol.* **183**: 1195-1204.

Deziel,E., Lepine,F., Milot,S., and Villemur,R. (2003) rhIA is required for the production of a novel biosurfactant promoting swarming motility in *Pseudomonas aeruginosa*: 3-(3-hydroxyalkanoyloxy) alkanoic acids (HAAs), the precursors of rhamnolipids *Microbiology* **149**: 2005-2013.

Doring,G., Maier,M., Muller,E., Bibi,Z., Tummler,B., and Kharazmi,A. (1987) Virulence factors of *Pseudomonas aeruginosa Antibiot.Chemother.* **39**: 136-148.

Drenkard,E., Ausubel,F.M. (2002) *Pseudomonas aeruginosa* biofilm formation and antibiotic resistance are linked to phenotypic variation *Nature* **416**: 740-743.

Dubrac,S., Touati,D. (2000) Fur positive regulation of iron superoxide dismutase in *Escherichia coli*: functional analysis of the sodB promoter *J.Bacteriol.* **182**: 3802-3808.

Dubrac,S., Touati,D. (2000) Fur positive regulation of iron superoxide dismutase in *Escherichia coli*: functional analysis of the sodB promoter *J.Bacteriol.* **182**: 3802-3808.

Eschenbrenner,M., Wagner,M.A., Horn,T.A., Kraycer,J.A., Mujer,C.V., Hagius,S., Elzer,P., and DelVecchio,V.G. (2002) Comparative proteome analysis of *Brucella melitensis* vaccine strain Rev 1 and a virulent strain, 16M *J.Bacteriol.* **184**: 4962-4970.

Escolar,L., Perez-Martin,J., and de Lorenzo,V. (1999) Opening the iron box: Transcriptional metalloregulation by the fur protein *Journal of Bacteriology* **181**: 6223-6229.

Feldman,M., Bryan,R., Rajan,S., Scheffler,L., Brunnert,S., Tang,H., and Prince,A. (1998) Role of flagella in pathogenesis of *Pseudomonas aeruginosa* pulmonary infection *Infect.Immun.* **66**: 43-51.

Foght,J.M., Westlake,D.W., Johnson,W.M., and Ridgway,H.F. (1996) Environmental gasoline-utilizing isolates and clinical isolates of *Pseudomonas aeruginosa* are taxonomically indistinguishable by chemotaxonomic and molecular techniques *Microbiology* **142 (Pt 9)** : 2333-2340.

Folschweiller,N., Schalk,I.J., Celia,H., Kieffer,B., Abdallah,M.A., and Pattus,F. (2000) The pyoverdin receptor FpvA, a TonB-dependent receptor involved in iron uptake by *Pseudomonas aeruginosa* (review) *Molecular Membrane Biology* **17**: 123-133.

Frederick,J.R., Elkins,J.G., Bollinger,N., Hassett,D.J., and McDermott,T.R. (2001) Factors affecting catalase expression in *Pseudomonas aeruginosa* biofilms and planktonic cells *Applied and Environmental Microbiology* **67**: 1375-1379.

Freeman,W.M., Walker,S.J., and Vrana,K.E. (1999) Quantitative RT-PCR: pitfalls and potential *Biotechniques* **26**: 112-115.

Frey,A.D., Farres,J., Bollinger,C.J., and Kallio,P.T. (2002) Bacterial hemoglobins and flavohemoglobins for alleviation of nitrosative stress in *Escherichia coli Appl.Environ.Microbiol.* **68**: 4835-4840.

Fridovich,I. (1995) Superoxide radical and superoxide dismutases *Annu.Rev.Biochem.* **64**: 97-112.

Galloway,D.R. (1991) *Pseudomonas aeruginosa* elastase and elastolysis revisited: recent developments *Mol.Microbiol.* **5**: 2315-2321.

Gerlai,R. (2002) Phenomics: fiction or the future? *Trends Neurosci.* **25**: 506-509.

Giaever,G., Chu,A.M., Ni,L., Connelly,C., Riles,L., Veronneau,S., Dow,S., Lucau-Danila,A., Anderson,K., Andre,B., Arkin,A.P., Astromoff,A., El Bakkoury,M., Bangham,R., Benito,R., Brachat,S., Campanaro,S., Curtiss,M., Davis,K., Deutschbauer,A., Entian,K.D., Flaherty,P., Foury,F., Garfinkel,D.J., Gerstein,M., Gotte,D., Guldener,U., Hegemann,J.H., Hempel,S., Herman,Z., Jaramillo,D.F., Kelly,D.E., Kelly,S.L., Kotter,P., LaBonte,D., Lamb,D.C., Lan,N., Liang,H., Liao,H., Liu,L., Luo,C., Lussier,M., Mao,R., Menard,P., Ooi,S.L., Revuelta,J.L., Roberts,C.J., Rose,M., Ross-Macdonald,P., Scherens,B., Schimmack,G., Shafer,B., Shoemaker,D.D., Sookhai-Mahadeo,S., Storms,R.K., Strathern,J.N., Valle,G., Voet,M., Volckaert,G., Wang,C.Y., Ward,T.R., Wilhelmy,J., Winzeler,E.A., Yang,Y., Yen,G., Youngman,E., Yu,K., Bussey,H., Boeke,J.D., Snyder,M., Philippsen,P., Davis,R.W., and Johnston,M. (2002) Functional profiling of the *Saccharomyces cerevisiae* genome *Nature* **418**: 387-391.

Gilligan,P.H. (1991) Microbiology of airway disease in patients with cystic fibrosis *Clin.Microbiol.Rev.* **4**: 35-51.

Gorg,A., Obermaier,C., Boguth,G., Harder,A., Scheibe,B., Wildgruber,R., and Weiss,W. (2000) The current state of two-dimensional electrophoresis with immobilized pH gradients *Electrophoresis* **21**: 1037-1053.

Govan,J.R., and Deretic,V. (1996) Microbial pathogenesis in cystic fibrosis: mucoid *Pseudomonas aeruginosa* and *Burkholderia cepacia Microbiol.Rev.* **60**: 539-574.

Hajnsdorf, E., and Regnier, P. (2000) Host factor Hfq of *Escherichia coli* stimulates elongation of poly(A) tails by poly(A) polymerase I. *Proc.Natl.Acad.Sci.U.S.A* **97**:1501-1505.

Hale,J.E., Butler,J.P., Knierman,M.D., and Becker,G.W. (2000) Increased sensitivity of tryptic peptide detection by MALDI-TOF mass spectrometry is achieved by conversion of lysine to homoarginine *Anal.Biochem.* **287**: 110-117.

Hanna,S.L., Sherman,N.E., Kinter,M.T., and Goldberg,J.B. (2000) Comparison of proteins expressed by *Pseudomonas aeruginosa* strains representing initial and chronic isolates from a cystic fibrosis patient: an analysis by 2-D gel electrophoresis and capillary column liquid chromatography-tandem mass spectrometry *Microbiology-Uk* **146**: 2495-2508.

Hannon,G.J. (2002) RNA interference *Nature* **418**: 244-251.

Hantke, K. (2003) Is the bacterial ferrous iron transporter FeoB a living fossil ? *Trends in Microbiol.* **11**: 192-195.

Hassett,D.J., Charniga,L., Bean,K., Ohman,D.E., and Cohen,M.S. (1992) Response of *Pseudomonas aeruginosa* to pyocyanin: mechanisms of resistance, antioxidant defenses, and demonstration of a manganese-cofactored superoxide dismutase *Infect.Immun.* **60**: 328-336.

Hassett,D.J., Woodruff,W.A., Wozniak,D.J., Vasil,M.L., Cohen,M.S., and Ohman,D.E. (1993) Cloning and characterization of the *Pseudomonas aeruginosa* sodA and sodB genes encoding manganese- and iron-cofactored superoxide dismutase: demonstration of increased manganese superoxide dismutase activity in alginate-producing bacteria *J.Bacteriol.* **175**: 7658-7665.

Hassett,D.J., Schweizer,H.P., and Ohman,D.E. (1995) *Pseudomonas aeruginosa* sodA and sodB mutants defective in manganese- and iron-cofactored superoxide dismutase activity demonstrate the importance of the iron-cofactored form in aerobic metabolism *J.Bacteriol.* **177**: 6330-6337.

Hassett,D.J. (1996) Anaerobic production of alginate by *Pseudomonas aeruginosa*: alginate restricts diffusion of oxygen *J.Bacteriol.* **178**: 7322-7325.

Hassett,D.J., Sokol,P.A., Howell,M.L., Ma,J.F., Schweizer,H.T., Ochsner,U., and Vasil,M.L. (1996) Ferric uptake regulator (Fur) mutants of *Pseudomonas aeruginosa* demonstrate defective siderophore-mediated iron uptake, altered aerobic growth, and decreased superoxide dismutase and catalase activities *Journal of Bacteriology* **178**: 3996-4003.

Hassett,D.J., Howell,M.L., Sokol,P.A., Vasil,M.L., and Dean,G.E. (1997) Fumarase C activity is elevated in response to iron deprivation and in mucoid, alginate-producing *Pseudomonas aeruginosa*: cloning and characterization of fumC and purification of native fumC *J.Bacteriol.* **179**: 1442-1451.

Hassett,D.J., Howell,M.L., Ochsner,U.A., Vasil,M.L., Johnson,Z., and Dean,G.E. (1997) An operon containing fumC and sodA encoding fumarase C and manganese superoxide dismutase is controlled by the ferric uptake regulator in *Pseudomonas aeruginosa*: Fur mutants produce elevated alginate levels *Journal of Bacteriology* **179**: 1452-1459.

Hassett,D.J., Elkins,J.G., Ma,J.F., and McDermott,T.R. (1999) *Pseudomonas aeruginosa* biofilm sensitivity to biocides: Use of hydrogen peroxide as model antimicrobial agent for examining resistance mechanisms *Biofilms* **310**: 599-608.

Hassett,D.J., Ma,J.F., Elkins,J.G., McDermott,T.R., Ochsner,U.A., West,S.E.H., Huang,C.T., Fredericks,J., Burnett,S., Stewart,P.S., McFeters,G., Passador,L., and Iglewski,B.H. (1999) Quorum sensing in *Pseudomonas aeruginosa* controls expression of catalase and superoxide dismutase genes and mediates biofilm susceptibility to hydrogen peroxide *Molecular Microbiology* **34**: 1082-1093.

Hassett,D.J., Cuppoletti,J., Trapnell,B., Lymar,S.V., Rowe,J.J., Yoon,S.S., Hilliard,G.M., Parvatiyar,K., Kamani,M.C., Wozniak,D.J., Hwang,S.H., McDermott,T.R., and Ochsner,U.A. (2002) Anaerobic metabolism and quorum sensing by *Pseudomonas aeruginosa* biofilms in chronically infected cystic fibrosis airways: rethinking antibiotic treatment strategies and drug targets *Adv.Drug Deliv.Rev.* **54**: 1425-1443.

Haussler,S., Tummler,B., Weissbrodt,H., Rohde,M., and Steinmetz,I. (1999) Small-colony variants of *Pseudomonas aeruginosa* in cystic fibrosis *Clin.Infect.Dis.* **29**: 621-625.

Haussler,S., Ziegler,I., Lottel,A., von Gotz,F., Rohde,M., Wehmhohner,D., Saravanamuthu,S., Tummler,B., and Steinmetz,I. (2003) Highly adherent small-colony variants of *Pseudomonas aeruginosa* in cystic fibrosis lung infection *J.Med.Microbiol.* **52**: 295-301.

Holloway,B.W., Romling,U., and Tummler,B. (1994) Genomic mapping of *Pseudomonas aeruginosa* PAO *Microbiology* **140 (Pt 11)**: 2907-2929.

Imlay,J.A., Linn,S. (1987) Mutagenesis and stress responses induced in *Escherichia coli* by hydrogen peroxide *J.Bacteriol.* **169**: 2967-2976.

Jasiecki, J., and Wegrzyn., G. (2003) Growth-rate dependent RNA polyadenylation in *Escherichia coli. EMBO Rep.* 4:172-177.

Jungblut,P.R., Schaible,U.E., Mollenkopf,H.J., Zimny-Arndt,U., Raupach,B., Mattow,J., Halada,P., Lamer,S., Hagens,K., and Kaufmann,S.H. (1999) Comparative proteome analysis of *Mycobacterium tuberculosis* and *Mycobacterium bovis* BCG strains: towards functional genomics of microbial pathogens *Mol.Microbiol.* **33**: 1103-1117.

Kadir,F.H., Moore,C.R. (1990) Bacterial ferritin contains 24 haemgroups *FEBS Lett* **271**: 141-143.

Kalapos, M. P., Paulus, H., and Sarkar., N. 1997. Identification of ribosomal protein S1 as a poly(A) binding protein in *Escherichia coli. Biochimie* **79:** 493-502**.**

Keyer,K., Imlay,J.A. (1996) Superoxide accelerates DNA damage by elevating free-iron levels *Proc.Natl.Acad.Sci.U.S.A* **93**: 13635-13640.

Keyer,K., Imlay,J.A. (1996) Superoxide accelerates DNA damage by elevating free-iron levels *Proc.Natl.Acad.Sci.U.S.A* **93**: 13635-13640.

Kim,E.J., Sabra,W., and Zeng,A.P. (2003) Iron deficiency leads to inhibition of oxygen transfer and enhanced formation of virulence factors in cultures of *Pseudomonas aeruginosa* PAO1 *Microbiology* **149**: 2627-2634.

Krause,E., Wenschuh,H., and Jungblut,P.R. (1999) The dominance of arginine containing peptides in MALDI-derived tryptic mass fingerprints of proteins *Analytical Chemistry* **71**: 4160-4165.

Kuruvilla,F.G., Shamji,A.F., Sternson,S.M., Hergenrother,P.J., and Schreiber,S.L. (2002) Dissecting glucose signalling with diversity-oriented synthesis and small-molecule microarrays *Nature* **416**: 653-657.

Lakey,D.L., Zhang,Y., Talaat,A.M., Samten,B., DesJardin,L.E., Eisenach,K.D., Johnston,S.A., and Barnes,P.F. (2002) Priming reverse transcription with oligo(dT) does not yield representative samples of Mycobacterium tuberculosis cDNA *Microbiology* **148**: 2567-2572.

Lamont,I.L., Beare,P.A., Ochsner,U., Vasil,A.I., and Vasil,M.L. (2002) Siderophore-mediated signaling regulates virulence factor production in *Pseudomonas aeruginosa Proc.Natl.Acad.Sci.U.S.A* **99**: 7072-7077.

Leidal,K.G., Munson,K.L., Johnson,M.C., and Denning,G.M. (2003) Metalloproteases from *Pseudomonas aeruginosa* degrade human RANTES, MCP-1, and ENA-78 *J Interferon Cytokine Res.* **23** : 307-318.

Letoffe,S., Redeker,V., and Wandersman,C. (1998) Isolation and characterization of an extracellular haem-binding protein from *Pseudomonas aeruginosa* that shares function and sequence similarities with the Serratia marcescens HasA haemophore *Mol.Microbiol* **28**: 1223-1234.

Licklider,L.J., Thoreen,C.C., Peng,J., and Gygi,S.P. (2002) Automation of nanoscale microcapillary liquid chromatography-tandem mass spectrometry with a vented column *Anal.Chem.* **74**: 3076-3083.

Lin,J., Huang,S.X., and Zhang,Q.J. (2002) Outer membrane proteins: key players for bacterial adaptation in host niches *Microbes and Infection* **4**: 325-331.

Linn,S., Imlay,J.A. (1987) Toxicity, mutagenesis and stress responses induced in *Escherichia coli* by hydrogen peroxide *J.Cell Sci.Suppl* **6**: 289-301.

Lyczak,J.B., Pier,G.B. (2002) *Salmonella enterica* serovar typhi modulates cell surface expression of its receptor, the cystic fibrosis transmembrane conductance regulator, on the intestinal epithelium *Infect.Immun.* **70**: 6416-6423.

Lyczak,J.B., Cannon,C.L., and Pier,G.B. (2002) Lung infections associated with cystic fibrosis *Clin.Microbiol.Rev.* **15**: 194-222.

Ma,J.F., Hager,P.W., Howell,M.L., Phibbs,P.V., and Hassett,D.J. (1998) Cloning and characterization of the *Pseudomonas aeruginosa* zwf gene encoding glucose-6-phosphate dehydrogenase, an enzyme important in resistance to methyl viologen (paraquat) *J.Bacteriol.* **180**: 1741-1749.

Ma,J.F., Ochsner,U.A., Klotz,M.G., Nanayakkara,V.K., Howell,M.L., Johnson,Z., Posey,J.E., Vasil,M.L., Monaco,J.J., and Hassett,D.J. (1999) Bacterioferritin A modulates catalase A (KatA) activity and resistance to hydrogen peroxide in *Pseudomonas aeruginosa Journal of Bacteriology* **181**: 3730-3742.

Macfarlane,E.L., Kwasnicka,A., and Hancock,R.E. (2000) Role of *Pseudomonas aeruginosa* PhoP-phoQ in resistance to antimicrobial cationic peptides and aminoglycosides *Microbiology* **146 (Pt 10)**: 2543-2554.

Malhotra,S., Silo-Suh,L.A., Mathee,K., and Ohman,D.E. (2000) Proteome analysis of the effect of mucoid conversion on global protein expression in *Pseudomonas aeruginosa* strain PAO1 shows induction of the disulfide bond isomerase, dsbA *J.Bacteriol.* **182**: 6999-7006.

Maringanti,S., Imlay,J.A. (1999) An intracellular iron chelator pleiotropically suppresses enzymatic and growth defects of superoxide dismutase-deficient *Escherichia coli J.Bacteriol.* **181**: 3792-3802.

Maringanti,S., Imlay,J.A. (1999) An intracellular iron chelator pleiotropically suppresses enzymatic and growth defects of superoxide dismutase-deficient *Escherichia coli J.Bacteriol.* **181**: 3792-3802.

Marlovits,T.C., Haase,W., Herrmann,C., Aller,S.G., and Unger,V.M. (2002) The membrane protein FeoB contains an intramolecular G protein essential for Fe(II) uptake in bacteria *PNAS* **99**: 16243-16248.

Martinez,A.a.R.K. (1997) Protection of DNA during oxidative stress by the nonspecific DNA-binding protein Dps. *J.Bacteriol.* **179**: 5188-5194.

Mathee,K., Ciofu,O., Sternberg,C., Lindum,P.W., Campbell,J.I.A., Jensen,P., Johnsen,A.H., Givskov,M., Ohman,D.E., Molin,S., Hoiby,N., and Kharazmi,A. (1999) Mucoid conversion of *Pseudomonas aeruginosa* by hydrogen peroxide: a mechanism for virulence activation in the cystic fibrosis lung *Microbiology-Uk* **145**: 1349-1357.

Mathesius,U., Imin,N., Chen,H., Djordjevic,M.A., Weinman,J.J., Natera,S.H., Morris,A.C., Kerim,T., Paul,S., Menzel,C., Weiller,G.F., and Rolfe,B.G. (2002) Evaluation of proteome reference maps for cross-species identification of proteins by peptide mass fingerprinting *Proteomics.* **2**: 1288-1303.

McCord,J.M., Fridovich,I. (1969) Superoxide dismutase: an enzymic function for erythrocuprein .*J.Biol.Chem.* **244**: 6049-6055.

Meyer,J.M., Neely,A., Stintzi,A., Georges,C., and Holder,I.A. (1996) Pyoverdin is essential for virulence of *Pseudomonas aeruginosa Infection and Immunity* **64**: 518-523.

Meyer,J.M. (2000) Pyoverdines: pigments, siderophores and potential taxonomic markers of fluorescent Pseudomonas species *Archives of Microbiology* **174**: 135-142.

Mohanty, B. K., and Kushner., S. R. 2000. Polynucleotide phosphorylase, RNase II and RNase E play different roles in the in vivo modulation of polyadenylation in *Escherichia coli*. *Mol.Microbiol* **36:**982-994.

Moore,G.R., Kadir,F.H., al Massad,F.K., Le Brun,N.E., Thomson,A.J., Greenwood,C., Keen,J.N., and Findlay,J.B. (1994) Structural heterogeneity of *Pseudomonas aeruginosa* bacterioferritin *Biochem.J.* **304 (Pt 2)**: 493-497.

Moreno-Vivian,C., Cabello,P., Martinez-Luque,M., Blasco,R., and Castillo,F. (1999) Prokaryotic nitrate reduction: molecular properties and functional distinction among bacterial nitrate reductases *J.Bacteriol.* **181**: 6573-6584.

Nouwens,A.S., Walsh,B.J., and Cordwell,S.J. (2003) Application of proteomics to *Pseudomonas aeruginosa Adv.Biochem.Eng Biotechnol.* **83**: 117-140.

Nouwens,A.S., Beatson,S.A., Whitchurch,C.B., Walsh,B.J., Schweizer,H.P., Mattick,J.S., and Cordwell,S.J. (2003) Proteome analysis of extracellular proteins regulated by the las and rhl quorum sensing systems in *Pseudomonas aeruginosa* PAO1 *Microbiology* **149**: 1311-1322.

O'Connor,C.D., Adams,P., Alefounder,P., Farris,M., Kinsella,N., Li,Y., Payot,S., and Skipp,P. (2000) The analysis of microbial proteomes: strategies and data exploitation *Electrophoresis* **21**: 1178-1186.

O'Malley,Y.Q., Reszka,K.J., Rasmussen,G.T., Abdalla,M.Y., Denning,G.M., and Britigan,B.E. (2003) The pseudomonas secretory product pyocyanin inhibits catalase activity in human lung epithelial cells *Am.J Physiol Lung Cell Mol.Physiol.*

Ochsner,U.A., Johnson,Z., Lamont,I.L., Cunliffe,H.E., and Vasil,M.L. (1996) Exotoxin A production in *Pseudomonas aeruginosa* requires the iron-regulated pvdS gene encoding an alternative sigma factor *Molecular Microbiology* **21**: 1019-1028.

Ochsner,U.A., Vasil,M.L. (1996) Gene repression by the ferric uptake regulator in *Pseudomonas aeruginosa*: Cycle selection of iron-regulated genes *Proceedings of the National Academy of Sciences of the United States of America* **93**: 4409-4414.

Ochsner,U.A., Johnson,Z., and Vasil,M.L. (2000) Genetics and regulation of two distinct haem-uptake systems, phu and has, in *Pseudomonas aeruginosa Microbiology-Uk* **146**: 185-198.

Ochsner,U.A., Vasil,M.L., Alsabbagh,E., Parvatiyar,K., and Hassett,D.J. (2000) Role of the *Pseudomonas aeruginosa* oxyR-recG operon in oxidative stress defense and DNA repair: OxyR-dependent regulation of katB-ankB, ahpB, and ahpC-ahpF *Journal of Bacteriology* **182**: 4533-4544.

Ochsner,U.A., Wilderman,P.J., Vasil,A.I., and Vasil,M.L. (2002) GeneChip((R)) expression analysis of the iron starvation response in Pseudomonas aeruginosa: identification of novel pyoverdine biosynthesis genes *Molecular Microbiology* **45**: 1277-1287.

Olsen,G.J., Woese,C.R., and Overbeek,R. (1994) The winds of (evolutionary) change: breathing new life into microbiology *J.Bacteriol.* **176**: 1-6.

Palma,M., Worgall,S., and Quadri,L.E. (2003) Transcriptome analysis of the *Pseudomonas aeruginosa* response to iron *Arch.Microbiol.*

Polack,B., Dacheux,D., DelicAttree,I., Toussaint,B., and Vignais,P.M. (1996) The *Pseudomonas aeruginosa* fumc and soda genes belong to an iron-responsive operon *Biochemical and Biophysical Research Communications* **226**: 555-560.

Polack,B., Dacheux,D., DelicAttree,I., Toussaint,B., and Vignais,P.M. (1996) Role of manganese superoxide dismutase in a mucoid isolate of *Pseudomonas aeruginosa*: Adaptation to oxidative stress *Infection and Immunity* **64**: 2216-2219.

Pond,M.N., Morton,A.M., and Conway,S.P. (1996) Functional iron deficiency in adults with cystic fibrosis *Respiratory Medicine* **90**: 409-413.

Poole,K., Neshat,S., Krebes,K., and Heinrichs,D.E. (1993) Cloning and nucleotide sequence analysis of the ferripyoverdine receptor gene fpvA of *Pseudomonas aeruginosa J.Bacteriol.* **175**: 4597-4604.

Rainey,P.B., Bailey,M.J. (1996) Physical and genetic map of the *Pseudomonas fluorescens* SBW25 chromosome *Mol.Microbiol.* **19**: 521-533.

Rainey,P.B., Travisano,M. (1998) Adaptive radiation in a heterogeneous environment *Nature* **394**: 69-72.

Ratledge,C., Dover,L.G. (2000) Iron metabolism in pathogenic bacteria *Annu.Rev.Microbiol.* **54**: 881-941.

Reid,D.W., Withers,N.J., Francis,L., Wilson,J.W., and Kotsimbos,T.C. (2002) Iron deficiency in cystic fibrosis - Relationship to lung disease severity and chronic *Pseudomonas aeruginosa* infection *Chest* **121**: 48-54.

Rindi,L., Lari,N., Gil,M.G., and Garzelli,C. (1998) Oligo(dT)-primed synthesis of cDNA by reverse transcriptase in mycobacteria *Biochem.Biophys.Res.Commun.* **248**: 216-218.

Ririe,K.M., Rasmussen,R.P., and Wittwer,C.T. (1997) Product differentiation by analysis of DNA melting curves during the polymerase chain reaction *Anal.Biochem.* **245**: 154-160.

Robey,M., Cianciotto,N.P. (2002) *Legionella pneumophila* feoAB promotes ferrous iron uptake and intracellular infection *Infect.Immun.* **70**: 5659-5669.

Romling,U., Fiedler,B., Bosshammer,J., Grothues,D., Greipel,J., von der,H.H., and Tummler,B. (1994) Epidemiology of chronic *Pseudomonas aeruginosa* infections in cystic fibrosis *J.Infect.Dis.* **170**: 1616-1621.

Romling,U., Wingender,J., Muller,H., and Tummler,B. (1994) A major *Pseudomonas aeruginosa* clone common to patients and aquatic habitats *Appl.Environ.Microbiol.* **60**: 1734-1738.

Romling,U., Tummler,B. (2000) Achieving 100% typeability of *Pseudomonas aeruginosa* by pulsed-field gel electrophoresis *J.Clin.Microbiol.* **38**: 464-465.

Sabra,W., Kim,E.J., and Zeng,A.P. (2002) Physiological responses of *Pseudomonas aeruginosa* PAO1 to oxidative stress in controlled microaerobic and aerobic cultures *Microbiology* **148**: 3195-3202.

Sachs,A.B., Sarnow,P., and Hentze,M.W. (1997) Starting at the beginning, middle, and end: translation initiation in eukaryotes *Cell* **89**: 831-838.

Sachs,A.B., Buratowski,S. (1997) Common themes in translational and transcriptional regulation *Trends Biochem.Sci.* **22**: 189-192.

Salunkhe,P., von Götz,F., Wiehlmann,L., Lauber,J., Buer,J., and Tummler,B. (2003) GeneChip Expression Analysis of the Response of *Pseudomonas aeruginosa* to Paraquat-Induced Superoxide Stress. *Genome Letters* **4**, 165-174. American Scientific Publishers

Sarkar,N. (1996) Polyadenylation of mRNA in bacteria *Microbiology* **142 (Pt 11)**: 3125-3133.

Sarkar,N. (1997) Polyadenylation of mRNA in prokaryotes *Annu.Rev.Biochem.* **66**: 173-197.

Sauer,K., Camper,A.K. (2001) Characterization of phenotypic changes in *Pseudomonas putida* in response to surface-associated growth *J.Bacteriol.* **183**: 6579-6589.

Sauer,K., Camper,A.K., Ehrlich,G.D., Costerton,J.W., and Davies,D.G. (2002) *Pseudomonas aeruginosa* displays multiple phenotypes during development as a biofilm *J.Bacteriol.* **184**: 1140-1154.

Schmitz,F.J., Fluit,A.C., Beeck,A., Perdikouli,M., and von Eiff,C. (2001) Development of chromosomally encoded resistance mutations in small-colony variants of *Staphylococcus aureus J.Antimicrob.Chemother.* **47**: 113-115.

Sherman,N.E., Stefansson,B., Fox,J.W., and Goldberg,J.B. (2001) *Pseudomonas aeruginosa* and a proteomic approach to bacterial pathogenesis *Dis.Markers* **17**: 285-293.

Shoemaker,D.D., Linsley,P.S. (2002) Recent developments in DNA microarrays *Curr.Opin.Microbiol.* **5**: 334-337.

Singh,P.K., Schaefer,A.L., Parsek,M.R., Moninger,T.O., Welsh,M.J., and Greenberg,E.P. (2000) Quorum-sensing signals indicate that cystic fibrosis lungs are infected with bacterial biofilms *Nature* **407**: 762-764.

Singh,P.K., Parsek,M.R., Greenberg,E.P., and Welsh,M.J. (2002) A component of innate immunity prevents bacterial biofilm development *Nature* **417**: 552-555.

Steege, D. A. (2000). Emerging features of mRNA decay in bacteria. *RNA*. **6:**1079-1090.

Stewart,V. (1998) Nitrate respiration in relation to facultative metabolism in Enterobacteria *Microbiol.Rev*: 190-232.

Stewart,V. (1993) Nitrate regulation of anaerobic respiratory gene expression in *Escherichia coli Mol.Microbiol.* **9**: 425-434.

Stover,C.K., Pham,X.Q., Erwin,A.L., Mizoguchi,S.D., Warrener,P., Hickey,M.J., Brinkman,F.S., Hufnagle,W.O., Kowalik,D.J., Lagrou,M., Garber,R.L., Goltry,L., Tolentino,E., Westbrock-Wadman,S., Yuan,Y., Brody,L.L., Coulter,S.N., Folger,K.R., Kas,A., Larbig,K., Lim,R., Smith,K., Spencer,D., Wong,G.K., Wu,Z., Paulsen,I.T., Reizer,J., Saier,M.H., Hancock,R.E., Lory,S., and Olson,M.V. (2000) Complete genome sequence of *Pseudomonas aeruginosa* PA01, an opportunistic pathogen *Nature* **406**: 959-964.

Stover,G.B., Drake,D.R., and Montie,T.C. (1983) Virulence of different Pseudomonas species in a burned mouse model: tissue colonization by *Pseudomonas cepacia Infect.Immun.* **41**: 1099-1104.

Tan,S.S., Weis,J.H. (1992) Development of a sensitive reverse transcriptase PCR assay, RT-RPCR, utilizing rapid cycle times *PCR Methods Appl.* **2**: 137-143.

Tong,A.H., Evangelista,M., Parsons,A.B., Xu,H., Bader,G.D., Page,N., Robinson,M., Raghibizadeh,S., Hogue,C.W., Bussey,H., Andrews,B., Tyers,M., and Boone,C. (2001) Systematic genetic analysis with ordered arrays of yeast deletion mutants *Science* **294**: 2364-2368.

Touati,D. (2000) Iron and oxidative stress in bacteria *Archives of Biochemistry and Biophysics* **373** : 1-6.

Tummler,B. (1987) Unusual mechanism of pathogenicity of *Pseudomonas aeruginosa* isolates from patients with cystic fibrosis *Infection* **15**: 311-312.

Tummler,B., Bosshammer,J., Breitenstein,S., Brockhausen,I., Gudowius,P., Herrmann,C., Herrmann,S., Heuer,T., Kubesch,P., Mekus,F., Romling,U., Schmidt,K.D., Spangenberg,C., and Walter,S. (1997) Infections with *Pseudomonas aeruginosa* in patients with cystic fibrosis *Behring Inst.Mitt.* : 249-255.

Tyers, M., and Mann, M., (2003) From genomics to proteomics *Nature* **422**: 193-197.

VanBogelen,R.A., Schiller,E.E., Thomas,J.D., and Neidhardt,F.C. (1999) Diagnosis of cellular states of microbial organisms using proteomics *Electrophoresis* **20**: 2149-2159.

Vasil,M.L., Ochsner,U.A., Johnson,Z., Colmer,J.A., and Hamood,A.N. (1998) The fur-regulated gene encoding the alternative sigma factor PvdS is required for iron-dependent expression of the LysR-type regulator PtxR in *Pseudomonas aeruginosa Journal of Bacteriology* **180**: 6784-6788.

Vasil,M.L., Ochsner,U.A. (1999) The response of *Pseudomonas aeruginosa* to iron: genetics, biochemistry and virulence *Molecular Microbiology* **34**: 399-413.

Velayudhan,J., Hughes,N.J., McColm,A.A., Bagshaw,J., Clayton,C.L., Andrews,S.C., and Kelly,D.J. (2000) Iron acquisition and virulence in Helicobacter pylori: a major role for FeoB, a high-affinity ferrous iron transporter *Mol.Microbiol.* **37**: 274-286.

Venturi,V., Weisbeek,P., and Koster,M. (1995) Gene regulation of siderophore-mediated iron acquisition in Pseudomonas: not only the Fur repressor *Mol.Microbiol.* **17**: 603-610.

Vijgenboom,E., Busch,J.E., and Canters,G.W. (1997) In vivo studies disprove an obligatory role of azurin in denitrification in *Pseudomonas aeruginosa* and show that azu expression is under control of RpoS and ANR *Microbiology-Uk* **143**: 2853-2863.

Visca,P., Leoni,L., Wilson,M.J., and Lamont,I.L. (2002) Iron transport and regulation, cell signalling and genomics: lessons from *Escherichia coli* and Pseudomonas *Molecular Microbiology* **45**: 1177-1190.

von Eiff,C., Proctor,R.A., and Peters,G. (2000) *Staphylococcus aureus* small colony variants: formation and clinical impact *Int.J.Clin.Pract.Suppl*: 44-49.

von Götz. (2003) Transkriptomanalyse verschiedener Morphotypen von *Pseudomonas aeruginosa*, isoliert von Patienten mit Cystischer Fibrose. Dissertation. 2003. Fachbereich Biologie, Universität Hannover.

von Götz, F., Haussler, S., Jordan, D., Saravanamuthu, S., Wehmhöner, D., Strussmann, A., Lauber, J., Attree, I., Buer, J., Tummler, B., and I. Steinmetz. **(**2004) Expression analysis of a highly adherent and cytotoxic small colony variant of *Pseudomonas aeruginosa* isolated from a cystic fibrosis lung. *J.Bacteriol.* in press.

Washburn,M.P., Yates,J.R., III (2000) Analysis of the microbial proteome *Curr.Opin.Microbiol.* **3**: 292-297.

Watnick,P., Kolter,R. (2000) Biofilm, city of microbes *J.Bacteriol.* **182**: 2675-2679.

Wechter,W.P., Begum,D., Presting,G., Kim,J.J., Wing,R.A., and Kluepfel,D.A. (2002) Physical mapping, BAC-end sequence analysis, and marker tagging of the soilborne nematicidal bacterium, *Pseudomonas synxantha* BG33R *Genomics* **6**: 11-21.

Wehmhoner, D. Proteomanalyse unterschiedlicher Morphotypen von *Pseudomonas aeruginosa*, isoliert von Patienten mit zystischer Fibrose. 2002. Fachbereich Biologie,Universität Hannover.

Wehmhoner,D., Haussler,S., Tummler,B., Jansch,L., Bredenbruch,F., Wehland,J., and Steinmetz,I. (2003) Inter- and intraclonal diversity of the *Pseudomonas aeruginosa* proteome manifests within the secretome *J.Bacteriol.* **185**: 5807-5814.

Wickens,M., Anderson,P., and Jackson,R.J. (1997) Life and death in the cytoplasm: messages from the 3' end *Curr.Opin.Genet.Dev.* **7**: 220-232.

WIlkins,M.R., Pasquali,C., Appel,R.D., Ou,K., Golaz,O., Sanchez,J.C., Yan,J.X., Gooley,A.A., Hughes,G., Humphery-Smith,I., Williams,K.L., and Hochstrasser,D.F. (1996) From proteins to proteomes: large scale protein identification by two-dimensional electrophoresis and amino acid analysis *Biotechnology (N.Y.)* **14**: 61-65.

Wilson,M.J., McMorran,B.J., and Lamont,I.L. (2001) Analysis of promoters recognized by PvdS, an extracytoplasmic-function sigma factor protein from *Pseudomonas aeruginosa J Bacteriol.* **183**: 2151-2155.

Wittwer,C.T., Ririe,K.M., Andrew,R.V., David,D.A., Gundry,R.A., and Balis,U.J. (1997) The LightCycler: a microvolume multisample fluorimeter with rapid temperature control *Biotechniques* **22**: 176-181.

Wittwer,C.T., Herrmann,M.G., Moss,A.A., and Rasmussen,R.P. (1997) Continuous fluorescence monitoring of rapid cycle DNA amplification *Biotechniques* **22**: 130-138.

Woodmansee,A.N., Imlay,J.A. (2002) Reduced flavins promote oxidative DNA damage in non-respiring *Escherichia coli* by delivering electrons to intracellular free iron *J.Biol.Chem.* **277**: 34055-34066.

Worlitzsch,D., Tarran,R., Ulrich,M., Schwab,U., Cekici,A., Meyer,K.C., Birrer,P., Bellon,G., Berger,J., Weiss,T., Botzenhart,K., Yankaskas,J.R., Randell,S., Boucher,R.C., and Doring,G. (2002) Effects of reduced mucus oxygen concentration in airway Pseudomonas infections of cystic fibrosis patients *J.Clin.Invest* **109**: 317-325.

Xiao,R., Kisaalita,W.S. (1997) Iron acquisition from transferrin and lactoferrin by *Pseudomonas aeruginosa* pyoverdin *Microbiology-Uk* **143**: 2509-2515.

Xiao,R., Kisaalita,W.S. (1998) Fluorescent pseudomonad pyoverdines bind and oxidize ferrous ion *Appl.Environ.Microbiol.* **64**: 1472-1476.

Yates,J.M., Morris,G., and Brown,M.R. (1989) Effect of iron concentration and growth rate on the expression of protein G in *Pseudomonas aeruginosa FEMS Microbiol.Lett.* **49**: 259-262.

Yoon,S.S., Hennigan,R.F., Hilliard,G.M., Ochsner,U.A., Parvatiyar,K., Kamani,M.C., Allen,H.L., DeKievit,T.R., Gardner,P.R., Schwab,U., Rowe,J.J., Iglewski,B.H., McDermott,T.R., Mason,R.P., Wozniak,D.J., Hancock,R.E., Parsek,M.R., Noah,T.L., Boucher,R.C., and Hassett,D.J. (2002) *Pseudomonas aeruginosa* anaerobic respiration in biofilms: relationships to cystic fibrosis pathogenesis *Dev.Cell* **3**: 593-603.

Zheng,M., Doan,B., Schneider,T.D., and Storz,G. (1999) OxyR and SoxRS regulation of fur *J.Bacteriol.* **181**: 4639-4643.

Zierdt,C.H., Schmidt,P.J. (1964) Dissociation in *Pseudomonas aeruginosa J.Bacteriol.* **87**: 1003-1010.

6.   Appendix

Primers used for real time PCR of *rpoD* and *feoB* homologue (PA4358) described in **section 3.1.7.**

Gene	Primer sequence	Binding region in the Coding sequence	Melting Temperature	GC %
rpoD	Forward Primer 5'-GGG GAT CAA CGT ATT CGA GA-3'	**159-178**	**57.3°C**	**50%**
	Reverse Primer 5'-TCA TCG GGA TCG ATA TAG CC-3'	**496-515**	**57.3°C**	**50%**
feoB	Forward Primer 5'-TGT ACC ATG TGC CAC ACC TT -3'	**1463-1482**	**57.3°C**	**50%**
	Reverse Primer 5'-GGT CGT AGC CTT CGT AGT CG -3'	**1800-1819**	**61.4°C**	**50%**

7.   Curriculum Vitae

Personal Details

Name	Senthil Selvan Saravanamuthu
Date of birth	28 April 1977
Place of birth	Chennai, India
Marital Satus	Unmarried
Email	sselvan19@yahoo.com

Education

Higher Schooling

1992 -1994 Jaigopal Garodia Vivekananda Vidhyalaya (JGVV),
U-44, Annanagar, Chennai – 600 040,
Tamil Nadu,
India

University

1995 – 2000 **M.Sc., in Life Sciences (Biotechnology)**
Master of Sciences in Life Sciences (5 year integrated degree course) with specialization in Biotechnology
School of Life Sciences, Bharathidasan University,
Tiruchirapalli, Tamil Nadu,
India

2000-2004 **Ph.D., Dissertation work**

Topic:
Proteome analysis of the differential adaptation of *Pseudomonas aeruginosa* morphotypes isolated from Cystic Fibrosis patients to iron limiting conditions, oxidative stress and anaerobic conditions.

Carried out at:
European Graduate College on *Pseudomonas aeruginosa* : Pathogenicity and Biotechnology at Medizinische Hochschule Hannover (MHH) and Gesellschaft für Biotechnologische Forschung (GBF), Braunschweig,Germany

Supervised by:
PD.Dr. Ivo Steinmetz, Institut für Medizinische Mikrobiologie und Krankenhaushygiene, MHH, Hannover.

.

Scientific meetings attended :
- **International conference cum workshop on Transcriptomics and Proteomics**, *'Decoding the microbe using advanced tools of Genomics,Transcriptomics and Proteomics'* organized by the Central Public Health Laboratories (CPHL), London, June 25-26,2001.
- Participation and presentation at the **International Summer School workshop of the European graduate college on Pseudomonas** at Denmark Technical University, Copenhagen, August 2001.
- Participation in the **Pseudomonas 2001,** Brussels, Belgium international congress for Pseudomonas research, September 17-21, 2001.
- **European seminar on Proteomics** by Amersham Biosciences, Charitie-Humboldt University, Berlin, July 2002.
- Participation and presentation at the **International Summer School workshop of the European graduate college on Pseudomonas** at the German Biotechnology Research Center, Braunschweig, August 2002.
- Poster presentation at the **Pseudomonas 2003**, September 06-10, 2003, Quebec, Canada

Courses organized :
Organized and conducted a Proteomics workshop for PhD students of the Deutsche Forschungs Gemeinschaft sponsored graduate college on Mucosal Host-Pathogen Interaction, June 6-7, 2002, at the GBF, Braunschweig.

Publications :

- **Saravanamuthu, S.,** Salunkhe, P., v.Götz, F., Rathinam C., Geffers, R., Buer, J., Tümmler, B., and Steinmetz, I. (2004). Evidence for polyadenlated mRNA in *Pseudomonas aeruginosa. J Bacteriol. -* Submitted

- v. Götz, F., Wehmhöner, D., **Saravanamuthu, S**., Häußler, S., Lauber, J., Attree, I., Jordan, D., Buer, J.,Tümmler, B. und Steinmetz, I. (2004) Expression analysis of a cytotoxic and biofilm forming small-colony variant of *Pseudomonas aeruginosa* isolated from a cystic fibrosis lung. *J.Bacteriol.* : in press

- Häußler, S., Ziegler, I., Lottel, A., v. Götz, F., Rohde, M., Tümmler, B., Wehmhöner, D., **Saravanamuthu, S**. und Steinmetz, I. (2003) Highly adherent small colony variants of *Pseudomonas aeruginosa* in cystic fibrosis lung infection. *J. Med. Microbiol.*, 52, 295–301

Erklärungen

Sehr geehrte Damen und Herren,

hiermit erkläre ich laut §6 Absatz 1 der Gemeinsamen Prüfungsordnung der naturwissenschaftlichen Fachbereiche für die Promotion zum Doktor der Naturwissenschaften (Dr.rer.nat) an der Universität Hannover, daß

ich die genehmigte Dissertation

1.selbständig verfasst und die zur Hilfeleistung herangezogenen Institutionen Vollständig angegeben und
2.nicht bereits als Diplomarbeit oder ähnliche Prüfungsarbeit verwendet habe.

von mir kein weiteres Promotionsverfahren bei einer andern Hochschule oder Fachbereich beantragt worden ist.

Eine vollständige Liste der wissenschaftlichen Publikationen finden Sie im Anhang der Dissertations-Schrift.

Senthil Selvan Saravanamuthu